

Phase Doppler Particle Analyzer (PDPA)/ Laser Doppler Velocimeter (LDV)

Operations Manual

*P/N 1990048, Revision E
February 2006*



Manual History

The following is a manual history of the Phase Doppler Particle Analyzer (PDPA)/Laser Doppler Velocimeter (LDV) Operations Manual (Part Number 1990048).

Revision	Date
Final	December 2001
A	December 2004
B	March 2005
C	May 2005
D	November 2005
E	February 2006

Warranty

Part Number
Copyright
Address
Fax No.
E-mail Address
**Limitation of Warranty
and Liability**
(effective July 2000)

1990048 / Revision E / February 2006

©TSI Incorporated / 2001–2006 / All rights reserved.

TSI Incorporated / 500 Cardigan Road / Shoreview, MN 55126 / USA

651-490-3824

fluid@tsi.com

Seller warrants the goods sold hereunder, under normal use and service as described in the operator's manual, shall be free from defects in workmanship and material for (12) months, or the length of time specified in the operator's manual, from the date of shipment to the customer. This warranty period is inclusive of any statutory warranty. This limited warranty is subject to the following exclusions:

- a. Hot-wire or hot-film sensors used with research anemometers, and certain other components when indicated in specifications, are warranted for 90 days from the date of shipment.
- b. Parts repaired or replaced as a result of repair services are warranted to be free from defects in workmanship and material, under normal use, for 90 days from the date of shipment.
- c. Seller does not provide any warranty on finished goods manufactured by others or on any fuses, batteries or other consumable materials. Only the original manufacturer's warranty applies.
- d. Unless specifically authorized in a separate writing by Seller, Seller makes no warranty with respect to, and shall have no liability in connection with, goods which are incorporated into other products or equipment, or which are modified by any person other than Seller.

The foregoing is IN LIEU OF all other warranties and is subject to the LIMITATIONS stated herein. **NO OTHER EXPRESS OR IMPLIED WARRANTY OF FITNESS FOR PARTICULAR PURPOSE OR MERCHANTABILITY IS MADE.**

TO THE EXTENT PERMITTED BY LAW, THE EXCLUSIVE REMEDY OF THE USER OR BUYER, AND THE LIMIT OF SELLER'S LIABILITY FOR ANY AND ALL LOSSES, INJURIES, OR DAMAGES CONCERNING THE GOODS (INCLUDING CLAIMS BASED ON CONTRACT, NEGLIGENCE, TORT, STRICT LIABILITY OR OTHERWISE) SHALL BE THE RETURN OF GOODS TO SELLER AND THE REFUND OF THE PURCHASE PRICE, OR, AT THE OPTION OF SELLER, THE REPAIR OR REPLACEMENT OF THE GOODS. IN NO EVENT SHALL SELLER BE LIABLE FOR ANY SPECIAL, CONSEQUENTIAL OR INCIDENTAL DAMAGES. SELLER SHALL NOT BE RESPONSIBLE FOR INSTALLATION, DISMANTLING OR REINSTALLATION COSTS OR CHARGES. No Action, regardless of form, may be brought against Seller more than 12 months after a cause of action has accrued. The goods returned under warranty to Seller's factory shall be at Buyer's risk of loss, and will be returned, if at all, at Seller's risk of loss.

Buyer and all users are deemed to have accepted this LIMITATION OF WARRANTY AND LIABILITY, which contains the complete and exclusive limited warranty of Seller. This LIMITATION OF WARRANTY AND LIABILITY may not be amended, modified or its terms waived, except by writing signed by an Officer of Seller.

Service Policy

Knowing that inoperative or defective instruments are as detrimental to TSI as they are to our customers, our service policy is designed to give prompt attention to any problems. If any malfunction is discovered, please contact your nearest sales office or representative, or call TSI at 1-800-874-2811 (USA) or (615) 490-2811.

Software License
(effective March 1999)

1. GRANT OF LICENSE. TSI grants to you the right to use one copy of the enclosed TSI software program (the "SOFTWARE"), on a single computer. You may not network the SOFTWARE or otherwise use it on more than one computer or computer terminal at the same time.
2. COPYRIGHT. The SOFTWARE is owned by TSI and is protected by United States copyright laws and international treaty provisions. Therefore, you must treat the SOFTWARE like any other copyrighted material (e.g., a book or musical recording) except that you may either (a) make one copy of the SOFTWARE solely for backup or archival purposes, or (b) transfer the SOFTWARE to a single hard disk provided you keep the original solely for backup or archival purposes.
3. OTHER RESTRICTIONS. You may not rent or lease the SOFTWARE, but you may transfer the SOFTWARE and accompanying written material on a permanent basis, provided you retain no copies and the recipient agrees to the terms of this Agreement. You may not reverse-engineer, decompile, or disassemble the SOFTWARE.
4. DUAL MEDIA SOFTWARE. If the SOFTWARE package contains multiple types of media, then you may use only the media appropriate for your single-user computer. You may not use the other media on another computer or loan, rent, lease, or transfer them to another user except as part of the permanent transfer (as provided above) of all SOFTWARE and written material.
5. U.S. GOVERNMENT RESTRICTED RIGHTS. The SOFTWARE and documentation are provided with RESTRICTED RIGHTS. Use, duplication, or disclosure by the Government is subject to the restrictions set forth in the "Rights in Technical Data and Computer Software" Clause at 252.227-7013 and the "Commercial Computer Software - Restricted Rights" clause at 52.227-19.
6. LIMITED WARRANTY. TSI warrants that the SOFTWARE will perform substantially in accordance with the accompanying written materials for a period of ninety (90) days from the date of receipt.
7. CUSTOMER REMEDIES. TSI's entire liability and your exclusive remedy shall be, at TSI's option, either (a) return of the price paid or (b) repair or replacement of the SOFTWARE that does not meet this Limited Warranty and which is returned to TSI with proof of payment. This Limited Warranty is void if failure of the SOFTWARE has resulted from accident, abuse, or misapplication. Any replacement SOFTWARE will be warranted for the remainder of the original warranty period or thirty (30) days, whichever is longer.
8. NO OTHER WARRANTIES. TSI disclaims all other warranties, either express or implied, including, but not limited to implied warranties of merchantability and fitness for a particular purpose, with regard to the SOFTWARE and the accompanying written materials.
9. NO LIABILITY FOR CONSEQUENTIAL DAMAGES. In no event shall TSI be liable for any damages whatsoever (including, without limitation, special, incidental, consequential or indirect damages for personal injury, loss of business profits, business interruption, loss of information or any other pecuniary loss) arising out of the use of, or inability to use, this SOFTWARE.

Laser Safety

The Phase Doppler Particle Analyzer System is a laser-based system. Laser light contains characteristics which present possible safety hazards. The laser is a source of extremely intense light which is very different from light emitted from conventional sources. You must be aware of the proper safety precautions before attempting to operate the system.

The energy level of the beam is high enough to cause serious damage to the eye, with possible loss of vision if the beam were to pass directly into the eye. Since the beam is collimated, the energy in the beam remains high and dangerous even at great distances from the laser source. In addition, the high voltages associated with laser operation also pose a safety hazard. You are, therefore, advised to observe the following safety precautions:

- ❑ Locate the warning labels on the individual components.
- ❑ Every laser or laser product contains instructions in the proper usage of the product. Follow the manufacturer's recommendations.
- ❑ Limit access to the laser. Keep the laser out of the hands of inexperienced or untrained personnel.
- ❑ Do **not** operate the laser in the presence of flammable, explosive, or volatile substances such as alcohol, gasoline, or ether.
- ❑ When the laser is on and the output beam is not terminated in an experiment or optics system, the beam should be blocked. Use the laser power meter or some other non reflective, nonflammable object.
- ❑ **Never** look directly into either the main laser beam or any of the stray beams. Never sight down a beam into its source.
- ❑ Do **not** allow reflective objects to be placed in the laser beam. Light scattered from a reflective surface can be as damaging as the original beam. Even objects such as rings, watch bands, or metal pencils can create a hazard.
- ❑ Post warning signs, and limit access to the laser area while the laser is in operation.
- ❑ Do **not** set up experiments with the laser at eye level.

- ❑ Protective eyewear is available for all varieties of visible laser light. Eyewear should be worn anytime that the laser is energized.
- ❑ In those cases when visual access to the beam is necessary (as in alignment), make sure that the area is clear of unnecessary personnel and that extreme caution is used to prevent exposure.

The system described in this manual is designed to operate using an Argon-ion or HeNe laser light source. There are two types of Argon-ion laser available; an air cooled version, and a water cooled version. The air cooled version is rated as a Class IIIB laser, while the water cooled is rated as a Class IV laser product. The HeNe laser is a Class IIIB laser.

The Center for Devices and Radiological Health's (CDRH) definition of Class IIIB and Class IV are listed below.

Class IIIB applies to devices that emit in the ultraviolet, visible, and infrared spectra. Class IIIB products include laser systems ranging from 5 to 500 milliwatts in the visible spectrum. Class IIIB emission levels are ocular hazards and direct exposure throughout the range of Class, and skin hazards at the higher levels of the Class.

Class IV levels exceed the limits of Class IIIB and are a hazard for scattered (diffuse) reflection as well as for direct exposure.

Warning labels are also required by the CDRH, and are attached to all components which contain laser radiation. For the specific Class of your laser, see the label located next to the output aperture.

Warning Labels

Warning labels are either attached to or printed on all TSI transmitters, transceivers, fiberlight™ Multicolor Beam Separators and Flow and Size Analyzers (FSA). Typical warning labels are depicted in Figure 1. TSI transmitters and transceivers in systems using Class IV lasers are labeled with information about the lasers wavelength (450–550 nm) and maximum power output.



Figure 1
Typical Warning Labels

Locations of Warning Labels

The locations of the warning labels on TSI transmitters, transceivers, fiberlight, and PDMs are shown in Figures 2 to 4.

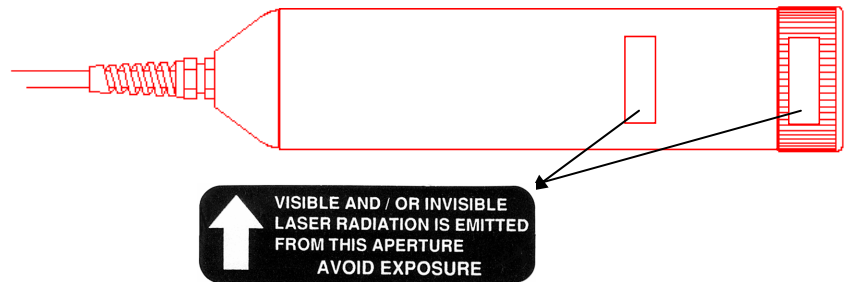


Figure 2
Location of Warning Labels on Transmitter/Transceiver

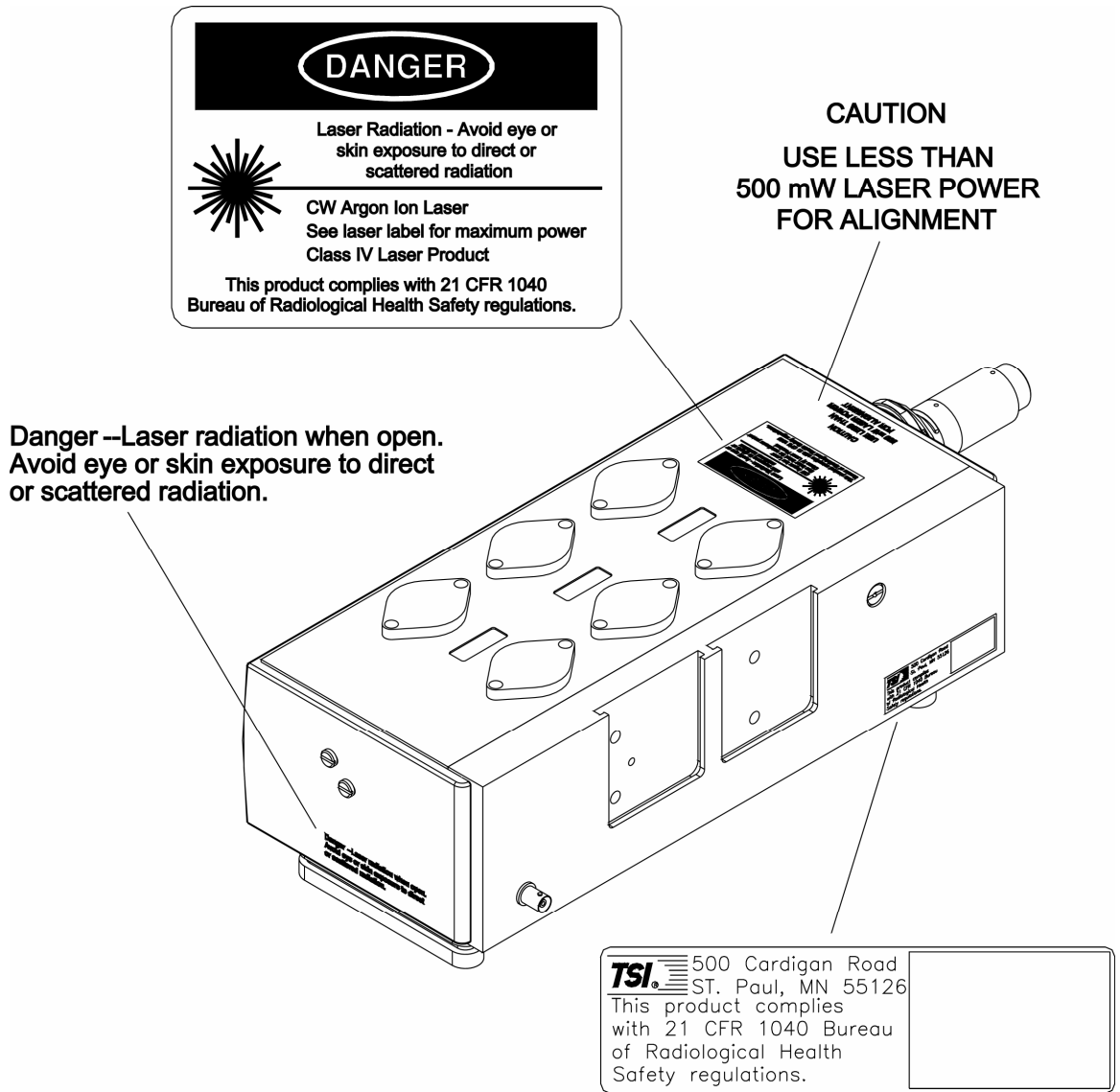


Figure 3
Location of Printed Warning Label on **fiberlight™**

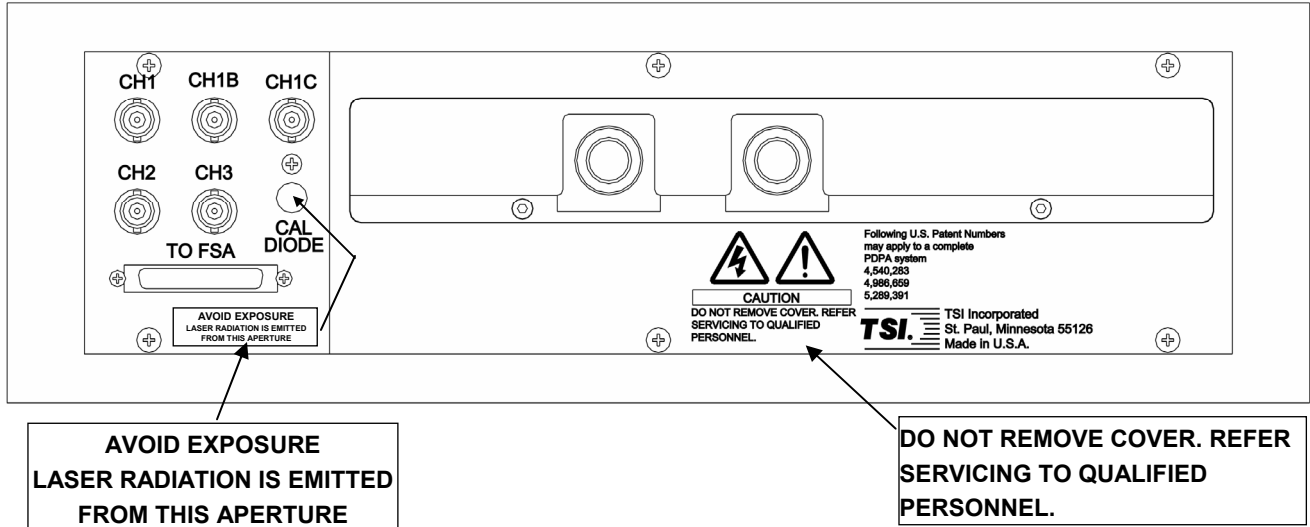


Figure 4
Location of Printed Warning Label on PDM

Power Output for fiberlight and Fiberoptic Probe Models

Typical values for the power output of the fiberlight and Transmitter/Transceiver Models as a percentage of input laser power are shown in the table below.

	Power Output as a Percentage of Laser Power (%)
fiberlight	80–90
Transmitter/Transceiver	50–65

Contents

Manual History	ii
Warranty	iii
Software License	iv
Laser Safety	v
Warning Labels	vii
Locations of Warning Labels.....	vii
Power Output for fiberlight and Fiberoptic Probe Models.....	ix
About This Manual	xix
Introduction.....	xix
Safety Labels.....	xix
Caution.....	xix
Warning.....	xx
Danger.....	xx
Caution, Warning, or Danger Symbols.....	xx
Getting Help.....	xxi
Submitting Comments	xxi

Chapters

1 Preparing the Computer to Store the Data	1-1
Installing the FLOWSIZER Software Package.....	1-1
Creating a New Structure for Data Storage.....	1-1
Selecting an Existing Project or Experiment Folder for Data Storage	1-3
2 Taking LDV Data	2-1
Direction of Fringe Motion Relative to Particle Motion for Velocity Measurements	2-3
Run Setup→Run Settings	2-3
Run Setup→Optics.....	2-6
Run Setup→Processor/Matrix.....	2-8
LDV Controls	2-11
Downmixing.....	2-12
Band Pass Filter.....	2-14
PMT Voltage	2-16
Burst Threshold	2-17
SNR	2-17

Hardware Status	2-18
3 Taking Size and Velocity Data	3-1
Phase Doppler Overview	3-1
Direction of Fringe Motion Relative to Receiver	
Orientation for Sizing Measurements	3-2
Setting Up the Software.....	3-3
Run Setup→Optics.....	3-4
Run Setup→Calibration	3-7
Run Setup→Diameter Measurement	3-8
Run Setup→Sweep Capture	3-9
Diameter Measurement	3-10
Run→Calibration→Laser Diode Calibration.....	3-15
4 Optimizing Particle Size Measurement and Obtaining Detailed Flow Information	4-1
Diameter Fitting.....	4-11
Rosin Rammler.....	4-11
Normal	4-12
Log Normal.....	4-12
5 Selecting an Optical Layout for Particle Sizing	5-1
6 Creating and Using Graphs.....	6-1
Showing a Graph	6-1
Designing a Graph	6-2
Deleting a Graph.....	6-3
Modifying a Graph	6-3
Modifying a Histogram Data Set	6-4
Customizing a Graph	6-5
7 Creating and Using Statistics Windows	7-1
Showing a Statistics Window.....	7-1
Velocity Statistics Window.....	7-2
Diameter Statistics Window	7-2
Volume Distribution Statistics Window	7-3
Velocity and Size Subrange Statistics Window.....	7-3
External Input Statistics Window	7-4
Transformed Velocity Statistics Window	7-4
Customizing a Statistics Window.....	7-5
Statistics Output Options.....	7-5
Statistics Summary Report.....	7-6
Design a Statistics Window	7-9
Example Statistics Windows.....	7-10
8 Using External Input	8-1
Analog.....	8-2
Converted Low	8-2
Converted High	8-2
Modulus.....	8-2
Offset	8-2
Analog Input Range.....	8-2
Digital	8-3

9 Power Spectrum Analysis	9-1
10 Using Subrange and Coincidence Modes	10-1
Inputting Subrange Values	10-2
Example Subrange Analysis	10-3
Velocity Subrange	10-4
Other Subrange Suggestions	10-6
Using Coincidence Mode	10-7
Coincidence Window Selection	10-8
Software Coincidence Mode of Operation	10-9
Software Coincidence Capture	10-10
Hints	10-10
Even-Time Sampling	10-11
Velocity Bias	10-11
Using the Even-Time Sampling Feature	10-12
11 Outputting Analog Data	11-1
12 Using RMR (Shaft Encoder or OPR)	12-1
Degrees Per Cycle	12-2
<u>3</u> 60	12-2
<u>7</u> 20	12-2
Direction	12-2
CCLW	12-2
CLW	12-2
Encoder Parameters	12-2
Mode	12-2
RMR Off	12-3
Once Per Rev.	12-3
Shaft Encoder x2	12-3
4x Shaft Encoder	12-3
Tolerance (Degree)	12-3
Pulses Per Revolution	12-3
Disable Inhibit Windows	12-3
Reset Time Stamp at OPR	12-4
Windows	12-4
RMR Windows Display Graphic	12-4
Modifying RMR Windows	12-4
Auto	12-4
Automatic RMR Window Generation Parameters	12-4
<u>N</u> umber of Windows	12-5
S <u>i</u> ze (degrees)	12-5
<u>O</u> ffset (degrees)	12-5
A <u>b</u> s Offset (degrees)	12-5
Windows	12-5
Selected	12-6
Max. Angle	12-6
Min. Angle	12-6
Post Processing	12-6
Apply	12-6

13 Setting Up and Using a Traverse	13-1
Setting the Traverse Parameters.....	13-1
Manual	13-2
Manual Setup.....	13-2
Communication Setup.....	13-4
Axis Setup.....	13-5
Auto	13-6
Auto Setup	13-7
Matrix	13-7
Parameter Description.....	13-8
Editing Commands.....	13-9
Creating a Simple Traverse Position List.....	13-9
14 Using the Burst Monitor	14-1
15 Exporting Data in ASCII Format	15-1
Export Format.....	15-2
Export Headings (first row).....	15-2
Export to 1 File	15-2
Apply Current Settings to All Runs.....	15-3
16 Matrix Transformation	16-1
Matrix Transformation Page	16-1
What is Transformation Matrix.....	16-1
Examples of Projection Matrix	16-1
Case 1. Three-Component Measurement Using Two Probes in the Same Plane	16-1
Case 2. Three-Component Measurement Using Two Probes not in the Same Plane	16-3
Case 3. Three-Component Measurement Using One 5-Beam Probe.....	16-5
Case 4. Two-Component Measurement Using One Probe.....	16-6
Case 5. Two-Component Near-Wall Measurement Using a Probe with Prism.....	16-7
Set Up the Transformation Matrix	16-8

Appendixes

A Laser Doppler Velocimetry (LDV) Technology	A-1
Components of an LDV System	A-2
Optimizing LDV Measurements	A-3
Laser Source	A-3
Doppler Frequency Measurement.....	A-3
Fringe Spacing	A-4
Measurement Volume Dimensions	A-4
Doppler Signal	A-5

LDV Signal Characteristics.....	A-6
Variation of Scattered Light Intensity	A-7
Typical Frequency versus Velocity Curves	A-8
Frequency Shifting	A-9
Acousto-Optic (Bragg) Cell.....	A-11
Signal Processors	A-11
Signal Processors Requirements	A-12
Types of Signal Processors.....	A-12
Components of Digital Signal Processors	A-13
Burst Detector.....	A-14
Low-Pass Filter	A-14
A/D Converter.....	A-14
Digital Signal Analyzer.....	A-14
Example Fourier Transforms.....	A-14
Velocity Bias	A-15
Noise in Laser Doppler Velocimetry	A-16
Particle Requirements for LDV	A-17
Particle Lag	A-18
Light Scattering.....	A-19
Number Concentration.....	A-19
Various Particle Generating Techniques	A-20
B Technical Paper	B-2

Figures

1 Typical Warning Labels	vii
2 Location of Warning Labels on Transmitter/Transceiver	vii
3 Location of Printed Warning Label on fiberlight.....	viii
4 Location of Printed Warning Label on PDM	ix
1-1 Create Project Directory Dialog	1-2
1-2 Manage Experiments and Runs Screen.....	1-3
1-3 Open Current Project Directory Dialog.....	1-4
2-1 Light Scattered by a Particle Passing Through the LDV Measurement Volume	2-2
2-2 Run Settings Screen	2-4
2-3 Optical Setup Page Screen.....	2-6
2-4 Hardware Status Screen	2-10
2-5 Processor/Matrix Screen	2-11
2-6 LDV Controls Menu	2-12
2-7 Example of a Good Frequency Histogram Taken with a Bandpass Filter Range of 1–10 MHz.....	2-15
2-8 Example of a Cut-Off Frequency Histogram Taken with a Bandpass Filter Range of 1–10 MHz.....	2-16
3-1 Run Settings Screen	3-4

3-2	Optical Setup Page Screen	3-5
3-3	Processor/Matrix Screen	3-6
3-4	Receiver Calibration Screen	3-7
3-5	Diameter Measurement Screen	3-8
3-6	Screen Capture Screen	3-9
3-7	Diameter/Channel 1 Velocity Control Menu	3-11
3-8	Mean Diameter as a Function of PMT Voltage	3-12
3-9	Data Rate as a Function of PMT Voltage	3-12
3-10	System Graph: Intensity Validation	3-13
3-11	Diameter Difference Screen Showing Differences Between Two Independent Measurements of Particle Diameter	3-14
3-12	Calibration Diode Setup Page After Taking Calibration Data	3-16
3-13	Typical Phase AB, Phase AC Graph After Capturing Calibration Diode Data	3-17
3-14	Calibration Diode Setup Page After Copying the Mean Phase Values	3-18
4-1	Capture Run Button on the Main Tool Bar	4-1
4-2	Settings to Utilize Intensity Validation and Probe Volume Correction	4-2
4-3	Warning Message Pertaining to Auto-Intensity Option	4-3
4-4	Playback Button on the Main Tool Bar	4-4
4-5	Velocity Statistics	4-5
4-6	Diameter Statistics	4-6
4-7	Measurement Volume Geometry	4-7
4-8	Volume Distribution Statistics	4-8
4-9	Various Size Distributions	4-11
4-10	Diameter Distribution and Fit: Log Normal Screen	4-14
4-11	Volume Distribution and Fit: Rosin Rammler Screen	4-14
4-12	Volume Distribution and Fit: Nukiyama-Tanasawa Screen with Too Many Bins	4-15
4-13	Volume Distribution and Fit: Nukiyama-Tanasawa Screen going from 0.1 $\mu\text{m}/\text{bin}$ to 1.0 $\mu\text{m}/\text{bin}$	4-16
5-1	Main Dialog Box for Selecting the Optical Layout	5-2
5-2	Optical Properties of Common Particle Materials	5-2
5-3	Scattering Domains Covering a Wide Range of Relative Refractive Indices and Off-Axis Angles	5-3
5-4	Feasible Scattering Modes for Various Domains, Attenuation Levels and Polarization	5-5
5-5	Error Message Pertaining to Inconsistent Entries for Auto Slope	5-7
6-1	Graph Designer Button	6-2
6-2	Graph Designer Screen	6-3
6-3	Edit Histogram Data Sets Screen	6-4
6-4	Text Parameters Dialog	6-5
6-5	Horizontal Axis Dialog	6-6
6-6	Axis Labels Dialog	6-6

6-7	Bar Graph Parameters Screen	6-7
6-8	Plot Parameters Screen	6-8
6-9	Graph Parameters Screen	6-8
6-10	Diameter Histogram Screen with Information Box	6-9
6-11	Graph Data	6-10
7-1	Statistics Selection Menu.....	7-1
7-2	Velocity Statistics Window	7-2
7-3	Diameter Statistics Window	7-2
7-4	Volume Distribution Statistics Window.....	7-3
7-5	Velocity and Size Subrange Statistics Window	7-3
7-6	External Input Subrange Statistics Window.....	7-4
7-7	Transformed Velocity Statistics Window	7-4
7-8	Customizing a Statistics Window	7-5
7-9	Statistics Output Options Window.....	7-6
7-10	Statistics Summary Report #1	7-7
7-11	Statistics Summary Report #2	7-8
7-12	Statistics Summary Report #3	7-8
7-13	Statistics Designer Button	7-9
7-14	Statistics Designer Screen	7-10
7-15	Example Custom Statistics Windows	7-10
8-1	External Input Screen.....	8-1
9-1	Power Spectrum/Correlation Screen.....	9-1
9-2	Processor/Matrix Screen	9-2
10-1	Subrange Input Menu.....	10-3
10-2	Diameter and Velocity Window for Subrange Example	10-4
10-3	FLowsizer Window for Lower Velocity Subrange	10-5
10-4	FLowsizer Window for Upper Velocity Subrange.....	10-6
10-5	Coincidence Window Setup.....	10-8
10-6	Examples of Software Coincidence Checking	10-9
10-7	Software Coincidence Button.....	10-9
10-8	Velocity Bias.....	10-12
11-1	Window for Selecting what Analog Signal to Output.....	11-1
12-1	RMR Screen.....	12-1
12-2	Automatic RMR Window Generation	12-5
13-1	Traverse Manager Screen.....	13-2
13-2	Communication Setup Dialog Screen.....	13-4
13-3	Axis Setup Dialog Screen	13-5
13-4	Auto Dialog Screen	13-6
13-5	Matrix Dialog Screen	13-8
13-6	Auto Fill-Column Screen.....	13-9
14-1	Burst Monitor Window.....	14-2
15-1	Export Data Dialog Box	15-1
16-1	Three-Component Velocity Measurement Using Two Probes in the Same Plane	16-2

16-2 Three-Component Velocity Measurement Using Two Probes not in the Same Plane	16-4
16-3 Three-Component Velocity Measurement Using a 5-Beam Probe.....	16-6
16-4 Two-Component Velocity Measurement Using One Probe.....	16-7
16-5 Schematic Drawing of Two-Component Near-Wall Velocity Measurement using a Probe with Prism.....	16-8
16-6 3-D Matrix Transformation Setup	16-9
16-7 3-D Matrix Transformation Test.....	16-10
A-1 LDV Technique.....	A-1
A-2 Dual-Beam Laser Anemometer	A-2
A-3 Fringe Descriptions	A-4
A-4 Measurement Volume Dimensions	A-5
A-5 Doppler Signal.....	A-6
A-6 Signal Characteristics Along the Measurement Volume	A-7
A-7 Scattered Light Intensity Variation	A-8
A-8 Typical Frequency versus Velocity Curves	A-9
A-9 Frequency Shifting	A-10
A-10 Acousto-Optic (Bragg) Cell.....	A-11
A-11 Example Fourier Transforms	A-15
A-12 Velocity Bias.....	A-15

Tables

2-1 Beam Separation Values for TSI Fiberoptic Probes.....	2-7
2-2 Beam Diameter Values for TSI Fiberoptic Probes	2-7
A-1 Sedimentation and Relaxation Time of Unit Density Sphere	A-19

About This Manual

Introduction

The purpose of this manual is to give step-by-step instructions for proper operation of a LDV or PDPA system. Primary focus of this manual is on the FLOWSIZER™ software package.

Please consult the LDV/PDPA System Installation Manual (P/N 1990024) for step-by-step installation and setup instructions. The TM/TR Series Fiberoptic Probe Manual (P/N 1990021) gives complete instructions on setup, care, and maintenance of your fiberoptic probe. The Model FSA 3500/4000 Signal Processor, Model PDM 1000 Photodetector Module LDV/PDPA System Manual (P/N 1990013) presents a detailed description and specifications of the associated LDV/PDPA electronics.



I m p o r t a n t
Before turning the FSA on, make sure all connections on the back of the FSA and PDM are secure. All cables should be sufficiently tightened. Failure to secure the connections can damage the PMT voltage supply.

Safety Labels

This section acquaints you with the advisory and identification labels on the instrument and used in this manual to reinforce the safety features built into the design of the instrument.

Caution



C a u t i o n
Caution means <i>be careful</i> . It means if you do not follow the procedures prescribed in this manual you may do something that might result in equipment damage, or you might have to take something apart and start over again. It also indicates that important information about the operation and maintenance of this instrument is included.

Warning



W A R N I N G

Warning means that unsafe use of the instrument could result in serious injury to you or cause irrevocable damage to the instrument. Follow the procedures prescribed in this manual to use the instrument safely.

Danger



D A N G E R

Danger means that unsafe use of the instrument could result in very serious injury or death to you. Follow the procedures prescribed in this manual to use the instrument safely.

Caution, Warning, or Danger Symbols

The following symbols may accompany cautions and warnings to indicate the nature and consequences of hazards:

	<p>Warns you that uninsulated voltage within the instrument may have sufficient magnitude to cause electric shock and/or death. Therefore, it is dangerous to make any contact with any part inside the instrument.</p>
	<p>Warns you that the instrument contains a laser and that important information about its safe operation and maintenance is included. Therefore, you should read the manual carefully to avoid any exposure to hazardous laser radiation.</p>
	<p>Warns you that the instrument is susceptible to electro-static dissipation (ESD) and ESD protection procedures should be followed to avoid damage.</p>
	<p>Indicates the connector is connected to earth ground and cabinet ground.</p>

Getting Help

To report damaged or missing parts, for service information or technical or application questions, contact:

TSI Incorporated
500 Cardigan Road
Shoreview, MN 55126 USA
Fax: (651) 490-3824
Telephone: 1-800-874-2811 (USA) or (651) 490-2811
E-mail Address: technical.service@tsi.com
Web site: service.tsi.com

Submitting Comments

TSI values your comments and suggestions on this manual. Please use the comment sheet, on the last page of this manual, to send us your opinion on the manual's usability, to suggest specific improvements, or to report any technical errors.

If the comment sheet has already been used, mail your comments on another sheet of paper to:

TSI Incorporated
500 Cardigan Road
Shoreview, MN 55126
Fax: (651) 490-3824
E-mail: fluid@tsi.com

CHAPTER 1

Preparing the Computer to Store the Data

Installing the FLOWSIZER™ Software Package

If you purchased your LDV/PDPA system computer from TSI, FLOWSIZER™ software is already installed. If you are supplying your own computer, FLOWSIZER software must be installed. A Windows® 98SE/2000/XP *Professional* Operating System is required. The preferred operating system is Windows XP *Professional* and the preferred amount of RAM is 1GB.

Locate the FLOWSIZER CD. Insert it, and if “AutoRun” does not initialize, open it and double-click the Setup.exe icon. Follow the steps in the installation wizard. Connect the FSA processor to the PC and switch the FSA on. Leaving the FLOWSIZER CD in the drive, restart the PC. You may notice a “New Hardware Found” message. If so, Windows is automatically accessing the FLOWSIZER CD and installing the FSA’s FireWire® (IEEE1394) driver. If you do not notice a “New Hardware Found” message, you will need to use the Control Panel’s “Add Hardware” Wizard. If required, browse to the CD drive, then to the FSA.INF file located in the “FSA IEEE-1394 Driver” folder. This will install the FSA’s FireWire (IEEE1394) driver.

Creating a New Structure for Data Storage

The basic storage structure for data taken with FLOWSIZER software consists of a main Project folder that contains various Experiment folders, each of which can contain many runs. Upon installation of FLOWSIZER, a default Project directory entitled *TSI Data* and a default experiment entitled *Default Experiment* will be created. There will also be several runs in the default experiment folder,

®Windows is a registered trademark of Microsoft Corporation in the United States and other countries.

®FireWire is a registered trademark of Apple Computer Inc.

which can be “played back” to view some examples of previously collected data.

The first step in setting up a place to store your data is to either create a new Project folder or to select an existing one.

To create a new Project folder select **File→New Project Directory**. A dialog box like the one shown in Figure 1-1 should open.

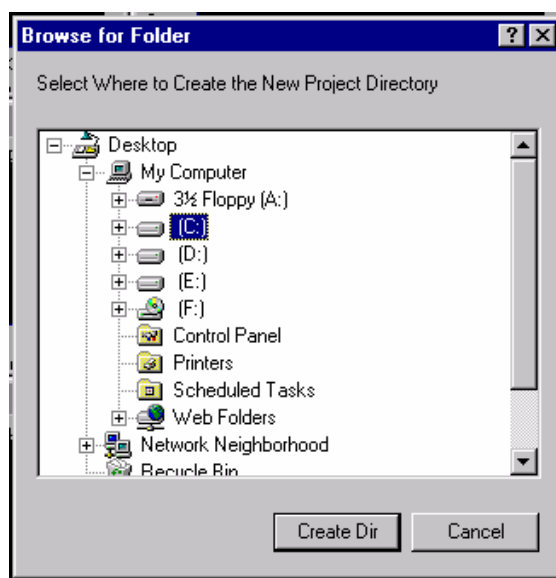


Figure 1-1
Create Project Directory Dialog

Select the target disk drive or folder the new project directory will reside in and click the **Create Dir** button. A dialog box prompting you to enter a new Project directory name will open. After entering a name for the Project folder click **OK**.

After creating a new Project directory you must create a new Experiment directory. To do this, select **File → Experiment Manager**. A dialog box similar to the one shown in Figure 1-2 will open. To create the new Experiment folder select the **New Experiment** button and then enter a desired name. (The default name will be *New Experiment*.) The name can be either a word (for example, 10 MPa) or a number (for example, 16). If you would like to use a previous run as a template for all FLOWSIZER software settings, browse to the appropriate Experiment and select (single-click) the Run you would like to clone. Press the **Copy** button. Then browse back to your new Experiment and press the **Paste** button. Select (single-click) this Run and press **Select**.

If you are not selecting a previous Run, after entering the new Experiment name, click the default Run 1 and press the **Select**

button. All settings from the most recently saved or opened run will be cloned over to the default Run1 file.

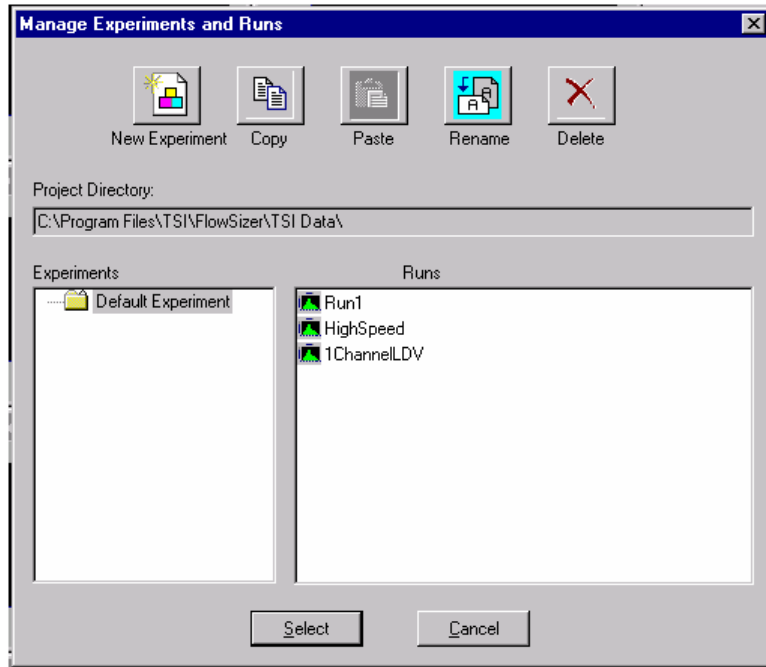


Figure 1-2
Manage Experiments and Runs Screen

Now that both a Project folder and an Experiment folder have been created the final step in setting up the data storage structure is to create a new run. To do this select **Run → New Run**. A dialog box prompting for a run name will open. Enter a name and hit the **OK** button. The data file structure is now complete and you are ready to begin taking data.

Selecting an Existing Project or Experiment Folder for Data Storage

If data is to be stored in a pre-existing Project or Experiment folder, do the following. To select a Project folder go to **File → Select Project Directory**. A dialog box like the one shown in Figure 1-3 will open. Select the folder name of an existing project and click **OK** to open.

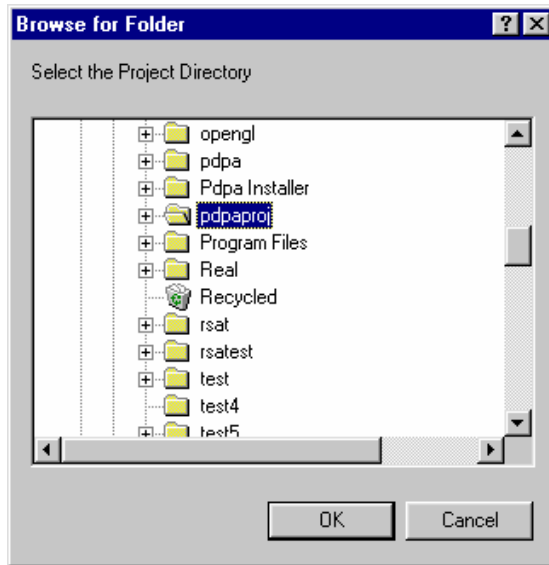


Figure 1-3
Open Current Project Directory Dialog

In order to select an existing Experiment folder, the correct Project folder, which contains the Experiment folder, to be opened must first be chosen. Then select **File → Experiment Manager**. The dialog box from Figure 1-2 will open. Highlight the Experiment folder that you wish to choose from the left window of the dialog box and hit the **Select** button. A run from the selected Experiment folder can also be chosen from the list in the right window of the dialog box. If a run is not chosen, a warning dialog box will open. You can ignore it by hitting **OK**. A run needs to be created before data can be taken in this case.

CHAPTER 2

Taking LDV Data

LDV Overview

Before getting into the details of taking LDV data with your system, a little background on the principle of LDV will be helpful. Laser Doppler Velocimeter measures the velocity of small particles that are moving in the fluid of interest. Assuming the particles are small, the velocity of these particles can be assumed to be the velocity of the fluid itself. The physical principle used to measure the particle velocities is the scattering of light by the particles. The intersection of the two laser beams (for each component of velocity) results in a fringe pattern—a series of light and dark fringes. As a particle moves through the measuring volume, it scatters light when it crosses a bright fringe, and scatters no light as it passes a dark fringe. This results in a fluctuating pattern of scattered light intensity with a frequency proportional to the particle velocity. Since the distance between fringes and the time for the particle to go from one fringe to the next (inverse of signal frequency) are known, the measured signal frequency can be converted to velocity. The scattered light is collected by optics and converted to electrical signals by Photomultiplier Tubes (PMTs). The frequency of the signal (also known as Doppler frequency f_D) is measured and then the velocity u is calculated by multiplying the frequency by the fringe spacing δ_f , i.e.

$$u = \delta_f f_D.$$

If the two laser beams that interfere are of exactly the same frequency, the fringes will be stationary in the measuring volume. One problem with this is that particles with a certain velocity moving one way across the fringes may have exactly the same frequency as particles (having the same magnitude of velocity) moving in the opposite direction. Thus there would be no way to determine if particles were moving in a positive or negative flow direction. To eliminate this problem in LDV systems, one of the two laser beams is frequency shifted by a Bragg cell by 40 MHz. This results in fringes that are essentially moving at a rate of 40 MHz in the measuring volume. Particles crossing the measurement volume will now have a frequency either above or below 40 MHz, depending on their direction. Thus the frequency of light scattered by a

particle will be 40 MHz plus or minus an amount due to its velocity. If a particle is moving against the fringes, it will have a frequency of 40 MHz plus the Doppler frequency (the frequency due to the particle velocity) and if a particle is moving with the fringes it will have a frequency of 40 MHz minus the Doppler frequency. Frequency shifting also allows you to measure velocities near zero, where without the shifting there would be no oscillating pattern of light scattered from the particle at all.

Another factor in the light scattering pattern is due to the Gaussian nature of the intensity laser beams. This results in bright fringes that have more intensity as you move towards the center of the ellipsoidal measuring volume. Thus a particle crossing through the measuring volume will result in a light scattering pattern similar to the one shown in Figure 2-1.

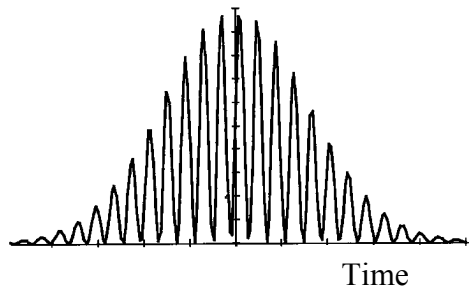


Figure 2-1
Light Scattered by a Particle Passing Through the LDV Measurement Volume

The scattered light is collected and transmitted to the PMTs through optical fibers. The PMTs generate electrical signals representing the incoming optical signals. The output of the PMT is first high-pass filtered to remove the low frequency portion of the signal due to the Gaussian beams. This low frequency envelope is called the pedestal. After removing the pedestal, the signal (consisting of the $40 \text{ MHz} \pm$ the Doppler shift) is mixed with another signal whose frequency can range from 0–40 MHz. The difference (low frequency portion of the mixed signal) signal is then passed through to a selectable series of bandpass filters. This process of mixing is often called downmixing. It allows you to select the optimum frequency shift to resolve reversing and zero flow situations. In cases where the flow is not reversing, downmixing by 40 MHz may be appropriate as it essentially removes the 40 MHz that was added by frequency shifting.

After downmixing, the signals are passed through a user selectable series of bandpass filters. Passing the signals through the bandpass filters helps improve the Signal to Noise Ratio (SNR) of the signals by eliminating noise. The signal frequencies are then measured using the signal processor.

Note: The following procedure will set up the system for general-purpose data collection, but may not be exactly appropriate for specific applications.

Direction of Fringe Motion Relative to Particle Motion for Velocity Measurements

The positive velocity direction for a given velocity component will be such that the particles cross the measurement volume against the motion of the fringes. To determine what direction the fringes are moving in the measuring volume, consider looking at the measuring volume from the vantage point of the transmitter. Determine which beam is the shifted beam and which is the unshifted for a particular pair of beams. (To do this, look on the fiberlight and close the shutter on either the shifted or unshifted beam, and see which one shuts off.) The fringe motion will be from the shifted to the unshifted beam.

Run Setup → Run Settings

After setting up and connecting the hardware and creating or selecting a Run to store your data the following will provide an overview of how to take data with the system. The first set of software settings to be checked is found by selecting **Run → Run Setup**. Then choose the **Run Settings** tab. A dialog box similar to the one shown in Figure 2-2 should now be open. The following parameters need to be selected.

1. *Maximum Particle Measurement Attempts*—This is the maximum total number of particle attempts to take in a run. This refers to the number of valid bursts detected, and not to the number of velocity or diameter measurements obtained from those bursts. In random (verified) mode, data acquisition will stop when the total samples from all active channels reaches this value. In hardware coincidence mode, data acquisition will stop when this number of samples is acquired from each channel enabled. In software coincidence mode, data acquisition will stop when this number of samples is acquired from each enabled channel. However, playback with different coincidence gate scale and/or coincidence interval settings will yield a different number of total samples captures. The reason for this is that with software coincidence, all samples are collected and saved—the non-coincident ones are simply not displayed or allowed to enter any statistics.

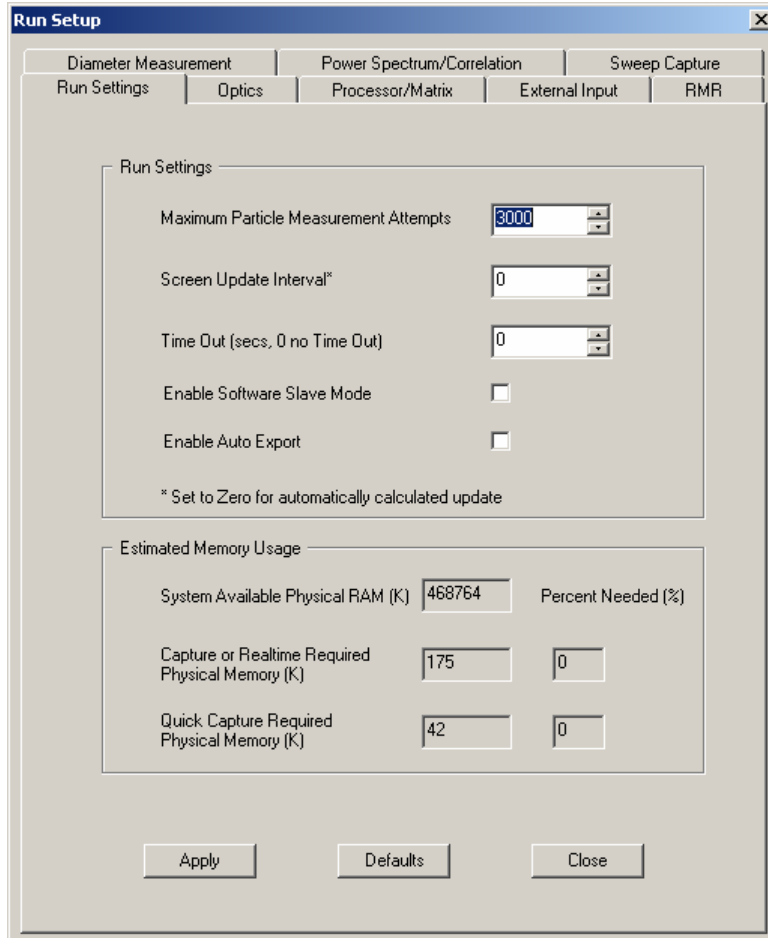


Figure 2-2
Run Settings Screen

2. *Screen Update Intervals*—The screen update size sets how often the screen is updated. During data acquisition, a value of zero shuts off this feature. A **Screen Update Interval** value of 1000 means the screen is updated after 1000 particle attempts are completed. It is suggested to use 0, which means the software will determine the screen update speed. This is especially useful in **Capture Run**, which captures data directly.
3. *Time Out*—This value is the length of time the run will stay open with no data being detected. A value of 0 means the run will not stop due to a data rate of zero.
4. *Enable Software Slave Mode*—By selecting this option an external computer could be used to control the data-taking computer. The control can be done through RS 232.
5. *Enable Auto Export*—This option instructs the FLOWSizer software to automatically do an ASCII Export of currently selected ASCII export values, each time a run is captured and saved.

Hints, Suggestions, and Comments

1. The *Maximum Particle Measurement Attempts* will be limited by the amount of memory that your computer contains. The recommended amount of memory is currently 1GB.
2. Unless there is a specific reason, set the *Screen Update Interval*, *Maximum Run Time*, and *Time Out* to 0. This means that your run will only stop due to the maximum number of particle measurement attempts.
3. With a highly varying data rate, such as from a pulsed spray device, setting a Screen Update Interval of 0 may result in data overflow. It is suggested that Screen Update Interval values of 1000 to 5000 be used to prevent this.
4. When collecting data from a high data rate flow, there is a possibility that the system will get a data overflow error, which will prematurely stop the run. To improve performance in this case, set the *Screen Update Interval* to a large value, or if even this is unsuccessful, try capturing data with the **Quick Capture** mode (<F8> or the button on the Main Menu box). In this mode, the system will capture data without updating the screen at all. After capture is complete, the data can then be saved and replayed without having any data overflow problems.

Run Setup → Optics

After selecting values for the **Run Settings** tab, click the **Optics** tab from the same dialog box. The dialog box should now look like the one shown in Figure 2-3.

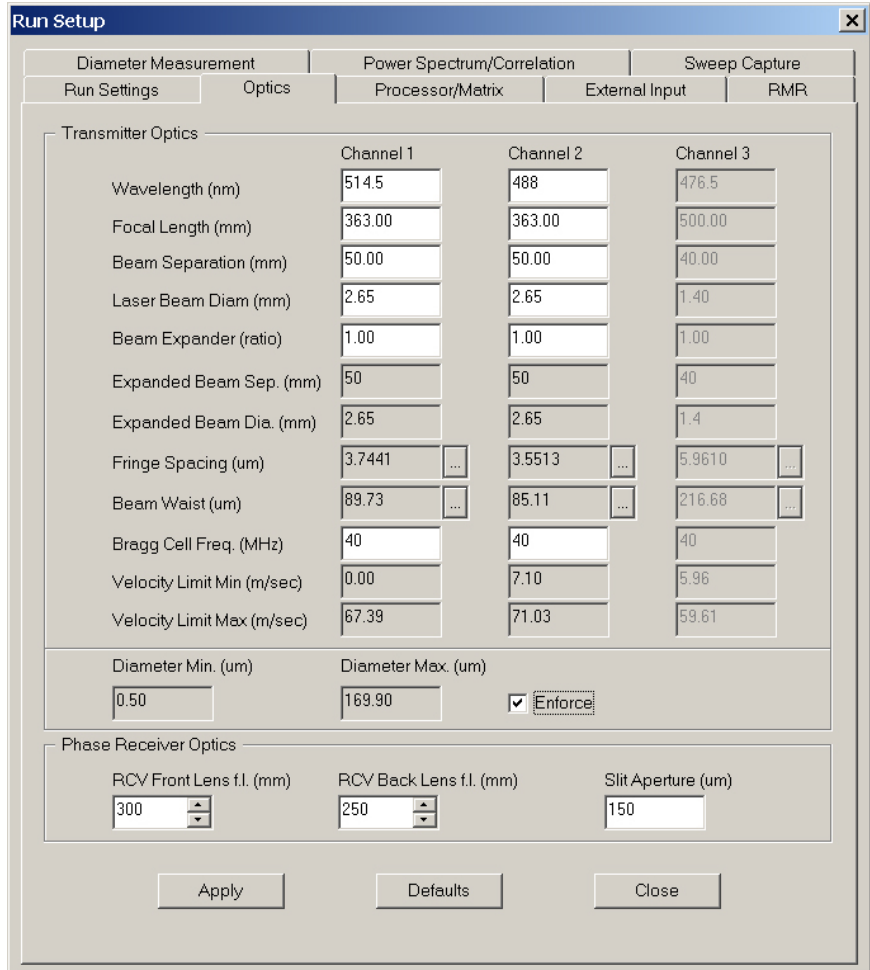


Figure 2-3
Optical Setup Page Screen

The following parameters need to be set correctly in order to take accurate velocity data.

1. **Wavelength**—Wavelength of the laser light for each channel (velocity component). This is laser dependent and should not be modified unless the laser is changed. Argon Ion laser wavelengths are 514.5 nm (green), 488.0 nm (blue), and 476.5 nm (violet).
2. **Focal Length**—Focal length of the front lens in the fiberoptic transmitter or transceiver probe usually found on the case of the lens. This parameter must be updated if the lens is changed.

3. *Beam Separation*—Distance between the two laser beams of one color from the probe, measured prior to the beam expander and the transmitter lens. See the table below for the correct value to use for your probe. If a beam expander is present, do *not* change the value—the software will account for the effect of the beam expander through the *Beam Expander* ratio.

Table 2-1
Beam Separation Values for TSI Fiberoptic Probes

Probe Series	Beam Separation
TR 10 Series 15 mm Diameter	7.5 mm
TR 20 Series 25 mm Diameter	15 mm
TM 50 Series 70 mm Diameter	20 mm
TR 60 Series 83 mm Diameter	50 mm
TR 360 Series 5 Beam Probe	25 mm (Green, Violet) 50 mm (Blue)

4. *Laser Beam Diam*—Gaussian diameter of the laser beam before the focusing lens and before the beam expander, if any. See the table below for the correct value to use for your probe. If a beam expander is present, do not change the value—the software will account for the effect of the beam expander through the *Beam Expander* ratio.

Table 2-2
Beam Diameter Values for TSI Fiberoptic Probes

Probe Series	Beam Diameter
TR 10 Series 15 mm Diameter	0.5 mm
TR 20 Series 25 mm Diameter	1.0 mm
TM 50 Series 70 mm Diameter	1.77 mm
TR 60 Series 83 mm Diameter	2.65 mm
TR 360 Series 5 Beam Probe	1.8 mm (All Beams)

5. *Beam Expander*—Expansion or contraction ratio of a beam expander or contractor. If an expander or contractor is not present, this field is set to **1**. The Model XPD50-I has an expansion ratio of 2.00 when installed as a beam expander, and an expansion ratio of 0.50 when installed as a beam contractor. The Model XPD60 has a fixed expansion ratio of 2.60. If a beam expander is present, do **not** change the *Laser Beam Diam* or

Beam Separation values—the software will account for the differences in these values through the *Beam Expander* ratio.

6. *Fringe Spacing*—Spacing between fringes in the measurement volume, dependent on other parameters. The fringe spacing (δ_f) is:

$$\delta_f = \frac{\lambda}{2 \sin(\kappa)}$$

λ = wavelength of laser

2κ = angle between beams

The *Fringe Spacing* will be automatically calculated by the software based on the previously entered optical parameters. You can also manually select the *Fringe Spacing* by clicking the “...” button (next to the computed fringe spacing value), checking the **Manual Input** checkbox, and then entering a value for the fringe spacing.

Note: *Once the “Manual Input” checkbox is enabled, future runs created from this run will also have this checkbox enabled. Remember this if optics are subsequently changed, you will again need to manually update the fringe spacing.*

7. *Bragg Cell Freq*—Amount of optical frequency shifting. For typical operation with fringe motion against the positive direction, this value is set to 40 MHz. For special operation with fringe motion in the positive direction, this value is set to -40 MHz.
8. The *Diameter Min* and *Diameter Max* limits are the theoretical measurement limits calculated by the system, with the standard assumption of a linear phase to diameter relationship. Uncheck the *Enforce* checkbox to disable adherence to these limits. Be aware that the smallest diameter droplets will have lower measurement reliability if this is done.
9. *Enforce*—Enforce the diameter units so diameters measured outside the range will be ignored.

Run Setup → Processor/Matrix

After setting the parameters from the **Optics** tab, click the **Processor/Matrix** tab from the same dialog box. The dialog box should now look like the one shown in Figure 2-5.

Check to see that the following parameters are set correctly:

1. *Channel Enable*—Enable the correct number of channels by checking or unchecking each box. Though not necessary, it is good practice to disable channels not currently being used.

- 2. High-Pass Filter**—Selects the high-pass filter which removes the signal pedestal (due to the Gaussian laser beams) from the Doppler signal. For most applications, choose 20 MHz. This filtering is performed on the signal in the PDM before downmixing. Use the 5 MHz filter for high velocity reversing flows because the raw PMT signal can drop below 20 MHz and be attenuated. Use the 20 MHz filter for very short transit time signals because the 5 MHz may not remove the entire pedestal.
- 3. Single Measurement/Burst**—For almost all applications, enable this check box. This will allow the processor to only take one valid measurement per particle, no matter the length of its gate time. Disable the check box only to arbitrarily break up continuous sinewave type signals into multiple bursts.
- 4. Burst Inhibit Connector**—Data collection for each channel can be inhibited using the burst inhibit connector on the back of the FSA. Bursts are inhibited when a logic high (+5V) is applied to this connector. These check boxes control which channels are affected by the signal at the connector. For example, checking the channel 2 box, but not the channel 1 and 3 boxes, would cause only channel 2 to be inhibited when a logic high is applied at the connector. When the connector is driven low, or nothing is connected to it, these boxes have no effect because nothing is being inhibited. See also the FSA hardware manual.
- 5. Enable Bragg Cell**—Checking this box enables the 40 MHz signal from the FSA to the fiberlight. It must be checked during normal operation. It would only be unchecked during some debugging situations to disable the shifted beams.

Items 6 through 9 are not selected in the example shown (Figure 2-5)

- 6. Enable Sync Pulse Input**—Check this box if you are using the sync pulse BNC connector on the back of the FSA. A rising logic level (+5V) applied to this connector will reset the time stamp during data collection (see FSA hardware manual). If this is being done, this box must be checked so the FLOWSizer software knows the time stamp will be resetting.
- 7. Enable Intensity Validation on Velocity**—Intensity validation is normally only used with phase Doppler systems. The height (or intensity) of the pedestal of each channel 1A particle is measured and compared to its size calculated by the phase Doppler method. This box does not have to be checked for phase Doppler measurements. However, intensity measurements can also be used with velocity (LDV) measurements, but only if you have a phase Doppler system, or if you ordered the intensity board as a special option. The intensity board is in the PDM and measures the pedestal

heights of channel 1A only. To use the intensity information with velocity data only, check this box. Select the range of intensities you wish to accept/exclude under the **Subrange (Under/Over)** tab, minimum and maximum intensity. Then enable this sub-ranging by selecting **Software Subrange** and **Software Coincidence**.

8. *Enable Gate-time Weighting*—Check this if you need to get velocity-bias corrected statistics. Gate time (transit time) is used as the weighting function. Velocity bias is caused by the fact that more of the faster particles go through the measuring volume per second. Therefore, the sampling of velocity is not representative of the true flow, but is biased with the faster ones. This causes the measured velocity mean to be higher than the actual, especially with a broad velocity distribution. Checking this box causes each velocity data point to be normalized or weighted with its own gate time. Slower particles have longer gate times and, therefore, more weight. With this weighting, the calculated mean velocity is closer to the actual mean. An even better method to remove velocity bias is to use even-time sampling, see Chapter 10 for more details.
9. *Hardware Coincidence*—Check this if you wish to enable hardware coincidence. This will require overlap of burst gates of active channels, in order for the data to be considered coincident. Note that hardware coincidence is only applicable to 2 and 3 channel systems. Non-Coincident data is discarded, which reduces file storage size, but remember that unlike software coincidence, there is no way to recover non-coincident data at a later time. Refer to Chapter 10 for more details on software coincidence.

When Hardware Coincidence is enabled, the Coincidence Data Rate will be enabled on the Hardware Status Screen (see Figure 2-4).

Hardware Status		
	Data Rate (Hz)	Burst Eff. (%)
Channel 1	0	0
Channel 2	0	0
Channel 3	0	0
Coincidence Data Rate		0

Figure 2-4
Hardware Status Screen

The next group of parameters allows selection of the value to send out the FSA processor Analog Out connector. This is a 0 to 10V signal, updated for every burst in the selected channel. The signal will remain at 0.0V until the first valid sample arrives. The user may connect a load up to 30mA on this line. For more details on

the frequency and phase to voltage conversion values, please see the Model FSA 3500/4000 Signal Processor, Model PDM 1000 Photodetector Module LDV/PDPA System Manual (P/N 1990013).

The final group of parameters is the 3D Transformation Matrix setup, for conversion of non-orthogonal or rotated coordinates to orthogonal coordinates. Please turn to Chapter 16 for more details on the Transformation Matrix values.

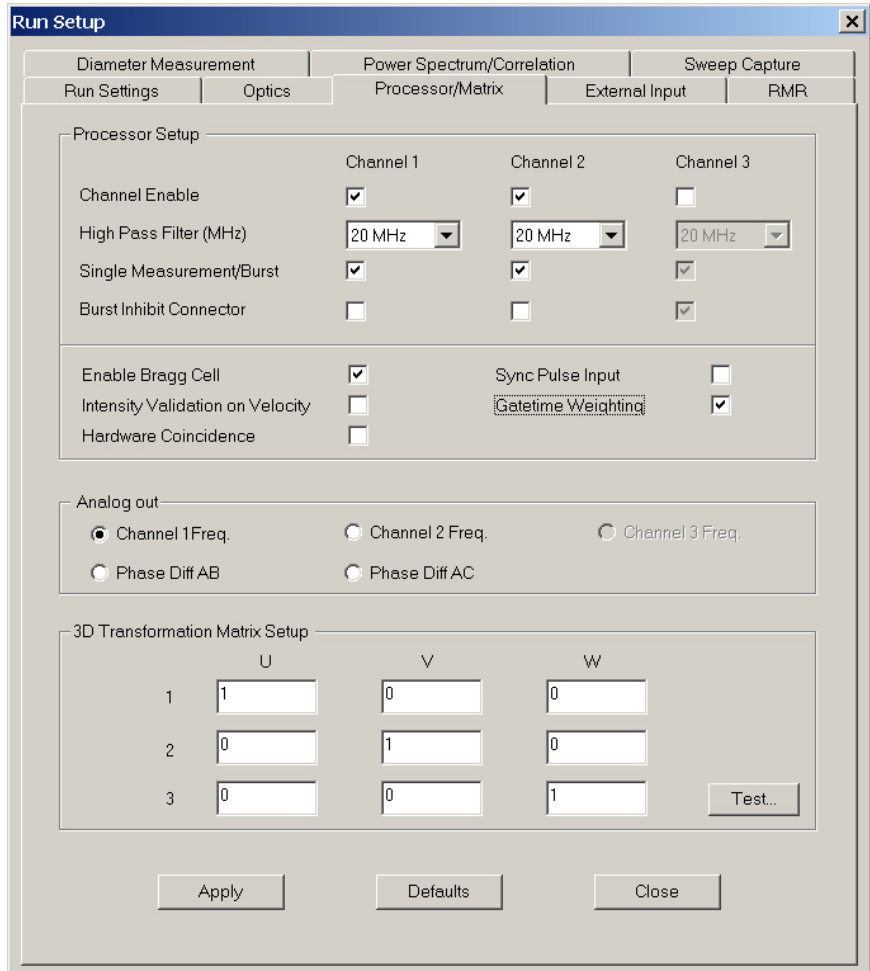


Figure 2-5
Processor/Matrix Screen

LDV Controls

The remaining set of controls that may need to be set is found on the main software window in the upper-right corner, the **LDV Controls** tab (see Figure 2-6). This figure shows the system setup to take two channels of velocity data.

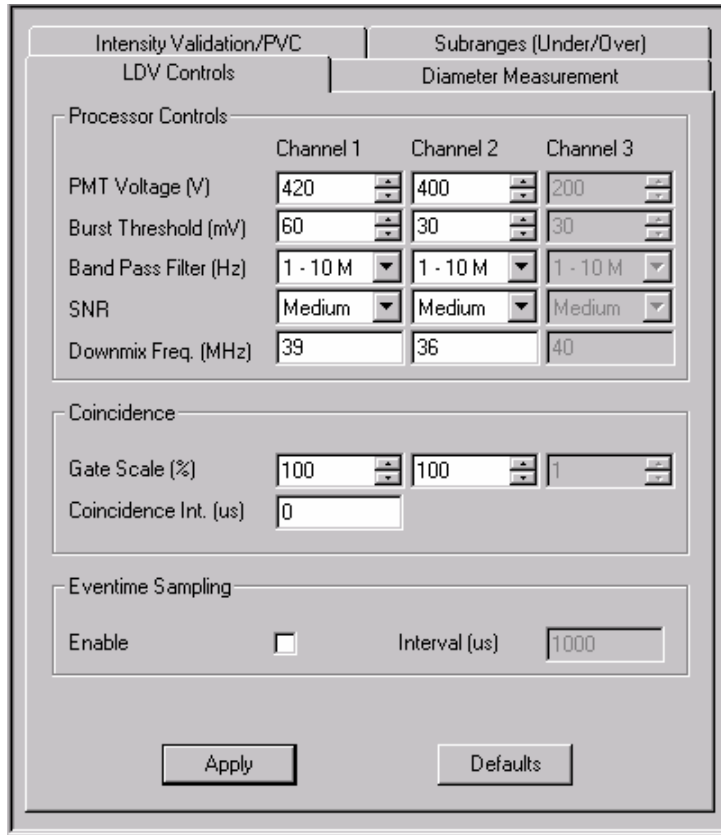


Figure 2-6
LDV Controls Menu

The selection of the parameters on the LDV Controls Menu is probably the most important for getting good velocity measurements. The process is often times slightly iterative among the various parameters. Following is a general procedure that will help you acquire good data in many applications. Keep in mind you will have to select parameters independently for each channel of velocity, you wish to measure.

Downmixing

The fiberlight's Bragg cell adds 40 MHz to the shifted beams, which causes the fringes for each color to move at 40 MHz. This causes 40 MHz to be added to the Doppler frequency of each burst. A particle, or solid surface, sitting stationary in the measuring volume will generate a 40 MHz signal. This allows flow reversals to be determined and also enables a range of frequencies to be compressed into a 1:10 range. Some or all of this 40 MHz can be removed by the downmixing done in the FSA. Downmixing subtracts

the downmix frequency from the input signal. The downmix frequency is entered in the **Downmix Freq. (MHZ)** box. Entering 40 MHz will eliminate all the 40 MHz Bragg Cell Shift, so only the Doppler frequency is left, which is proportional only to the particle velocity. Entering 39 means 39 MHz is subtracted from the 40 MHz Bragg cell shift, leaving 1 MHz still added onto the Doppler frequency. This will allow flow reversals up to 1 MHz to be measured. With a 5 μm fringe spacing, this would correspond to flow reversals up to 5 m/s. Entering 36 means 36 MHz is subtracted from the 40 MHz Bragg cell shift, leaving 4 MHz still added onto the Doppler frequency. This would correspond to 20 m/s (assuming 5 μm fringe spacing), in terms of the maximum flow reversal velocity. Entering 0 means downmixing is bypassed so the entire 40 MHz is still left on the signal.

When your Doppler frequency is 20 MHz or lower, you should always use downmixing. This allows you to use the narrowest bandpass filter range on the signal after downmixing to remove the most possible noise. A common starting point is to use a 36 MHz downmix frequency, and the 1–10 MHz bandpass filter setting.

When the Doppler frequency is above 40 MHz you should bypass downmixing. This is because downmixing produces two frequency components, the sum and difference between the input signal and the downmix frequency. The bandpass filters remove the sum term, leaving the difference term, which is what we want. When the difference term is near or above 40 MHz, the sum term cannot be fully filtered out resulting in a distorted signal that may give erroneous frequency readings. A Doppler frequency which is between 20 and 40 MHz is in a transition region where downmixing or bypassing downmixing both may work.

For this reason, signals being downmixed pass through an 80 MHz low-pass filter. This prevents downmixing from being used for Doppler frequencies over 40 MHz. When downmixing is bypassed, this 80 MHz low-pass filter is also bypassed.

Leaving some or all of the 40 MHz on the signal is necessary when your flow is going both directions through the measuring volume. This way the flow direction can be determined, and the FLOWSIZER software then calculates the actual velocity since it knows the amount of frequency that was left on. Even without reversing flows, if your range of Doppler frequencies doesn't fit within one of the bandpass filter ranges, you must downmix by less than 40 and leave some shift on the signals. A third reason for leaving some shift on is if some particles are traveling nearly parallel to the fringes in the measuring volume. In this case they wouldn't cross many fringes and not generate enough frequency cycles to be detectable by the processor. Leaving shift on adds cycles to each

burst, making them easily distinguishable from noise. Other than for these reasons, you should generally not leave shift on because adding many cycles to a burst begins to put it out of the region where the processor was optimized, i.e., short bursts in the neighborhood of 5–50 cycles each.

Band Pass Filter

Normally the first parameter to select is the *Band Pass Filter* setting. If you know the range of frequencies that will be in the flow, you can select the setting directly. Remember that the signal frequency (without frequency shift) is equal to the particle velocity divided by the fringe spacing. To estimate the frequency of the signal input to the signal processor, add the effective frequency shift (equal to 40 MHz minus the downmix frequency). If you are unsure, select the 1–10 MHz setting (also use a *PMT Voltage* of 400, a *Burst Threshold* of 30, an *SNR* of medium, and a *Downmix Freq.* of 36). Then check the *Data Rate* found on the *Hardware Status* portion of the main software page. If the data rate is zero, try a different filter range until a non-zero data rate is detected.

At this point, you can view the data by capturing in real-time mode. To do this, go to **Run** → **Real Time View** (or hit <F6>). Before capturing data you want to have the *Frequency Histogram* graph open for the channel that you are working with (e.g., use **Graphs** → **Frequency1 Histogram** for data on Channel 1). (See Chapter 6, “Using and Creating Graphs,” if you are unsure of how to do this.)

As data is being updated to the screen, you should see a frequency histogram appearing. You will know whether or not you have the correct bandpass filter selected depending on how the histogram looks. If the histogram count drops close to zero on both ends of the distribution within the selected bandpass filter range, you can be confident you have selected the correct filter range. Figure 2-7 is an example of a run with the correct bandpass filter selection. Figure 2-8, on the other hand, is an example of an incorrectly chosen bandpass filter range. Notice how the distribution is clipped on the upper end of the frequency distribution. In this example you should change the bandpass range to 2–20 MHz. If a distribution has a frequency range that does not fit within any of the bandpass filter ranges (for example, a frequency distribution ranging from 500 kHz to 4 MHz), you may need to increase the frequency shift (or decrease the downmix frequency) value to make the frequency distribution fit within one of the bandpass ranges. To do this you change the *Downmix Freq.* to a smaller number. The frequencies of your signals will then be increased by whatever the difference is between the number you select and 40 MHz. For example, changing

the *Downmix Freq.* to 39 MHz will increase all the frequencies by 1 MHz ($40-39=1$ MHz). In the example given previously (a frequency distribution ranging from 500 kHz to 4 MHz), changing the *Downmix Freq.* to 39 MHz will result in a frequency distribution ranging from 1.5 MHz to 5 MHz. The distribution will now fit in the 1–10 MHz bandpass filter range.

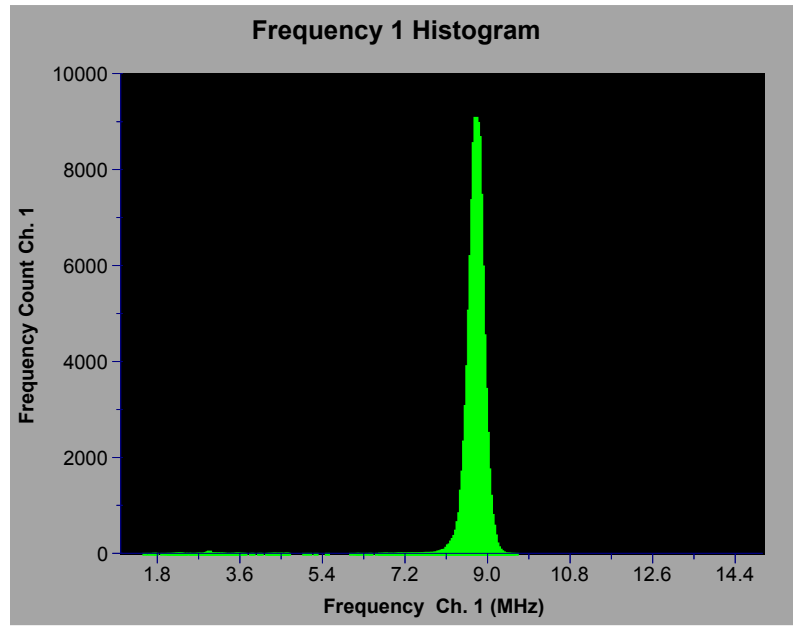


Figure 2-7

Example of a Good Frequency Histogram Taken with a Bandpass Filter Range of 1–10 MHz

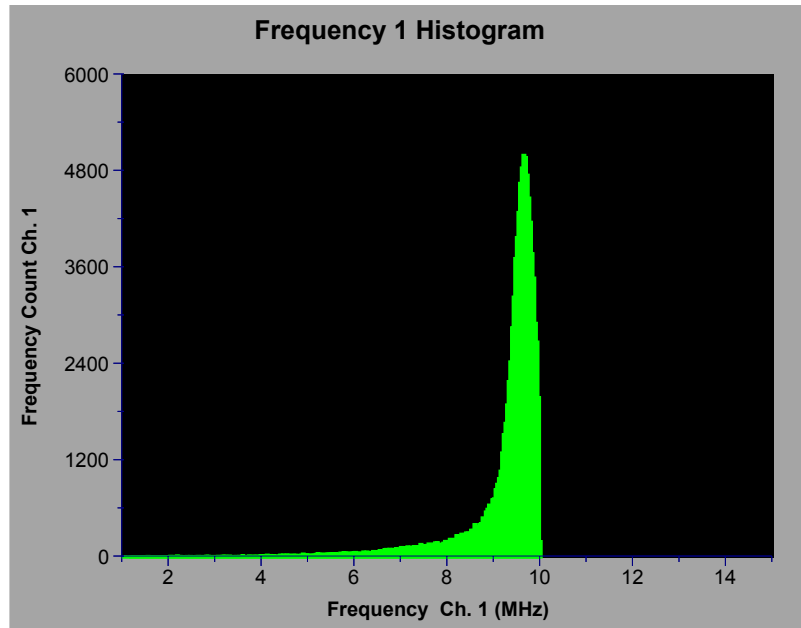


Figure 2-8

Example of a Cut-Off Frequency Histogram Taken with a Bandpass Filter Range of 1–10 MHz

After the correct *Band-Pass Filter* range has been selected you will want to optimize the *PMT Voltage*, *Burst Threshold*, and *SNR* parameters for your specific application. A discussion of important considerations follows:

PMT Voltage

This parameter sets the voltage that is applied to the PMT for each channel. Increasing the voltage increases the gain of the PMT in a roughly linear fashion. This increase in gain applies not only to the signal, but also to any associated noise. In order to choose an optimum voltage, the following considerations are important. As the voltage is increased, signals from smaller particles (which scatter less light) will be gained up enough to be detected by the processor. Thus increasing the voltage should in general increase the data rate. At a certain point, however, increasing the voltage will not provide much benefit and may actually reduce the data rate. Since the signal will generally have larger amplitude than noise, and since the electronics begin clipping a signal at a certain point, increasing the voltage beyond a certain point will simply reduce the SNR. For many applications, the optimum voltage range will fall between 350 V and 600 V.

Burst Threshold

The *Burst Threshold* is another very important variable in taking LDV data. Often times, the best way to optimize your data is to iterate between adjusting the *PMT Voltage* and the *Burst Threshold*. The *Burst Threshold* is the analog voltage level that a signal must reach before the burst gate in the processor will open. (**Note:** Burst Threshold is only one of the two requirements for opening the burst gate. The other requirement is a certain SNR-level based on a real-time Fourier transform).

In general larger particles scatter more light and thus will have higher signal amplitudes. Also, increasing the *PMT Voltage* will increase the signal amplitudes, which is why the *Burst Threshold* level cannot be adjusted without considering the *PMT Voltage*. Typical *Burst Threshold* values will range from 30 mV to 300 mV. For applications with small particles (<10 μm) the optimum will probably be 30 mV or slightly higher than that. On the other hand, with large particles an optimized value might be 100 mV or 200 mV. In situations with high background light levels, such as near wall measurements or measurements in a dense medium, Burst thresholds over 500 mV may be needed to achieve the best data rate.

The signal out BNC connector on the FSA front panel shows the signal as it is when it passes the burst threshold circuit. When the connector is attached to an oscilloscope 50 ohm input, the amplitude seen on the scope matches the burst threshold in millivolts. For example, if the burst threshold is set to 100 mV, a burst signal showing an amplitude of ± 100 mV on the scope is just at the threshold.

SNR

The *SNR* (signal-to-noise ratio) sets the validation threshold used by the FSA's burst validation subsystem, when evaluating bursts passed on from the burst detector. An *SNR* of "High" means only the best quality bursts pass validation. This results in more accurate frequency and phase data, but also a lower data rate. An *SNR* setting of "Very Low" means noisier bursts are validated, resulting in higher data rates. These noisier bursts still represent valid flow or size data, but just not as accurately. The *SNR* setting has no effect on the FSA's burst detector, but only on its burst processing validation. Because of this, choosing a higher *SNR* level will result in a decrease in the burst efficiency. The selection of *SNR* also sets a minimum number of cycles required for a burst to be

validated. Thus you would use an SNR setting of “Very Low” when measuring bursts with just a few cycles or to measure bursts of very short transit time.

Hardware Status

The hardware status window is in the lower right-hand corner of the screen. The **Data Rate (Hz)** is the number of bursts passing validation per second for each channel. In phase Doppler systems, channel 1 indicates the phase data rate. This data rate reflects the processor output and is unaffected by software settings such as subranging, coincidence, or even-time sampling.

Burst Eff (%) is percent burst efficiency. It is the ratio of burst detector triggers to valid bursts. For example, the burst detector puts out 10,000 bursts per second, each one having one burst gate and 2,500 per second were considered valid after burst processing. The data rate would be 2,500 and burst efficiency 25%. Poor SNR signals will have lower burst efficiencies.

PMT Volt Sat. will light up if the PMTs are saturated from getting too much light. These indicators mirror exactly the lights on the PDM front panel. When saturation is indicated, the PMT voltage is clamped to some value lower than that requested. During saturation only, this actual PMT voltage is shown under **Sat. Volt. (V)**. Note that the channel 1A, 1B, 1C PMTs share one common high voltage supply, but may not match in saturation because of different light levels to each PMT. When one of the three saturates, it clamps the high voltage for all three.

FSA Connection shows whether the FSA has established a communication link to the computer. It also shows the FSA model, 4000 or 3500. Connection will be automatically established when the FSA is powered on and the FireWire cable is connected between the FSA and computer.

Coincidence Data Rate displays the hardware coincidence data rate when it is enabled.

CHAPTER 3

Taking Size and Velocity Data

Note: *This section assumes that the system hardware is set up correctly, i.e., an optical layout has been chosen for sizing (see Chapter 5, “Selecting An Optical Layout for Particle Sizing”). You should also already be familiar with operating the system to take velocity data. The following procedure will help optimize the system for general applications. Difficult applications may require changes from the standard procedure and nothing can substitute for experience in using the system.*

Phase Doppler Overview

Before going into the details of taking size data, a brief overview of the phase Doppler (sizing) technique will be given. Phase Doppler measurements allow for the sizing of spherical particles (typically liquid sprays, but also some bubbles and solid spheres). Along with size information, the velocity of the particle is also obtained, so in this sense the phase Doppler technique is an extension of LDV. The size of particles that can be measured is limited, at the low end by the amount of light (which depends on particle size, laser power, and light collecting optics) that is scattered by very small particles, and is limited at the high end by the Gaussian nature of the laser beams (and the far field condition). Typical limits for common configurations might be 1 or 2 μm on the lower end and 500 μm to 1 mm on the upper end.

To explain the physical principle used to measure the size of particles, the explanation of the measuring volume consisting of a series of moving fringes will again be used. As a particle moves through the measuring volume, it “scatters these fringes” all around, including some towards the optical receiver. The frequency of the scattered light determines the velocity of the particle. Only one detector is required to get this temporal frequency of the scattered light. However, the spatial frequency (spacing between the scattered fringes at the light collecting optics) of the scattered fringes contains information about the size of the particle being

measured. In order to measure this spatial frequency a minimum of two detectors is required. The spatial frequency is measured as a phase shift between the two electrical signals resulting from the scattered light. This phase shift can then be related to particle size provided the correct optical layout is used. In TSI phase Doppler systems, three separate detectors are used. Thus, two independent measurements of size are obtained. This allows for redundancy in measuring size as well as an improved dynamic size range with high sensitivity.

One problem with measuring size (phase difference or phase shift) is to ensure that the phase shift measured by the processing electronics is only “caused” by the particle.

Because electronic circuitry can introduce its own phase shifts between two signals, it is often necessary to calibrate away the shift introduced by the electronics. This is done by measuring the phase shift from a light source with a known phase difference. Any deviation from the expected phase shift is then due to the electronics and can be calibrated away. In TSI systems a red laser diode is used as the calibration light source. By splitting the diode light into three parts we can be sure there is no phase shift in the optical signals themselves. Thus any measured phase shift must be due to electronics.

Another important sizing feature that TSI systems provide is a measurement of the scattered light intensity for each particle. Intensity measurement is useful because it helps eliminate erroneous size measurements and also provides a better characterization of the measuring volume size, which is useful in calculating certain flow properties.

Direction of Fringe Motion Relative to Receiver Orientation for Sizing Measurements

(For more information, see “Direction of Fringe Motion Relative to Particle Motion for Velocity Measurements” in Chapter 2.)

When taking size data, it is critical that the PDPA receiver be oriented properly with respect to the direction of the fringe motion. When looking in the PDPA receiver eyepiece, the arrow you see should be pointing in the positive velocity direction when you are using refraction or internal reflection lightscatter modes. This means that the fringe motion will be upward when the arrow in the

receiver is pointing down (upward and downward being with respect to gravity, i.e., the usual understanding of up and down). If you are collecting light that is due to reflection off of the particles, the receiver must be rotated 180 degrees. In this case, the fringe motion and the arrow in the receiver will be in the same direction.

For the special case of inverting the transmitter/transceiver probe to “subtract” 40 MHz from high-speed flows, the above rules hold. For example, with refraction or internal reflection, the receiver arrow will still point in the positive flow direction. Remember to enter “-40MHz” as the Bragg cell frequency in the optics setup page. See “**Run Setup** → **Optics**” in Chapter 2 for details.

Setting Up the Software

The following will go through the operation of the software required to take size data. Many of the same screens that were set up for taking velocity data will have to be set for taking size data. The first thing to do is to make sure you have an appropriate file structure (project, experiment, and run) to save data to. See the Chapter 1, “Preparing the Computer to Store Data,” for more details if you are unclear on how to do this.

The first screen to set up is found under **Run** → **Run Setup**. Then select the **Run Settings** tab, as shown in Figure 3-1. Explanations of how to set up this screen are found in Chapter 2, “Taking Velocity Data.”

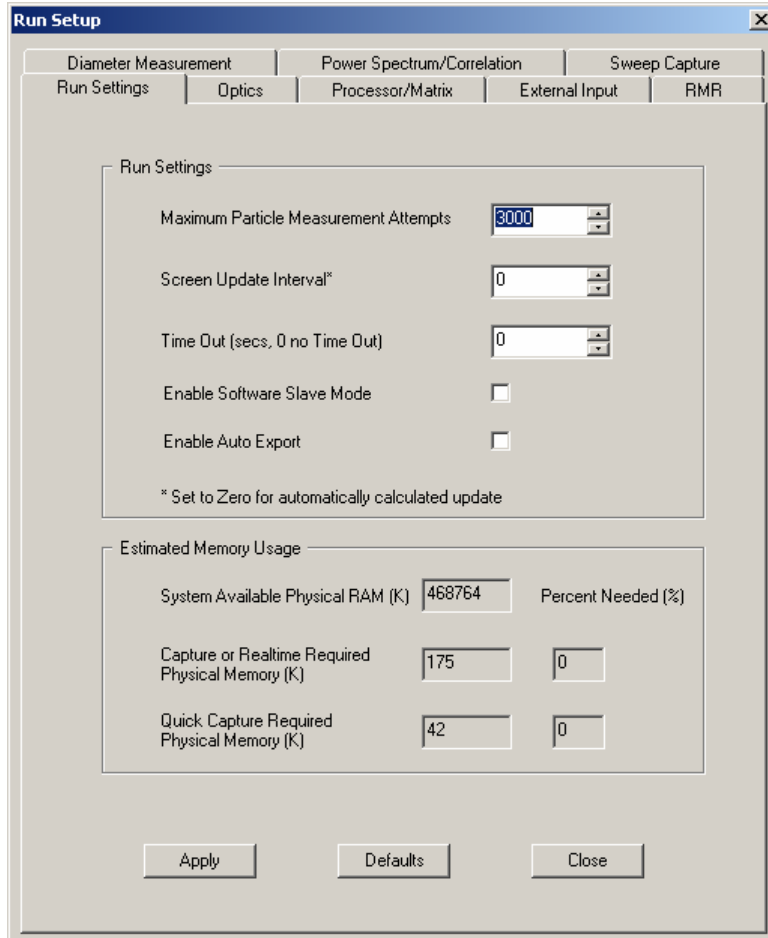


Figure 3-1
Run Settings Screen

Run Setup → Optics

The second screen to set up is the **Optics** tab that is also found under **Run → Run Setup** (Figure 3-2). Most of the setup explanations found on this screen are also found in Chapter 2, “Taking LDV Data.” However, a few additional comments are in order:

1. *Diameter Limit Min*—The smallest measurable particle size with the current optical setup. This value will depend on the transmitter fringe spacing, the PDPA receiver focal length, and the “slope,” which is calculated on the **Run → Run Setup, Diameter Measurement** tab.
2. *Diameter Limit Max*—The largest measurable particle size with the current optical setup. Depends on the same parameters as the *Diameter Limit Min*.

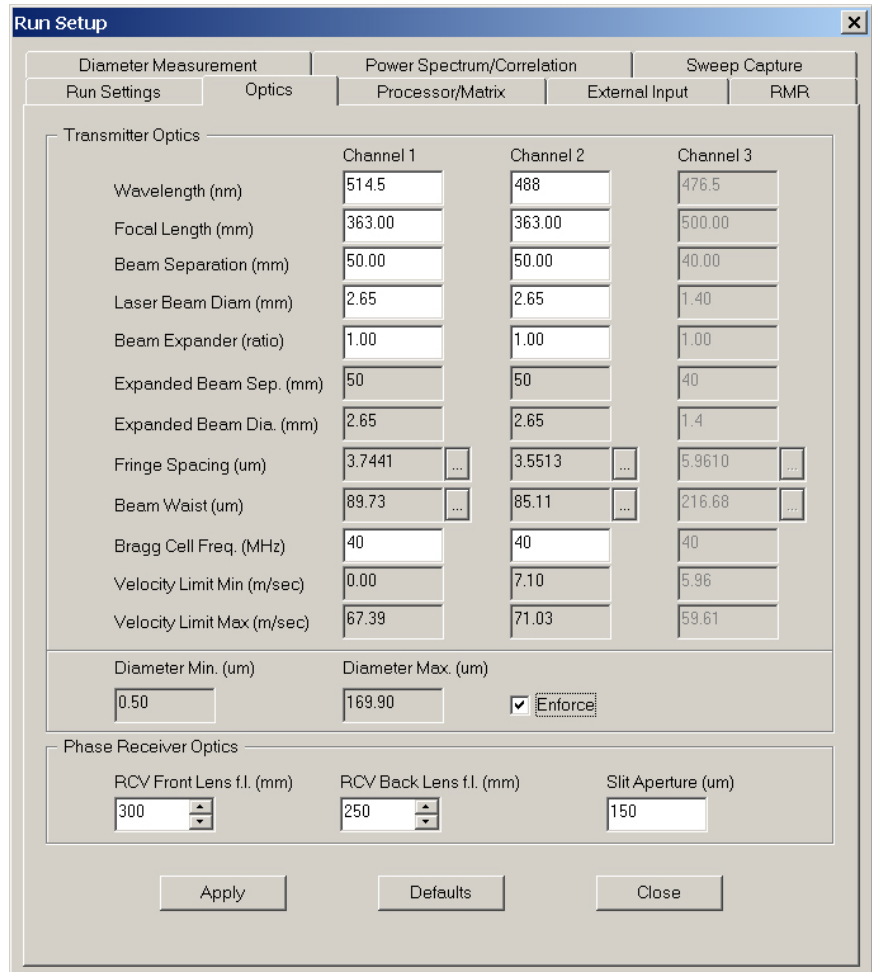


Figure 3-2
Optical Setup Page Screen

3. *RCV Front Lens f.l.*—The focal length of the front lens in the PDPA receiver.

Note: This value is not altered when performing underwater measurements.
4. *RCV Back Lens f.l.*—The focal length of the internal lens in the PDPA receiver. This value should always be set to 250 mm for RV 70 series receivers and 370 mm for RV 100 series receivers.
5. *Slit Aperture*—The width of the slit in the PDPA receiver. The slit width affects the size of the measuring volume in which particles will be detected. It is important to have this parameter correct when measuring number density or volume flux. The slit width can be read through the eyepiece in the PDPA receiver, and the standard value is 150 μm . Optional slits are available from TSI with widths of 25 μm and 50 μm for better measurement of dense flows.

After finishing the setup of the *Optics* page you will need to set up the *Processor/Matrix* tab (Figure 3-3). You must have at least Channel 1 enabled to take size data. See Chapter 2, “Taking Velocity Data,” for more discussion of the parameters on this screen.

Note: *The positive direction of any velocity component is given by the direction that goes from the unshifted beam to the shifted beam, at the transmitting lens. Using this, you can set up the transmitting probe(s) to have the proper coordinate system.*

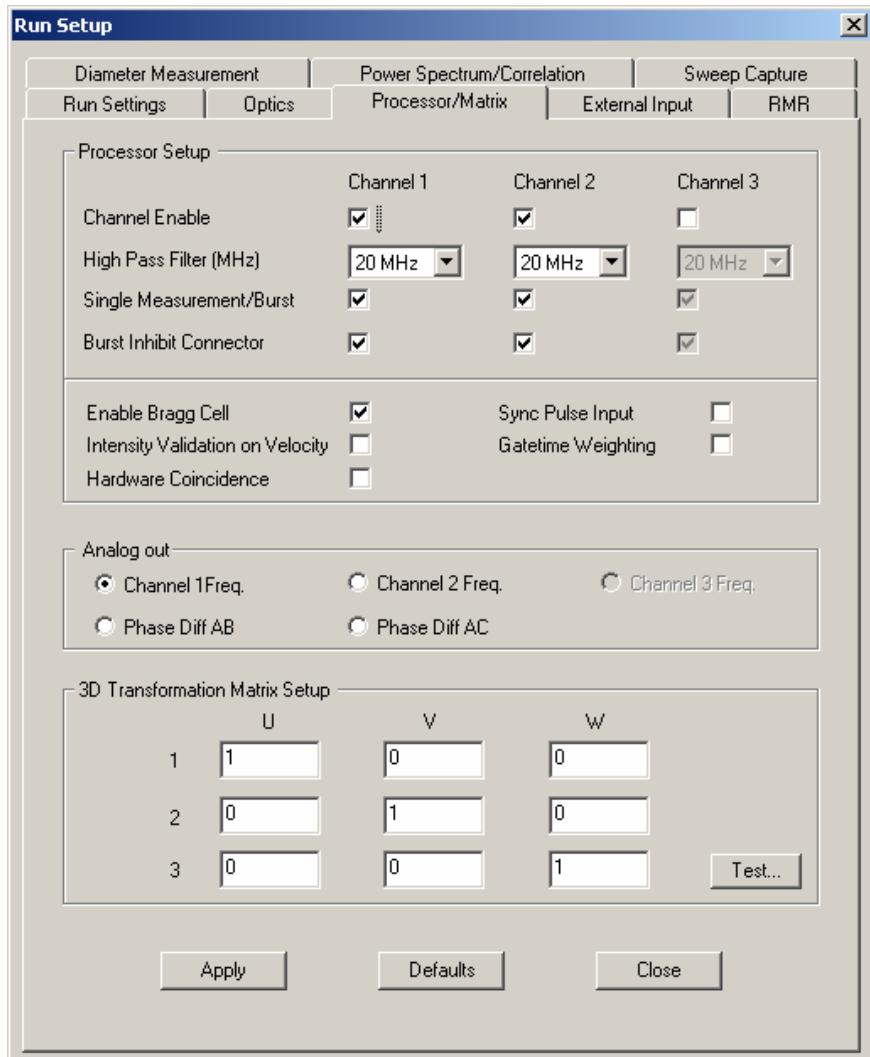


Figure 3-3
Processor/Matrix Screen

Run Setup → Calibration

The next screen to setup is found by clicking **Run → Calibration**, and then selecting the *Receiver Calibration* tab (Figure 3-4). You should verify that the *Detector Separation* values for AB and AC are entered correctly. Each PDPA receiver has slightly different values that are determined at TSI prior to delivering the system. The values should be found on your receiver.

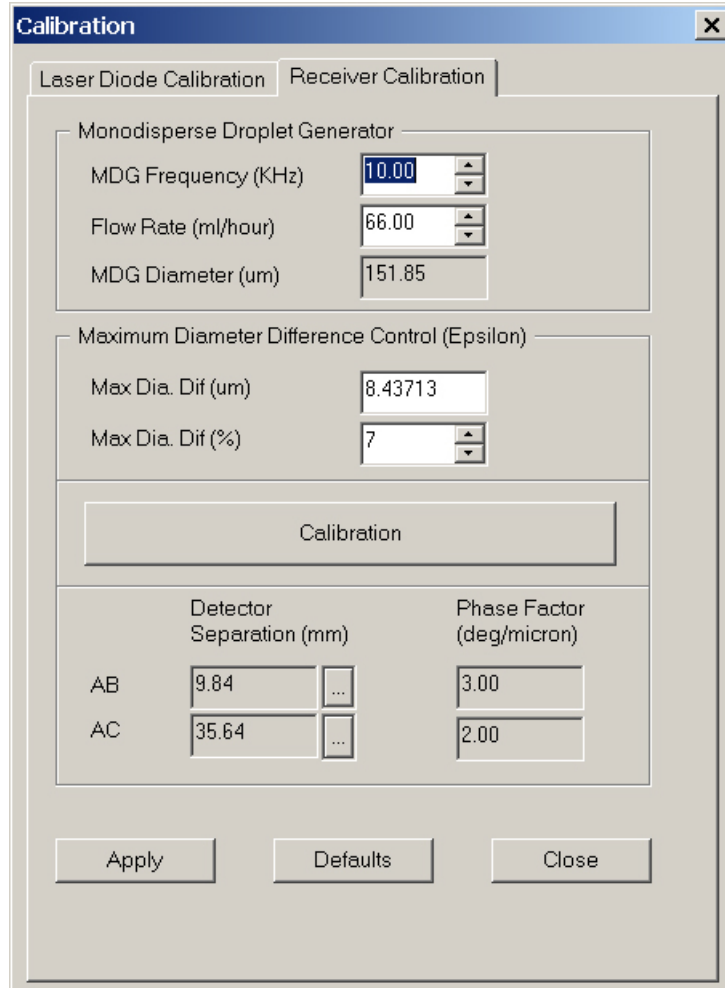


Figure 3-4
Receiver Calibration Screen

Run Setup → Diameter Measurement

The next screen is reached through **Run** → **Run Setup, Diameter Measurement** tab (Figure 3-5).

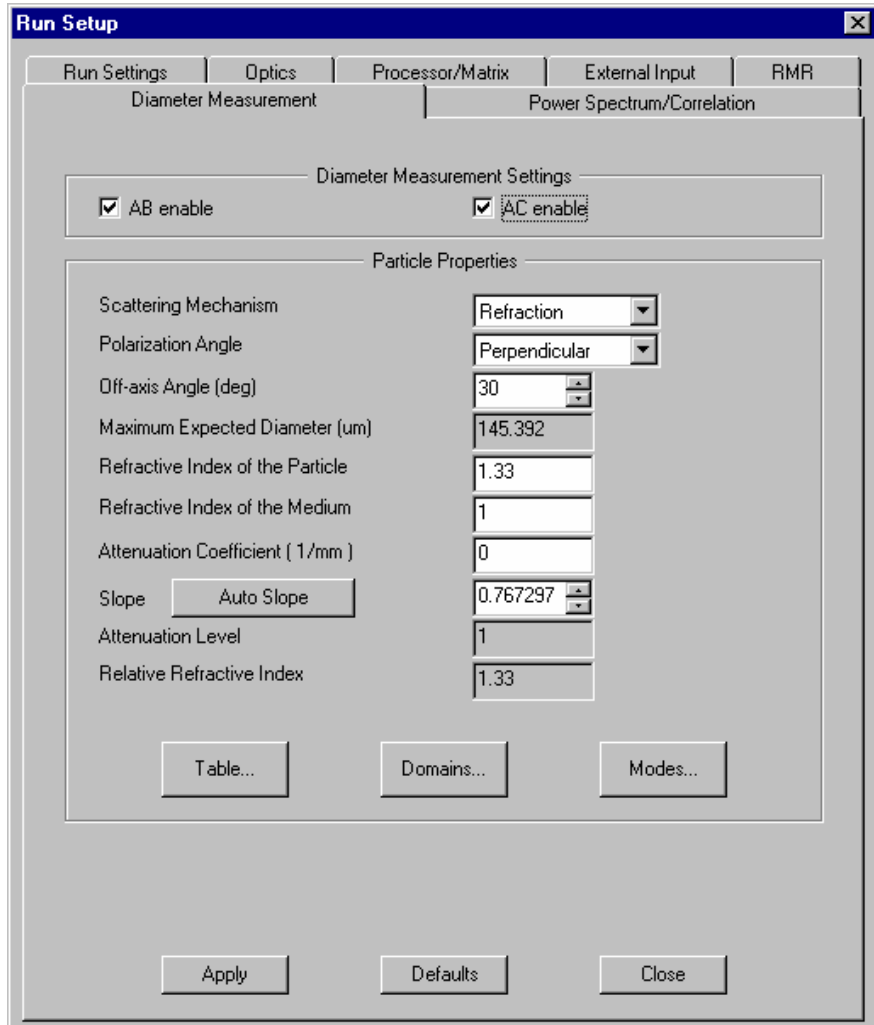


Figure 3-5
Diameter Measurement Screen

To enable particle sizing you should enable both the *AB enable* and the *AC enable* check boxes. Enabling both boxes will provide the two independent size measurements that will provide the most accurate data. It is possible to enable only one of the boxes, but this is not a normal mode of operation. The mode of checking only AB or AC is used if you only have two input signals into the FSA.

The *Particle Properties* portion of the screen also needs to be set up correctly. The correct selection of these parameters is covered in Chapter 5, "Selecting an Optical Layout for Particle Sizing."

Run Setup → Sweep Capture

The next screen is reached through **Run → Run Setup, Sweep Capture** tab (Figure 3-6).

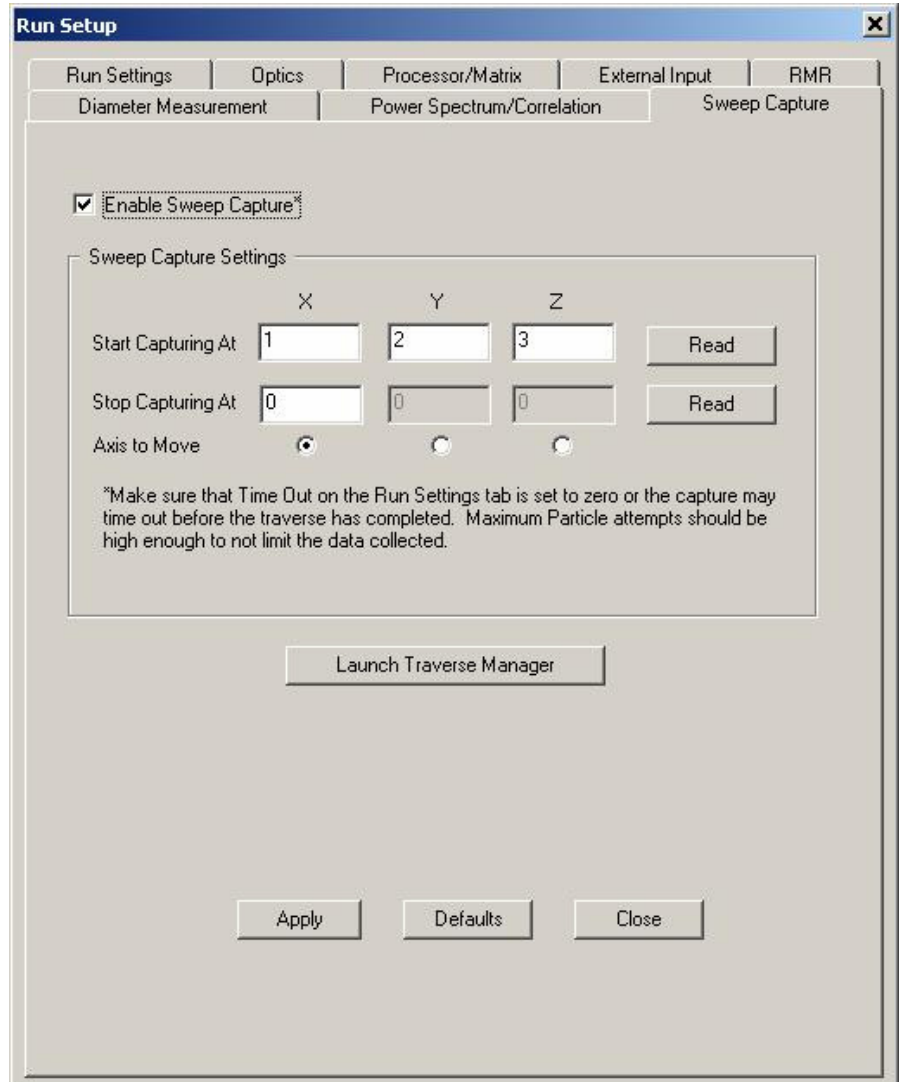


Figure 3-6
Sweep Capture Screen

Sweep Capture is used to record data *while the traverse is in motion*. This method of data collection is used to rapidly acquire data across an entire spray plume. Keep in mind that the final averaged values are number-density (concentration) weighted.

You must have traverse hardware installed to use this feature. The traverse movement is limited to one axis.

When a Sweep Capture Starts:

- ❑ If the Traverse Manager is not active it will be activated.
- ❑ The Traverse is moved to the starting position.
- ❑ The recording of data begins.
- ❑ The Traverse is moved along the selected axis.
- ❑ When the end position is reached the traverse stops and data collection ends.

Diameter Measurement

Now go to the *Diameter Measurement* tab (Figure 3-7) found in the upper right corner of the main software window. If you are using more than one channel of velocity you will control channels 2 and/or 3 from the *LDV Controls* tab. Since size data is taken on channel 1, you will control the channel 1 velocity from the *Diameter Measurement* tab.

Many of the same considerations are important to choosing these parameters as when taking velocity data, so reviewing the *LDV Controls* tab explanations in Chapter 2 would be very helpful at this point. Remember, you must select the bandpass filter range so that you aren't cutting off any frequencies that may correspond to particle velocities in the flow.

The PMT voltage setting for sizing is more critical than for velocity because it affects the measurable size range of the instrument. The voltage must be large enough to detect the smaller particles in the flow, yet low enough so that excessive PMT saturation does not occur. Particles scatter light in proportion to the diameter squared (d^2).

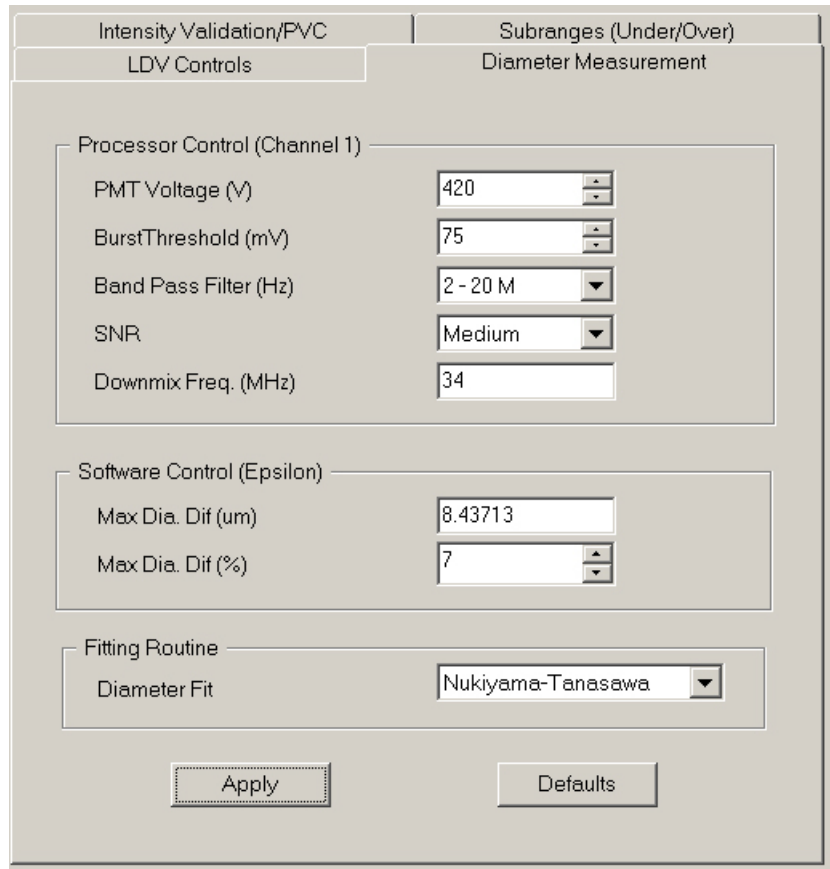


Figure 3-7
Diameter/Channel 1 Velocity Control Menu

In order to set the voltage level for taking size data, the following procedure is recommended. With the system taking data, observe the D_{10} (diameter mean). Increase the PMT voltage until the value of the diameter mean is stable with PMT voltage. As you increase the voltage, the smaller particles will become measurable. When the voltage is large enough, most of the smaller particles will be detected, and the D_{10} will stabilize. Figure 3-8 illustrates the relationship of D_{10} with PMT voltage. Notice that after 400 V (in this example) that the D_{10} diameter mean is fairly constant with increasing PMT voltage. As with LDV, the Data Rate also increases with increasing voltage (Figure 3-9). For *this* example, the recommended PMT voltage would be around 400 V.

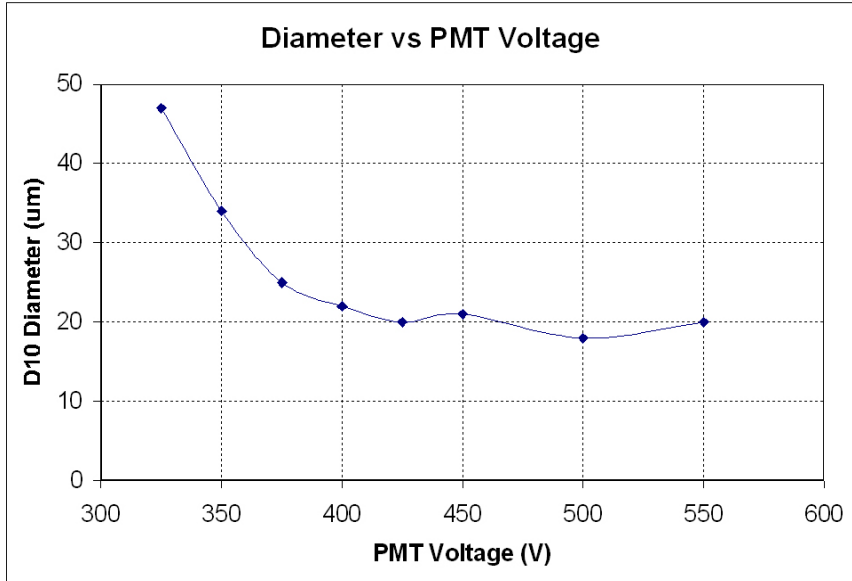


Figure 3-8
Mean Diameter as a Function of PMT Voltage

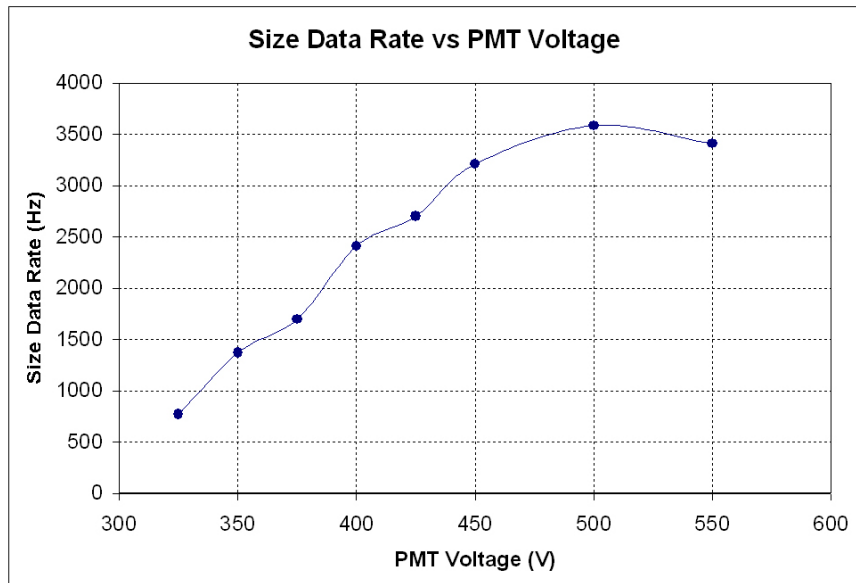


Figure 3-9
Data Rate as a Function of PMT Voltage

Another important consideration in optimizing your size data is to observe the intensity data as a function of particle size. This data can be viewed on the *Intensity Validation Graph* (**Graphs** → **System Graphs** → **Intensity Validation**). An example of this graph is shown in Figure 3-10.

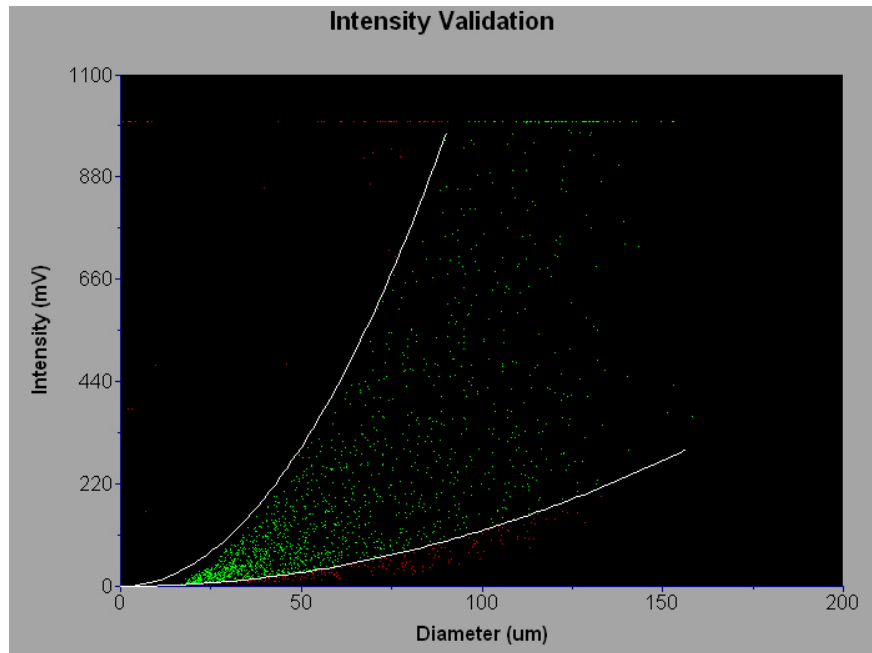


Figure 3-10
System Graph: Intensity Validation

As can be seen in Figure 3-10, there is a relatively sharp upper bound on the intensity for any given size particle. This bound should follow a roughly diameter squared relationship. There is no clear lower limit to intensity because of the Gaussian nature of the measuring volume. A few comments on the intensity versus size plot are in order. First, if you are measuring particles with a very narrow size distribution, you will get more of a blob on your *Intensity Validation* plot. You can also use the *Intensity Validation* plot to help select a PMT voltage. The goal is to pick a PMT voltage so that your larger particles have intensities that are very near saturation (intensity of 1000). If you pick too high of a voltage, even at small particle sizes you will have saturated intensities. This helps provide a rough guide to a range of voltages that will produce the best data.

An explanation of a couple more of the graphs used in sizing will now be given. Consider first the Diameter Difference graph shown in Figure 3-11. This graph takes the diameter difference between the two independent size measurements and plots it versus the diameter, which is actually a weighted average of the two size measurements. By setting bounds on the allowable diameter difference we can reject data points where the system obviously failed to perform a good sizing measurement. To select the diameter difference limits you use the *Epsilon* control found on the bottom of the *Diameter Measurement* tab (Figure 3-7). Based on years of

experience in measurement of a wide variety of sprays and flows, 7% is the accepted value for the “Max. Dia. Dif. (%)” setting.

If your system is set up correctly the data on the diameter difference graph should look like a line roughly centered at a diameter difference of 0. When the data are centered at a diameter difference of zero, this is your primary indication that a phase calibration is **not** needed. When the data are shifted away from zero, this indicates that a phase calibration should be performed.

There may be a slight angle to the roughly linear shape, but if it angles sharply over at least one-half the measurable diameter range, it indicates a problem with the *Detector Separation* values from Figure 3-4.

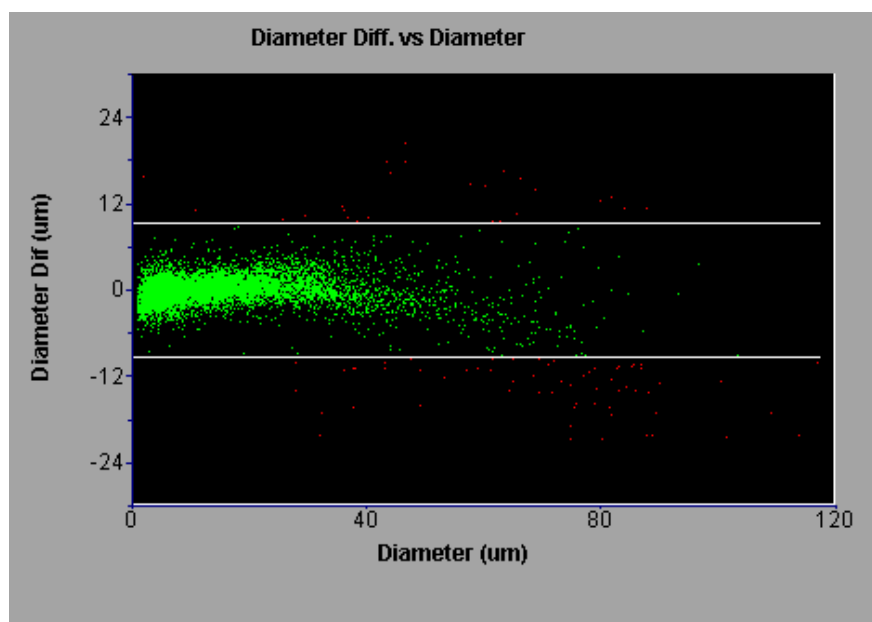


Figure 3-11
Diameter Difference Screen Showing Differences Between Two Independent Measurements of Particle Diameter

After optimizing the five processor control parameters (*PMT Voltage*, *Burst Threshold*, *Band-Pass Filter*, *Downmix Freq.*, and *SNR*) and verifying that the Intensity graph and Diameter Difference graphs are reasonable looking, a phase calibration may be performed to eliminate the influence of the PMTs and processing electronics on the phase shift measurement. But before starting the calibration, you should note several important characteristics of the data you just captured. First, note the mean frequency for channel one. Second, look at the intensity distribution and note a rough value for what the average intensity might be. In addition to noting these two parameters, before performing the calibration, first either cover the PDPA receiver or stop the particle flow through the measuring

volume. You also need to perform the calibration with the optimized processor settings that you just used to capture your flow data.

Run → Calibration → Laser Diode Calibration

To start the calibration process select **Run → Calibration → Laser Diode Calibration**. A window will open like the one shown in Figure 3-12. To perform the calibration, enable the Cal. Diode checkbox and set the *Doppler Frequency* parameter to the mean frequency of the real flow. The value to enter will be that before downmixing, so you need to add the downmix frequency to the mean flow frequency. For example, if you had a mean flow frequency of 5 MHz and you were using a downmix frequency of 40 MHz, you would enter a *Doppler Frequency* of 45 MHz. Set the intensity to 100 and then take data like you would with a real flow. The *Data Rate* will be automatically calculated based on the chosen *Doppler Frequency*, and the *Downmix Freq* and *Bandpass Filter* settings from the *Diameter Measurement* screen.

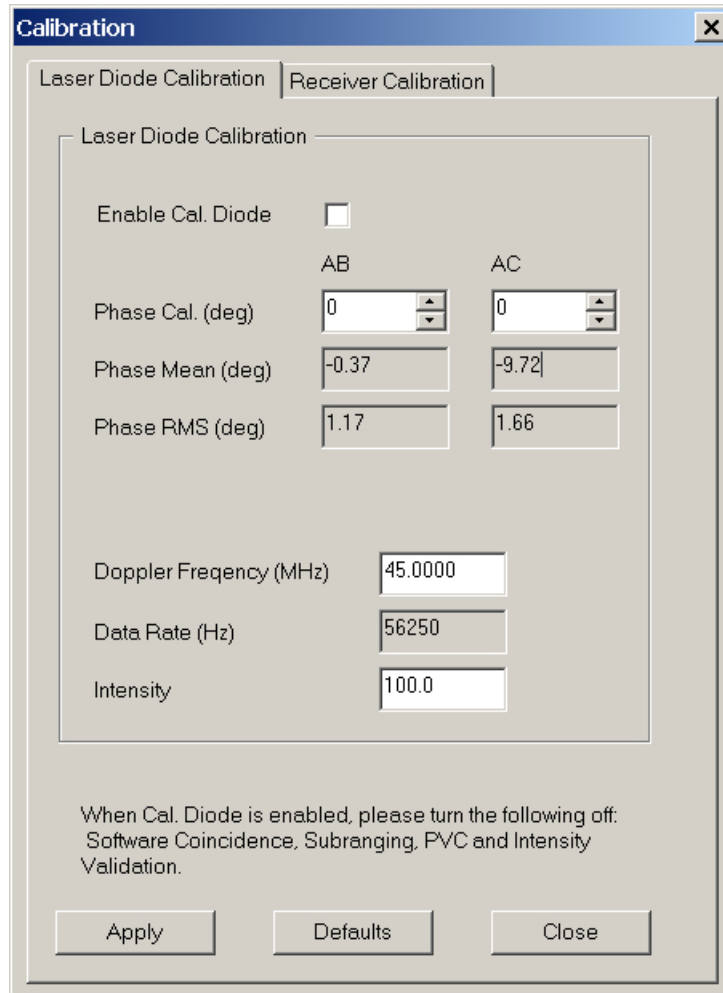


Figure 3-12
Calibration Diode Setup Page After Taking Calibration Data

It would be very useful to open up the system graph showing the phase shifts for both detector pairs AB and AC. To do this go to **Graphs → System Graphs → Phase AB, Phase AC**. After taking a set of data, the graph should look something like the one shown in Figure 3-13.

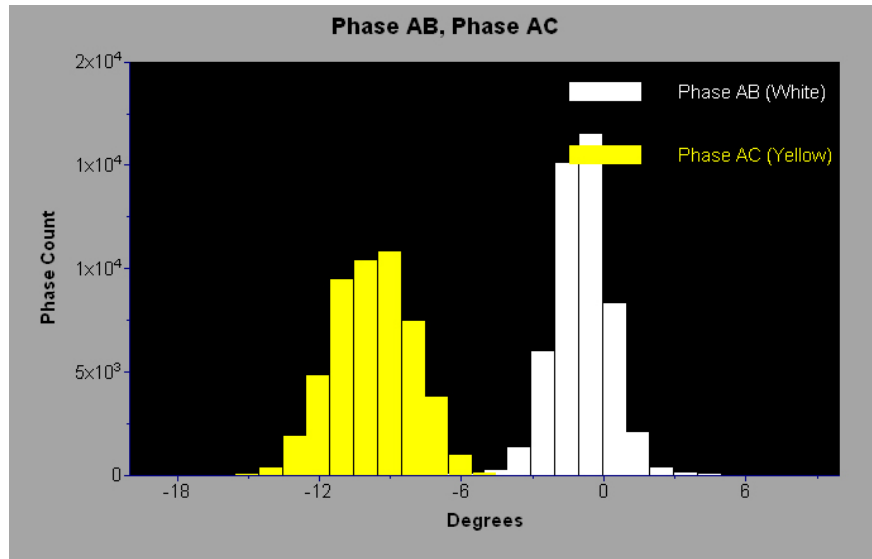


Figure 3-13
Typical Phase AB, Phase AC Graph After Capturing Calibration Diode Data

In the *Laser Diode Calibration* page (Figure 3-12) both the *Phase Mean* and *Phase RMS* parameters should update after capturing data to reflect the mean and RMS of the two phase distributions (AB and AC). The mean values should be near zero (± 30) for lower frequency flows. For higher frequencies (above 20 MHz) the phase mean values will gradually move further away from zero. The RMS values should typically be less than or around 3 degrees. In the example data shown in Figure 3-13 and Figure 3-14, the mean phase for AB is -0.37 degrees and the RMS is 1.17. The distribution for AC has a mean of -9.72 degrees and an RMS of 1.66 degrees.

You should now check the intensity values by looking at the intensity versus size graph. There will probably be very few points on the graph, as most will be rejected as a particular error type. However, the few points there should be clustered around a certain intensity value. If this intensity is higher than the mean intensity value you noted from your real flow data, then you should lower the *Intensity* parameter below 100 and retake data. Keep lowering the *Intensity* until the two intensities are roughly the same. If the intensity from the calibration data is lower than the mean intensity data of your flow even with an *Intensity* parameter of 100 then you can stop. The phase calibration is actually affected very weakly by the signal intensity, so you can expect an accurate correction.

After checking the above you should copy the *Phase Mean* values for both the AB and AC distributions into the *Phase Cal* edit boxes. For the example we have been displaying, Figure 3-14 shows what the page should look like after copying the values. Uncheck

(disable) the Enable Cal. Diode checkbox. You have now completed the calibration procedure.

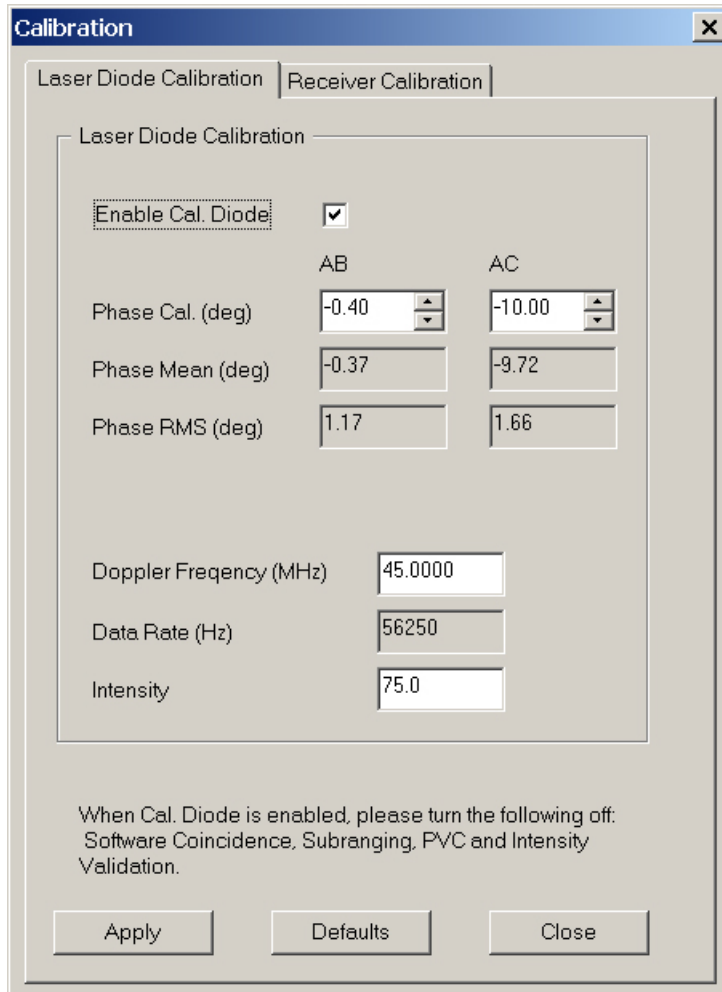


Figure 3-14
Calibration Diode Setup Page After Copying the Mean Phase Values

CHAPTER 4

Optimizing Particle Size Measurement and Obtaining Detailed Flow Information

After completing Chapters 1–3, you are ready to do the final capture of data with your PDPA system. Remember that the diode calibration was done in Chapter 3 with a particular set of processor parameters. If you change these you may need to do a new calibration.

Using **Graphs** → ..select the graphs that you want to view during data capture. From **System Graphs** menu, you may want to select *Intensity Validation*, *Diameter Diff. Vs. Diameter*, and *Velocity vs Diameter*. Other graphs of interest would be Diameter Histogram, Velocity, Frequency and Gate Time Histograms for the Channels in use.

You may also want to display some of the numerical statistics as well. You are recommended to use **Statistics** → **System Statistics** and select *Velocity Statistics*, *Diameter Statistics* and *Volume Distribution Statistics*.

You can arrange the graphs and statistics windows manually or use the options (Tile Horizontally, Tile Vertically or Cascade) available under menu item **Window**. Start a new run (see Chapter 1) and collect data by pressing <F9> or the **Capture Run** button on the main tool bar as shown in Figure 4-1.



Figure 4-1
Capture Run Button on the Main Tool Bar

After capturing a run, you can examine the plots and statistics to decide whether this data makes sense. For example, the diameter difference should be small and velocity versus diameter should follow an expected trend (e.g., in the spray of a pressure atomizer, larger drops move faster due to higher inertia. **Note:** the white

curve on the Velocity vs Diameter plot represents the average correlation).

If you think that the collected data is valuable, it is advised that you save it immediately. For this purpose, use **Run** → **Save Run** or the **Save** button on the tool bar. Now your data cannot be overwritten and you cannot capture more data without creating a new run. However, you can playback the saved data and try out various data reduction options that are discussed below.

When you have a reasonable looking intensity versus size plot (something similar to Figure 3-10), you can turn on the intensity validation. To do this go to the *Intensity Validation/PVC* tab found in the upper-right window of the main software screen. See Figure 4-2 for the contents of this page. To enable intensity validation click on the *Enable Intensity Validation* checkbox.

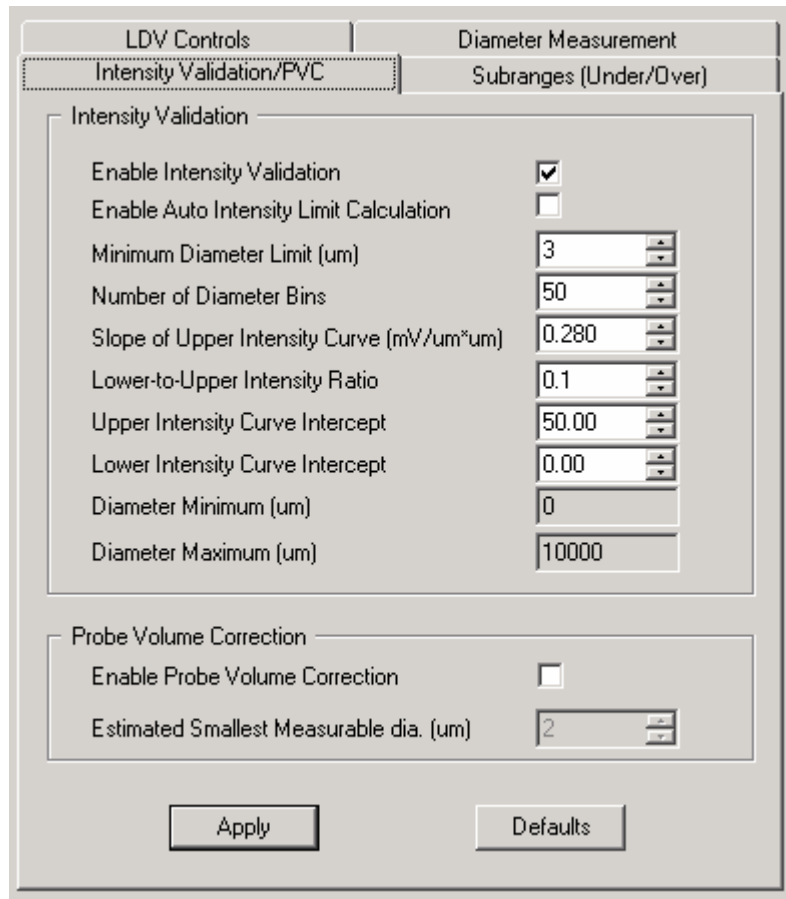


Figure 4-2
Settings to Utilize Intensity Validation and Probe Volume Correction

As shown in Figure 3-10, the intensity-diameter relation has a natural upper limit that follows a d^2 law (scattered light intensity

being proportional to the square of particle diameter). However, there may be some out-liers that need to be eliminated by setting an upper threshold curve that closely matches the natural upper limit. The slope of the upper threshold curve may be calculated automatically by checking **Enable Auto Intensity Limit Calculation**. If this choice is made, the **Number of Diameter Bins** should be set to a large number, e.g., 100 or 200. (You may find the auto-intensity option convenient in at least getting close to the natural upper limit. Or, you may opt to use manual settings iteratively to arrive at the correct upper limit).

When you choose auto-intensity option, the following message (Figure 4-3) may appear. Please activate software coincidence and/or software subrange using the guidelines given under Chapter 10.

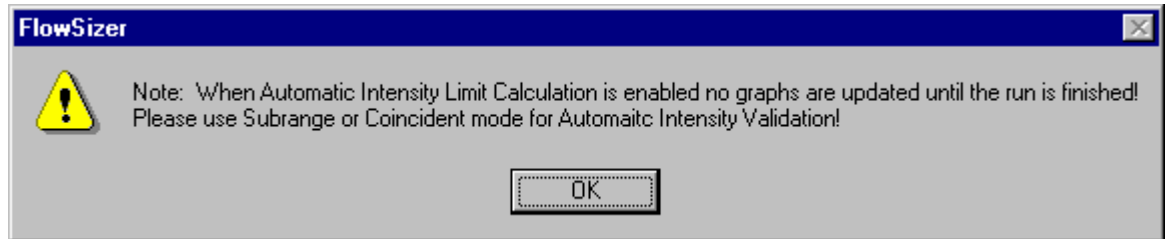


Figure 4-3
Warning Message Pertaining to Auto-Intensity Option

The d^2 law is based on the geometrical optics and does not apply to very small particles. You can set a *Minimum Diameter Limit* (μm) below which the d^2 law is not applied. This parameter can be ascertained from the intensity versus diameter scatter plot or can be determined through light scattering simulations. The value of this parameter would typically be 1–5 μm .

The *Slope of Upper Intensity Curve* ($mV/\mu m*\mu m$) needs to be specified for the manual intensity validation. A good start would be $1000/d_{max}*d_{max}$, where d_{max} is the largest measurable diameter.

Lower-to-Upper Intensity Ratio determines the position of the lower intensity threshold curve relative to the upper curve. This ratio is obviously less than 1. If it is too close to 1, a large amount of data would lie below the lower threshold and will be rejected. On the other hand, if it is too close to 0, some weak signals with erroneous particle size information would be included in the valid data set. Simulations have shown that a value of 0.1–0.2 is appropriate for this parameter.

A physical interpretation of the above parameter is as follows. Signals from a given size particle have different intensities because

they cross the Gaussian laser spot at different locations. Those going through the center of the Gaussian spot generate the strongest signal with the largest intensity. Those grazing the measurement volume at its $1/e^2$ limits will generate signals with an intensity that is 0.135 times the largest intensity. Hence, by setting the lower-to-upper intensity ratio at 0.2, we truncate the measurement volume to a spot smaller than the Gaussian spot. By setting the above ratio to 0.1, we truncate it to a spot somewhat larger than the Gaussian spot.

Theoretically, the upper and lower intensity curves should have zero intercept. However, there may be some electronics-related offset in the measurement that may be corrected by setting the intercept to a non-zero value. In most applications the default value of zero would be satisfactory for *Upper/Lower Intensity Curve Intercept*. We do not recommend using an intercept outside the ± 50 mV range.

After entering appropriate intensity validation settings, press **Apply** (they are not applied automatically). You are now ready to playback the data just taken with intensity validation. Use the playback button from the main tool bar as shown in Figure 4-4.



Figure 4-4
Playback Button on the Main Tool Bar

The intensity validation plot now has two white curves, showing the upper and the lower intensity thresholds. In agreement with the d^2 law, these curves are parabolic. The upper curve becomes flat for the diameter values smaller than the Minimum Diameter Limit. The data points lying outside the two limiting curves are rejected and shown in red.

You would notice changes in the Diameter Histogram and Diameter Statistics. You have probably gotten rid of some of the unrealistically large particles. This is a good time to review the information on the statistics displays.

Velocity Statistics, as shown in Figure 4-5, provides the mean and the root-mean-square (RMS) values of velocity for each component that is enabled. The *Turbulence Intensity* is the ratio of RMS to mean velocity expressed as a %. The mean, RMS and % fluctuation are also reported for the signal frequency. Note that the frequency includes a shift and the frequency statistics are not simply a scaling factor different from the velocity statistics.

	Channel 1	Channel 2	Channel 3
Velocity Mean (m/sec)	8.7320	0.4629	0.2584
Velocity RMS (m/sec)	2.3668	0.1029	0.1213
Turbulence Intensity (%)	27.11	22.24	46.96
Frequency Mean (MHz)	7.7461	7.3499	7.1995
Frequency RMS (MHz)	1.6930	0.0778	0.0937
Frequency TI (%)	21.86	1.06	1.30
Gate Time Mean (usec)	7.95	5.46	5.73
Gate Time RMS (usec)	2.91	1.67	2.13
Data Rate (Hz)	1795	2052	2968
Valid Count	3465	3465	3465
Invalid Count	0	0	0
Elapsed Time (sec)	2.5373		

Figure 4-5
Velocity Statistics

The Velocity Statistics screen also reports the mean and RMS values of the “gate time.” The gate time represents the duration of the individual signals. This can be used as a check for the quality of the measurements. The gate time multiplied by the main velocity component results in a distance that should roughly represent the size of the measurement volume. If the above distance is too much smaller or larger than the nominal size of the measurement volume, one may expect some problems with the measurements. The gate time is also used for correcting the sampling bias in the velocity or probe volume bias in the size measurement.

The Velocity Statistics screen also provides the *Data Rate*, the number of valid signals collected (*Valid Count*) and the total duration of the measurement (*Elapsed Time*). In velocimetry applications, a high data rate is desirable in order to resolve the fine time scales of turbulence. The valid count would vary from channel to channel, unless coincidence is enabled. In the case of coincidence, individual data rates are reported for each channel, but the valid count represents the coincident data only.

Invalid Count refers to the number of samples that were coincident but which did not result in a valid velocity. This category is relevant for hardware coincidence only.

The Diameter Statistics, as shown in Figure 4-6, consists of various mean diameters, i.e., number mean D10, surface mean D20, volume mean D30, Sauter mean D32 and D43. The following general definition applies to all of the above mean diameters:

$$D_{mn} = \left(\frac{\sum D^m}{\sum D^n} \right)^{\frac{1}{m-n}}$$

		PVC	Spatial
D10 (um)	6.58	6.23	5.62
D20 (um)	9.04	8.69	7.93
D30 (um)	11.66	11.30	10.45
D32 (um)	19.41	19.09	18.12
D43 (um)	26.20	25.91	
Size Data Rate (Hz)	3539		
Size Valid Count	5028		
Epsilon Exception	409		
Diameter Exception	0		
Intensity Invalid	3234		

Figure 4-6
Diameter Statistics

The mean diameters are computed in three different ways. The first column represents the raw means, based on the data as it is. The second column is titled *PVC*, which stands for *Probe Volume Correction*. The effective probe volume in phase Doppler applications is a function of particle diameter. Large particles are able to scatter discernible signals from the outer regions of the measurement volume, where illumination intensity is weak due to the Gaussian distribution. On the other hand, small particles scatter less light per unit illumination. Hence, they generate measurable signals only from the central region of the measurement volume.

This probe volume bias favors larger particles. It must be pointed out that the intensity validation tends to undo the above effect by validating signals within certain boundaries, regardless of the particle size. However, the probe volume bias may be present at the lower end of the size distribution.

The values in the PVC column are zero, unless *Enable Probe Volume Correction* is checked on **Intensity Validation/PVC** screen.

After probe volume correction, the mean values represent temporal averages; i.e., average values seen by an observer who is examining the particles passing by a given point in space. This observer sees more of the faster moving particles.

Another kind of average is called spatial average (3rd column), which is seen by an observer who takes a snapshot of the entire particle field. This observer reports averages based on a region around the observation point that is large enough to provide good statistics.

Spatial averages can be deduced from the PDPA data. Although the actual algorithm is quite complex, the basic idea is to use the transit time weighting in order to cancel out the bias towards the faster particles.

This may be the time to play back the data one more time with **Enable Probe Volume Correction** checked. The subsequent parameter on the **Intensity Validation/PVC** page is **Estimated Smallest Measurable Dia. (um)**. This represents your best guess as to the smallest diameter that the system is currently measuring. It depends on several parameters, including the laser power and the PMT voltage. It should be reassuring for you to know that this parameter is meant for “emergency use” and is not normally employed for probe volume correction. Before explaining the purpose of the above parameter it would be appropriate to describe the PVC algorithm itself.

The corrections to the probe volume are based on the dimensions of the measurement volume. As shown in Figure 4-7, the cross-section of the measurement volume is defined by its length L and width $W(d_p)$. L is fixed and depends on the slit width and the lens combination in the receiving optics. Hence, the probe volume corrected particle counts are inversely proportional to $W(d_p)$, which is very small for the smallest particles and increases with the increasing particle diameter. Its value for a given size class is closely related to the largest path length (gate time multiplied by the velocity) generated by that size class.

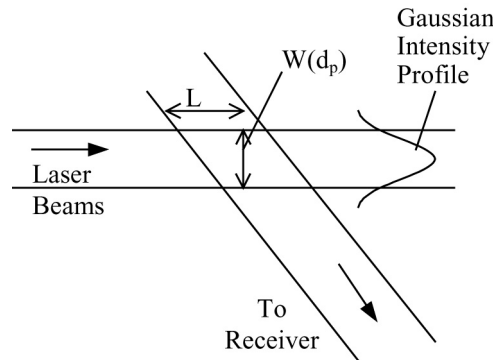


Figure 4-7
Measurement Volume Geometry

A curve of $W(d_p)$ versus particle diameter d_p is generated using the measured path length data. If the measured data is insufficient or inconsistent, a theoretical curve is used that is based on the user-specified *Smallest Measurable Dia.*

If intensity validation is enabled, the value of $W(d_p)$ is not allowed to exceed the value set by the intensity limits, i.e.,

$$W_c = d_{mv} \sqrt{\frac{1}{2} \ln\left(\frac{1}{\gamma}\right)},$$

where d_{mv} is the $1/e^2$ probe volume diameter and γ is the *Lower-to-Upper Intensity Ratio*.

When the data is played back with PVC enabled, several changes happen in the output. In the Diameter Statistics, non-zero values appear in the columns titled PVC and Spatial.

You may notice your probe volume corrected mean diameters are about the same as the uncorrected values. This happens when the small particles do not play a significant role and the intensity validation based W is practically valid over the entire size range. In other words, intensity limits make the probe volume fixed and eliminate the probe volume bias.

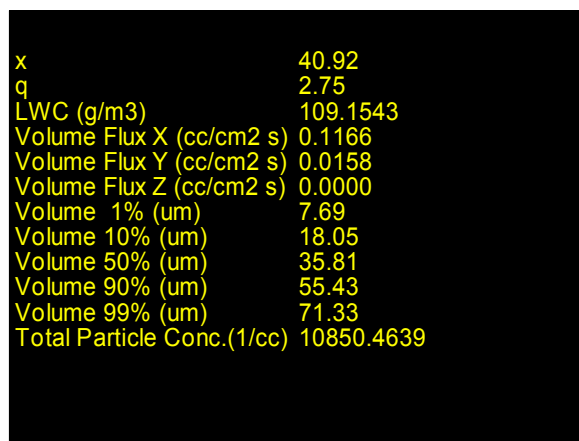
If the small particles, with W values smaller than W_c , are significant, the probe volume corrected mean diameters are smaller than the uncorrected values.

Figure 4-8 shows the *Volume Distribution Statistics*. Non-zero values are available here.

The parameters x and q define the best fit of PVC corrected data to Rosin-Rammler distribution, given by

$$1 - Q = \exp\left[-(D/x)^q\right]$$

where Q represents the fraction of the total volume contained in drops of diameter less than D .



x	40.92
q	2.75
LWC (g/m3)	109.1543
Volume Flux X (cc/cm2 s)	0.1166
Volume Flux Y (cc/cm2 s)	0.0158
Volume Flux Z (cc/cm2 s)	0.0000
Volume 1% (um)	7.69
Volume 10% (um)	18.05
Volume 50% (um)	35.81
Volume 90% (um)	55.43
Volume 99% (um)	71.33
Total Particle Conc.(1/cc)	10850.4639

Figure 4-8
Volume Distribution Statistics

LWC represents the liquid water content in grams per cubic meter. It is based on the assumptions that the particles are water drops. For other kind of particles, multiply this number by the specific gravity of the particulate matter in order to determine the mass per unit volume of the particles.

The x , y and z components of the flow rate of particle material per unit area are expressed as *Volume Flux X, Y and Z*, respectively. These components of the volume flux correspond to the first, second and third velocity component. Each component of volume flux is the summation of bin-by-bin volume fluxes for that component.

The bin-resolved x (y or z)-component of volume flux is given as the volume fraction times the mean x (y or z) velocity component for the size bin under consideration.

The volume fraction for the j th size bin is expressed as

$$L_j = \frac{\pi}{6} \frac{\sum D_j^3 t_j}{V_{probe_j} T},$$

where summation is done for all the particle diameters D_j and their transit times t_j in the j th size bin. T represents the total measurement time and V_{probe_j} is the volume of the probe region for the j th size bin.

As discussed above, the effective volume of the probe region may increase with the increasing particle diameter, due to increasing signal strength. The following definition of V_{probe_j} provides the necessary size dependency of the probe region on the particle size,

$$V_{probe_j} = \left(\frac{s f_{rf}}{f_{rb} \sin \phi} \right) W_j h_j,$$

where s , f_{rf} , f_{rb} and ϕ are the slit width, focal length of the front receiver lens, focal length of the back receiver lens and the collection (off-axis) angle, respectively. The term in the parentheses represents the length of the probe region, whereas W_j and h_j are the size-dependent width and height of the probe region.

h_j is the mean path length for the j th size class.

Referring to Figure 4-8, the following will describe the remaining parameters.

Volume 1 represents the drop diameter in microns such that 1% of total liquid volume is in drops of smaller diameter.

Volume 10 represents the drop diameter in microns such that 10% of total liquid volume is in drops of smaller diameter.

Volume 50 is the drop diameter in microns such that 50% of total liquid volume is in drops of smaller diameter. This is also referred to as the mass median diameter (MMD), or volume median diameter (VMD, MVD).

Volume 90 represents the drop diameter in microns such that 90% of total liquid volume is in drops of smaller diameter.

Volume 99 represents the drop diameter in microns such that 99% of total liquid volume is in drops of smaller diameter.

The number of particles (all size bins) per unit volume in cc^{-1} is represented by *Total Particle Conc. (1/cc)*.

Further information about the particulate two-phase flow is given in the graph reached by **Graphs → System Graphs → Particle Diameter Distribution**. This plot (Figure 4-9) has five size distributions. The first two histograms represent the uncorrected and probe volume corrected particle counts. The particle counts are normalized with the width of the size bin (in microns), so that the area under the curve is always 100%. In the case of *Corrected Area* and *Corrected Volume* curves, the vertical scale represents the surface area and the volume of the drops. Normally, the peak of the area distribution is shifted to the right of the number distribution and that of volume distribution is shifted to the right of the area distribution.

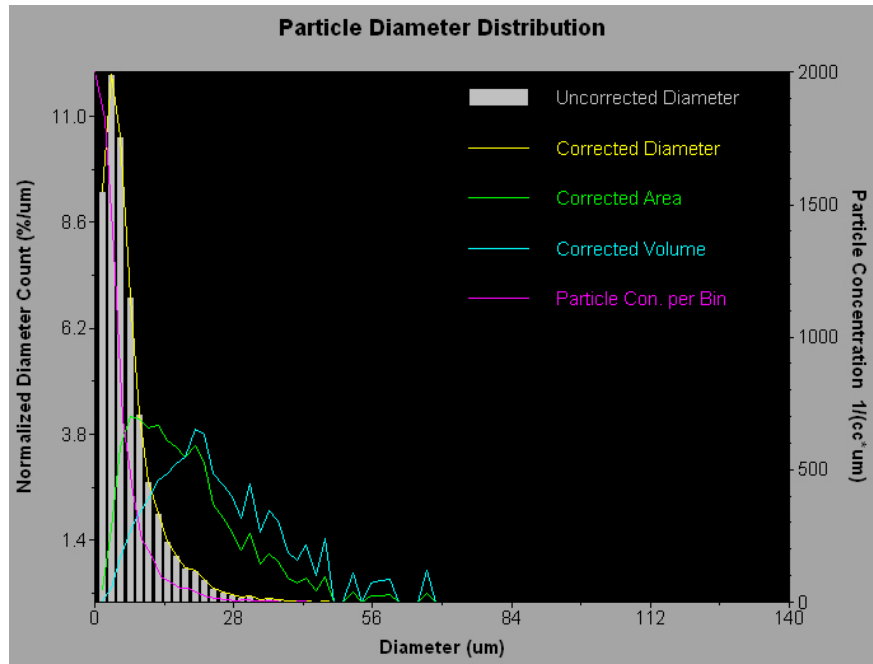


Figure 4-9
Various Size Distributions

The concentration distribution is also normalized with the bin width, so that the area under the curve represents the total concentration in 1/cc as given in Volume Distribution Statistics (Figure 4-8).

All the distributions in Figure 4-9 represent the temporal data, except the concentration distribution, which is spatial by definition.

Diameter Fitting

There are five Diameter Fit Routines available to help transfer measured results to numerical models. Selection is made in the Diameter Measurement tab (Figure 3-7), press the Playback button to force FLOWSIZER to recompute the fit.

Rosin Rammler

This is the most widely used expression for drop size distribution, although it was originally developed to approximate the crushing of solids into powders. It is expressed in the form:

$$1 - Q = \exp - (D / X)^q$$

Where Q is the fraction of the total volume contained in drops of diameter less than D , and X and q are constants.

Fit Var: x in FLOWSIZER represents X .

Fit Var: q in FLOWSIZER represents Q .

Normal

The Normal distribution function is based on processes that are random in nature and where no specific bias is present. Atomizers, humidifiers, and some air-assist spray generators produce normally distributed droplet diameters. This fit usually models the number distribution best.

$$\frac{dN}{dD} = f(D) = \frac{1}{\sqrt{2\pi}s_n} \exp\left[-\frac{1}{2s_n^2}(D - \bar{D})^2\right]$$

Where s_n is a measure of the deviation of values of D from a mean value \bar{D} .

Fit Var: Mean in FLOWSIZER represents the mean value.

Fit Var: Variance in FLOWSIZER represents the deviation value.

Log Normal

Many particle size distributions that occur in nature have been found to follow the Gaussian or Normal distribution law if the logarithm of the particle diameter is used as the variable. Pressure atomizers and hole-type fuel injectors typically have diameter distributions that follow this model. This fit does a better job of modeling the number distribution, rather than the volume distribution.

$$\frac{dN}{dD} = f(D) = \frac{1}{\sqrt{2\pi}Ds_g} \exp\left[-\frac{1}{2s_g^2}(\ln D - \ln \bar{D}_{ng})^2\right]$$

where \bar{D}_{ng} is the number geometric mean drop size and s_g is the geometric standard deviation.

Fit Var: Mean in FLOWSIZER represents the mean value.

Fit Var: Variance in FLOWSIZER represents the deviation value.

Fit Var: XBar = exp(Mean) in FLOWSIZER represents the exp of the mean value.

Figure 4-10 shows a Log-Normal Fit to a Diesel injectory spray.

Matsumoto-Takahashi

It is also known as Modified Log Normal. It is used when values of either D_{min} or D_{max} (or both) are known, and restrict the values of the particle sizes.

$$\frac{dN}{dD} = f(D) = \frac{1}{\sqrt{2\pi}Ds_g} \exp\left[-\frac{1}{2s_g^2} \left(\ln \frac{(D - D_{min})(D_{max} - D_{Min})}{\bar{D}_{ng}(D_{max} - D)}\right)^2\right]$$

Where D_{max} is the maximum diameter and D_{min} is the minimum diameter.

Fit Var: Mean in FLOWSIZER represents the mean value.

Fit Var: Variance in FLOWSIZER represents the deviation value.

Fit Var: XBar = exp(Mean) in FLOWSIZER represents the exp of the mean value.

Fit Var: Max in FLOWSIZER represents the maximum diameter.

Nukiyama-Tanasawa

The expression contains two independent constants, namely b and q . This expression is sometimes found to be a better model for pressure atomizers and hole type fuel injectors, compared to the above models. It performs better as a volume distribution fit.

$$\frac{dN}{dD} = D^2 \exp-(bD)^q$$

Fit Var $B = \exp(r)$ in FLOWSIZER represents b .

Fit Var: q in FLOWSIZER represents Q .

Two system graphs use the currently selected Diameter Fit routines (Figure 4-10 and Figure 4-11). These plots are accessed under **Graphs → System Graphs → Diameter Distribution and Fit** and **Graphs → System Graphs → Volume Distribution and Fit**. These system graphs allow you to view the number-based and volume-based distributions and fits.

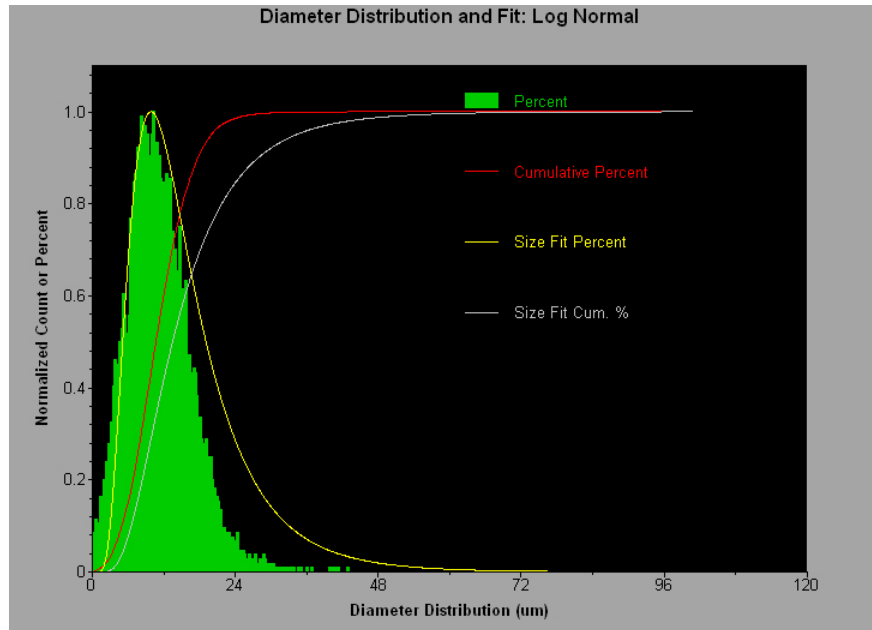


Figure 4-10
Diameter Distribution and Fit: Log Normal Screen

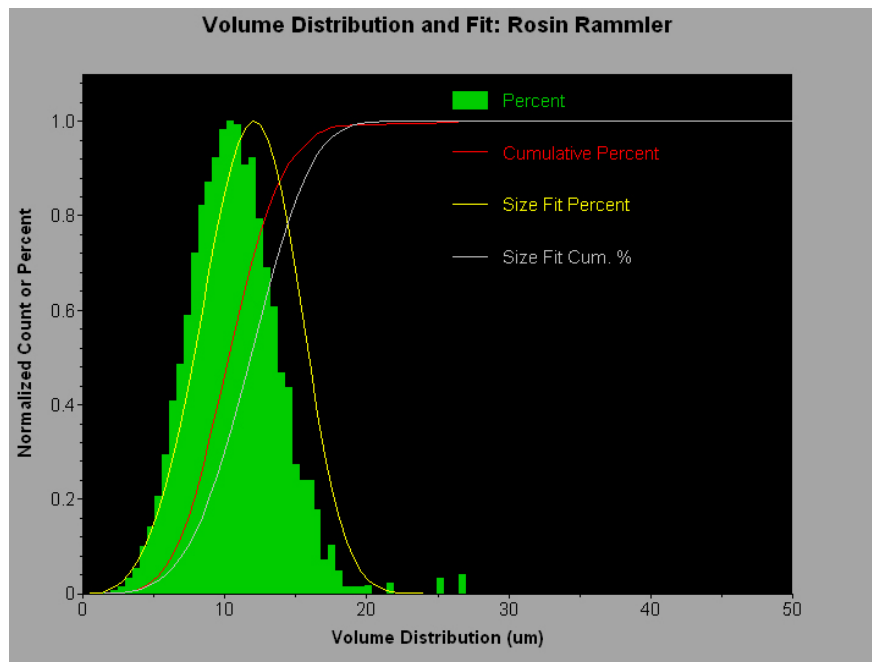


Figure 4-11
Volume Distribution and Fit: Rosin Rammler Screen

The quality of fit is affected by the bin settings. Too many bins introduce artificial variations, too few bins mask the actual trends. Figure 4-12 shows an example fit with too many bins. Right-click on the plot, select **Edit Histogram Data Sets...** then select

Diameter Count from the list. “Bin Count” should be set to give a “Bin Range” of about 1 $\mu\text{m}/\text{bin}$. Press **OK** when finished.

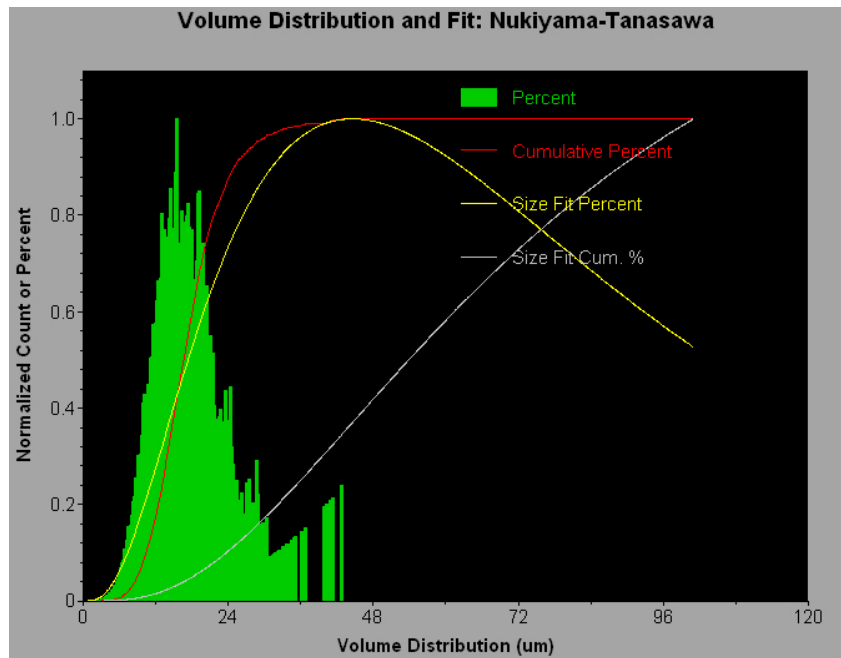


Figure 4-12
Volume Distribution and Fit: Nukiyama-Tanasawa Screen with Too Many Bins

Figure 4-13 shows the result after going from 0.1 $\mu\text{m}/\text{bin}$ (Figure 4-12) to 1.0 $\mu\text{m}/\text{bin}$.

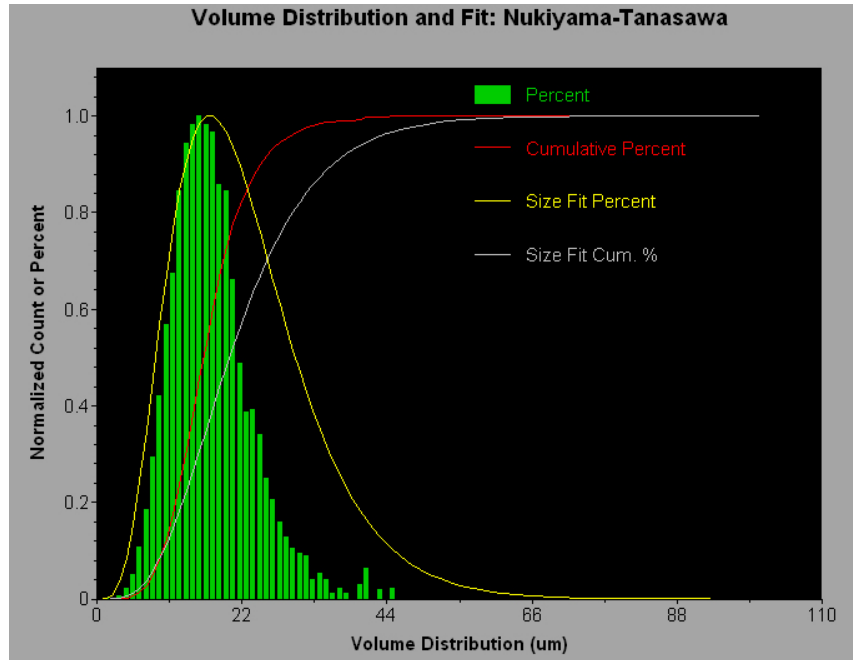


Figure 4-13
Volume Distribution and Fit: Nukiyama-Tanasawa Screen going from 0.1 $\mu\text{m}/\text{bin}$ to 1.0 $\mu\text{m}/\text{bin}$

All the above discussion pertains to a single measurement point in a particle flow. In order to cover a flow field the above measurements need to be repeated at multiple points. The present software can control a traverse and automate the process of moving the measurement volume from one location to the other. See Chapter 13, "Setting up and Using a Traverse."

Sometimes you may want to correlate the size and velocity data with the measurements taken with other devices (e.g., pressure and temperature sensors). This is accomplished using the external input option discussed under Chapter 8, "Using External Input."

Many flows are periodic, e.g., a pulsed spray. FLOWSIZER software allows the analysis of periodic flows, i.e., phase averaging (see Chapter 12, "Using RMR").

CHAPTER 5

Selecting an Optical Layout for Particle Sizing

For particle sizing applications, it is important that the transmitting and the receiving probes are positioned correctly relative to each other, polarization is set right and the slope of the phase-diameter curve is specified correctly.

FLowsizer helps to select the above parameters. To start using FLowsizer for this purpose, choose **Run → Run Setup → Diameter Measurement**. A dialog box, shown in Figure 5-1 appears. In order to use this utility, you should know the refractive index and light attenuation coefficient of the particles. If the particles are suspended in a liquid, the refractive index of the liquid is also needed.

These data for some of the common materials is given in a table, which can be accessed by pressing the button labeled “Table.” It opens the dialog box shown in Figure 5-2. In many applications involving drops of special liquids, e.g., paints, adhesives, fuels, you have to measure the optical properties. An Abbe refractometer can be used to measure the refractive index. Attenuation coefficient α can be determined using measurement of the transmission of a laser beam through a liquid film of known thickness. The following correlation is used for this purpose:

$$\frac{P_{out}}{P_{in}} = e^{-\alpha L},$$

where P_{in} and P_{out} are the laser power entering and leaving the liquid film respectively. L is the thickness of the film.

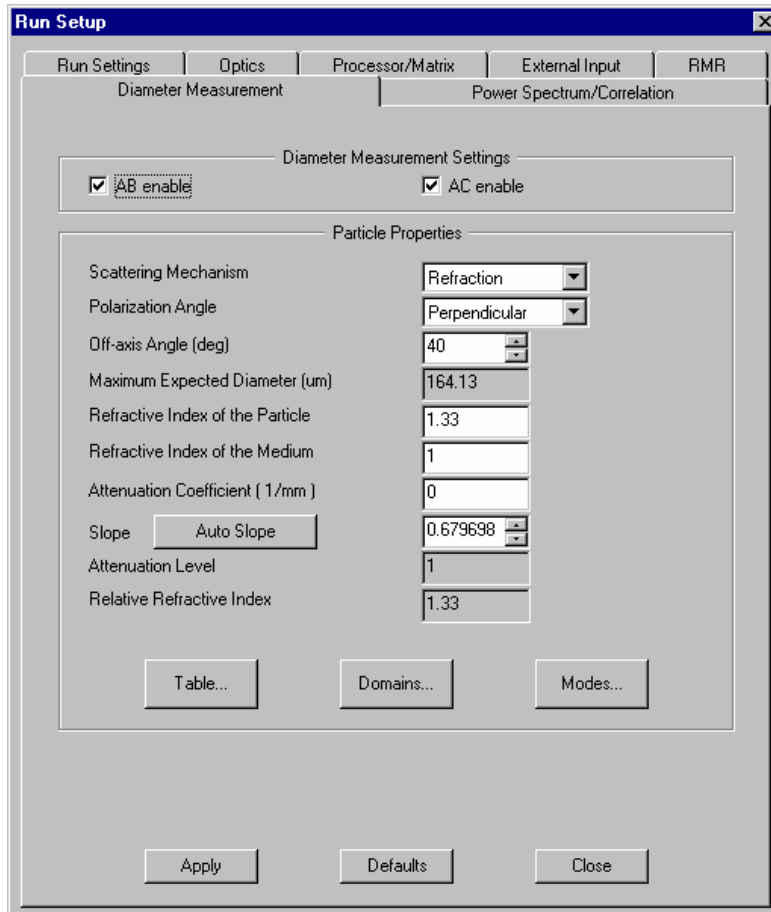


Figure 5-1
Main Dialog Box for Selecting the Optical Layout

Particle Material	Refractive Index	Attenuation Coefficient (1/mm)
Air	1	0
Water	1.33	0
Glass	1.52	0
Jet-A Fuel	1.45	50
Mil-C Fuel	1.45	0.05
Silver	0.2	84,000
Aluminum	1.44	128,000
Copper	0.62	63,000

Figure 5-2
Optical Properties of Common Particle Materials

You should proceed with the following steps to select the optical arrangement:

1. Enter the values of *Refractive Index of the Particle*, *Refractive Index of the Medium* and the *Attenuation Coefficient* on the **Diameter Measurement** page of **Run Setup**. Now, hit *Apply* and the values of the *Attenuation Level* and the *Relative Refractive Index* will be updated. Attenuation Level is based on the product of Attenuation Coefficient and the Maximum Expected Particle Diameter. It is read from the following table.

Attenuation Level	$\alpha(\text{mm}^{-1}) \times d_{p\text{max}}(\mu\text{m})/1000$
1	< 0.005
2	0.005—0.05
3	0.05—500
4	500—4000
5	> 4000

Relative refractive index is the ratio of the particle refractive index to the medium refractive index.

2. Click on the button labeled *Domains*. The graph of Figure 5-3 will appear.

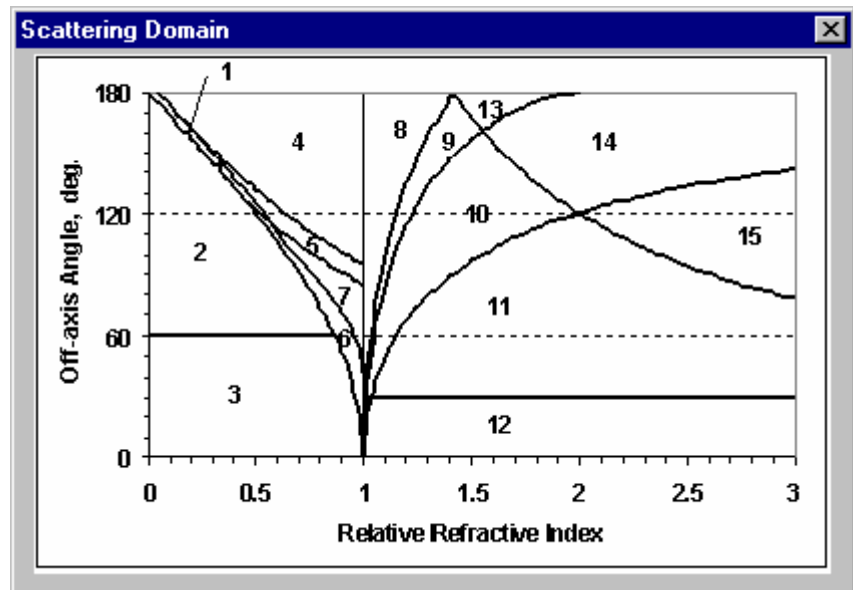


Figure 5-3
Scattering Domains Covering a Wide Range of Relative Refractive Indices and Off-Axis Angles

At this point, you should select one or more domains that are available for the present application. For most liquid sprays in a gaseous environment, the relative refractive index is 1.3–1.4, so that the scattering domains 8–12 are available for further evaluation. If you do not have optical access in the near forward direction (i.e., off-axis angles $<90^\circ$ are not available), only Domain 8, 9, and 10 would be available.

For gas bubbles in a liquid, the relative refractive index would be in the range of 0.7 to 0.8, making scattering domains 2–7 available for further evaluation.

3. Click on the button labeled “Modes.” This will display the **Scattering Mode Charts**, as shown in Figure 5-4. The two charts pertain to the two cases of polarization of light. Standard TSI systems use perpendicular polarization, meaning the electric vector is perpendicular to the beam plane. You can now examine the scattering mechanisms pertaining to the present set of domains and the attenuation level.

Circles, triangles and squares are used to represent the scattering mechanisms of reflection, refraction and internal reflection, respectively. Closed symbols mean a high level of confidence in the choice of the scattering mechanism. In this case, FLOWSIZER will compute the slope of the phase-diameter curve using both geometric and Mie-based light scattering theories.

Open symbols signify a lower level of confidence and the estimated slope may deviate by more than 5% from the actual slope. In this case, it is recommended that you use a more rigorous theory of light scattering, i.e., Mie theory, to examine the phase-diameter relationship. Contact TSI if you think this is needed.

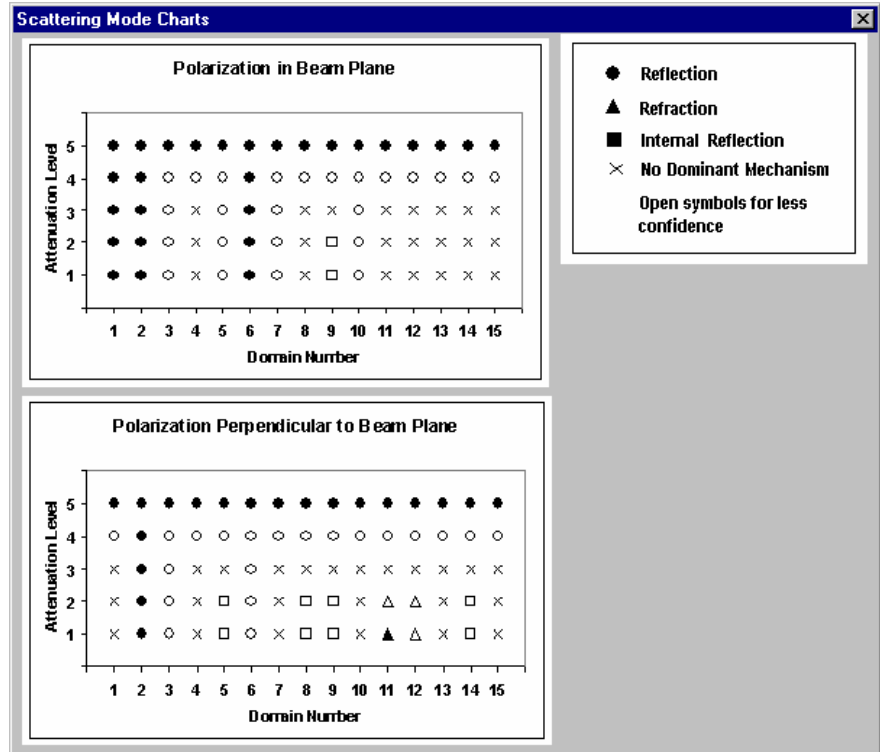


Figure 5-4
Feasible Scattering Modes for Various Domains, Attenuation Levels and Polarization

Let us consider a few examples.

For water drops in air, the attenuation level is 1 and the available modes are 8–12. The scattering mode charts show that perpendicular polarization and domain 11, with refraction as the scattering mechanism, are the best choice. You can also use domain 8 or 9, if domain 11 is not available due to some physical constraints in the experimental setup.

For air bubbles in water, parallel polarization (i.e., polarization in the beam plane) and domain 6 offer a good combination. *Normally, PDPA systems are built to have electric vector of polarization perpendicular to the plane of the laser beams (2nd chart). If parallel polarization is needed, contact TSI for a modification of your fiberoptic couplers to enable switching of the polarization.*

Another choice for bubble sizing is Domain 2 with either case of polarization.

For particles with attenuation level of 5, e.g., metallic particles, surface reflection is the only scattering mechanism and hence, any domain or polarization can be used.

Most paints and fuels have attenuation levels of 1 or 2 and hence, domain 11 and perpendicular polarization are feasible. Also, due to their higher refractive index, backscatter modes 8 and 9 are usually not available.

Very opaque fluids, with attenuation levels of 3 or 4, can only be measured in Domain 10 with parallel polarization.

4. So far we have selected the scattering mechanism and the polarization angle. These may be entered on the **Diameter Measurement** page. We also know the scattering domain, which restricts the choice of off-axis angles to a certain range (see Figure 5-3). For water drops in air (relative refractive index: 1.33), if Domain 11 is selected, the available off-axis angles are 30-75°. It is your choice to select one of these angles. It is preferable to be well inside the domain and not too close to the boundaries.

For air bubbles in water (relative refractive index: 0.75), domain 2 requires the off-axis angle to be in 60-80° range and domain 6 restricts it to 80-90°. Domain 2 is a better choice, because signals are stronger and the standard case of polarization, i.e., perpendicular, can be used.

Enter the selected off-axis angle on the **Diameter Measurement** page.

5. With all the entries current on the Diameter Measurement page, click *Auto Slope*. This will compute the non-dimensional slope of the phase-diameter curve, defined through the following relationship:

$$\frac{\text{Phase}}{360} = \frac{\text{"Slope"}}{\text{Slope}} \times \frac{\text{Detector Separation}}{\text{Receiver Focal Length}} \times \frac{\text{Particle Diameter}}{\text{Fringe Spacing}}$$

A message will appear on the message screen (bottom right corner of the FLOWSizer screen). This message may read, "Orient the PDPA receiver in its ring mounts, such that the white arrow seen through the eye piece, points in the positive flow direction,"

or,

"Orient the PDPA receiver in its ring mounts, such that the white arrow seen through the eye piece, points against the positive flow direction."

The positive flow direction is from unshifted to shifted beam, that is, against the fringe motion. All cases of external reflective

scatter, including Domain 2 for bubbles, use the arrow pointing against the positive flow direction. All cases of refraction, including internal reflection, use the white arrow pointing in the positive flow direction.

During the installation of the system, you may have already set the “white arrow” in the right direction. If you are not sure how to do this, please consult the installation manual.

If the entries on the diameter measurement page are not self-consistent, you may get a message like the one shown in Figure 5-5. Please revisit Figure 5-3 and Figure 5-4 and make sure that your entries are consistent.

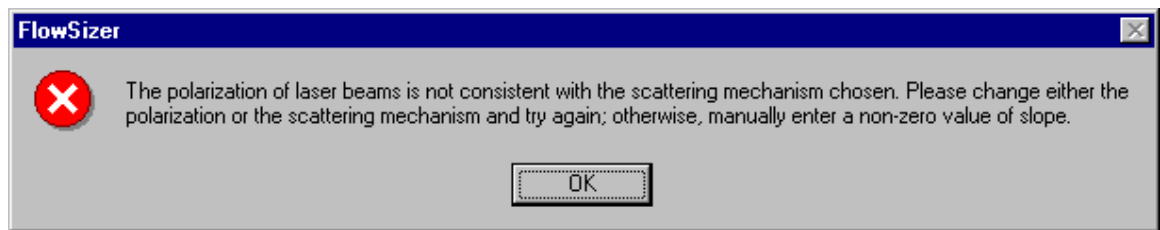


Figure 5-5
Error Message Pertaining to Inconsistent Entries for Auto Slope

Slope can also be entered manually. This would be the case when Mie scattering calculations show a slope significantly different than the Auto Slope.

6. Hit **Apply** and switch to the Optics page of Run Setup. You will see an updated value of *Diameter Limit Max (um)*. If it is less than your expected maximum, you should change at least one of the following optical parameters in the suggested manner:

- Increase the Transmitter Focal Length;
- Reduce the Beam Separation (for example, using a Model XPD50-I beam expander in 0.5:1 contraction position);
- Increase the Receiver Front Lens focal length

The relationship between the above parameters and the maximum diameter is linear, i.e., doubling the transmitter focal length would double the size range. Reducing the beam separation to half would have the same effect.

You may also want to modify the optics if *Diameter Limit Max (um)* is much larger (more than twice) the expected maximum diameter.

Contact TSI for the available choices of the transmitter and receiver lenses as well as the beam expanders.

The above steps should complete your selection of the optical layout for particle sizing. You may still have to do the necessary hardware changes and optical alignments before proceeding with the measurements.

CHAPTER 6

Creating and Using Graphs

The graphing capabilities of the FLOWSIZER™ Data Acquisition and Analysis Software add a unique dimension of flexibility to the software. You can create histogram plots, scatter plots, smoothed line plots, etc. After creating a plot, it is immediately available in a drop-down list. The FLOWSIZER graphing system is based on a set of variables—some measured, some derived—that can be plotted one versus another, as you choose.

Showing a Graph

Press <Alt><G> (or **Graphs**) and use the **Up/Down** arrow keys or click the Graphs menu item to select an existing graph. Seven graphs located in the **System Graphs** submenu are pre-defined because of their importance to phase/Doppler applications. These include the **Intensity Validation** graph, **Diameter Difference vs Diameter** graph, **Phase AB Phase AC** graph, **Velocity vs Diameter** plot, **Particle Diameter Distribution** graph, **Diameter Distribution and Fit** graph, and **Volume Distribution and Fit** graph. All user-defined graphs are listed below the System Graphs submenu. Simply select the one you wish to display. The current data needs to be replayed, or, new data acquired, to appear in the graph.

Each graph entry in the **Graph** menu corresponds to a pair of files in the current Project folder. A graph named **Diameter Histogram**, for example, is associated with the file pair Diameter Histogram.grf and Diameter Histogram.bin. If you create a new Project folder, the existing graphs can be copied into it so that you don't have to redesign all the graphs.

A variety of plots are included with FLOWSIZER, but oftentimes you will need to display other data by creating a new graph. The following section will guide you through this process.

Designing a Graph

Press <Ctrl><G>, or select **Graphs → Graph Designer**, or press the **Graph Designer** button (shown in Figure 6-1) to design your own graph. The dialog shown in Figure 6-2 will appear.



Figure 6-1
Graph Designer Button

Press the **New** button to bring up a dialog box so you can begin to create a new graph. You will first be prompted to enter a title for the new plot, then you will be returned to Figure 6-2 to select the plot style and variables. First select the Graph Type to create—either XY or Histogram. XY plots can have a variety of styles, including Line, Line + symbol, Scattered, Vert Bars, Horiz Bars, 3D Ver Bars, 3D Horz Bars. Next, from the Data Set column, select the variable to plot on each axis (XY plot) or the variable to display in a histogram. X and Y values can be scaled up or down by the Scale Factor. You may also modify the maximum number of data points to be displayed on the graph. Remember that this is independent of the Maximum Particle Measurement Attempts in the (**Run → Run Setup**) Run Settings tab. Finally, press **Save** to save your plot, and **Close** to return to FLOWSIZER.

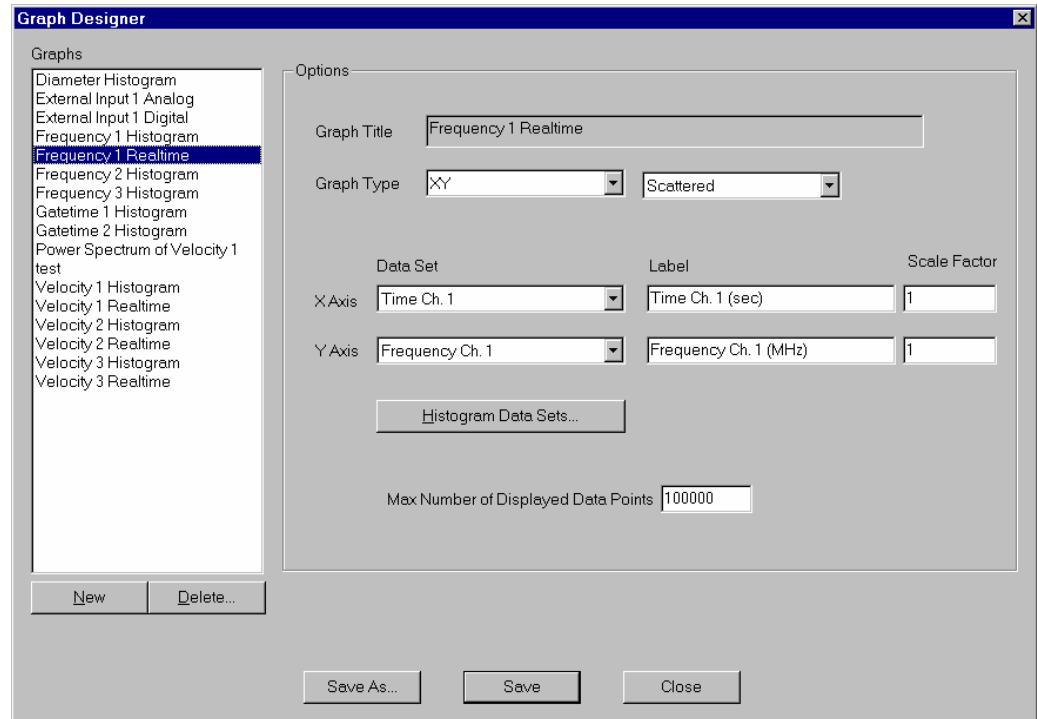


Figure 6-2
Graph Designer Screen

Deleting a Graph

Press **<Ctrl><G>**, or select **Graphs** → **Graph Designer**, or press the **Graph Designer** button (shown in Figure 6-1). The dialog shown in Figure 6-2 will appear. Highlight the graph you wish to delete. Press the **Delete** button. This will delete the graph currently highlighted.

Modifying a Graph

Press **<Ctrl><G>**, or select **Graphs** → **Graph Designer**, or press the Graph Designer button (shown in Figure 6-1). The dialog shown in Figure 6-2 will appear. Highlight the graph you wish to modify. You are now free to alter the graph type, X and Y Data Set, X and Y Label, and Scale Factor. You may also modify the maximum number of data points to be displayed on the graph. Remember that this is independent of the Maximum Particle Measurement Attempts in the (**Run** → **Run Setup**) Run Settings tab. Press **Save** to save your changes.

Modifying a Histogram Data Set

Right-click on any graph, or press the histogram Data Sets button in the Graph Designer Screen. The dialog shown in Figure 6-3 will appear. Highlight the histogram data set you wish to modify. You are now free to alter the Maximum, Minimum, and Bin Count. Using an excessively large bin count can cause meaningless features (peaks, gaps, etc.) to appear in the histogram.

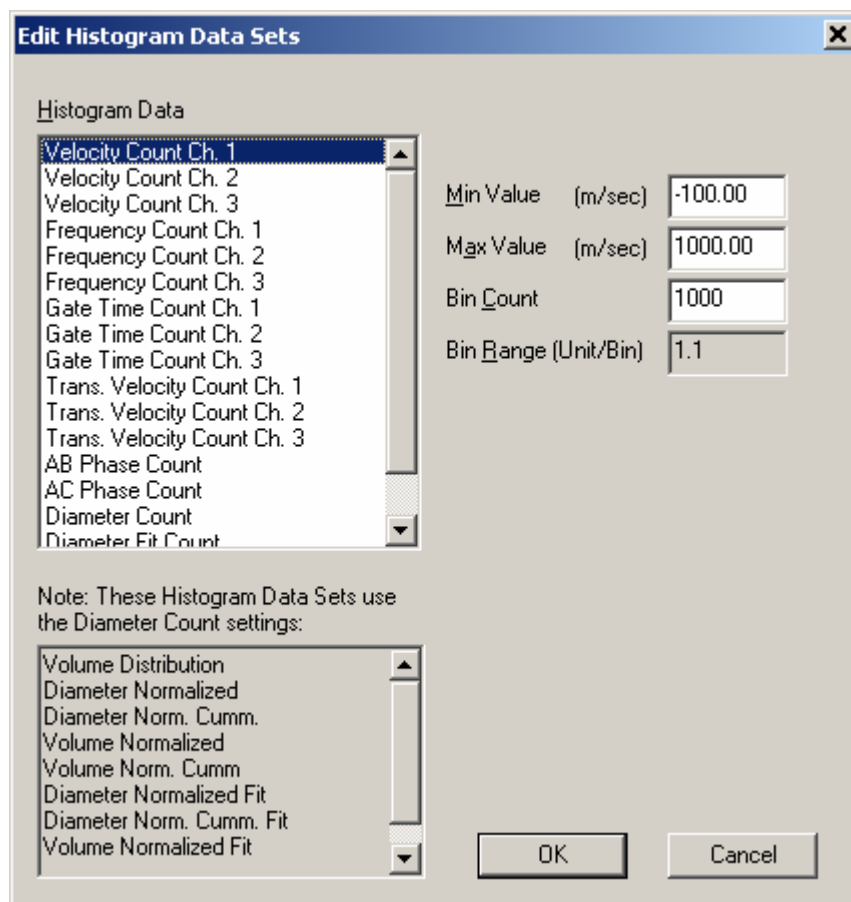


Figure 6-3
Edit Histogram Data Sets Screen

Note: Several data sets are dependent on the Diameter Count Histogram settings. Changing the Diameter Count settings will change the settings for the dependent data sets automatically.

Customizing a Graph

You can modify graph titles, axis labels, and even the graph type by double-clicking on the graph object you wish to modify.

By double-clicking the graph title or an axis title, you can access the Text Parameters dialog box, shown in Figure 6-4. The title or label itself, and the font parameters can be modified here.



Figure 6-4
Text Parameters Dialog

Double-clicking a plot axis (not the labels), brings up the axis edit dialog box. Figure 6-5 shows the Horizontal Axis dialog (the Vertical Axis dialog is similar). Axis limits are specified in the From/To fields. Enable Fixed Range to lock in the limits you specify when replaying the data and taking new data. Click the Line Attributes button to modify the axis line. Tick intervals and gridlines can be specified in the lower part of the dialog. The gridline style can also be modified if gridlines are enabled.

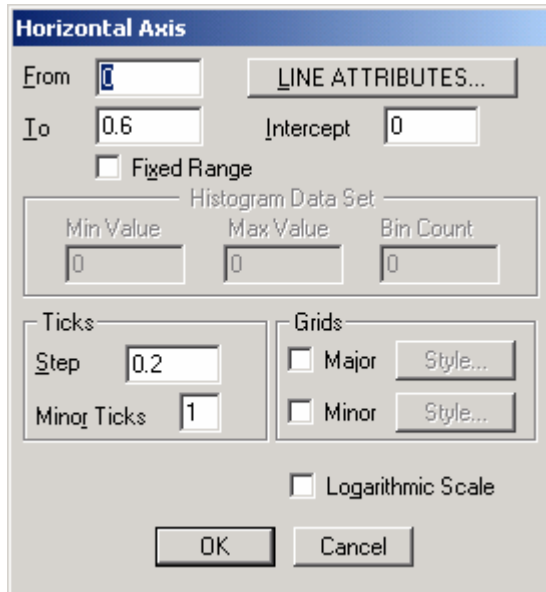


Figure 6-5
Horizontal Axis Dialog

Double-clicking the axis labels (the numbers near major tick marks) brings up the Text Parameters dialog box, shown in Figure 6-6. The position, format, and font format can be modified here.

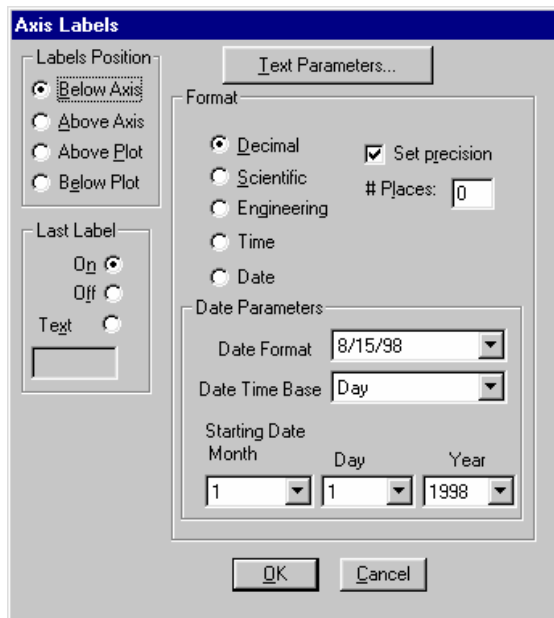


Figure 6-6
Axis Labels Dialog

Double-clicking a histogram graph (on the bars themselves) brings up the Bar Graph Parameters dialog box, shown in Figure 6-7. The type, format, position, and color can be set in this dialog. Pressing the **Data** button brings up a spreadsheet-like display of the actual data plotted. This useful feature will be explained in more detail later.

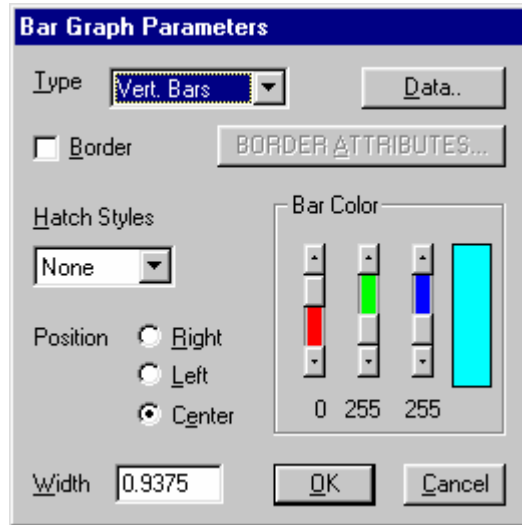


Figure 6-7
Bar Graph Parameters Screen

Double-clicking any non-histogram graph (on the points or line) brings up the Plot Parameters dialog box, shown in Figure 6-8. The plot type and other attributes can be set in this dialog. Pressing the **Data** button brings up a spreadsheet-like display of the actual data plotted. This useful feature will be explained in more detail later.

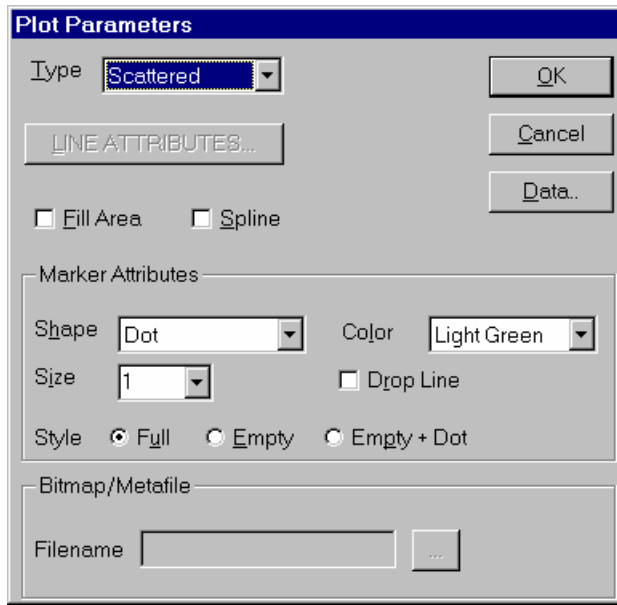


Figure 6-8
Plot Parameters Screen

By right-clicking on a graph and selecting **Edit Graph → Edit Graph Window** you can edit the graph window attributes. A dialog will appear, as shown in Figure 6-9. This important dialog allows you to alter the plot color scheme if, for example, you are pasting plots into a word processing type application where a black background is undesirable.

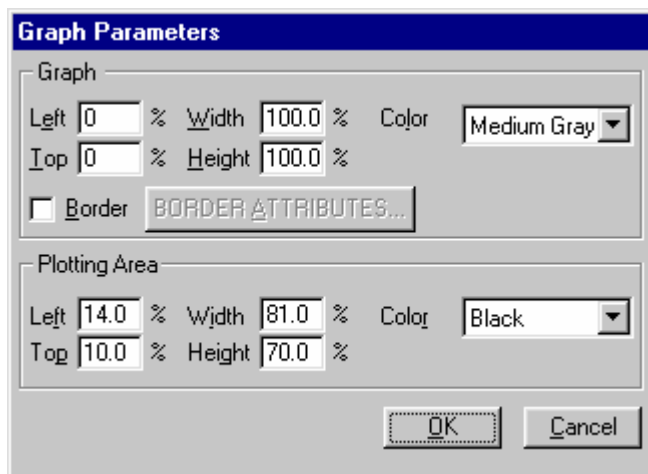


Figure 6-9
Graph Parameters Screen

Left-click on or near any point or bar of a plot to view the coordinates (X and Y value) of that point in a floating information box, as shown in Figure 6-10. This is a useful way to identify peaks

in histograms, and outliers in scatter plots, as well as other plot features.

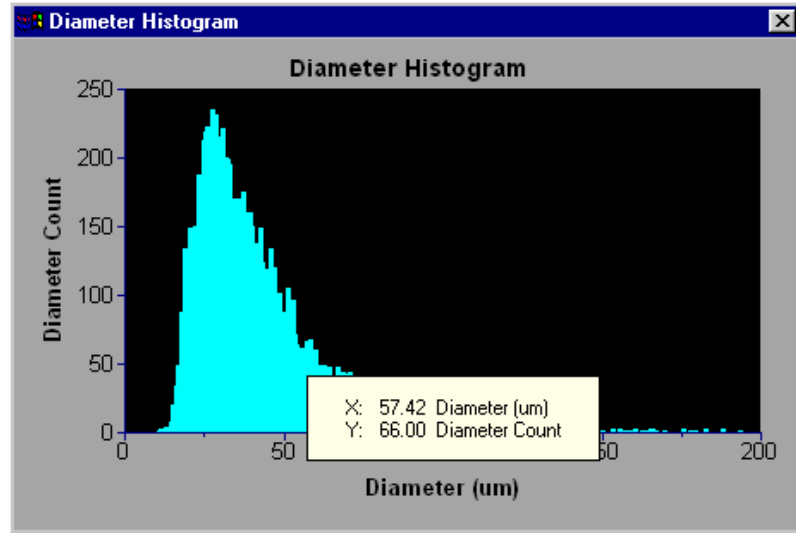


Figure 6-10
Diameter Histogram Screen with Information Box

Right-click on a graph and select **Edit Graph** → **Edit Plot** and then click the **Data** button to bring up the actual data in a spreadsheet-like window. Use **Copy** to copy the data and paste it into a spreadsheet application like Excel.

#	X	Y
0	9.76563	0
1	10.5469	1
2	11.3281	2
3	12.1094	2
4	12.8906	4
5	13.6719	3
6	14.4531	7
7	15.2344	20
8	16.0156	33
9	16.7969	49
10	17.5781	87
11	18.3594	78
12	19.1406	133
13	19.9219	110
14	20.7031	148
15	21.4844	143
16	22.2656	150
17	23.0469	187
18	23.8281	187
19	24.6094	212
20	25.3906	218
21	26.1719	222
22	26.9531	206
23	27.7344	234
24	28.5156	231
25	29.2969	202
26	30.0781	214

Figure 6-11
Graph Data

Other useful hints are as follows:

- ❑ Right-click on any graph and select **Print Graph** to print a graph.
- ❑ Right-mouse click on a graph and select **Miscellaneous → Increase Font Size** or **Miscellaneous → Decrease Font Size** to change the font size of the plot text. You can also select (highlight) the graph and press <+> or <-> to accomplish the same effect.
- ❑ If you have severely adjusted one or more graph attributes and do not know how to “undo” it and get a useful plot back, right click a graph and select **Miscellaneous → Reset Plot** to clear all the customized settings for the graph and restore its default settings.
- ❑ Right-click on any graph and select **Copy Graph to Clipboard** to copy a graph to the Windows clipboard, after which you can paste it into any other Windows application.
- ❑ Right-click on any graph and select **Save Graph** to save graph as an image file. Bitmap (larger file size) and several metafile (smaller file size) formats are available in the submenu.

- ❑ By double-clicking on the title bar of a plot window, you toggle the plot window between full screen size and current size.
- ❑ Press <Ctrl><H> or select **Graphs → Tile Graphs Horizontally** to horizontally arrange all the graphs and statistics windows in your display.
- ❑ Select **Graphs → Tile Graphs Vertically** to vertically tile all graphs and statistics windows in your display.
- ❑ Select **Graphs → Cascade Graphs** to cascade all graphs and statistics windows.
- ❑ Select **Graphs → Hide All Graphs** to hide all graphs and statistics windows in your display.

CHAPTER 7

Creating and Using Statistics Windows

The statistics capabilities of TSI's FLOWSIZER™ Data Acquisition and Analysis Software are very similar to the graphics capabilities, and so you can expect to become proficient rather quickly. The FLOWSIZER statistics system is based on a set of variables—some measured, some derived—that can be displayed in user-defined windows that can be moved and resized just like graph windows.

Showing a Statistics Window

Press <Alt><S> and use the Up/Down arrow keys or click the **Statistics** menu item to select an existing statistics window. As shown in Figure 7-1, six statistics windows located in the System Statistics submenu are pre-defined because of their importance. These include:

- Velocity Statistics
- Diameter Statistics
- Volume Distribution Statistics
- Velocity and Size Subrange Statistics
- External Input Subrange Statistics
- Velocity Transformed Statistics

Any or all these can be displayed as you choose.

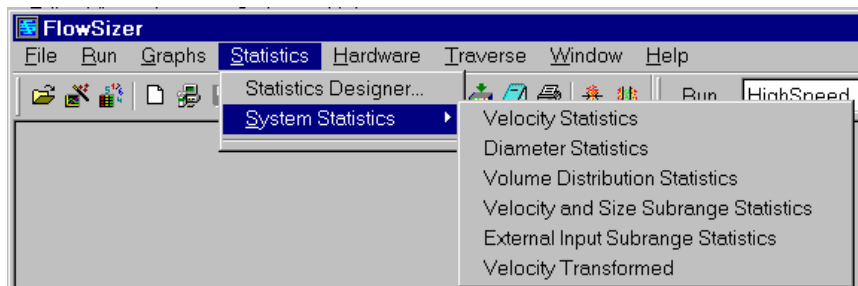


Figure 7-1
Statistics Selection Menu

Velocity Statistics Window

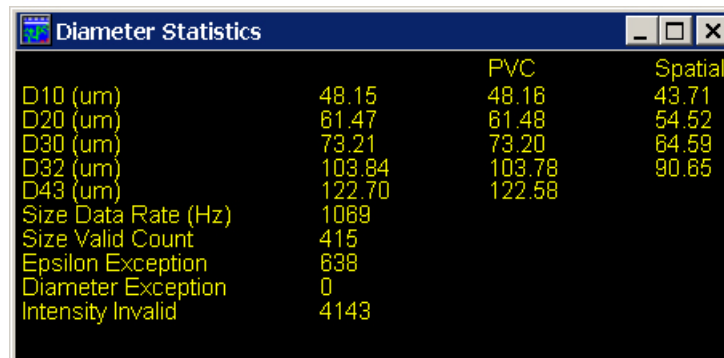
Figure 7-2 shows the Velocity Statistics Window. Three-channel coincident data are shown in this example.

	Channel 1	Channel 2	Channel 3
Velocity Mean (m/sec)	8.7320	0.4629	0.2584
Velocity RMS (m/sec)	2.3668	0.1029	0.1213
Turbulence Intensity (%)	27.11	22.24	46.96
Frequency Mean (MHz)	7.7461	7.3499	7.1995
Frequency RMS (MHz)	1.6930	0.0778	0.0937
Frequency TI (%)	21.86	1.06	1.30
Gate Time Mean (usec)	7.95	5.46	5.73
Gate Time RMS (usec)	2.91	1.67	2.13
Data Rate (Hz)	1795	2052	2968
Valid Count	3465	3465	3465
Invalid Count	0	0	0
Elapsed Time (sec)	2.5373		

Figure 7-2
Velocity Statistics Window

Diameter Statistics Window

Figure 7-3 shows the Diameter Statistics Window. The software algorithms require you to select coincident mode and enable the probe volume correction (PVC) algorithm in order to see the PVC and Spatially corrected values. Otherwise, they are all zeros.

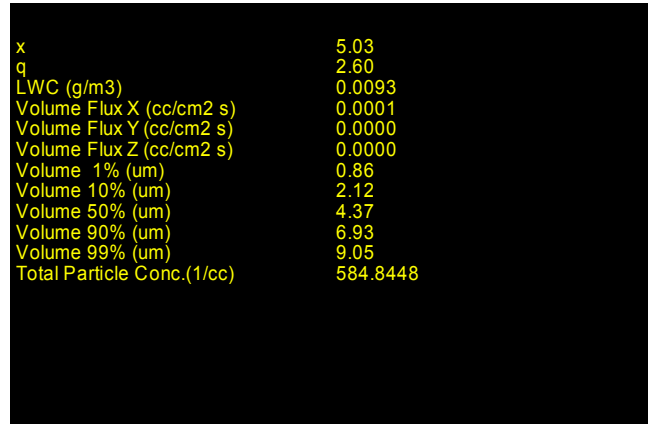


		PVC	Spatial
D10 (um)	48.15	48.16	43.71
D20 (um)	61.47	61.48	54.52
D30 (um)	73.21	73.20	64.59
D32 (um)	103.84	103.78	90.65
D43 (um)	122.70	122.58	
Size Data Rate (Hz)	1069		
Size Valid Count	415		
Epsilon Exception	638		
Diameter Exception	0		
Intensity Invalid	4143		

Figure 7-3
Diameter Statistics Window

Volume Distribution Statistics Window

Figure 7-4 shows the Volume Distribution Statistics Window. The software algorithms require you to select coincident mode and enable the probe volume correction (PVC) algorithm in order to see these values. Otherwise, they are all zeros.



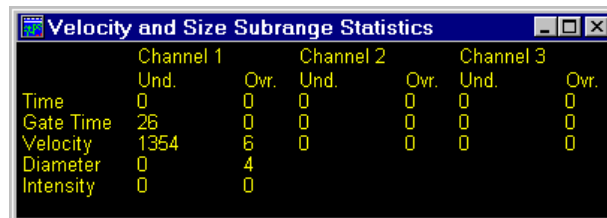
x	5.03
q	2.60
LWC (g/m3)	0.0093
Volume Flux X (cc/cm2 s)	0.0001
Volume Flux Y (cc/cm2 s)	0.0000
Volume Flux Z (cc/cm2 s)	0.0000
Volume 1% (um)	0.86
Volume 10% (um)	2.12
Volume 50% (um)	4.37
Volume 90% (um)	6.93
Volume 99% (um)	9.05
Total Particle Conc.(1/cc)	584.8448

Figure 7-4
Volume Distribution Statistics Window

Velocity and Size Subrange Statistics Window

Figure 7-5 shows the Velocity and Size Subrange Statistics Window. The software algorithms require you to select subranged mode and enter appropriate subrange values in order to see these values. Otherwise, they are all zeros.

Refer to Chapter 10 for more details on how to use the subrange feature.

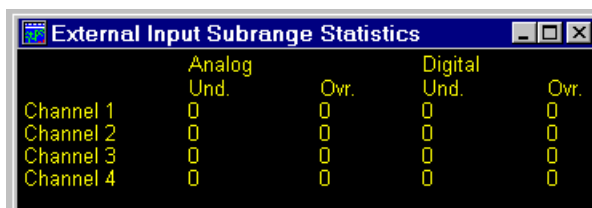


	Channel 1		Channel 2		Channel 3	
	Und.	Ovr.	Und.	Ovr.	Und.	Ovr.
Time	0	0	0	0	0	0
Gate Time	26	0	0	0	0	0
Velocity	1354	6	0	0	0	0
Diameter	0	4				
Intensity	0	0				

Figure 7-5
Velocity and Size Subrange Statistics Window

External Input Statistics Window

Figure 7-6 shows the External Input Subrange Statistics Window. Here you have to be using the external input option, and enter appropriate subrange values. Otherwise, they are all zeros, as they are here, since an external input option was not used.

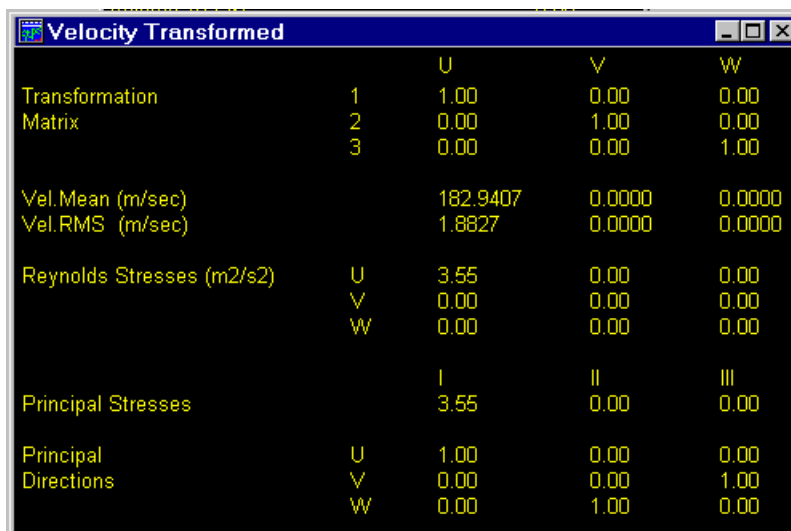


	Analog		Digital	
	Und.	Ovr.	Und.	Ovr.
Channel 1	0	0	0	0
Channel 2	0	0	0	0
Channel 3	0	0	0	0
Channel 4	0	0	0	0

Figure 7-6
External Input Subrange Statistics Window

Transformed Velocity Statistics Window

Figure 7-7 shows the Transformed Velocity Statistics Window. The software algorithms require you to select coincident mode and use a multi-channel PDPA or LDV. Otherwise, the results shown are not very meaningful, as they are here, since a 1D system was used for this data.



	U	V	W	
Transformation	1	1.00	0.00	0.00
Matrix	2	0.00	1.00	0.00
	3	0.00	0.00	1.00
Vel. Mean (m/sec)		182.9407	0.0000	0.0000
Vel.RMS (m/sec)		1.8827	0.0000	0.0000
Reynolds Stresses (m2/s2)	U	3.55	0.00	0.00
	V	0.00	0.00	0.00
	W	0.00	0.00	0.00
Principal Stresses	I	3.55	0.00	0.00
Principal Directions	U	1.00	0.00	0.00
	V	0.00	0.00	1.00
	W	0.00	1.00	0.00

Figure 7-7
Transformed Velocity Statistics Window

Customizing a Statistics Window

You can modify the appearance and colors used in statistics windows. Right-click in the window and select **Edit Statistics** → **Edit Statistics Window...** (Figure 7-8). Customize the colors used in the “Graph Parameters” window. Select **OK** when done.

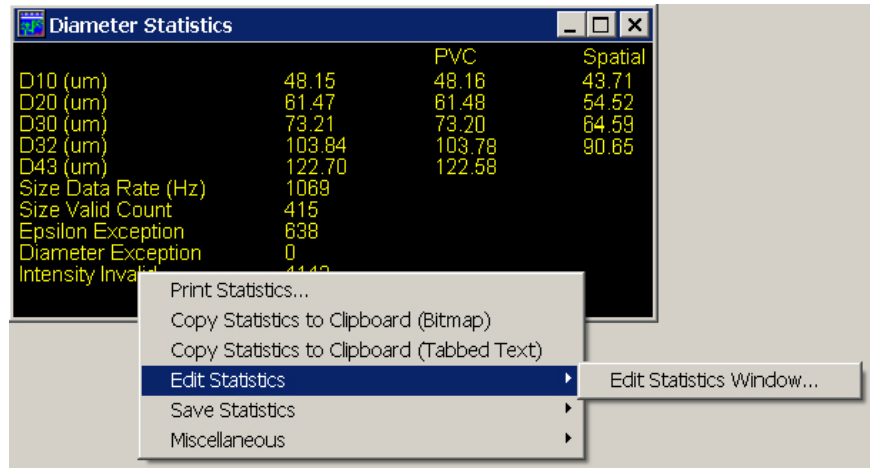


Figure 7-8
Customizing a Statistics Window

Statistics Output Options

Statistics windows can be copied and pasted into graphics software applications using the right-click **Copy Statistics to Clipboard (Bitmap)** option. When you want to copy statistics to other applications such as Microsoft Word, Excel, or PowerPoint, the **Copy Statistics to Clipboard (Tabbed Text)** option gives better results (Figure 7-9).

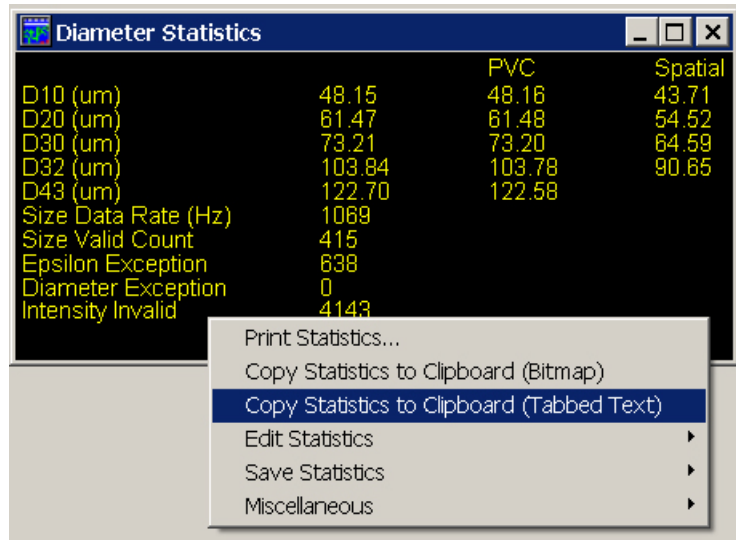


Figure 7-9
Statistics Output Options Window

Like Graph windows, Statistics windows can be saved to a variety of bitmap and metafile type files. These options are available under the right-click **Save Statistics** selection.

Statistics Summary Report

All the above diameter, volume, velocity and transformed velocity statistics are also available in an ASCII (text) based screen. Select **File → Statistics Report**. The report can be printed, saved, or **<Ctrl><C>** copied to the clipboard. The contents of the Statistics Summary Report are shown in Figure 7-10, Figure 7-11, and Figure 7-12.

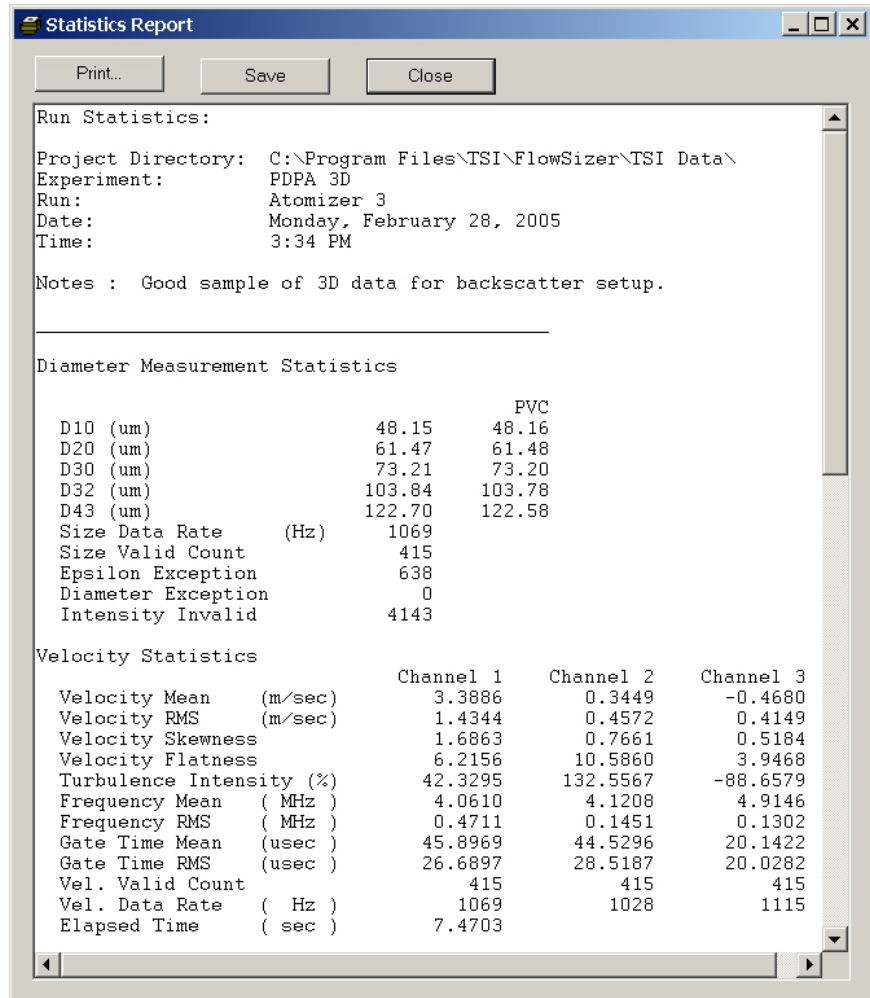


Figure 7-10
Statistics Summary Report #1

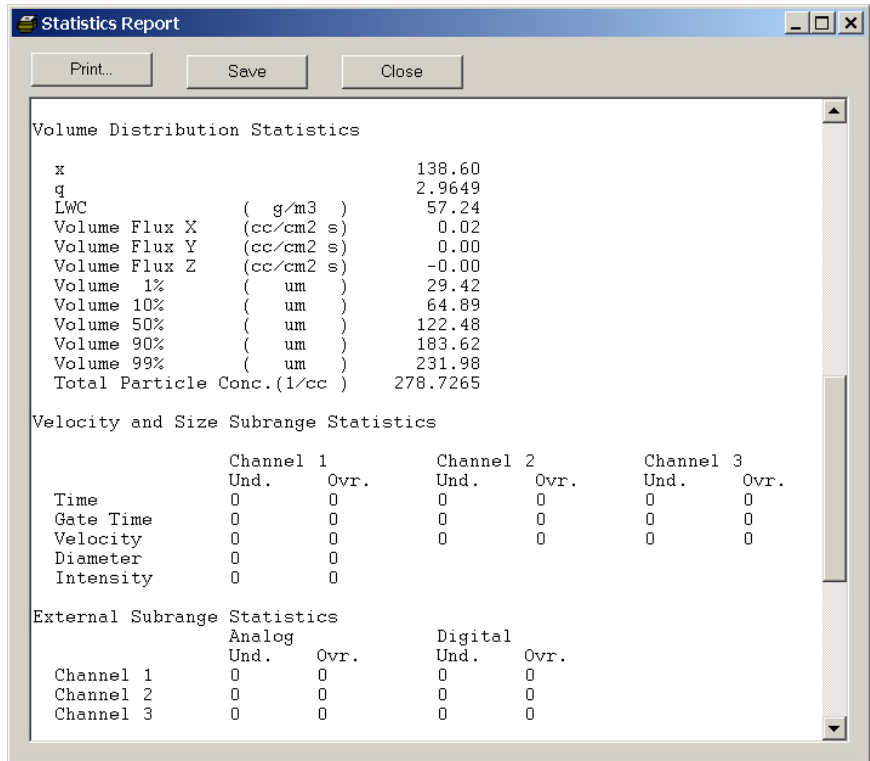


Figure 7-11
Statistics Summary Report #2

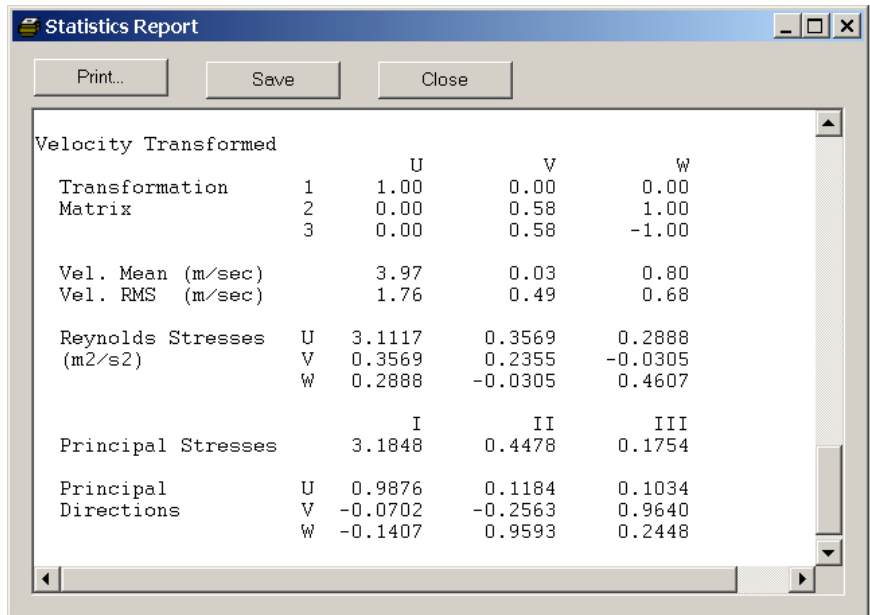


Figure 7-12
Statistics Summary Report #3

A variety of statistics windows is included with FLOWSIZER, but oftentimes you will need to display your own set of statistics. One reason may be that the statistics useful to you happen to be

scattered among many system statistics windows, which leads to an extremely cluttered display. The following section will guide you through the process of creating your own Statistics Window.

Designing a Statistics Window

Press <Ctrl><G>, or select **Statistics → Statistics Designer**, or press the **Statistics Designer** button (shown in Figure 7-13) to design your own graph. The dialog shown in Figure 7-14 will appear.



Figure 7-13
Statistics Designer Button

Press the **New** button to bring up a dialog box so you can begin to create a new statistics window. You will first be prompted to enter a title for the new statistics window, then you will be returned to Figure 6-2 to select the variables to include. First, increment the number of rows and columns to make room for your data. Next, from the second column, select the variable to show using the drop-down menu. Enter a name for it in the left field. Repeat this for each item you wish to include. Finally, press **Save** to save your statistics window, and **Close** to return to FLOWSIZER.

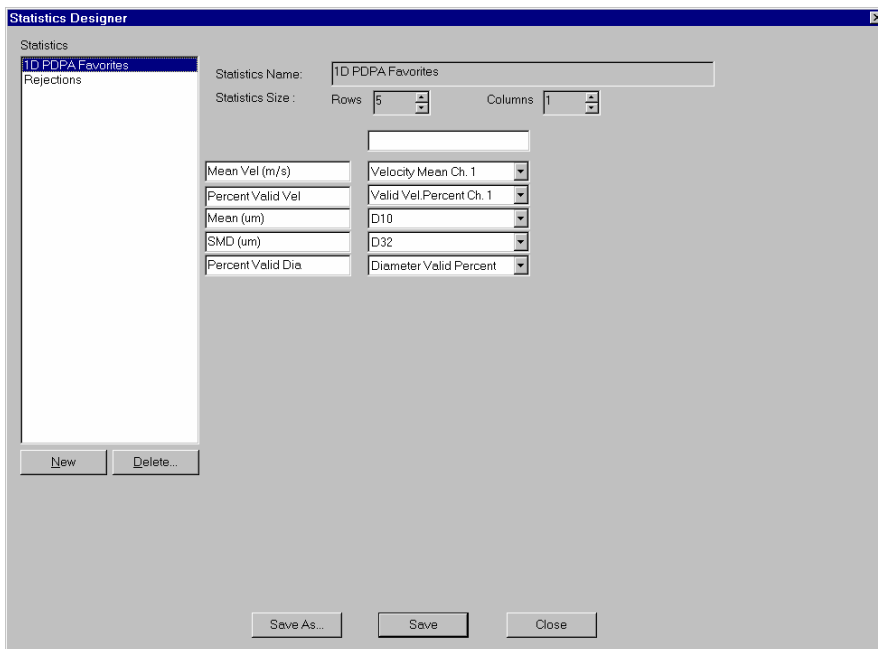


Figure 7-14
Statistics Designer Screen

Example Statistics Windows

Figure 7-15 shows two example statistics windows for 1D PDPA. The first is a convenient and compact grouping of some basic measured parameters. The second is a collection of PDPA rejections—useful to monitor while taking data to maintain reliability of the results.

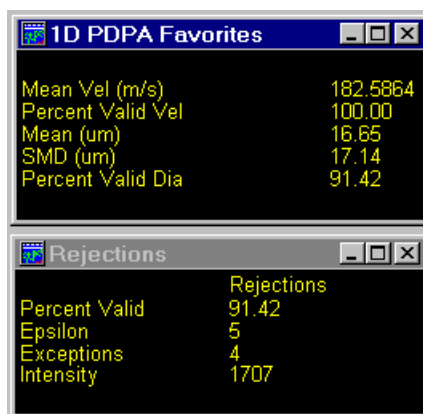


Figure 7-15
Example Custom Statistics Windows

CHAPTER 8

Using External Input

This chapter briefly covers the approach to input external data (Analog or Digital).

The first screen is found under **Run** → **Run Setup**. Then select the **External Input** tab, as shown in Figure 8-1.

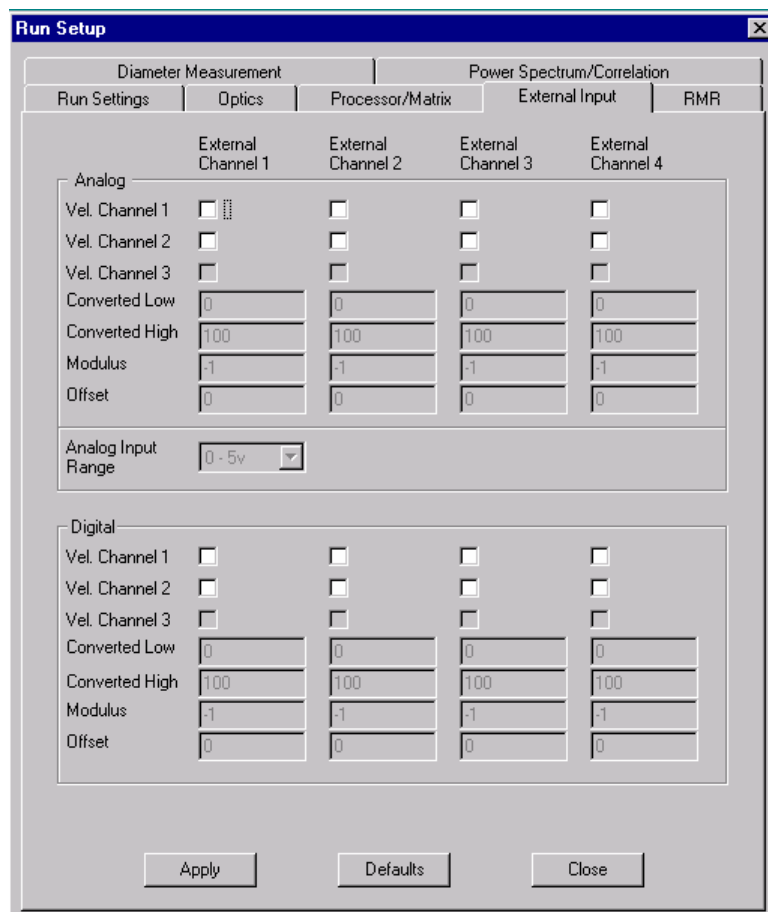


Figure 8-1
External Input Screen

If RMR is enabled and the timestamp is reset each cycle, Digital Channel 1 will not be available for use. Four channels of analog and/or digital data can be captured and tagged with the selected velocity data.

Analog

If each channel data taking is to be triggered along with *Vel. Channel 1* data, select the row of boxes for Channel 1. If external data taking is to be synchronized with other Velocity channels, select the appropriate boxes (please note that Figure 8-1 shows only two velocity channels—i.e., 2D LDV/PDPA system).

The incoming external signal voltage can be converted to a range of values. To do this the following items need to be selected.

Converted Low

Set this to be the low value for the converted signal for the external input channel. For example, the low value can be set to zero for the minimum input voltage.

Converted High

Set this to be the high value for the converted signal for the external input channel. For example, the high value could be set to 100. If the converted low value is zero, you would then have values ranging from 0–100, similar to a “percent full-scale” reading.

Modulus

Modulus needs to be selected as a number between the **Converted Low** and **Converted High** values. For example, if this value is selected as 50, the Converted values go from 0 to 50 as the input voltage goes from the minimum value (0 volts) to midrange (2.5 volts). As the input voltage crosses the mid range, the converted values again go from 0 to 50 (instead of 51 to 100). In other words, the converted values show “two cycles.” Selecting the modulus to be 25 would generate 4 cycles (the maximum converted value would be 25, for this case). Default value of –1 indicates that this feature is inactive.

Offset

The offset value selected is added to the converted values.

Analog Input Range

Analog Input range shows the range of analog voltage signals that the External Input will measure. These values correspond to the

Converted Low and **Converted High** values. The three ranges available are 0–5 volts, –5 to 5 volts and 0–10 volts.

Digital

The setup procedure here is the same as that for **Analog** signals.

Converted Low and **Converted High** are the low and high-end converted values corresponding to input digital signals of 0 and 2^{16} (65,536).

CHAPTER 9

Power Spectrum Analysis

This chapter briefly covers the approach to get the power spectrum of the velocity field. Since particle arrivals (at the measuring volume) occur at random times the velocity output from the signal processor is random. This makes the Spectrum analysis of LDV data different from standard approaches.

The first screen is found under **Run** → **Run Setup**. Then select the **Power Spectrum/Correlation** tab, as shown in Figure 9-1.

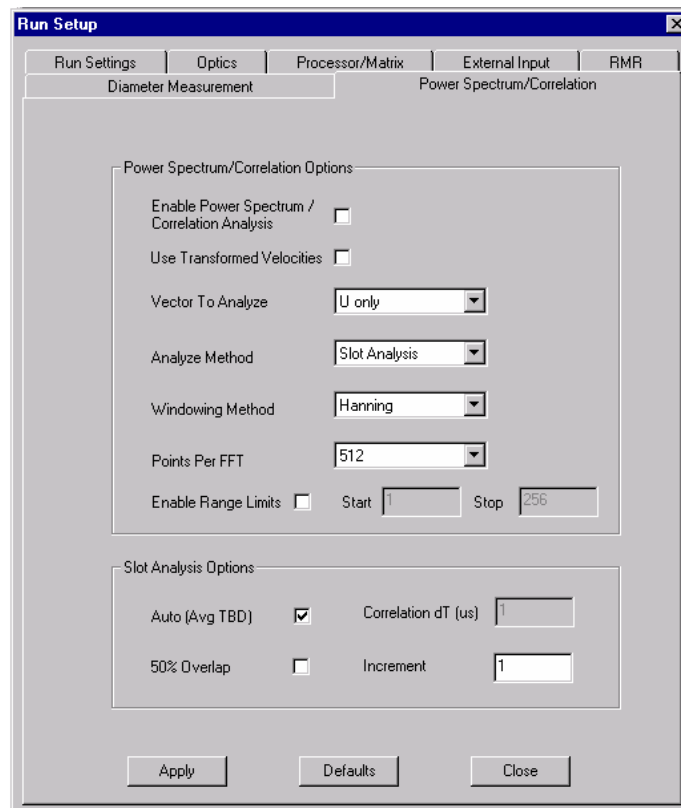


Figure 9-1
Power Spectrum/Correlation Screen

To do the spectrum analysis, first select **Enable Power Spectrum/Correlation Analysis**.

Use Transformed Velocities; allows computation of the power spectrum of the velocity components after the matrix transformation (see Figure 9-2).

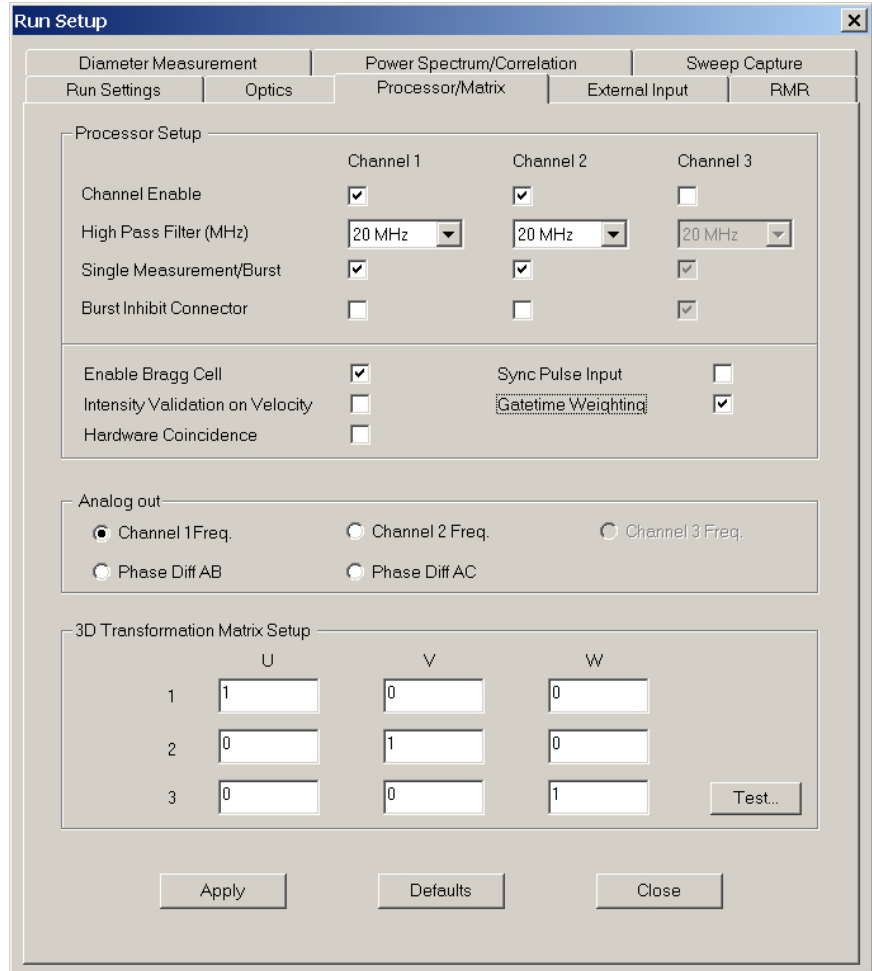


Figure 9-2
Processor/Matrix Screen

Vector to Analyze: Velocity component or components whose power spectrum needs to be computed.

Analyze Method: There are two methods of analysis—*Slot Analysis* and *Even-Time Analysis*.

Slot Analysis: This method allows for the random arrival of velocity data. The process involves first a computation of the autocorrelation of raw data. This would generate an Autocorrelation function with random values of the time delay. This Autocorrelation function is “binned” to have equal ΔT values. In other words, the autocorrelation values are computed for equally spaced delay times. Fourier transform of this provides the power spectrum values. Please see Appendix B for more details on the technique.

Even-Time Analysis - Data needs to be collected in *Even-Time Sampling* mode (See Figure 9-2). This approach is used when the data rate high enough so that even-time sampling mode of data collection would be feasible—i.e., there is a new data point every time the sampling is done. This approach would not need Velocity bias correction to compute the statistics. *Slot Analysis* is the default Analysis Method.

Windowing Method: Lists the different windows that can be selected for FFT. Default selection is Hanning. You can also select No Windows.

Points per FFT: The range of values are 512–4096. As this value increases, the frequency resolution also increases. Default value is 512.

Enable Range Limits: Selecting this option would allow you to select portions of the data file to compute the spectrum. For example, selecting this option and choosing **Start** to be 1 and **Stop** to be 1024 would result in computing spectrum for the first 1024 points. If this is not selected, the entire data file (in blocks of 512) will be used for the computations.

Slot Analysis Options include:

Auto (Avg TBD): Selecting this would estimate the average dT for Autocorrelation to be computed from the average value of time between data (TBD). This is the default selection.

Correlation dT : If *Auto (Avg TBD)* was not selected, the value for Correlation dT (in microseconds) needs to be entered manually. The Autocorrelation function will be “binned” into an equally spaced distribution based on this value of dT .

50% Overlap: Choosing this will generate the Autocorrelation function using 50% overlap of the data.

Increment: Increment of 1 uses all the data to compute the Power Spectrum. Increment of 2 implies that every other data point will be skipped. In this case, only half the number of data points would be used for computing the spectrum. This approach could be used to get higher resolution at the lower end of the frequency spectrum, provided that a large number of data points have been collected.

CHAPTER 10

Using Subrange, Coincidence Modes and Even-Time Sampling

The FLOWSIZER™ Data Acquisition and Analysis Software can process and display your data in three different ways. By default, all the data that the processor can process are transferred to the host computer via the FireWire interface. FLOWSIZER displays this data as you acquire it, and it is also displayed during Playback. This means, using a 2D PDPA example, that a droplet could pass through the measurement volume and only allow a U component velocity measurement to be made (i.e., no diameter, no V velocity component). The default FLOWSIZER view (i.e., neither Subrange nor Coincidence button selected) would show the U velocity measurement in all the U velocity plots and histograms, even though its accompanying diameter and V velocity measurement cannot be included anywhere. This is often not desirable, such as when looking for diameter-velocity correlations, or velocity-velocity correlations. For these situations, the data can be “filtered” or “sorted” to select only those particles with no missing measurements—in the 2D PDPA example, the Diameter, U component velocity, and V component velocity must all be present. This is known as coincident data, and is explained in more detail later in this section. The data can also be “filtered” or “sorted” to select only those particles whose diameter, velocity, etc. fall within certain limits. This is known as subranged data and is explained in the following paragraphs. No data is ever deleted or lost when using the subrange and/or software coincidence features. It is simply not shown.

The analysis capabilities of FLOWSIZER are very powerful, and part of that power comes from the capability to set limits on a measured variable and then investigate other measured data that falls inside those limits. To do this, we need to use both Subrange AND Coincidence buttons in FLOWSIZER. Subranging sets bounds for the variables we are examining. Coincidence sorts out all the other data so that we are left with only those that are associated with data within the subrange.

You may have a 1D PDPA system, for example, and measure a velocity histogram with two distinct peaks. You ask whether the flow really has a bimodal velocity distribution, and if it does, is each peak associated with different diameter characteristics? The lower velocity peak may be associated with a larger droplet diameter, for example.

You may have a 2D PDPA system, for example, and measure a transient (pulsed) spray. The independent variable in this case is time, specifically time After Start of Injection (ASOI). The axial velocity will vary greatly with time ASOI, initially being very high (near the nozzle exit velocity, depending on how far from the nozzle you are measuring) and after injection stops, decaying exponentially. The diameter and radial velocity will also vary greatly with time ASOI. You will want to subrange out various portions of the injection process to examine the diameter during actual injection, for example. You may also need to quantify the entrainment of ambient gas by examining the radial velocity during and/or after the actual injection process. You may want to examine the diameter of droplets entrained into the spray after injection stops.

Subranging and coincidence allows you to investigate these types of questions and analyze your data quickly and in great depth.

Inputting Subrange Values

Click the **Subranges (Over/Under)** tab in the controls area (right part of the FLOWSIZER window). As shown in Figure 10-1, five measured parameters can be subranged. These include:

- Velocity
- Gate Time
- Diameter
- Intensity
- Time

If the system is equipped with the External Input option, four additional analog and four additional digital subrange inputs are also available. The system shown in Figure 10-1 was not equipped with the External Input option, so the relevant fields are disabled.

For each variable, you can select a lower limit only, an upper limit only, or both an upper and lower limit.

LDV Controls		Diameter Measurement		
Intensity Validation/PVC		Subranges (Under/Over)		
	Channel 1	Channel 2	Channel 3	
Min Velocity (m/sec)	179	-2000	-2000	
Max Velocity (m/sec)	190	2000	2000	
Min Gate Time (usec)	0.1	0	0	
Max Gate Time (usec)	200	16960	16960	
	Diameter (um)	Intensity (mV)	Time (sec)	
Minimum	5	0	0	
Maximum	30	1000	300	
External	Analog		Digital	
	Minimum	Maximum	Minimum	Maximum
Channel 1	0	65535	0	65535
Channel 2	0	65535	0	65535
Channel 3	0	65535	0	65535
Channel 4	0	65535	0	65535
Apply		Defaults		

Figure 10-1
Subrange Input Menu

Example Subrange Analysis

Figure 10-2 shows the Velocity and Diameter Histogram Windows for a 2D PDPA run with a bimodal U velocity histogram. In this section, we will analyze this data using subranges, to show the capabilities of subrange analysis.

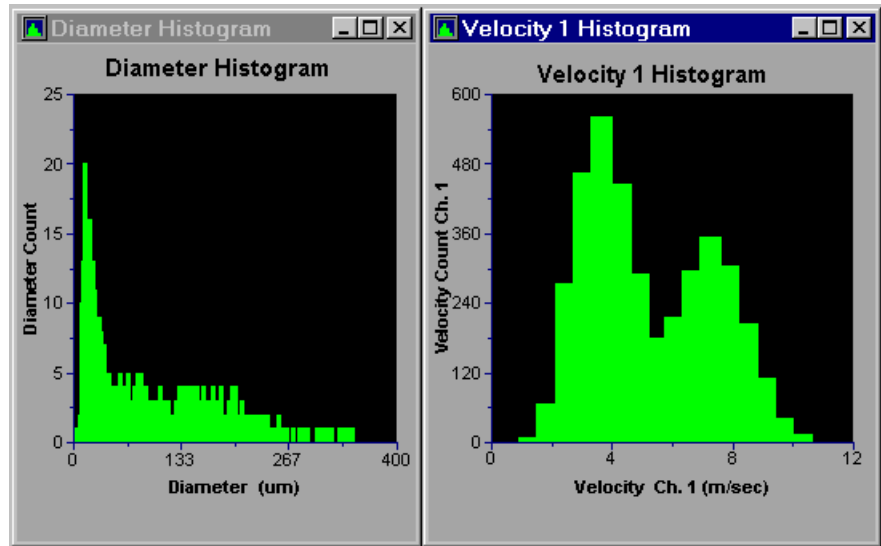


Figure 10-2
Diameter and Velocity Window for Subrange Example

Velocity Subrange

The descriptive statistical variables describing a bimodal velocity distribution, such as that shown in Figure 10-2, may not be very meaningful. In this case, we can subrange the Channel 1 Velocity between the two peaks—or, at 5.6 m/s in this example. We then have two populations or “subranges,” one below 5.6 m/s and one above 5.6 m/s. We will use only the U Velocity (Channel 1) subrange. Figure 10-3 shows the FLOWSizer Window. All the results displayed here are associated with only those particles having a velocity under 5.6 m/s, i.e., those in the lower peak. Note the following:

- A value of 5.6 m/s is entered in the subrange on the right
- The Subrange button is pressed
- The Coincidence button is pressed
- Only the lower channel 1 velocity peak is present
- These slower-moving droplets tend to be smaller

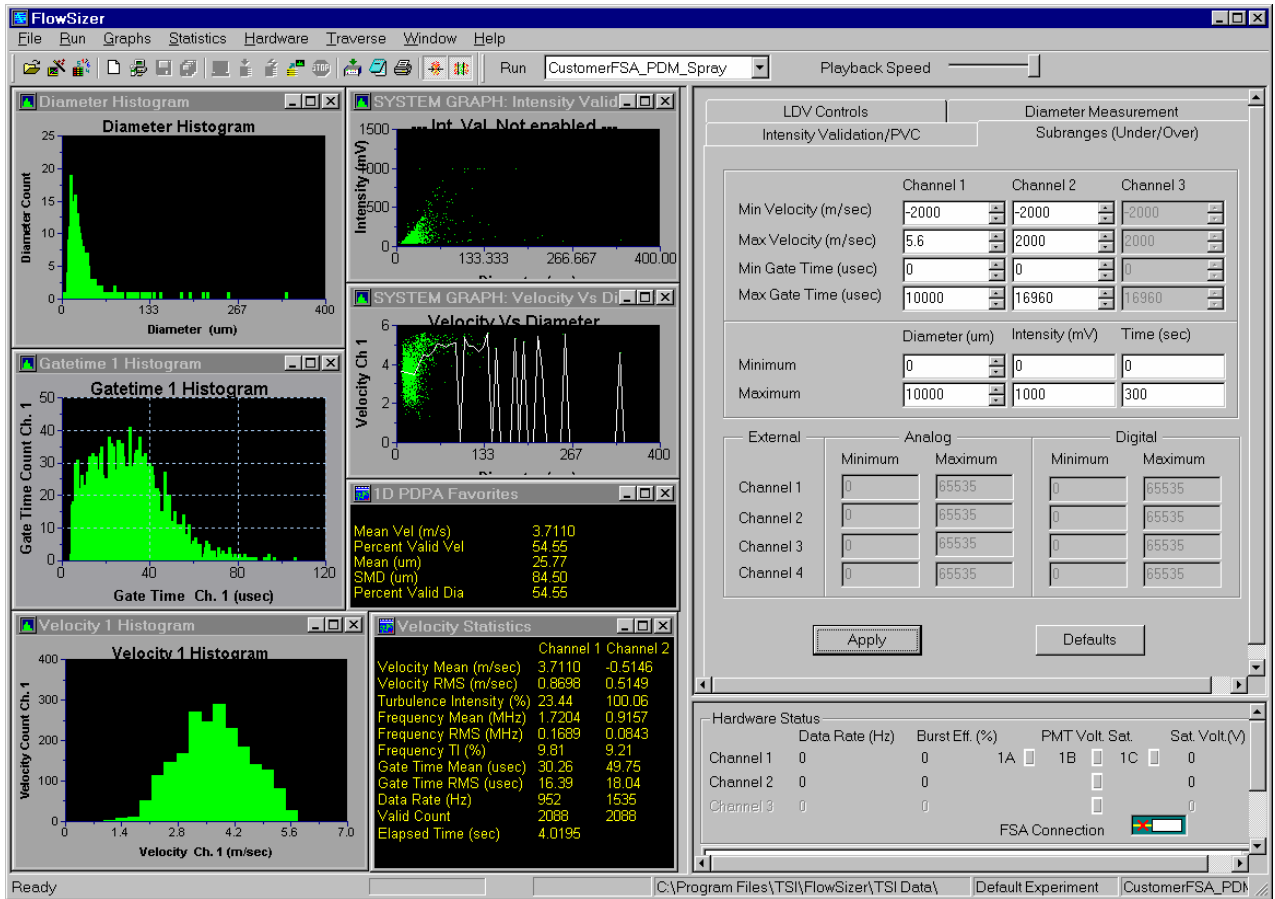


Figure 10-3
 FLOWSizer Window for Lower Velocity Subrange

Next we will examine the particles in the upper channel 1 velocity peak. Figure 10-4 shows the FLOWSizer window for this data. All the results displayed here are associated with only those particles having a velocity above 5.6 m/s, i.e., those in the upper peak. Note the following:

- ❑ A value of 5.60001 m/s is entered in the Ch.1 Min. Velocity subrange, on the right
- ❑ The Subrange button is pressed
- ❑ The Coincidence button is pressed
- ❑ Only the upper channel 1 velocity peak is present
- ❑ These faster-moving droplets tend to be larger, although all diameters appear to be represented

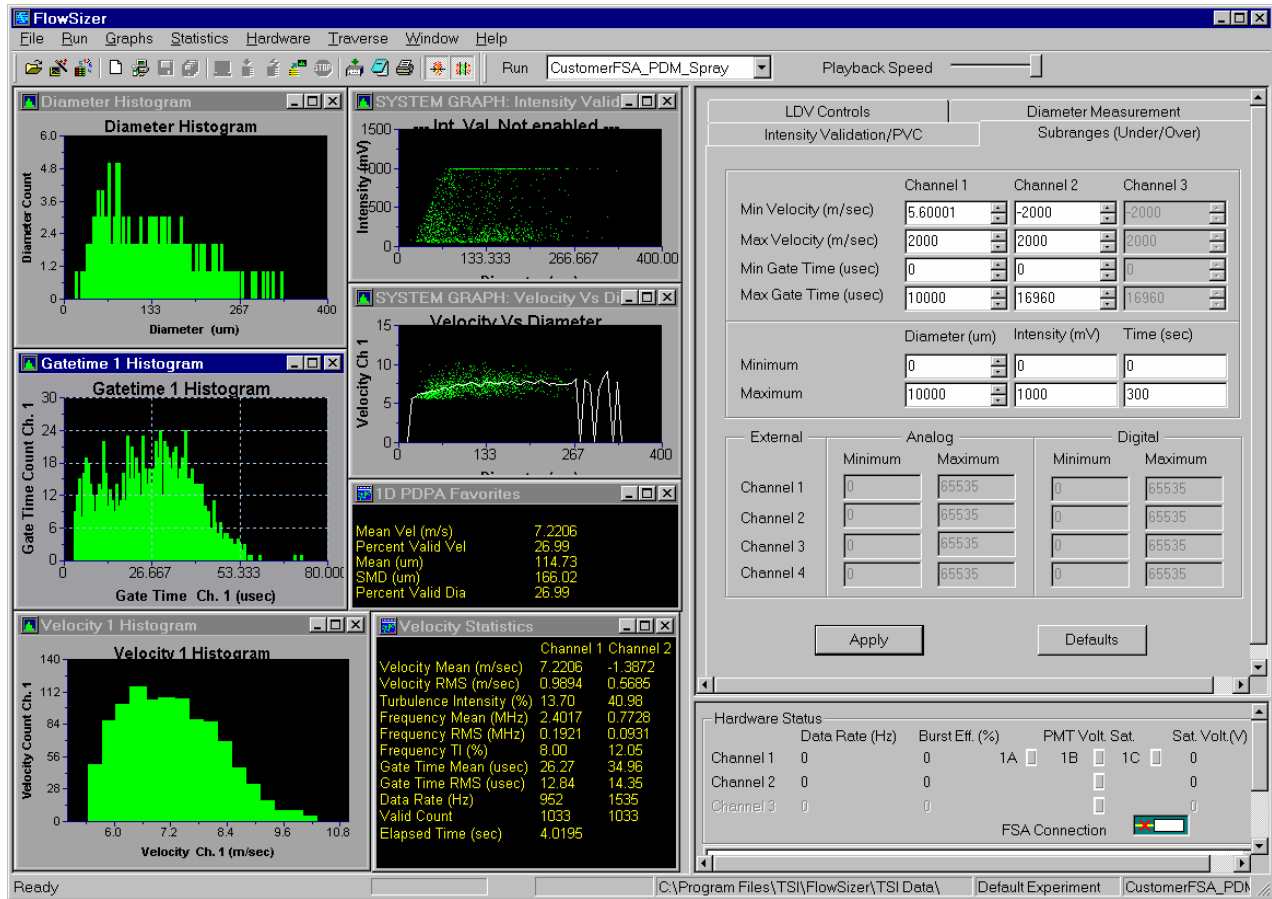


Figure 10-4
FLOWSizer Window for Upper Velocity Subrange

Other Subrange Suggestions

As mentioned above, other variables can be subranged as well. Any component of Velocity or Gate Time, Diameter, Intensity, Time, or External data may be used. The case of a transient (pulsed) spray presents many possibilities of subranging. You may wish to examine nearly saturated intensity droplets, nearly zero intensity droplets, various time intervals, or velocity intervals (reversing flow, for example).

Subranging can improve the reliability of your data by verifying that known characteristics are indeed present. Do larger droplets tend to have a higher velocity, for example. Subranging can expose characteristics of your data that are covered up by other parts of the data. A relatively few large droplets may have a fluctuating velocity, for example. But when displayed in non-subranged, non-coincident mode, the effect is covered up by all the other droplets.

So the best solution is to explore your data using subranges and coincidence.

Software Coincidence Mode

This mode of operation is used when two quantities (e.g., velocity components) need to be collected or sampled simultaneously. For example, the coincidence mode of operation is used to obtain Reynolds stress values, instantaneous velocity vector and velocity-size and other correlations.

Simultaneous sampling or collection of two quantities is done when both the measurements are obtained within a preselected small time window. This window is generally referred to as the Coincidence Window.

To set up the Coincidence window, go to the set of controls on the upper right corner of the main software window. Select the **LDV Controls** tab (Figure 10-5).

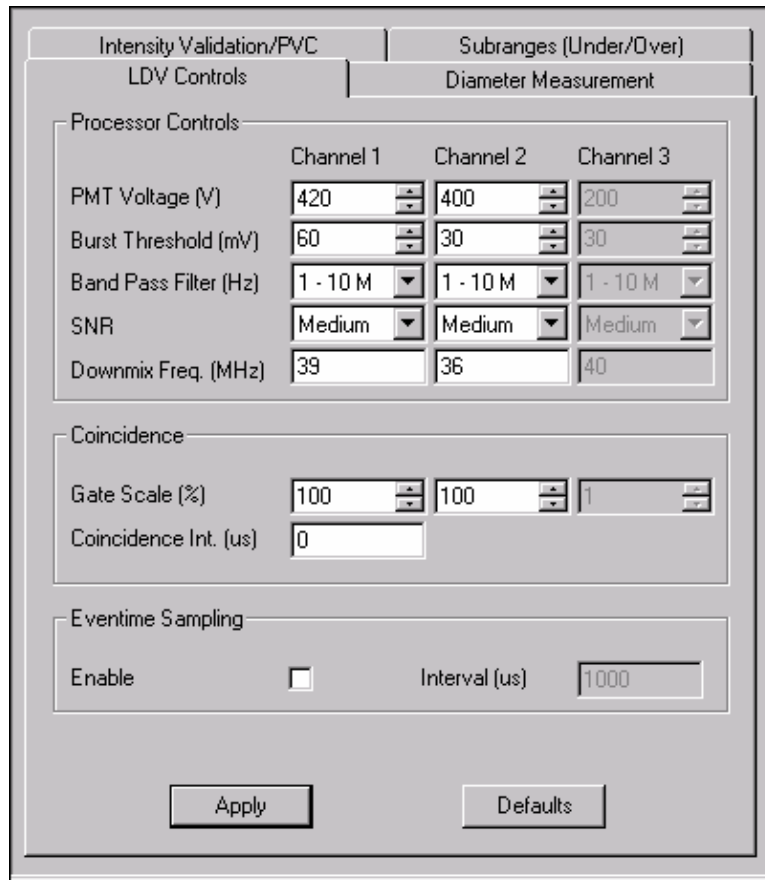


Figure 10-5
Coincidence Window Setup

Coincidence Window Selection

Gate Scale (%)—The Gate Scale controls how many gate widths the software looks forwards and backwards from the gate on one channel to find a gate on another channel. This value is set for each enabled channel and ranges from 0–1000%. A typical value is 250%. The Gate Scale is measured from the center of the burst gate on the corresponding channel. With a Gate Scale of 100%, for instance, the software will look half a gate forward and behind the center of the gate. This is essentially the same as hardware coincidence. Refer to “**Run Setup** → **Processor Matrix**” in Chapter 2 for details on hardware coincidence.

The upper burst gates in Figure 10-6 would be coincident with a 100% gate scale on each channel. With a gate scale of 200%, FLOWSizer lengthens each burst gate by 100% forward and 100% behind. The upper burst gate in Figure 10-6 would again be coincident at this gate scale. The lower burst gate would not be coincident at 100% or 200% gate scale but are coincident at 300% gate scale.

Coincidence Int. (μs)—This specifies a coincidence interval in microseconds. This value is added to each coincidence window. Thus, coincidence is determined by a combination of percent of gate time and a fixed window. Just one of the methods can be used by setting the other to zero. Coincidence interval becomes important with very short gate times because time stamp resolution limits the ability of particles to exhibit overlapping. In flows where the mean gate time is less than $2 \mu\text{s}$, consider using a $1 \mu\text{s}$ Coincidence Interval. When the mean gate time is less than $1 \mu\text{s}$, you should always use a Coincidence Interval of $1 \mu\text{s}$ to $2 \mu\text{s}$.

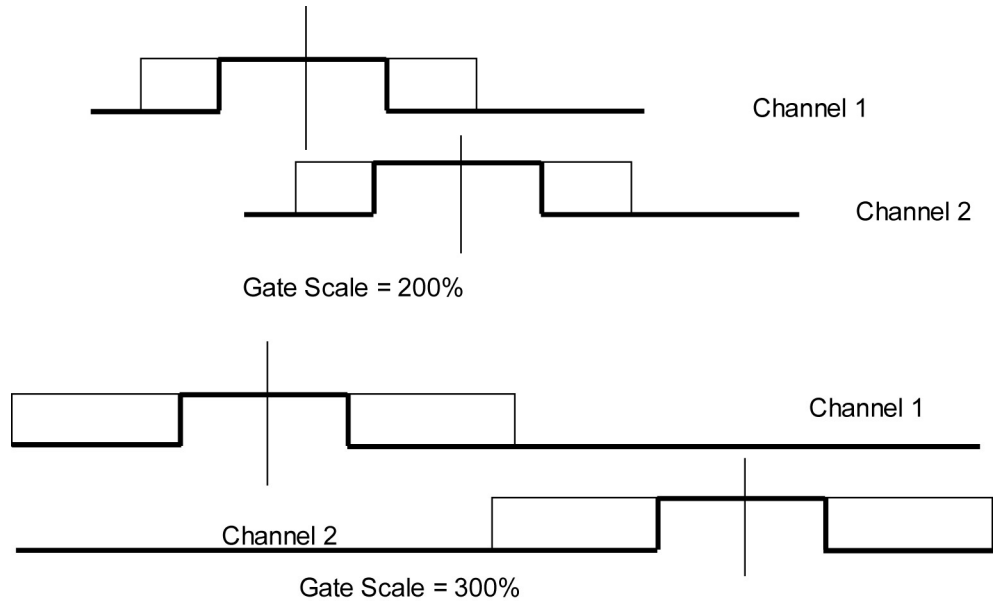


Figure 10-6
Examples of Software Coincidence Checking

Software Coincidence Mode of Operation

To activate Software Coincidence mode of operation go to the main software window.



Figure 10-7
Software Coincidence Button

Press the button identified as **Software Coincidence** (Figure 10-7). This will activate Software Coincidence mode of operation.

When data are played back, you may notice more or less total samples present. This is normal and results from the fact that for software coincidence, no data is discarded, it is simply not shown. Thus, if the coincidence window is increased, you could possibly

increase the Maximum Particle Measurement Attempts and obtain more total samples.

For a one-component PDPA system, Coincidence mode selection would result in using only data points that have both velocity and size information. In other words, data points with only velocity and no size measurements would not be displayed. For multi-component PDPA systems, Coincidence selection would result in using or selecting data points that have both size and the multiple components of velocity measurements. For size-velocity correlation results, the system needs to be operated in Coincidence mode.

In the case of three-component LDV systems, selecting coincidence would result in only using data points that have all three-component measurements. This means that all three velocity component measurements occurred within the specified Coincidence window time. The same comments are valid for a two-component LDV system. If the LDV or PDPA system is collecting external data (e.g., pressure), to calculate velocity-pressure or size-pressure correlations, the system needs to be operated in Coincidence mode.

Coincidence is also used with Subranging. Subranging sets bounds for the variables we are examining. Coincidence sorts out all the other data so that we are left with only those that are associated with data within the subrange.

No data is ever deleted or lost when using the subrange and/or coincidence features. It is simply not shown.

Software Coincidence Capture

To this point, software coincidence has been discussed in terms of playing back saved data. When new data are acquired with software coincidence enabled, you will obtain the same number of samples on each channel enabled. Be aware that additional noncoincident data are also saved. As a result, the computer's memory could be consumed by noncoincident samples and could cause capture to be terminated (in low coincidence situations).

Hints

1. Optical overlap of the measurement volumes determines your coincidence ratio. Unreasonably long gate scales (>500%) cannot compensate for misaligned measurement volumes—including 3D probe layouts. It is advisable to use your microscope objective to verify overlap of the measurement volumes before you begin taking data. See the “TM/TR Series Fiberoptic Probe” manual for more details.

2. When using hardware coincidence with PDPA systems, you must use software coincidence as well, to ensure each diameter measurement also has a velocity measurement. Hardware coincidence only checks for internal overlap of the gates (in the FSA), *not* the presence of a valid diameter.
3. Typical Gate Scale settings are 250%. Typical Coincidence Interval settings are 1 or 2 μs and become necessary when mean gate times are less than 1 μs .
4. Good 3D coincidence starts with use of the pinhole and then the microscope objective, to achieve good overlap of measurement volumes. Then the FLOWSIZER Burst Monitor or an oscilloscope can be used to achieve the best overlap of channel 1/2 burst gates with channel 3 burst gates.

Even-Time Sampling

LDV is a technique where the flow's velocity is sampled, and particles crossing the measuring volume determine when samples are taken. Enabling Even-Time Sampling causes the software to not use all the possible samples, but only one sample out of a given time period. The main benefit of this approach is to remove velocity bias. Even-Time Sampling is not done in the processor, but in the FLOWSIZER software. The software selects one data point from each time interval using the data's time stamp.

Velocity Bias

The concept of velocity bias is easiest to explain in terms of mean velocity. By "mean" we are referring to a time average. In other words, the "mean" of a continuous but fluctuating analog signal is the value obtained with a sufficiently long averaging time so a second reading of the same flow would provide the same value within an acceptable error band.

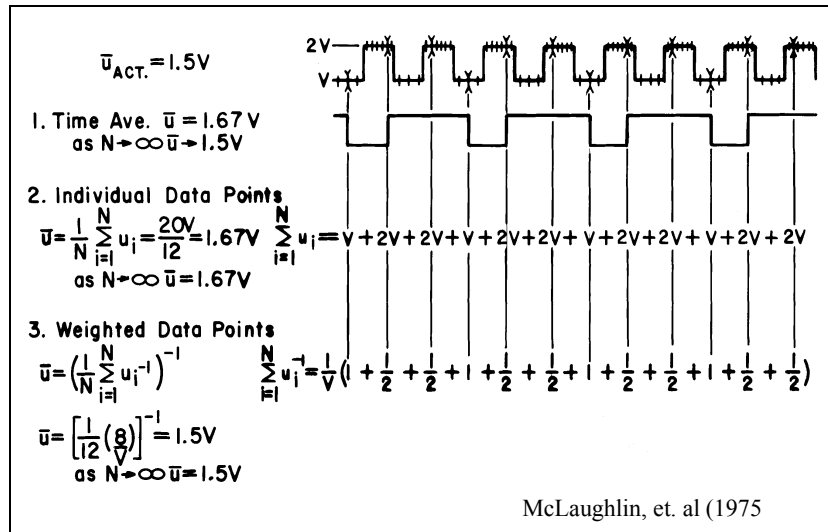


Figure 10-8
Velocity Bias

In LDV, the measurement is on individual particles as they traverse the measurement volume. It is quite clear that as the velocity increases, more particles will traverse the measurement volume per unit of time. In fact the number should be proportional to the velocity. Therefore, if you simply average the individual measurements being made, the result will be biased to the high velocity side since there will be more measurements per unit of time at the higher velocities.

As shown in Figure 10-8, in a one-dimensional flow situation, simply applying a correction based on the measured velocity works. But the flow is not normally one-dimensional. Also, any bias correction must consider all biases in the system, not just velocity.

The best solution is to provide a high enough seed density so that uniform time sampling or some similar technique can be used.

Using the Even-Time Sampling Feature

Even-Time Sampling is enabled under the LDV Controls tab on the upper right corner of the screen. Checking the enable box causes the software to use only one data point, the first point in time, from each time interval. Enter the time interval in microseconds. When selecting the time interval, the main thing to keep in mind is that the processor data rate must be several times larger than the even-time sampling data rate. The processor data rate is displayed in the hardware status box in the lower right corner of the screen. The even-time sampling rate is $1/\text{sampling interval}$. The result of even-time sampling is that the samples obtained are at equally spaced

time intervals. The data arrival (due to particle arrival in the measuring volume) is random. In the even-time sampling process, the first available data point in each time interval is taken as the sample. Hence, the data rate needs to be much higher (say, about 10 times) than the sampling rate, so that the collected samples occur very close to the sampling time. Consequently, the minimum even-time sampling interval you can use will be determined by your processor data rate.

CHAPTER 11

Outputting Analog Data

In some cases you may want to output an analog signal, which is proportional to the signal frequency (particle velocity) or phase (particle size) of the signal. This is a simple two-step process. First set up the software and second connect to the Analog Out BNC that is found on the back of the FSA processor. To set up the software go to **Run → Run Setup**. Then select the **Processor/Matrix** tab. You should now see a window similar to the one shown in Figure 11-1.

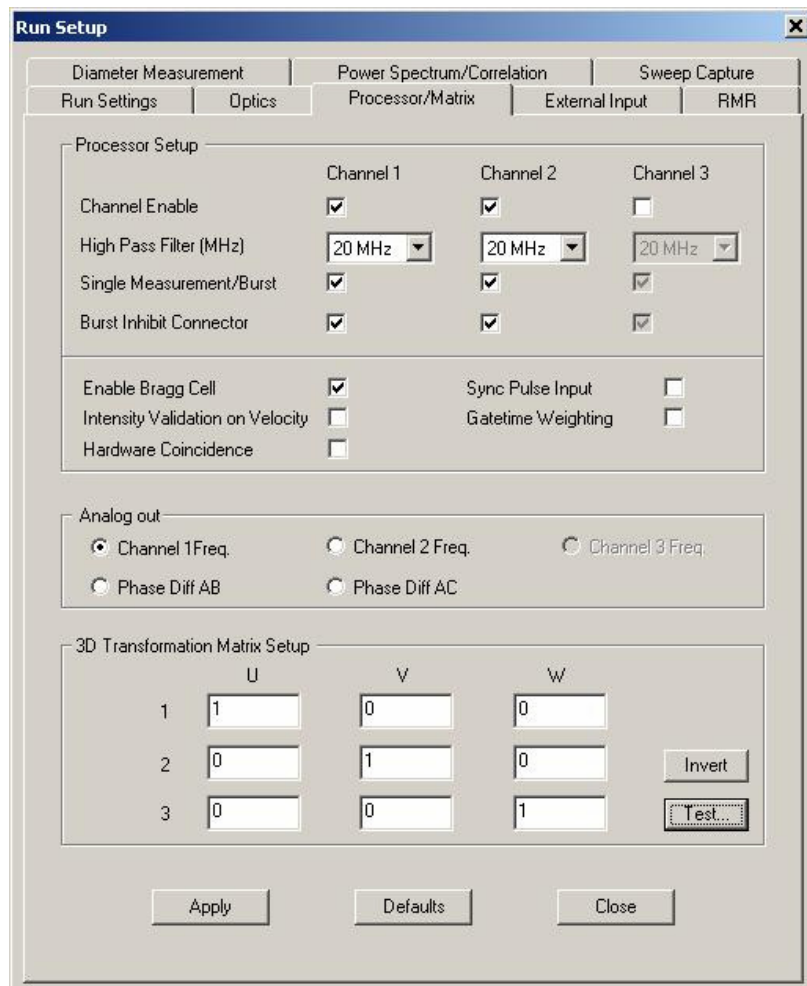


Figure 11-1
Window for Selecting what Analog Signal to Output

Look at the **Analog out** portion of the window. Depending on how many channels of velocity you have enabled and whether or not you have sizing enabled, you will see certain parameters grayed out. In this example, the system is set up for two channels of velocity and size. Thus the **Channel 3 Freq** is grayed out. Select the parameter that you wish to output as an analog signal. You can only output one signal at a time. In this example, we are outputting the channel 1 frequency.

Next connect a standard BNC cable to the BNC connection on the back of the FSA labeled **Analog Out**. This BNC output provides a 0- to 10-volt signal corresponding to the frequency or phase that you have selected. The output is updated for every valid burst from the selected parameter. When data capture is started from the software, the output resets to 0 volts until the first valid burst occurs.

The range of frequencies indicated by the analog out voltage depends on the bandpass filter range selected in the FLOWSizer software as shown in the following table. Note that this output indicates frequency, not velocity, so there may not be a 1 to 1 relation between the two depending on the type of downmixing used. If phase is selected, 0 volts corresponds to 0 degrees and 10 volts corresponds to 360 degrees. This output can supply up to 30 milliamps of current.

Bandpass Filter Range	Frequency	Voltage	Frequency	Voltage
0.3-3 kHz	0.3	1	3	10
1-10 kHz	1	1	10	10
3-30 kHz	3	1	30	10
10-100 kHz	10	1	100	10
30-300 kHz	30	1	300	10
100-1000 kHz	100	1	1000	10
0.3-3 MHz	0.3	1	3	10
1-10 MHz	1	1	10	10
2-20 MHz	2	1	20	10
5-30 MHz	5	1	30	6
5-40 MHz	5	1	40	8
5-50 MHz	5	1	50	10
10-65 MHz	10	1	65	6.5
20-80 MHz	20	2	80	8
10-100 MHz	10	1	100	10
50-100 MHz	50	5	100	10
40-120* MHz	40	2	120	6
60-150* MHz	60	3	150	7.5
20-175* MHz	20	1	175	8.75
75-175* MHz	75	3.75	175	8.75

*FSA 4000 only

CHAPTER 12

Using RMR (Shaft Encoder or OPR)

This chapter briefly covers the approach to input RMR—Shaft encoder or OPR (once-per-rev).

The first screen is found under **Run** → **Run Setup**. Then select the **RMR** tab, as shown in Figure 12-1.

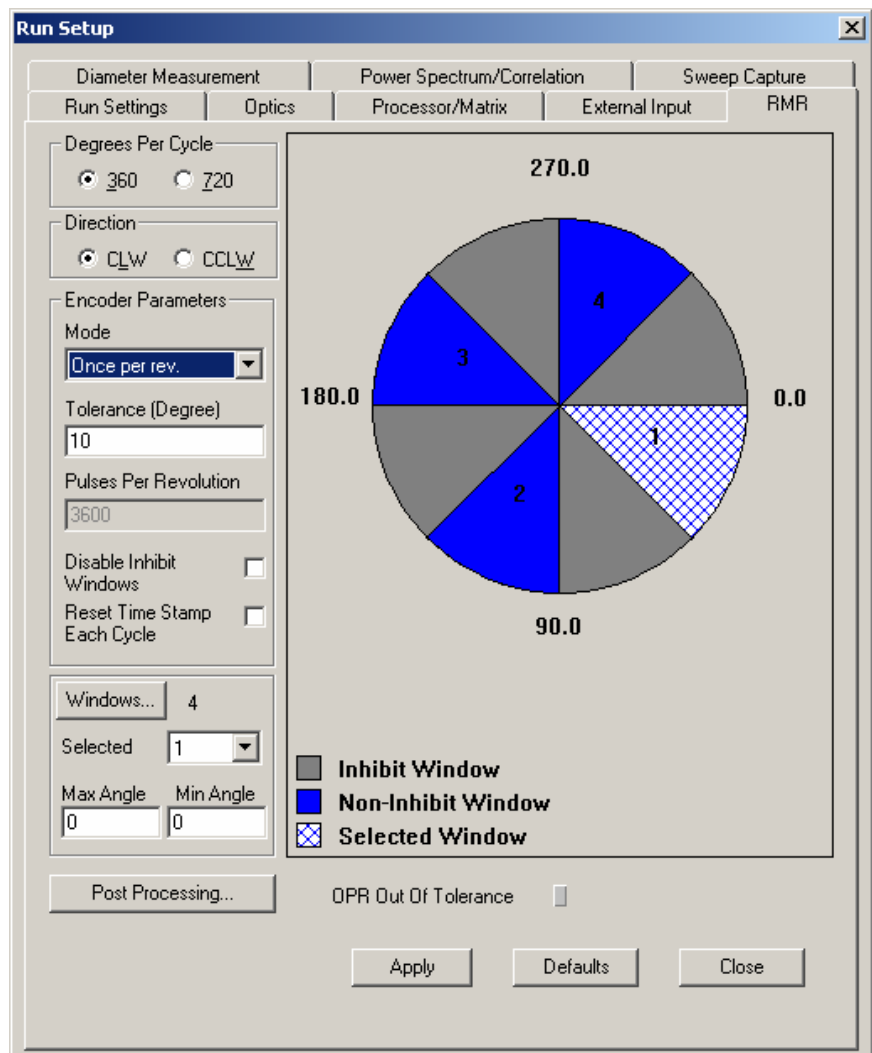


Figure 12-1
RMR Screen

Degrees Per Cycle

The resolver attaches a once-per-revolution pulse for every rotation (360 degrees) or every two rotations (720 degrees).

360

Select if the experiment test range is over a 360-degree cycle.

720

Select if the experiment test range is over a 720-degree cycle.

To create a 720-degree period, every other “once-per-rev pulse” is ignored. Use the active real-time displays to make sure that the windows are synchronized with the right “once-per-rev pulse.”

Direction

The graphical RMR window selection control can be changed to make it easier to visualize the selected windows. This control reflects the direction selected.

CCLW

Choose this to select *counterclockwise* direction. The displayed angles increase counterclockwise

CLW

Choose this to select *clockwise* direction. The displayed angles increase in a clockwise direction.

Encoder Parameters

Allows you to specify the following parameters:

Mode

The following modes of operation are available.

RMR Off

This is the default selection and corresponds to a case when no RMR is used.

Once Per Rev.

Choose this when the signal input into the RMR is the once-per-rev (OPR) signal. The RMR will use a once-per-rev pulse as a synchronizing input and divide the revolution period into 3600 pulses. This method relies on a stable time period between once-per-rev pulses.

If the periods are not stable, the **OPR Out Of Tolerance** will flash and the data for that cycle will be marked as Out of Lock. Use the “Tolerance” to select the maximum fluctuation allowed to be considered in lock.

Shaft Encoder x2

This mode multiplies the shaft encoder resolution by 2. For example, if the shaft encoder has a basic resolution of 500 then the Resolver Points Per Cycle value will be equal to 1000.

Shaft Encoder x4

This mode multiplies the shaft encoder resolution by 4. For example, if the shaft encoder has a basic resolution of 500 then the Resolver Points Per Cycle value will be equal to 2000.

Tolerance (Degree)

This selection determines how stable the once-per-rev pulse needs to be and still be considered in lock. The value needs to be expressed in degrees. This means that a nominal 3600 pulses per Revolution OPR with 1 degree selected can vary from 3610 to 3590 pulses per revolution and still be considered in lock.

Pulses Per Revolution

The number of encoder points per revolution output by the shaft encoder installed on the system. If (operating) **Mode: Once per rev.** is selected, the only choice is the default value of 3600.

Disable Inhibit Windows

The inhibit windows enable you to inhibit data collection at certain angular positions, such as when a rotating blade is in the

measuring volume. Checking this box disables this feature and allows data collection at all angles. Unchecking this box causes data collection inhibiting to follow the windows you setup as defined below.

Reset Time Stamp at OPR

This provides the option to reset the time stamp, if desired, when the once-per-revolution signal is received. This applies to once-per-revolution or shaft encoder mode.

Windows

This set of parameters controls the creation and adjustment of acquisition windows.

To update the RMR hardware to match the display, press the **Apply** button.

RMR Windows Display Graphic

The screen contains a display control in the shape of a circle with the current selected windows displayed as pie-shaped wedges at the defined angles. The quadrant angles are marked in degrees based on direction. Each window is marked with its window number. If a window is selected, it will be drawn in a cross-hatch pattern. Max. Angle and Min. Angle provide the beginning and end of the window.

Modifying RMR Windows

To modify windows follow these procedures:

Auto

This selection brings up a set of controls to generate equally spaced windows.

Automatic RMR Window Generation Parameters

The following describes the Automatic RMR Window Generation parameters.

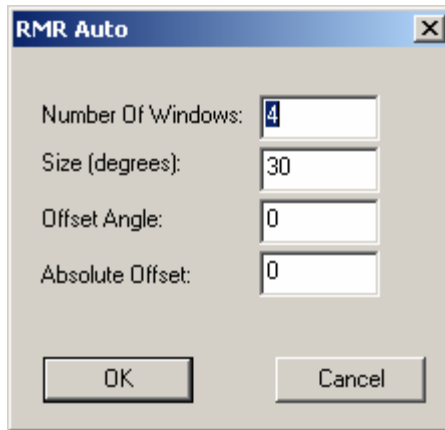


Figure 12-2
Automatic RMR Window Generation

Number of Windows

The number of windows desired per period. The windows are evenly divided into 360 (720 if selected) degrees.

Size (degrees)

The size of each window in degrees.

Offset Angle (degrees)

The offset that will be added to the placement of all of the windows. In effect the whole window pattern is shifted in degrees by this amount. Use the offset to adjust the window pattern.

Abs Offset (degrees)

The amount by which the graphic display is shifted. Use this to adjust the display to match the actual model so that the “0” angle is at a more intuitive point rather than the default position.

OK	<i>Selects choices made.</i>
Cancel	<i>Exits without saving any changes made.</i>

After using the Auto. Approach to select the window duration, each window width could be altered by typing in Min. and Max. Angle desired for the window.

Windows

This information field displays the number of windows per cycle.

Selected

Displays the number of the selected window. This window is displayed in the graphic control in a cross-hatch pattern with minimum and maximum values displayed in the Max and Min boxes. To change the “Selected” window, type in the window you want to select in the entry field or left click on the window you want to select.

Max. Angle

Edge of the selected window with the largest angle value.

Min. Angle

Edge of the selected window with the smallest angle.

Post Processing

RMR post processing enables you to view the mean and rms of diameter, volume, and velocity data binned by RMR angles. You can bin your data either by angle or by time interval.

Apply

Sends the settings from the graphic control to the RMR hardware. Window settings **do not** become effective until this button is pressed.

CHAPTER 13

Setting Up and Using a Traverse

If you are using a traverse in your experiment, you need to set up the mode in which you want to operate it and also set the parameters through the **Traverse** menu option.

Select **Traverse** → **Start** to open the main traverse interface.

Select **Traverse** → **Scan Capture** to start the automatic capture process based on the Matrix of positions and filenames you selected. Matrix can be entered manually or automatically. The spreadsheet within this module is fully compatible with Microsoft® Excel. Therefore, you can copy and paste to and from both applications.

Please refer to “Sweep Capture” section in Chapter 3 to capture data while traverse is moving.

Setting the Traverse Parameters

To specify the traverse parameters, select the Traverse option from the command menu bar and then select one of the three control options:

- Manual
- Auto
- Matrix

The following paragraphs describe these parameters.

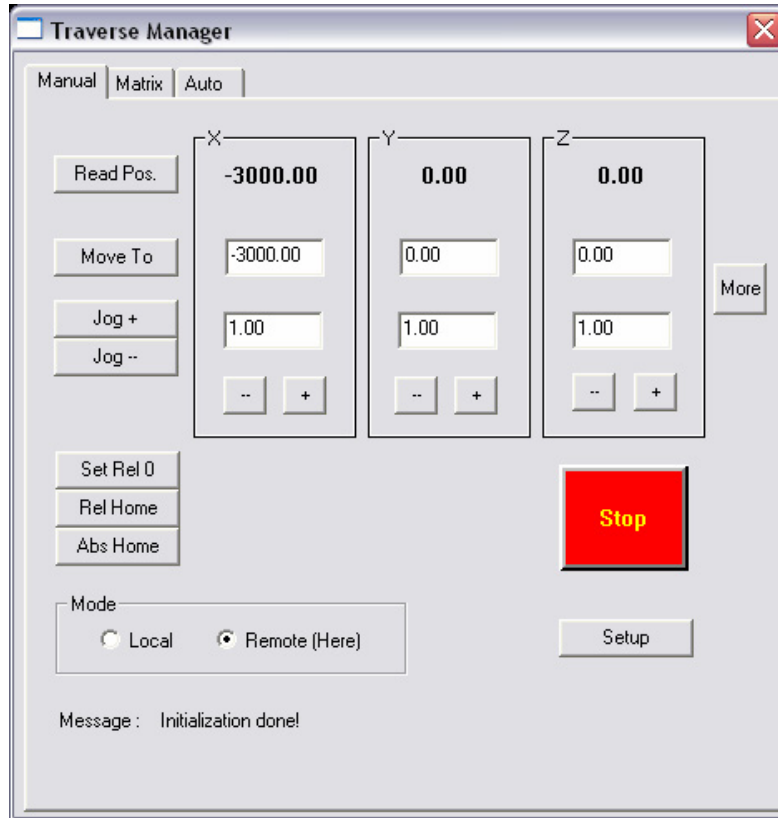


Figure 13-1
Traverse Manager Screen

Manual

This option allows manual control of the traverse.

The following parameters or options are available:

Manual Setup

Parameter	Description
Stop	Halts traverse motion. Motion on the <i>x</i> , <i>y</i> , <i>z</i> , <i>u</i> , <i>v</i> , and <i>w</i> axes stops and the current position of the traverse is read and displayed in the X, Y, Z, U, V, and W group boxes.
Move To	Moves all connected axes to the position entered in the X, Y, Z, U, V, W, Move boxes.
Jog+	Moves all connected axes by the displacement value entered in the X, Y, Z, U, V, W, Jog boxes in the positive direction.
Jog-	Moves all connected axes by the displacement value entered in the X, Y, Z, U, V, W, Jog boxes in the negative direction.

Parameter	Description
X, Y, Z	<ul style="list-style-type: none"> • The X, Y, Z, group boxes do the following: The top lines in each box show the current positions of the x, y, and z axes of the traverse. • The boxes next to the Move button allow you to enter a new position for each axis. When you press the Move button, all three axes of the traverse move to this new position. • The boxes next to the Jog button allow you to enter a displacement value by which you can move all three axes of the traverse. For example, if you specify .1 in the Jog boxes, when you hit Jog, all three axes move by .1. • The + or - buttons next to the displacement value boxes allow you to individually move, each axis of the traverse—plus or minus the selected displacement value.
More	Displays three more axis U, V, W.
Local	Releases the traverse control from the computer to a hardware hand control (joystick).
Remote	Restores computer control of the selected traverse.
Abs Home	Moves the traverse to its hardware zero reference point. This puts the traverse at a known reference location, indicated as 0,0,0. All future indicated positions are displacements from this point.
Rel Home	Moves the traverse to its relative zero position using the “Set Rel 0” command.
Set Rel 0	Assigns the current traverse position as the 0,0,0 reference point. All future indicated positions are displacements from this point. Current position will be set to display 0,0,0.
Setup	Set up all the driver settings, communication settings, and axis settings.

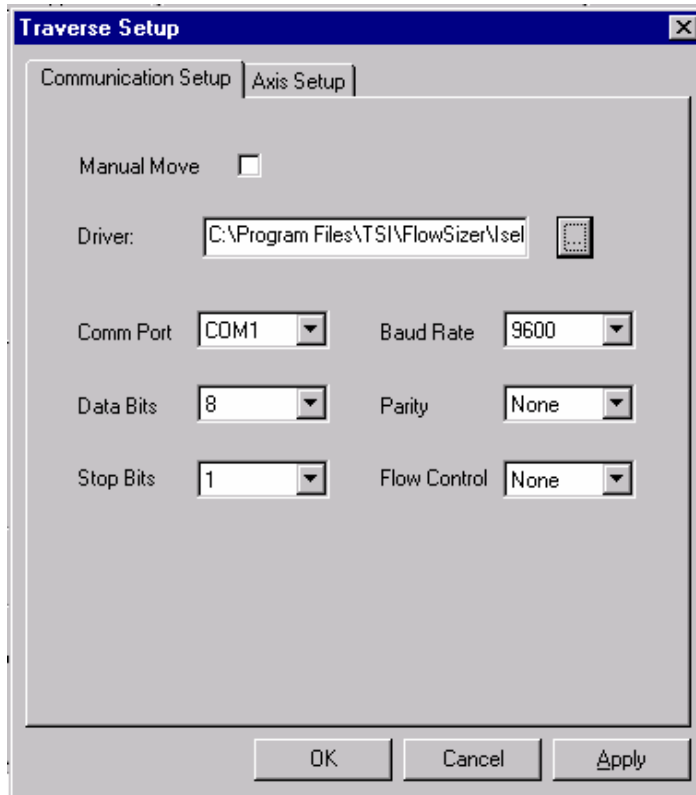


Figure 13-2
Communication Setup Dialog Screen

Communication Setup

Parameter	Description
Manual Move	Move the traverse by yourself. There will be no driver and communications needed.
Driver	Select which traverse driver to use.
Comm Port	Set the serial port the traverse is connected to.
Baud Rate	RS-232 setting determined by your traverse controller.
Data Bits	RS-232 setting determined by your traverse controller.
Parity	RS-232 setting determined by your traverse controller.
Stop Bits	RS-232 setting determined by your traverse controller.
Flow Control	RS-232 setting determined by your traverse controller.

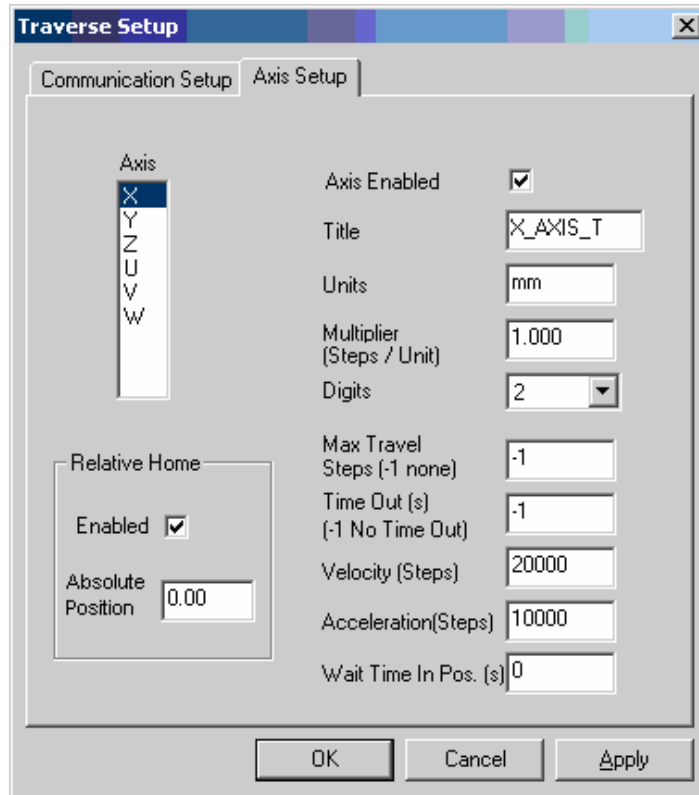


Figure 13-3
Axis Setup Dialog Screen

Axis Setup

Parameter	Description
Axis	Select which axis to set up.
Axis Enabled	Enable/Disable this axis.
Title	Name of this axis.
Units	Units of this axis, e.g., mm or inch
Digits	How many decimal points to use.
Max Travel Steps	Specify the maximum number of step the traverse can travel along each axis.
Time Out (s)	Set the timeout limit of the axis.
Velocity (steps)	Velocity of the axis, -1 means not supported.
Acceleration (steps)	Acceleration of the axis, -1 means not supported.
Wait Time In Pos. (s)	Wait time in seconds after traverse moves to specified position before data capture starts.
Relative Home	Enabled: Enable/Disable relative home. Your traverse controller should give its feedback to this setting. Absolute Position: Absolute position of the relative home of this traverse.

Auto

This selection moves the traverse step-by-step along the path stored in the current traverse position list. Use this option to test or pre-run the traverse position list for any problems before making an actual acquisition run. You can also use this option to determine if, and where, instrument commands need to be added to a position file. The current position list is displayed at the bottom of the dialog box. To select a different position list, select **Matrix** → **Open** to open an existing traverse file.

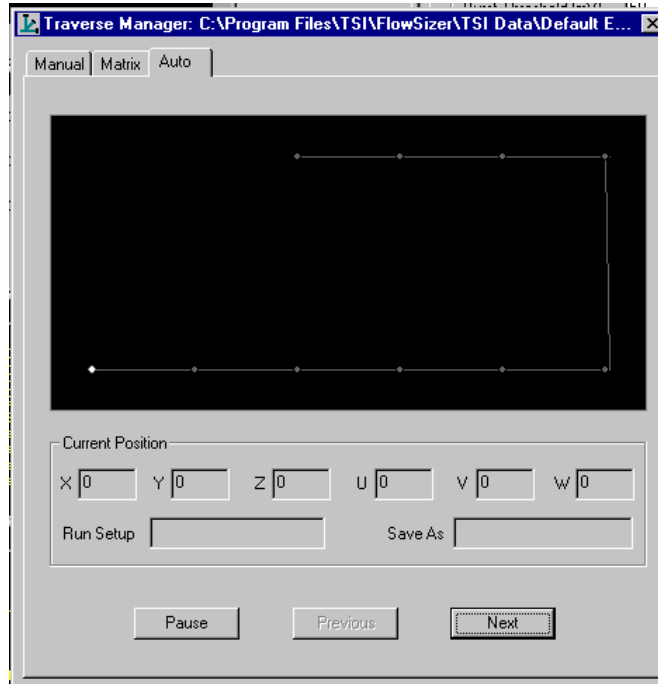


Figure 13-4
Auto Dialog Screen

Auto Setup

Parameter	Description
Previous	Moves the traverse backwards one position. Each press of this button moves the traverse to the previous position, sends out any embedded commands, and updates the position displays. Use the Matrix control to edit traverse position or commands.
Next	Moves the traverse forward one position. Each press of this button moves the traverse to the next position, sends out any embedded commands, and updates the position displays. Use the Matrix control to edit traverse position or commands.
Current Position	X: Current entry of X axis in the Matrix. Y: Current entry of Y axis in the Matrix. Z: Current entry of Z axis in the Matrix. U: Current entry of U axis in the Matrix. V: Current entry of V axis in the Matrix. W: Current entry of W axis in the Matrix. Run Setup: Current entry of Run Setup in the Matrix. Save As: Current entry of Save As in the Matrix.

Matrix

This option provides you with a spreadsheet that can be used to create and maintain traverse position lists. Traverse position lists can contain, besides position information, embedded Run Setup files and Save As files. This allows you to optimize the settings for these instruments for each position in a list without relying on a general setting for all cases.

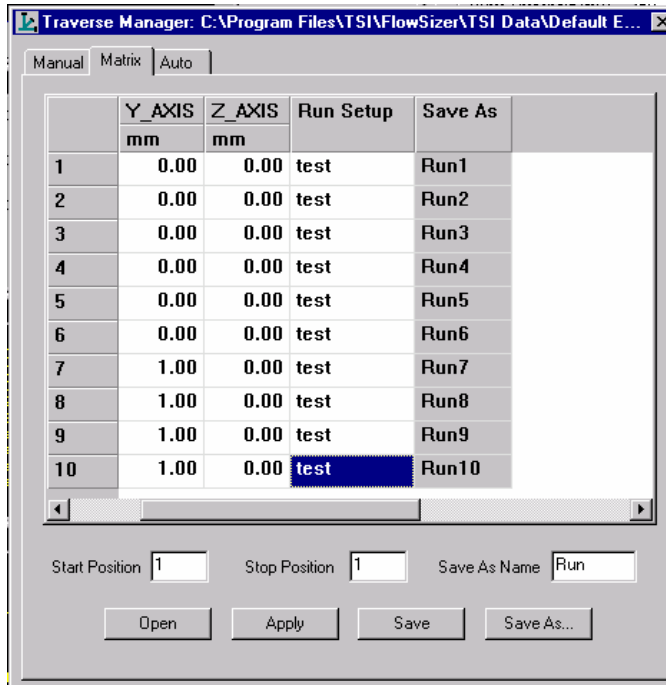


Figure 13-5
Matrix Dialog Screen

Parameter Description

The traverse position list is displayed in the spreadsheet in columns. The following describes the contents of each of these columns.

Parameter	Description
X	Contains X position.
Y	Contains Y position.
Z	Contains Z position.
U	Contains U position.
V	Contains V position.
W	Contains W position.
Run Setup	Name of the Setup file for this position. During scan capture, FLOWSizer software will load this setup file and take data based on all the settings stored in the file.
Save As	Name of the Save As file for this position. During scan capture, FLOWSizer software will save captured data to this file automatically.
Open	Open an existing .trv traverse file.
Apply	Apply all the matrix information to the software.
Save	Save current matrix to a .trv traverse file.
Save As	Save current matrix to a different .trv traverse file.

Editing Commands

The right mouse button brings up the following pop-up menu of specific traverse file editing commands.

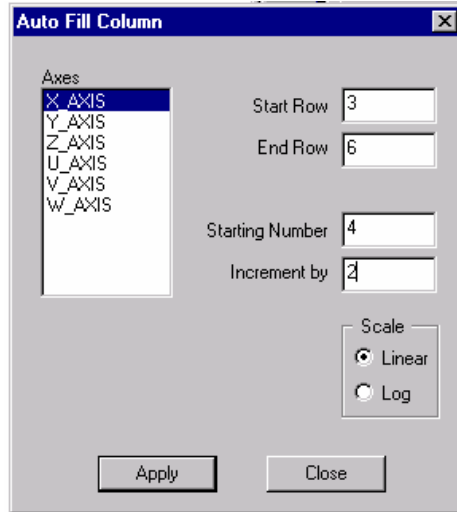


Figure 13-6
Auto Fill-Column Screen

Command	Description
Insert Row	Adds a new line at the cursor position. Use in create space for an embedded command in the traverse position list.
Delete Row	Deletes the line at the cursor position.
Auto	Axes: Select the axis to do auto fill. Start Row: Start row number. End Row: End row number. Starting Number: Start value. Scale: Linear increase linearly, while Log increase logarithmically.
Cut	Cuts highlighted text.
Copy	Copies cut text to the clipboard.

Creating a Simple Traverse Position List

This list starts at position 0,0,0 and moves in the positive x, y, and z directions ten positions, 1-mm per position. This example uses a linear relation to do the automatic position generation.

1. From the Matrix page, click the left mouse button to bring up the Edit menu.
2. From the Edit menu option, select **Insert Row**. This inserts a new row into current spreadsheet.

3. Repeat step 2 ten times to create ten rows.
4. Enter 0 in the first row of columns X, Y, Z. This will be the initial position.
5. Click the left mouse button to bring up the Edit menu, select **Auto Fill** option.
6. In the Auto Fill dialog box, select **X axis**, enter 1 in the start row, enter 10 in the end row, enter 0 in the starting number, enter 1 in increment, and select **Apply**.
7. Make similar steps for the other two axes.
8. Enter a Run Setup filename in the uppermost Run Setup box. You only need to enter the name to the first position that has a setup file change, the software will fill the rest automatically once you click the **Apply** button.
9. Enter a filename in the **Save As** box. The software will generate the rest automatically once you click the **Apply** button.

CHAPTER 14

Using the Burst Monitor

The capabilities of FLOWSIZER™ Data Acquisition and Analysis Software to display acquired data are very powerful and versatile. But in addition to that, FLOWSIZER also has the capability to display the actual Doppler bursts as they are being processed! This feature is useful in optimizing your settings to improve the data rate, validation rate, and data reliability. It is also useful in troubleshooting, when a good digital oscilloscope is not available.

Select **Hardware** → **Burst Monitor** to open the Burst Monitor Window. Figure 14-1 shows the Burst Monitor Window. First select the channel you wish to display. For PDPA systems, select channel 1 and the channel 1A, 1B and 1C signals will be displayed. An LDV system will display only individual channels. Then select either **Continuous** or **Single Read** to continuously monitor the burst stream, or, capture single “snapshots” of the burst stream.

The burst monitor shows the signal after downmixing and bandpass filterings as it appears when being sampled, or digitized. This is the same signal seen on the signal out BNCs on the FSA front panel. In fact, the amplitude, into 50 ohms, at this connector corresponds to the amplitude shown in the burst monitor.

The main use of this monitor is to check the quality of the burst signals being processed, specifically their amplitude and noise level. The PMT voltage should be high enough so that some of the signals are close to ± 5 volts in amplitude, which is the full scale of the 8-bit A/D converters. Having some very large signals peg, or max out the A/D full scale is not a problem and even desirable so that the smaller particles have enough gain. Noisy signals don't have a clean looking sinewave and also have only a few samples. Good quality signals will have a large proportion of the bursts with the maximum number of samples, 256.

The portion of the signal shown is not the whole burst, but only the center portion used by the burst processing DSPs to calculate frequency + phase. The 10–1 bandpass filter ranges are further divided into three subranges to optimize samples/cycle. The subrange is indicated by showing time scale x1, x2, or x4. If the time scale is x2, the frequency displayed is actually $\frac{1}{2}$ of the x1 range. If it is x4, the frequency is $\frac{1}{4}$ of the x1 range. Note also that the FSA's maximum data rate is lower when the burst monitor

window is open, because the FSA is busy transferring raw data to the computer.

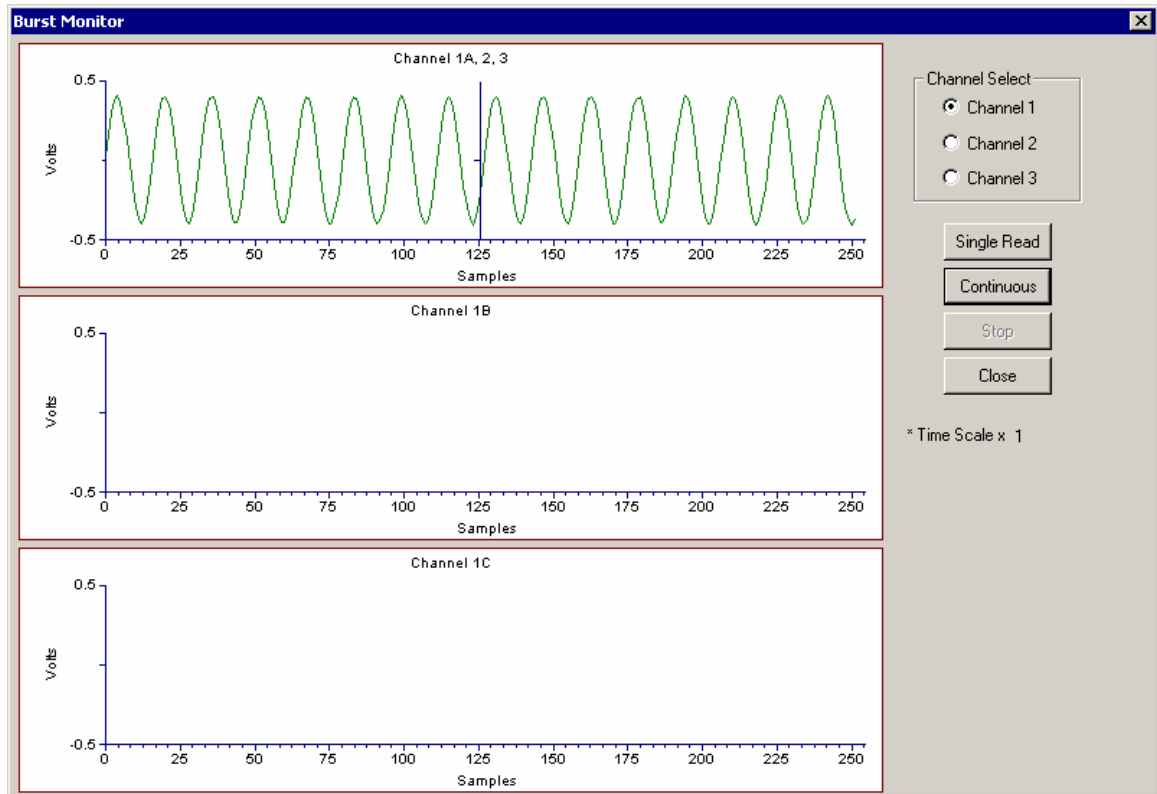


Figure 14-1
Burst Monitor Window

CHAPTER 15

Exporting Data in ASCII Format

To export your data go to **File** → **Export Data**. A dialog box like the one shown in Figure 15-1 should open.

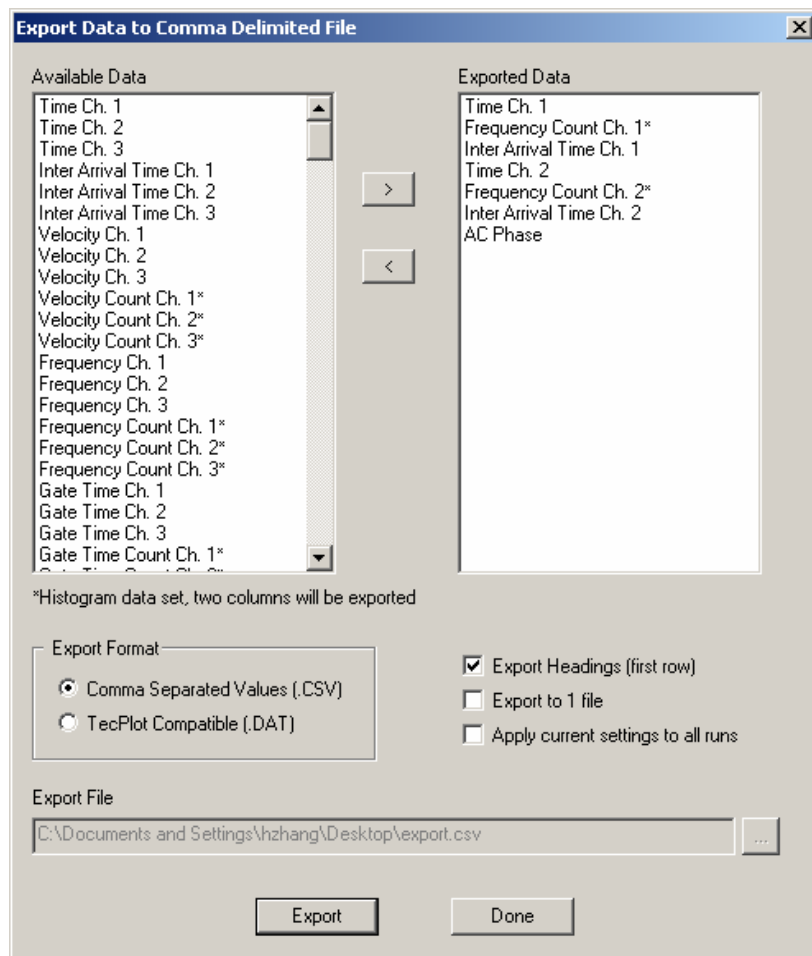


Figure 15-1
Export Data Dialog Box

You can then choose which parameters you would like to export. To select parameters for export simply click on the parameter you would like to export and then click the > button. (To remove a parameter that you already selected, click the < button.) When you

have chosen all the parameters you want to export, click the **Export** button. A text file will then be created and stored in the location shown in the **Export File** edit box.

Export Format

This allows you to choose the format of your export files. Both of them are text files. .csv files can be loaded directly into Microsoft Excel, .dat can be loaded directly into TecPlot.

Export Headings (first row)

If this check box is selected, the first row of the exported file will contain which parameters you have chosen (along with the units) and the order they were exported in.

Export to 1 File

Checking this box allows you to export the data from multiple FLOWSizer runs into one *.csv file. If you only have one run selected and you check this box, it will just export that one run into the *.csv file. If this box is unchecked, the **Export File** edit box will be grayed out and the current run you are processing will be saved with the same name and in the same folder as the data file you are processing. If this box is checked, you can select where to save the resulting *.csv file by clicking on the ..button which is to the right of the **Export File** edit box.

To select multiple FLOWSizer runs to process into one *.csv file, you must select all the runs you want to process by going to **File** → **Experiment Manager**, and selecting the runs you want to process (use the Ctrl key to select more than one run). Then open the **Export File Dialog Box**, make sure the **Export to 1 file** edit box is checked, and select a location and name for the resulting *.csv file. Then export the data and the data from all the runs will be put in one *.csv file.

Apply Current Settings to All Runs

This box applies only when you are exporting multiple FLOWSIZER runs into one *.csv file. By checking this box the settings from the very first run will be applied to all selected runs when creating the *.csv file. It is probably not likely to be used very often.

When you are done exporting the data, click on the **Done** button to close **the Export File Dialog Box**. The set of parameters that you last exported will be saved, so the next time you choose to export data, these parameters will automatically be selected when the **Export File Dialog Box** is opened.

Matrix Transformation

Matrix Transformation Page

In two- and three-component LDV/PDPA systems, the measured velocity directions do not always coincide with the desired world coordinate system. The FLOWSIZER™ Data Acquisition and Analysis Software can transform the measured non-orthogonal velocity (V_1 , V_2 , V_3) to the orthogonal velocity components (u , v , w) in the world coordinate system (x , y , z). To perform this transformation, you need to setup a transformation matrix in the FLOWSIZER software.

What is Transformation Matrix?

The transformation matrix can be derived from the projection of the orthogonal velocity (u , v , w) along the measurement directions

$\vec{e}_k = (e_1, e_2, e_3)$:

$$\begin{bmatrix} V_1 \\ V_2 \\ V_3 \end{bmatrix} = E \cdot \begin{bmatrix} u \\ v \\ w \end{bmatrix} = \begin{bmatrix} e_{1x} & e_{1y} & e_{1z} \\ e_{2x} & e_{2y} & e_{2z} \\ e_{3x} & e_{3y} & e_{3z} \end{bmatrix} \cdot \begin{bmatrix} u \\ v \\ w \end{bmatrix}$$

The inverse of projection matrix E is the final transformation matrix that is used to convert the non-orthogonal velocity components (V_1 , V_2 , V_3) to the orthogonal velocity (u , v , w). In the next section, you can find the projection matrix E for some typical LDV measurement configurations. Since the FLOWSIZER software automatically calculates the inverse of matrix E to get the transformation matrix, what you need to enter in the software is simply the projection matrix E itself.

Examples of Projection Matrix

Case 1. Three-Component Measurement Using Two Probes in the Same Plane

Figure 16-1 shows the typical setup of two-probe measurements, in which probe A has a two-component transmitter and both probes

are in the YZ plane. The projections of orthogonal velocity components (u, v, w) onto the measurement directions are:

$$V_1 = u$$

$$V_2 = -v \cdot \cos \alpha - w \sin \alpha$$

$$V_3 = -v \cdot \cos \beta + w \sin \beta$$

where V_1 and V_2 are measured by probe A, and V_3 by probe B. α and β is the angle between the axis z and the optical axis of probe A and probe B, respectively. γ is the angle between the optical axis of probe A and the YZ plane. α, β and γ are defined between 0 and 90 degrees.

The projection matrix E to be entered in the FLOWSIZER software, for the world coordinate system shown in Figure 16-1, is given below,

	x	y	z
1	1	0	0
2	0	$-\cos \alpha$	$-\sin \alpha$
3	0	$-\cos \beta$	$\sin \beta$

If the world coordinate system is different from that shown in Figure 16-1, the sign of e_{ij} in the projection matrix is determined by the angle between the measurement direction V_i and the axis x_j : e_{ij} is positive if the angle is less than 90 degrees, and negative if the angle is between 90 and 180 degrees.

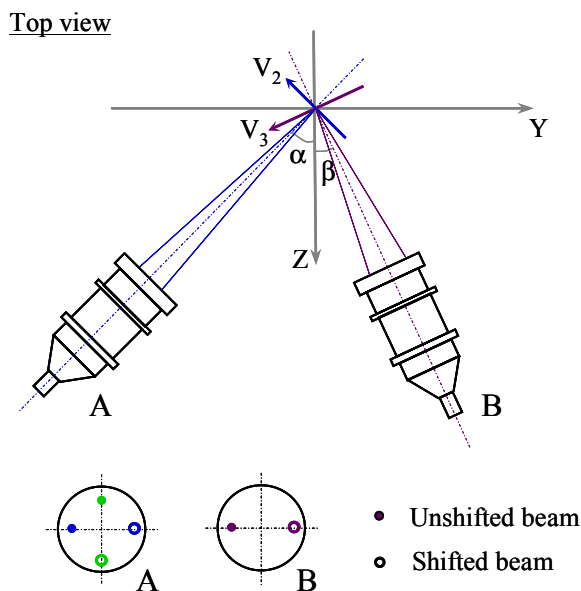


Figure 16-1
Three-Component Velocity Measurement Using Two Probes in the Same Plane

Case 2. Three-Component Measurement Using Two Probes not in the Same Plane

Figure 16-2 shows the setup of two-probe measurement similar to that shown in Figure 16-1 except that probe A is not in the YZ plane. The projections of orthogonal velocity components (u, v, w) onto the measurement directions are:

$$V_1 = u \cdot \cos \gamma - v \cdot \sin \alpha \cdot \sin \gamma + w \cos \alpha \cdot \sin \gamma$$

$$V_2 = -v \cdot \cos \alpha - w \sin \alpha$$

$$V_3 = -v \cdot \cos \beta + w \sin \beta$$

where V_1 and V_2 are measured by probe A, and V_3 by probe B. α and β is the angle between the axis z and the optical axis of probe A and probe B, respectively. γ is the angle between the optical axis of probe A and the YZ plane. α, β and γ are defined between 0 and 90 degrees.

The projection matrix E to be entered in the FLOWSIZER software, for the world coordinate system shown in Figure 16-2, is given below:

	x	y	z
1	$\cos \gamma$	$-\sin \alpha \cdot \sin \gamma$	$\cos \alpha \cdot \sin \gamma$
2	0	$-\cos \alpha$	$-\sin \alpha$
3	0	$-\cos \beta$	$\sin \beta$

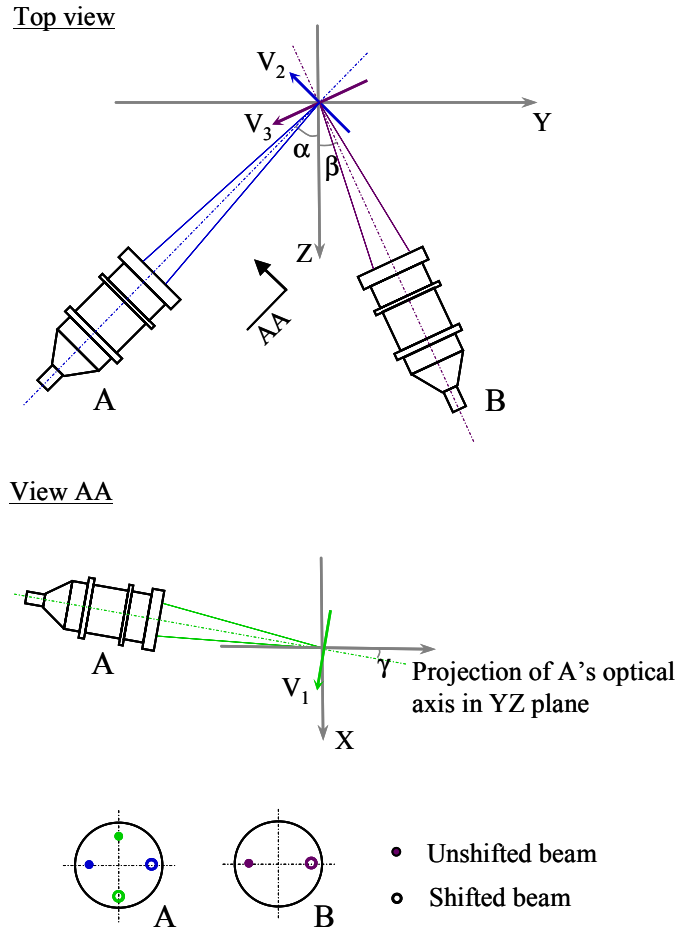


Figure 16-2
Three-Component Velocity Measurement Using Two Probes not in the Same Plane

If the world coordinate system is different from that shown in Figure 16-2, the sign of e_{ij} in the projection matrix is determined by the angle between the measurement direction V_i and the axis x_j ; e_{ij} is positive if the angle is less than 90 degrees, and negative if the angle is between 90 and 180 degrees, except for the two special cases given below:

- a. e_{iy} is positive if the angle between the probe A's projection in YZ plane and the measurement direction V_1 AND the angle between the projection and the axis y are BOTH less than or BOTH greater than 90 degrees;
- b. e_{iz} is positive if the angle between the probe A's projection in YZ plane and the measurement direction V_1 AND the angle between the projection and the axis z are BOTH less than or BOTH greater than 90 degrees..

Case 3. Three-Component Measurement Using One 5-Beam Probe

Figure 16-3 shows the typical setup of 5-beam probe measurement, in which three velocity components are measured by a single three-component transceiver probe. The projections of orthogonal velocity components (u, v, w) onto the measurement directions are:

$$V_1 = u \cdot \cos\alpha + w \cdot \sin\alpha$$

$$V_2 = v \cdot \cos\gamma + w \sin\gamma$$

$$V_3 = u \cdot \cos\beta - w \sin\beta$$

where V_1 is measured by green beam, V_2 by blue beam, and V_3 by violet beam. α and β is the angle between the Z axis and the optical axis of the green and violet beam pairs, respectively. γ is the angle between the optical axis of the 5-beam probe and the axis z. α , β and γ are defined between 0 and 90 degrees.

The projection matrix E to be entered in the FLOWSizer software, for the world coordinate system shown in Figure 16-3, is given below,

	x	y	z
1	$\cos\alpha$	0	$\sin\alpha$
2	0	$\cos\gamma$	$\sin\gamma$
3	$\cos\beta$	0	$-\sin\beta$

If the world coordinate system is different from that shown in Figure 16-3, the sign of e_{ij} in the projection matrix is determined by the angle between the measurement direction V_i and the axis x_j ; e_{ij} is positive if the angle is less than 90 degrees, and negative if the angle is between 90 and 180 degrees.

A special case of 5-beam probe measurements is when $\gamma = 0$; i.e., the optical axis of the probe is perpendicular to the Y axis.

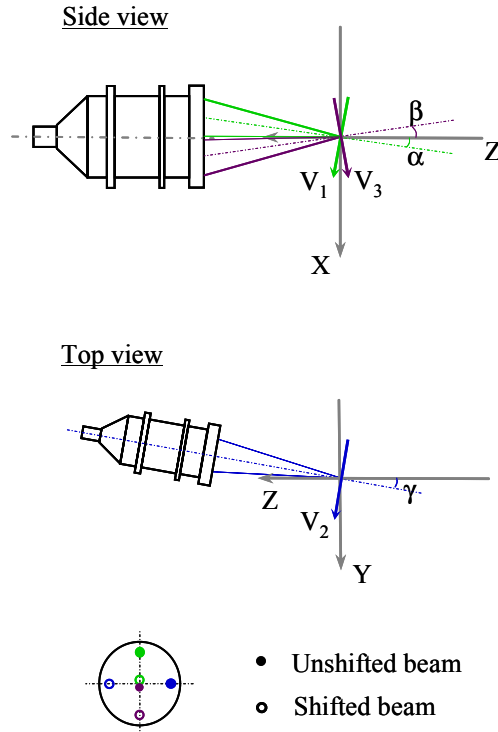


Figure 16-3
Three-Component Velocity Measurement Using a 5-Beam Probe

Case 4. Two-Component Measurement Using One Probe

Figure 16-4 shows the setup of single-probe measurement of two velocity components. Normally no transformation is needed for this case since the two measurement directions are orthogonal. However, sometimes the world coordinate system is rotated (along the axis z) from the measurement coordinate system (as seen in the end view in Figure 16-4), and an affine transform is needed to obtain the velocity components (u, v, w) in the world coordinate system. The projections of orthogonal velocity components (u, v, w) onto the measurement directions are:

$$V_1 = u \cdot \cos \alpha - v \sin \alpha$$

$$V_2 = u \cdot \sin \alpha + v \cos \alpha$$

where α is the angle from the axis x to the measurement direction V_1 and is defined between -180 degrees to 180 degrees with clockwise direction being the positive.

The projection matrix E to be entered in the FLOWSIZER software is given below. Please note that the signs of the elements in this matrix are fixed and the angle α can be negative values.

	x	y	z
1	$\cos\alpha$	$-\sin\alpha$	0
2	$\sin\alpha$	$\cos\alpha$	0
3	0	0	1

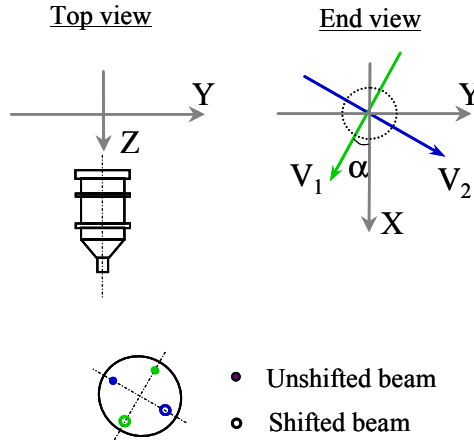


Figure 16-4
Two-Component Velocity Measurement Using One Probe

Case 5. Two-Component Near-Wall Measurement Using a Probe with Prism

Figure 16-5 shows the setup of near-wall velocity measurement using a probe with two-beam transmitter. A prism is used to move the bottom beam to the center to facilitate near-wall measurement. The projections of orthogonal velocity components (u , v , w) onto the measurement directions are:

$$V_1 = u \cdot \cos \gamma + w \cdot \sin \gamma$$

$$V_2 = v$$

where the angle γ is determined by the green beam separation and the focal length of the probe. Since the angle γ is very small, the measurement direction V_1 is almost aligned with the axis x and the contribution from velocity component w to V_1 can be neglected.

The projection matrix E to be entered in the FLOWSizer software, for the world coordinate system shown in Figure 16-5, is given below,

	x	y	z
1	$\cos\gamma$	0	0
2	0	1	0
3	0	0	1

where e_{1x} is negative if the angle between the measurement direction V_1 and the axis x is greater than 90 degrees, and e_{2y} is -1 if the direction of V_2 is opposite to the axis y .

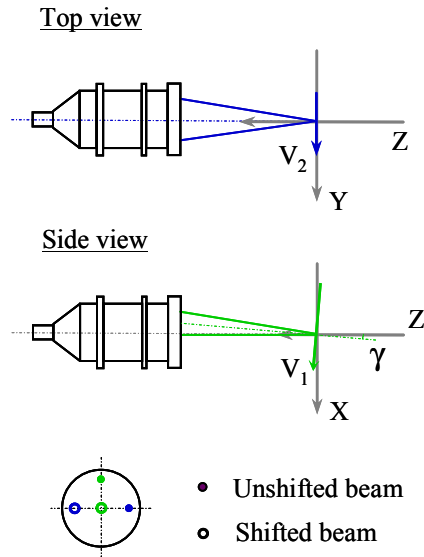


Figure 16-5
Schematic Drawing of Two-Component Near-Wall Velocity Measurement using a Probe with Prism

Set Up the Transformation Matrix

To setup the transformation matrix, select **Run → Run Setup Processor/Matrix** to open the transformation page (see Figure 16-6). Enter the matrix parameters (the projection matrix E , as explained in the previous sections). Once data has been taken, view the transformed velocity components under **Statistics → System Statistics → Velocity Transformed**.

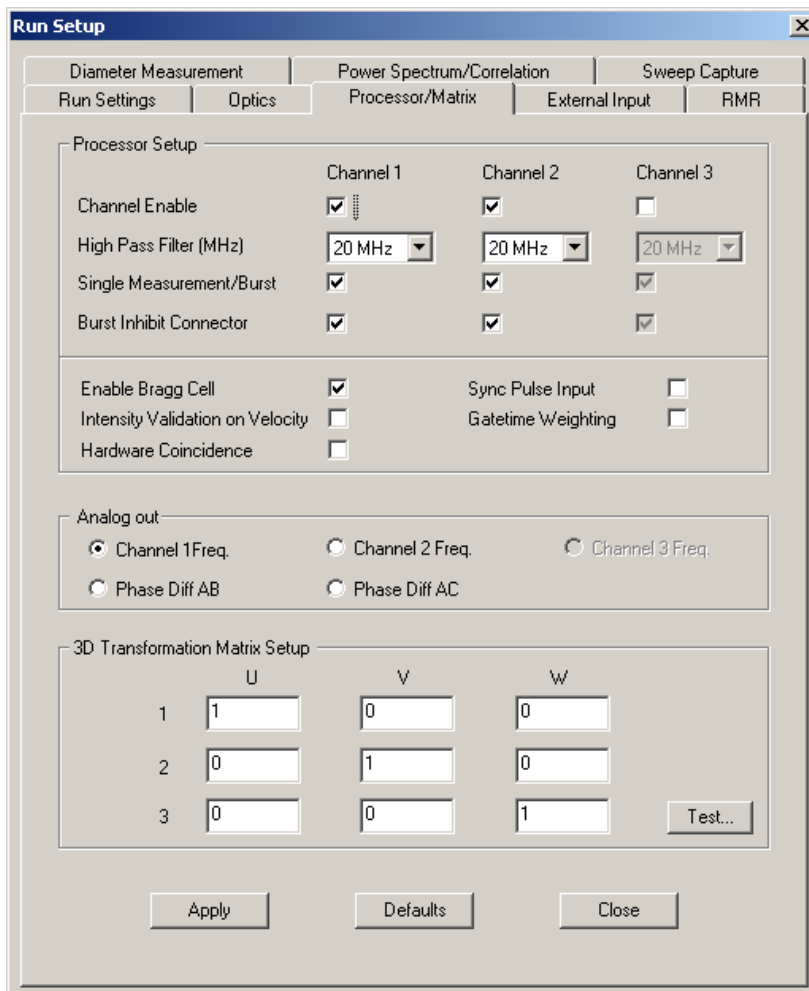


Figure 16-6
3-D Matrix Transformation Setup

The Test button allows you to test the current matrix (see Figure 16-7). If you enter the measured mean values, the “Output” column will show resulting in orthogonal values.

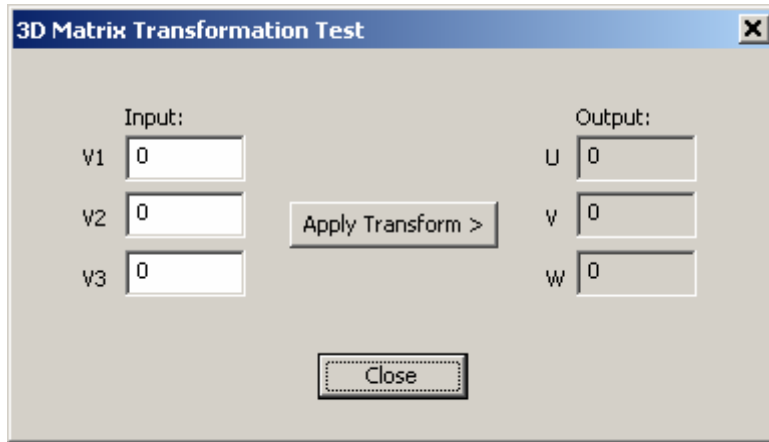


Figure 16-7
3-D Matrix Transformation Test

APPENDIX A

Laser Doppler Velocimetry (LDV) Overview

The Laser Doppler Velocimetry (LDV) measurement technique uses a laser to generate a coherent (fixed frequency) beam to illuminate a moving particle in the flow. This particle movement creates a Doppler shift in the light frequency directly proportional to its velocity. Thus the measurement of such Doppler shift frequency is a measurement of the particle's velocity. Since the particle is very small, one can be quite certain that the particle velocity is very close to that of the fluid velocity. By not inserting any sensor into the flow, this technique provides a noncontact way of measuring velocity.

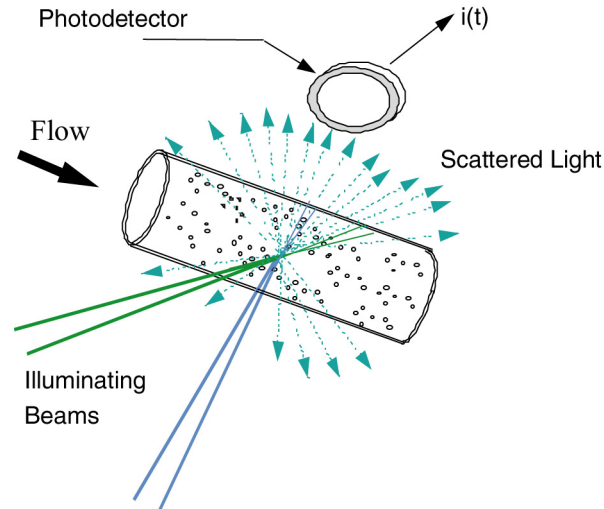


Figure A-1
LDV Technique

Some of the key aspects of this noncontact flow measuring technique are:

- ❑ Measurement is, generally, independent of the property of the medium
- ❑ Desired component of velocity can be measured by suitably orienting the laser beams
- ❑ The signal exists only when a detectable particle is in the measurement volume and, hence, is discontinuous.

Components of an LDV System

The components of an LDV system are:

- ❑ Laser—Monochromatic light source, provides coherent, collimated beam
- ❑ Transmitting optics
- ❑ Receiving Optics, Detector
- ❑ Signal processor, Data Analysis system

The dual-beam approach is the most common optical arrangement. Figure A-2 shows the basic components of a complete LDV system for velocity measurements.

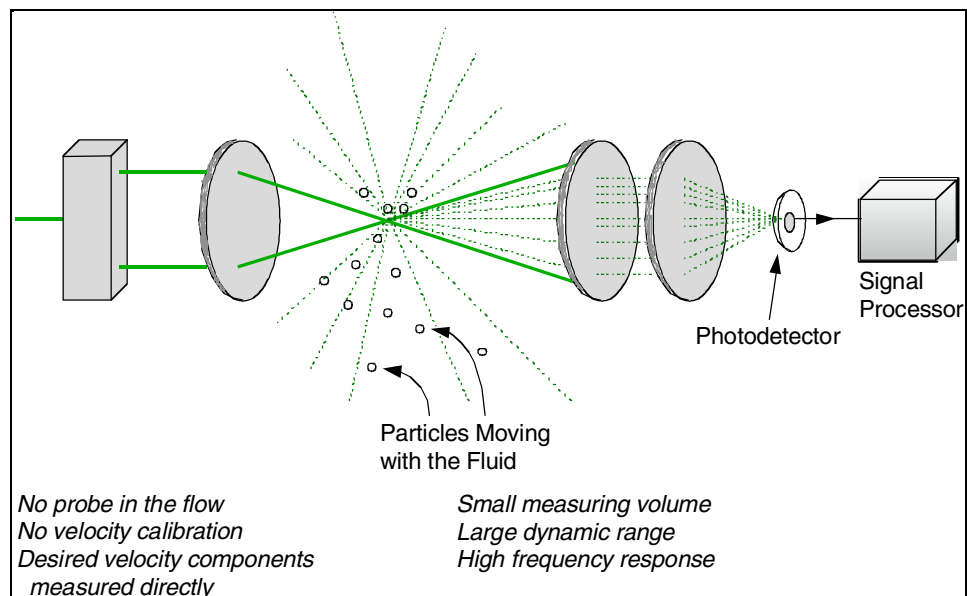


Figure A-2
Dual-Beam Laser Anemometer

Optimizing LDV Measurements

To optimize a measurement, you must have:

- ❑ Particles that follow the flow and provide an adequate signal.
- ❑ Laser, optics, and photodetector that provide a signal with optimum signal-to-noise ratio at the photodetector output.
- ❑ A signal processor that extracts the maximum amount of information from the photodiode signal.
- ❑ Data processing techniques that provide the needed flow properties from the output of the signal processor.

In many flows, if all these criteria are handled properly, very good data can be obtained that is simply not available by any other technique.

Laser Source

Typically, an argon-ion laser is used as the laser source. This laser output has multiple wavelengths. The three wavelengths used for LDV/PDPA applications are 514.5 nm (green), 488.0 nm (blue), and 476.5 nm (violet).

Doppler Frequency Measurement

The Doppler shift frequency created by a moving particle is typically from a few kHz to more than 100 MHz, but is contained in its light frequency which is typically around 440 GHz. If we use two laser beams, each to create a Doppler effect on the moving particle, and mix the scattered light from the particle at the photodiode, the basic light frequency is subtracted, only the Doppler shift frequency which is much lower, is detected.

In a one-channel LDV/PDPA system, two beams of equal intensity are generated. The two beams are then focused and crossed at an angle (half angle = κ) at the focal length of the lens. When a small particle in the fluid flows past the beam crossing, its scattered light is collected and focused onto a photodetector, creating the (Doppler) signal for velocity measurement. Scattered light from particles outside of the crossing point fall outside of the photodetector and do not get measured.

Fringe Spacing

At the crossing point of the two beams, an interference fringe pattern is actually created by the coherence of the laser light source. This fringe pattern provides the necessary light pattern to illuminate the particles and is often used as an alternate method to explain the creation of the Doppler frequency signal (Figure A-3).

The fringe spacing, (d_f) in an LDV system, depends only on the wavelength of light, (λ), and half angle, (κ). The amplitude variation of the signal reflects the Gaussian intensity distribution across the laser beam. Collection (receiving) optics for the dual-beam system can be placed at any angle. The resulting signal from the receiving system still gives same frequency. However, signal quality and intensity varies greatly with angle.

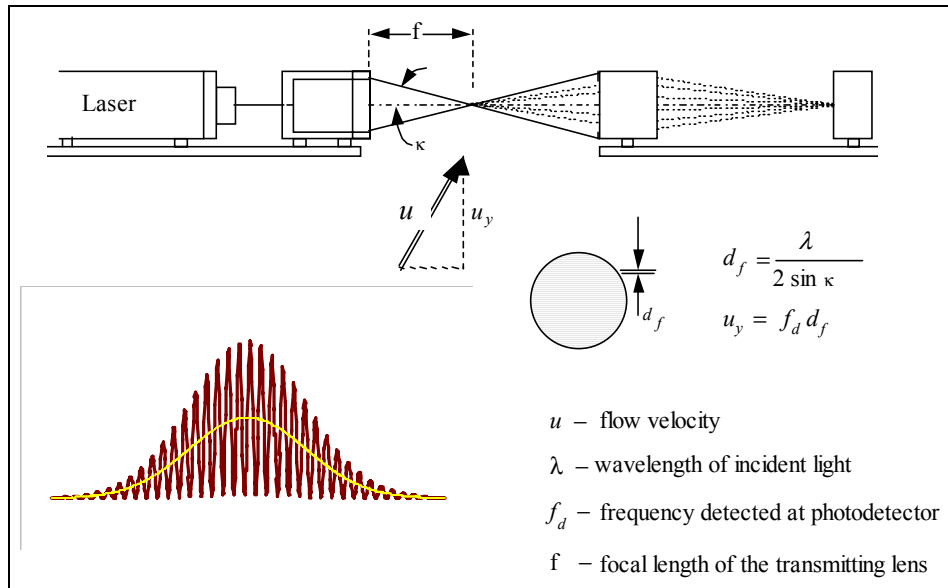


Figure A-3
Fringe Descriptions

Measurement Volume Dimensions

The measurement volume is the body bound by the ellipsoidal surface shown in Figure A-4, and it corresponds to the surface on which the light intensity of the fringes is $1/e^2$ of the maximum intensity, which occurs at the center of the measurement volume. Fringe spacing decreases with increasing angle κ .

N_{FR} = number of fringes
 V = volume of measurement volume
 d_f = fringe spacing
 d_m = diameter of the measurement volume
 l_m = length of the measurement volume
 f = focal length of the lens
 λ = laser wavelength

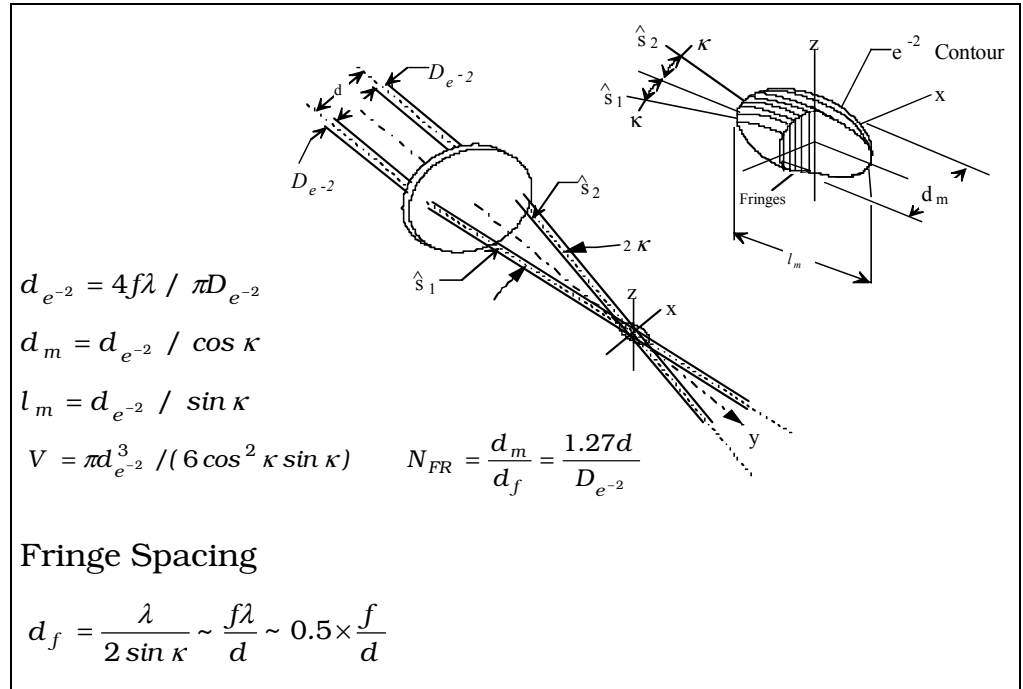


Figure A-4
Measurement Volume Dimensions

Doppler Signal

The light scattered by a particle passing through the fringes in the measurement volume is optically collected and focused onto the photomultiplier tube (PMT). The PMT produces an electrical current proportional to this light flux. Variations in this electrical current caused by the particle passing the fringes are subsequently analyzed to determine the velocity of the particle.

The signal output from the PMT can, typically, be decomposed to the following components:

- Low frequency "pedestal" caused by the particle passing through the focused Gaussian-intensity laser beams.

- ❑ Doppler frequency, f_d , signal that is superimposed on the pedestal and has a regular sinusoidal pattern related to how fast the particle crosses the fringes in the measurement volume.
- ❑ Wide bandwidth electronic noise generated by stray light, the PMT, and associated electronics.

Signal (a) in Figure A-5 is the sum of the pedestal component, the Doppler component and the noise from the photodiode. Since the pedestal is undesirable for good signal processing, it is usually removed by simply filtering the signal through a high-pass filter. The resulting signal, with pedestal-removed, is shown in (b). High frequency noise can be reduced by low-pass filtering the noise at a frequency which must be greater than f_d in order to avoid filtering the Doppler signal. The low-pass filtered signal is shown in (c).

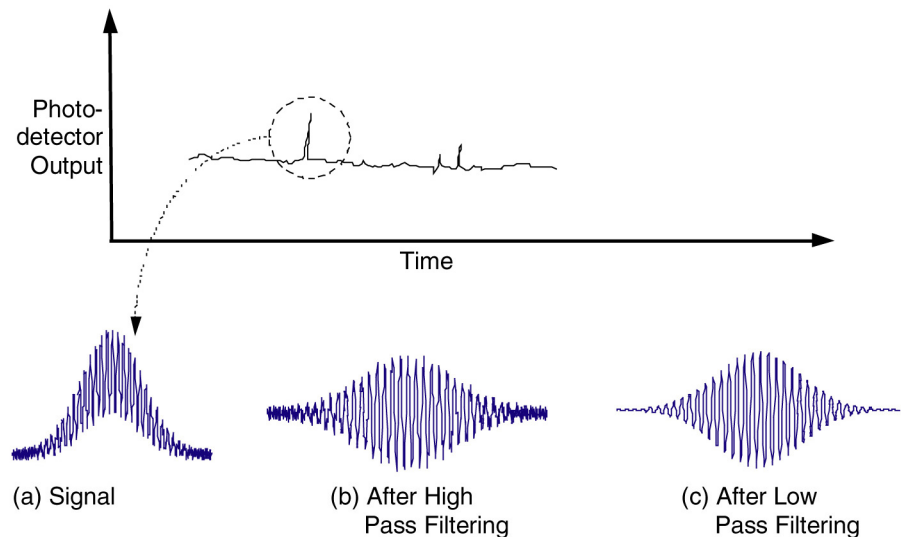


Figure A-5
Doppler Signal

LDV Signal Characteristics

Figure A-6 represents the variations in intensity distribution at the intersection region of two Gaussian beams. These would represent the output of a photodetector as a single particle passes along the indicated paths if:

- ❑ The beams are polarized normal to the plane of the beams
- ❑ The light scattered by the particle from two incident beams mixes to give 100 percent modulation depth on the photodetector output.

- ❑ The scattered light intensity is sufficient to give an essentially continuous signal.

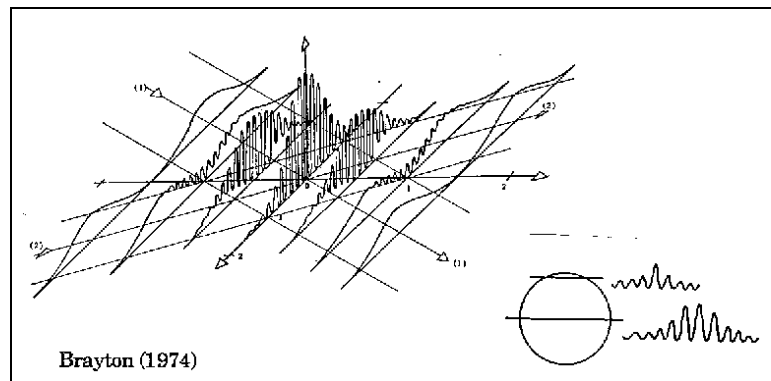


Figure A-6
Signal Characteristics Along the Measurement Volume

A particle that is small compared with the fringe spacing, d_f , normally produces a scattered light signal proportional to the light intensity incident on the particle. Under these conditions, the Doppler component of the signal, for example, the sinusoidal oscillating component, always has a Gaussian envelope, even though the sum of the Doppler component and the pedestals change shape substantially for various particle trajectories.

Variation of Scattered Light Intensity

Figure A-7 shows the variation of the scattered light intensity as a function of receiver position for polarization perpendicular to the beams. The intensity values are obtained from the Mie scattering calculations. For a dual-beam system, the component of velocity measured is independent of the location of the scattered light collection system.

The backscatter mode is a very convenient arrangement since all the optics are on one side of the measuring point, requiring only one window and providing easier traversing arrangement of the LDV system. In this case, the same lens is used for focusing the two beams and for collecting and collimating the scattered light.

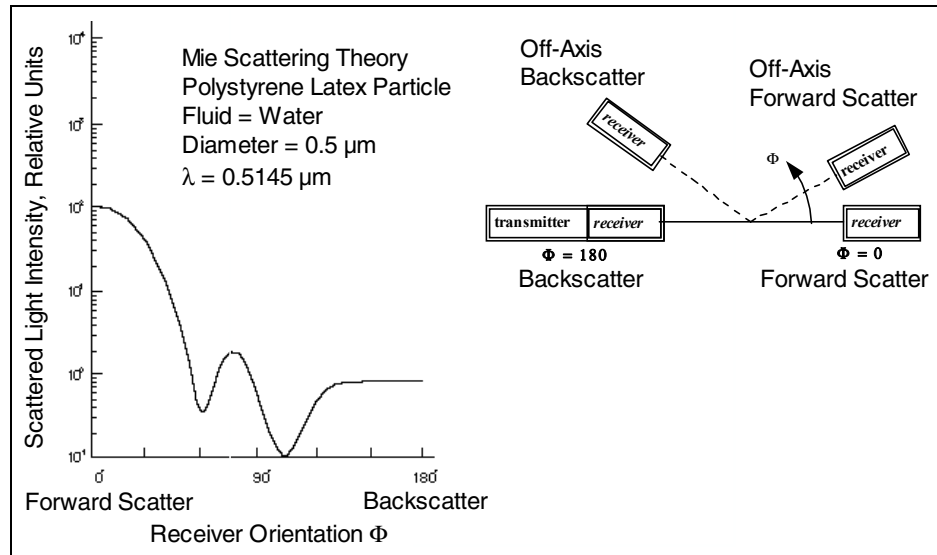


Figure A-7
 Scattered Light Intensity Variation

If direct backscatter is not used, then a separate receiving system, appropriately positioned to collect the scattered light, is used. Once the receiving optics is separate from the transmitting optics, the direct forward-scatter arrangement provides the strongest signal. In practice, to avoid reflections, an off-axis forward-scatter location for the receiver is often preferred.

Typical Frequency versus Velocity Curves

Figure A-8 shows the frequency versus velocity for two values of half-angle (k) between the two beams. Figure A-3 has the equation showing the relationship between frequency and velocity. Generally, velocity dynamic range of over 10^3 is achieved by LDV systems and for most common flows, the corresponding Doppler frequencies are in the kHz to MHz range.

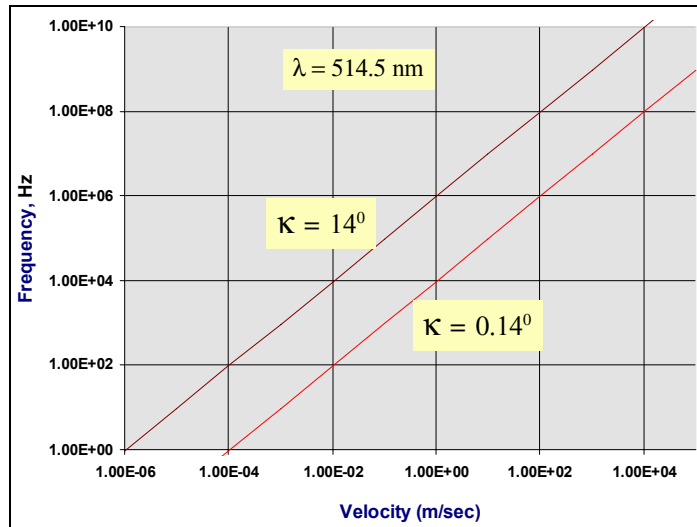


Figure A-8
Typical Frequency versus Velocity Curves

The value of $k = 14^\circ$ represents a lens with an F-number (focal length/diameter) of 2. At $k = 0.14^\circ$, the F-number would be about 200. These are reasonable limits using a single-focusing lens. The absolute minimum fringe spacing, d_f , is the laser wavelength divided by 2 (that is when $\sin k = 1$, $k = 90^\circ$). This gives frequencies of about 4 MHz per m/s of velocity for visible wavelength lasers ($\lambda = 0.5$).

Velocity measurements from 1 $\mu\text{m}/\text{sec}$ to over 1,000 m/sec which corresponds to a dynamic range of over 10^9 , have been made with LDV.

Frequency Shifting

The purpose of frequency shifting in LDV is to:

- Measure flow reversal.
- Measure small fluctuations of velocity (in the presence of a large average velocity).
- Extend the range of low and high velocities that can be measured by a processor.
- Measure flow velocities in highly turbulent flows.

Figure A-9 shows the linear relationship between velocity and Doppler frequency f_d . For the case of no frequency shift, the frequency of the Doppler signal (photodiode output) goes to zero as the velocity goes to zero and remains positive when the velocity becomes negative. Further, the Doppler signals generated by two

particles, A and B, having equal velocity magnitude but opposite direction (one positive and other negative) will have the same frequency value f_{AB} . From a fringe model standpoint, the fringes are stationary in a system with no frequency shift.

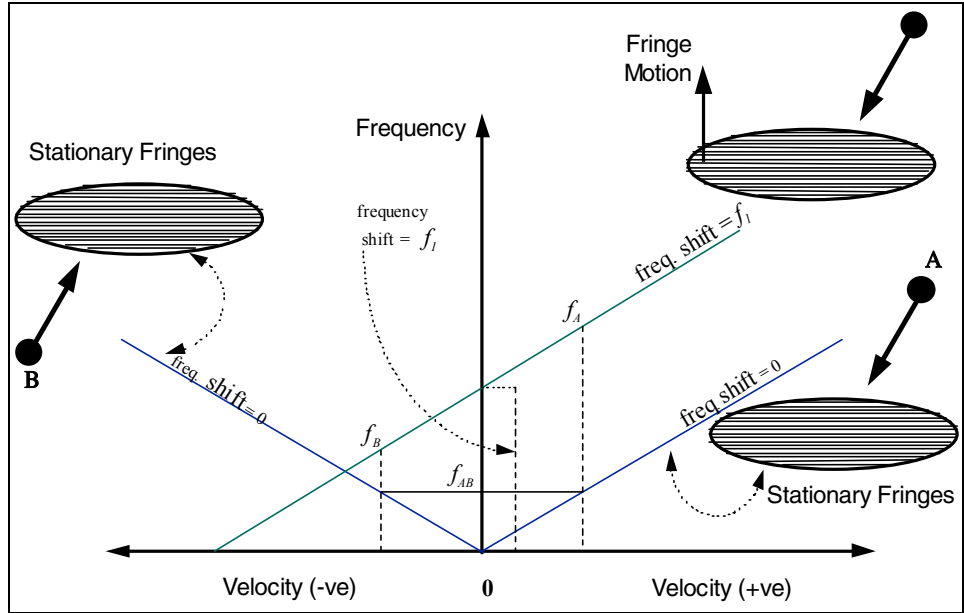


Figure A-9
Frequency Shifting

A system with frequency shift effectively offsets the frequency-velocity curve along the y-axis by the frequency shift value. In Figure A-9, the frequency-velocity curve for a system with a frequency shift value of f_i is shown. For this system, a particle with zero velocity generates a signal of frequency f_i . And as the velocity decreases, the frequency of the signal will be less than f_i . The two particles A and B generate signals with frequencies f_A and f_B , respectively. From a fringe model standpoint, the system with frequency shift corresponds to a case where the fringes are moving. In Figure A-9, the fringe motion is opposite the velocity direction of particle A. This creates a higher number of fringe crossings and hence the frequency f_A is higher (by f_i) than f_{AB} . For a frequency-shifted system, frequency input to the processor is f , where:

$$f = \text{Shift frequency} \pm |\text{Velocity}| / \text{fringe spacing}$$

Acousto-Optic (Bragg) Cell

Bragg interaction is characterized by the diffraction of a high percentage of the incident light intensity (>80 percent) into the first-order beam. Typically, more than two beams exit the Bragg cell. By adjusting the angle between the cell and the incident beam, the intensity of the first-order output beam can be maximized. By adjusting input signal strength, the intensity of the two beams coming out (zero-order and first-order) can also be equalized. Used in this manner, the cell can be both a frequency shifter and beamsplitter. The major disadvantage of this approach is the very small angle ($2\alpha = 0.31^\circ$ for a 40 MHz cell and $\lambda = 514.5$ nm) between the two beams.

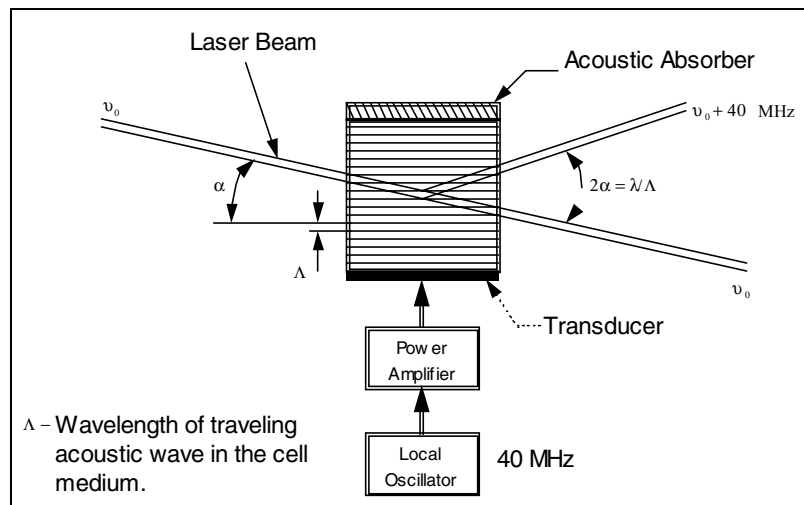


Figure A-10
Acousto-Optic (Bragg) Cell

Signal Processors

This section discusses the signal processor requirements and lists the different types of processors. It also discusses the components of digital processors.

Signal Processors Requirements

- Accurate individual burst measurements
- Large total frequency range
- Large dynamic range
- High maximum data rates
- Measures low SNR signals
- Low cost

In any measurement, accuracy is always important and to avoid phase noise, it is important to measure individual bursts accurately rather than averaging over a number of bursts.

Since the basic input to the processor is a frequency, this permits a very wide potential range of velocities from millimeter per second to over 1000 meters per second.

A large dynamic range permits measurements, for example, in high-speed flows where the flow actually reverses (with frequency shifting).

In high-speed flows, data rates need to be very high if flow variations are to be followed in real-time or if spectrum analysis on the velocity is to be done.

Even with an optimum optical setup, the processor must either make measurements on low SNR signals or reliably reject them.

Low-cost means that the system is affordable for more applications.

Types of Signal Processors

This section discusses the following types of signal processors.

- Spectrum Analyzers
- Photon Correlators
- Trackers
- Counters
- Covariance Processor
- Digital Signal Processors

Since it is frequency that needs to be measured, the natural first step was to use a spectrum analyzer. However, a standard spectrum analyzer can only provide information on the average frequency and the deviation from that average over a period of time.

Photon correlators had a similar problem, but they could in theory operate at a much lower SNR since individual photons were being counted.

The tracker was designed to “track” the Doppler frequency as it changed and was especially applicable to high-burst density signals. However, at low-data densities where large changes in velocity could take place between measurable particles, the tracker would “lose” the signal because of its relatively narrow filter bandwidth.

The counter used a high-speed clock and logic to essentially measure the time for a fixed number of cycles (typically 8). This measured individual particles very well and has been used extensively. Its primary limitation was an inability to measure at low SNRs.

The covariance processor was designed for phase-Doppler measurements. It can be used for velocity where limited accuracy is acceptable.

Digital signal processors represent the state of the art in signal processors for velocity.

Note: *In the following section we will discuss only digital signal processors, especially those built by TSI.*

Components of Digital Signal Processors

While the order may change, all digital signal processors have the following functions:

- High-pass filter to remove low frequency components (pedestal)
- Low-pass filter to limit noise and bandwidth
- A/D converter
- Burst detector
- Digital signal analyzer
- I/O port to computer for data analysis

Burst Detector

In modern processors, the burst detector is a key component and is designed to detect “coherency” in the signal. This is much more effective than simply depending on the amplitude of the Doppler signal, although in some cases both are used. A burst detector is required so the processor is not wasting time processing signals that contain only noise.

Low-Pass Filter

Besides reducing noise in the signal, it is necessary to avoid aliasing.

A/D Converter

With advancement in performance and reduction in cost, electronics are enabling multi-bit digitization to become feasible for higher and higher sampling rates. Current state-of-the-art is an 8-bit A/D converter operating at up to 800 MHz.

Digital Signal Analyzer

Either a Fourier transform with a method to accurately establish the peak location or auto-correlation with a method to accurately establish the zero-crossing locations are the primary techniques used.

Example Fourier Transforms

Figure A-11 shows example transforms. In essence, the transform compares the actual signal with a series of similar signals at a range of frequencies. When the comparison is strong, a peak is generated. The frequency represented by the peak is the dominant frequency in the original signal. In LDV, only the primary peak is of interest.

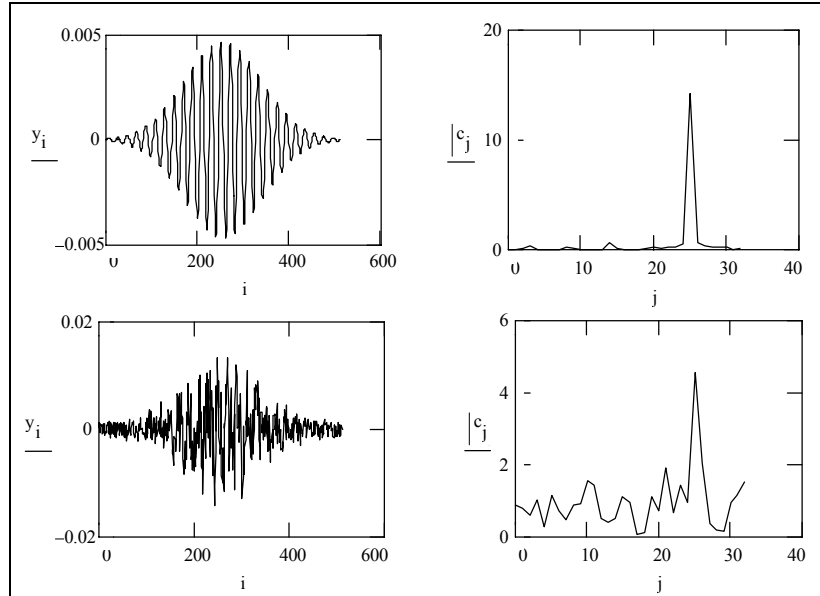


Figure A-11
Example Fourier Transforms

Velocity Bias

The concept of velocity bias is easiest to explain in terms of mean velocity. By “mean” we are referring to a time average. In other words, the “mean” of a continuous but fluctuating analog signal is the value obtained with a sufficiently long averaging time so a second reading of the same flow would provide the same value within an acceptable error band.

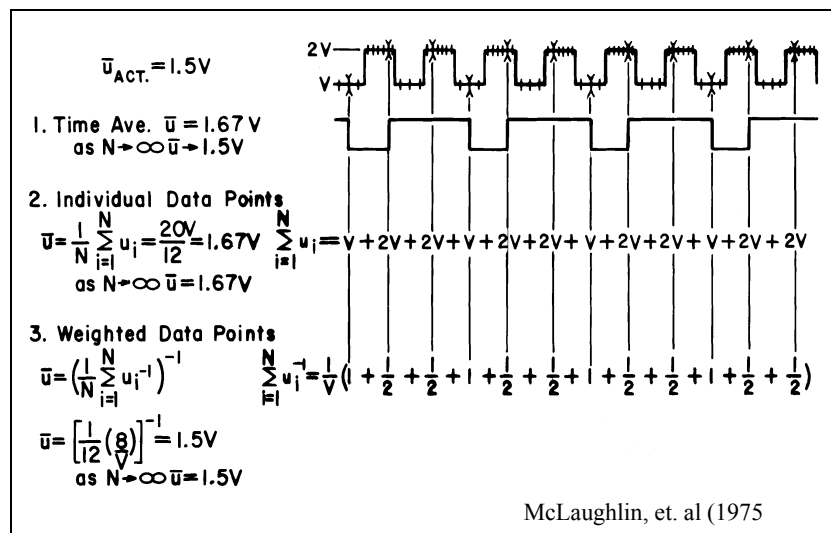


Figure A-12
Velocity Bias

In LDV, the measurement is on individual particles as they traverse the measurement volume. It is quite clear that as the velocity increases, more particles will traverse the measurement volume per unit of time. In fact the number should be proportional to the velocity. Therefore, if you simply average the individual measurements being made, the result will be biased to the high velocity side since there will be more measurements per unit of time at the higher velocities.

As shown in Figure A-12, in a one-dimensional flow situation, simply applying a correction based on the measured velocity works. But the flow is not normally one-dimensional. Also, any bias correction must consider all biases in the system, not just velocity.

The best solution is to provide a high enough seed density so that uniform time sampling or some similar technique can be used.

Noise in Laser Doppler Velocimetry

It is desirable that all light reaching the photodetector comes from incident laser light scattered from signal producing particles in the measurement volume. In theoretical calculations of signal-to-noise ratio this is the usual assumption. However, there are many other possible light sources including room lights, reflections or scattering of laser light from walls, windows, or optical components, and radiation from the fluid (e.g., flames or plasmas). These all add random shot noise to the photodetector signal. In addition, the photodetector itself generates inherent "shot noise" due to dark currents that exist in the absence of any light.

The optimum approach to coping with extraneous light sources is to try to eliminate them. Techniques include:

1. Using high-quality and clean optics and windows for minimum flare.
2. Eliminating direct reflections by masking or appropriate orientation of the optics (e.g., off-axis collection).
3. Using a second aperture on the receiving optics as a spatial filter.
4. Using optical filters so only scattered light near the laser wavelength is transmitted to the photodetector.
5. Coating solid surfaces near the measurement volume with light absorbing paint or, alternatively, fluorescent paint that fluoresces at a wavelength different than the incident laser light.

6. If not (5), sometimes a highly reflecting wall (mirror) is most effective in reducing the amount of light scattered from the wall in random directions.
7. Turning off room lights or other sources of extraneous light.
8. Using “light traps” to absorb the light from the incident beams after they have passed the measurement volume.

In many cases, none of the above precautions are necessary. However, you should try and use as large a particle as possible that will still follow the flow. Then you will need to test them to see if you get enough signal.

Particle Requirements for LDV

In some cases (e.g., water flow in forward-scatter) the natural particles occurring in the fluid are adequate seed. In other cases, experimental conditions require that only natural particles can be used. However, in most LDV applications, the data can be improved by adding appropriate seed particles to the flow.

The presence of the right type of particles in the flow is vital for successful LDV measurements. The three basic requirements for the seeds are:

1. They should follow the flow with adequate fidelity.
2. They must scatter sufficient light to produce measurable signals.
3. They should be present in desirable numbers.

It is often prudent to assess the requirements for the seed particles during the planning stage of the LDV system and plan for a suitable seeder along with the LDV system. Unfortunately, complete information regarding light scattering properties, size and number density of the particles from various seeders is usually not available. To make things worse, in a given application it is not the mean particle diameter and total number of particles produced by the seeder that are important, it is the size and number of the particles that produce measurable signals that are important. Following is a brief discussion of the three basic requirements of seed particles.

Particle Lag

The ability of the particle to follow the flow is characterized by its aerodynamic diameter. The aerodynamic diameter of a particle is defined as the diameter of a unit density sphere with the same settling velocity as the particle in question. The aerodynamic diameter primarily depends on the size, density and shape of the particle.

The particle velocity at any time, t , after a step change in fluid velocity is given by ($\rho_g \ll \rho_p$):

$$\frac{V_g - V_p}{V_{gi} - V_{pi}} = e^{-t/\tau}$$

where:

V_g = gas velocity after a step change

V_p = particle velocity at time t

V_{gi} and V_{pi} = gas and particle velocity before the step change

and

$$\tau = \frac{\rho_p d_p^2}{18\mu} = \text{relaxation time of the particle.}$$

The frequency response can be calculated from τ as follows:

$$f = \frac{1}{2\pi\tau} \left[\frac{1}{A_r^2} - 1 \right]^{1/2}$$

where A_r = particle oscillation amplitude divided by fluid oscillation amplitude.

For $A = 0.707$ (-3 dB point)

$$f = \frac{1}{2\pi\tau}$$

Table A-1 gives settling velocity and relaxation time of unit density spheres. Particles with the same aerodynamic diameter will have approximately the same settling velocity and relaxation time.

Table A-1
Sedimentation and Relaxation Time of Unit Density Sphere

Particle Diameter (μm)	Sedimentation Velocity (cm/sec)	Relaxation Time (sec)
0.5	7.5×10^{-4}	7.7×10^{-7}
0.6	1.1×10^{-3}	1.1×10^{-6}
0.7	1.5×10^{-3}	1.5×10^{-6}
0.8	1.9×10^{-3}	2.0×10^{-6}
0.9	2.4×10^{-3}	2.5×10^{-6}
1.0	3.0×10^{-3}	3.1×10^{-6}
2.0	1.2×10^{-2}	1.2×10^{-5}
3.0	2.7×10^{-2}	2.8×10^{-5}
4.0	4.8×10^{-2}	4.9×10^{-5}
5.0	7.5×10^{-2}	7.7×10^{-5}

Table for air. Dynamic viscosity $\mu = 1.81 \times 10^{-4}$ poise.

Light Scattering

The amount of light reaching the photodetector is a complex function of particle size, shape, refractive index, and the geometry of the collection optics. For a given system, it is possible to estimate the minimum diameter of the spherical particle that will scatter enough light to produce a measurable signal through computer calculations. However, you should try and use as large a particle as possible that will still follow the flow. Then you will need to test to see if you get enough signal.

Number Concentration

The number of particles that are large enough to produce a measurable signal is of interest. The smaller particles usually add more noise than signal, and so are undesirable. Very large particles are also undesirable as they are not likely to follow the flow. Thus for LDV applications, aerosols of nearly uniform size are desirable. Monodispersity is a measure of the uniformity of particle size. This is expressed by σ_g , the geometric standard deviation, defined by the equation:

$$\sigma_g = \frac{d_{84\%}}{d_{50\%}}$$

(The diameter of 84% of the particles is smaller than $d_{84\%}$ and the diameter of 50% of the particles is smaller than $d_{50\%}$). Ideally, $\sigma_g = 1$, but an aerosol is called monodisperse when $\sigma_g \leq 1.2$.

The desired particle concentration in the flow depends on the type of signal analysis. Often, the desirable situation is to find one and only one particle in the viewing volume while still maintaining a high data rate. If N_p (particles/cm³) is the number of particles in the flow and V (cm³) is the volume of the measurement volume, then the probability of finding one and only one particle in the measurement volume is greatest when $N_p V = 1$. Then, about 37% of the time there is one particle in the measurement volume, 37% of the time there are no particles in the measurement volume and the remainder of the time there is more than one particle in the measurement volume. If more than one particle in the measurement volume is desirable, then $N_p V \gg 1$, and if more than one particle is unacceptable, then $N_p V \ll 1$.

The particle concentration in the flow can be calculated from the equation:

$$N_p = \frac{Q_s \cdot N_s}{Q_T}$$

where:

Q_s = aerosol output of the seeder.

N_s = particle concentration of the seeder.

Q_T = total flow rate.

Various Particle Generating Techniques

There are several techniques to generate particles. The following is a brief discussion of the three basic techniques most often used to generate particles for LDV seeding.

1. **Atomization:** Atomization is a process of generating liquid droplets with compressed air. Many simple, reliable, and inexpensive atomizers are available. However, the generated aerosol is polydisperse. Atomizers can be used in any of the three following ways.
 - a. To generate liquid droplets—Droplets of any oil can be generated in an atomizer. However, such aerosols contain some very large droplets (10–15 μm). Although large particles will generally give the strongest signals, they probably are not following the flow field to be measured. In addition, they often cause practical difficulties by depositing on windows.
 - b. To generate solid particles of a solute—Solid particles from material like salt or sugar can be generated by atomizing a

APPENDIX B

Technical Paper

This appendix contains the technical paper “Spectral Analysis of Laser Velocimeter Data with the Slotted Correlation Method.”

SPECTRAL ANALYSIS OF LASER VELOCIMETER DATA
WITH THE SLOTTED CORRELATION METHOD

W. A. Bell*

Lockheed - Georgia Company
Marietta, Georgia 30063

ABSTRACT

This paper presents a theoretical and experimental investigation of the slotted correlation method for determining power spectra from laser velocimeter (LV) measurements. The estimate of the autocorrelation function is analyzed regarding aliasing, variance, and velocity biasing. The bias of the estimate is predictable and increases with increasing width of the lagged time slot $\Delta\tau$. When $\Delta\tau$ is sufficiently large, aliasing occurs and can be detected and avoided by decreasing $\Delta\tau$ until a stable estimate of the power spectral density is obtained. Expressions for the variance of the estimate of the autocorrelation function are derived and agree with results obtained by numerical experiment. The variance can be decreased by increasing the sampling rate, total sampling time, $\Delta\tau$, and the time between restarts of the estimate of the autocorrelation function. When velocity biasing occurs with LV data, the histogram of the number of points per lagged time slot shows a dependency on the autocorrelation function. This dependency can be used as an indication of the presence of velocity biasing.

LIST OF SYMBOLS

b - biasing coefficient
e - exponential function
f - frequency
 f_{max} - Nyquist frequency based on lagged time slot width $\Delta\tau$. $f_{max} = 1/2\Delta\tau$
i - index or $\sqrt{-1}$
j - index
k - lagged time slot number
l - index
N - number of points per lagged time slot
 N_B - number of points per lagged time slot with velocity biasing present
 N_C - number of times the computation of the autocorrelation function estimate must be restarted because of interruptions in the data acquisition process

N_{CT} - number of flow correlation times within the total sampling interval
 N_T - total number of samples taken
P - probability
R - autocorrelation function
r - sampling rate
s - independent time variable
t - independent time variable
 τ' - random variable
T - total sampling time
 $\Delta\tau$ - width of the lagged time slot
 η - independent variable
 τ - lagged time
 τ_c - correlation time of the unsteady process
 τ_k - value of τ at the kth lagged time slot
 ω - angular frequency
 ω' - folding angular frequency

I. INTRODUCTION

Background

Determining spectral estimates from laser velocimeter (LV) data presents unique problems. Since the LV relies on seeding particles to obtain velocity data, samples can only be taken when a particle traverses the measurement volume. Assuming randomly distributed particles throughout the flow, the time between samples is nonuniform, and follows an exponential distribution.

The nonuniform distribution of the time between samples precludes the use of standard spectral estimates, based on equidistant times between samples. The standard methods rely primarily on the fast Fourier transform (FFT) because of the speed at which it can compute the spectral estimates. However, the FFT does not apply to randomly sampled data. Thus, spectral estimation using LV data require special algorithms, which tend to be much slower than the standard, FFT-based methods. Another difference between periodic and random sampling occurs with aliasing. With periodic sampling, aliasing arises when the sampling rate falls below the Nyquist frequency. However, for the exponential distribution of the time between

*Senior Scientist, Member AIAA
Released to AIAA to publish in all forms.

samples exhibited by the LV data, alias-free spectral estimates are obtained (1).

A consideration unique to the analysis of LV data is velocity biasing. Since more particles per unit time cross the measurement volume with high velocities than with low, more measurements are taken at the higher velocities. McLaughlin and Tiederman (2) developed a method for taking this effect into account. However, more recently it has been shown that several factors can impact the degree and presence of velocity biasing (3). These include particle arrival times, sampling statistics, and flow correlation time scales. The impact of the recent developments in velocity biasing on spectral estimation of LV data needs to be addressed.

Previous Studies of the Slotted Correlation Method

This paper investigates the slotted correlation technique, which is widely used to obtain spectra from LV measurements. With this method an estimate of the auto- or cross-correlation function is first determined. This estimate is formed by dividing the lagged time axis of the correlation function into equidistant intervals, or slots. The LV data, consisting of discrete points in time along with the time between samples, are then used to compute the estimate of the correlation function. This is done by forming the product of two successive data points, determining the time difference (or lag) between them, and finding the lagged time slot that best approximates the time difference. The sum of the products at each slot are then formed. The average value of the lagged product within each slot is taken as an estimate of the correlation function at the center of the lagged time slot. Since the time slots are equidistant, the FFT can be applied to the resulting estimate to provide the power spectrum.

As with any spectral analysis method, of major concern are aliasing, variance, and, with LV data, velocity biasing. These topics have been the subject of several investigations (4-9). Scott (6) and Mayo (7) find that aliasing can occur in the slotted correlation function estimate if the frequency based on the slot width does not satisfy the Nyquist criterion. They show analytically that aliasing can be eliminated by decreasing the size of the lagged time slots. Their analysis needs to be experimentally verified and a technique for determining the presence of aliasing developed.

An expression for the variance of the estimates of the correlation function is derived by Scott (6). He shows that increasing the number of points per lagged time slot decreases the variance. Thus, it is important to determine the parameters that influence the number of points per slot. In another investigation of variance using a direct Fourier transform to obtain spectra from randomly sampled data, Roberts and Gaster (5) obtain significant decreases in variance. Their technique consists of filtering out part of the spectral energy at discrete frequencies from the input data and recomputing the spectra with the remaining data set, which then has a smaller mean square value. For application to the slotted correlation method, this approach must be modified and the governing

equations for variance of the estimates of the correlation function reformulated.

In the area of velocity biasing, Buchhave (9) reports the results of both analytical and experimental investigations into the impact of biasing on the estimate of the correlation function. Assuming the data rate to be proportional to the velocity, he uses residence time weighting to account for the presence of biasing. However, the assumption of direct proportionality between sampling rate and velocity does not apply in many cases (3,8,10,11). As a result a more general technique is needed to determine both the presence and degree of velocity biasing to account for its effect on spectral estimation.

Scope

Since the computation of the correlation function forms the basis of the slotted correlation approach, this paper concentrates on the estimation of this function. The purpose of this paper is to extend the previous work done concerning aliasing, variance analysis, and LV velocity biasing and their influence on the estimate of the autocorrelation function. The first part of the paper is an analytical investigation into each of these three areas. Based on the expressions derived in Refs. 6 and 7, an algorithm is developed for detecting and avoiding aliasing. Next, expressions are derived for determining the variance of the estimates of the correlation function. Since the number of points per lagged time slot strongly affects the variance, the factors influencing this parameter are derived based on an exponential distribution of time between samples. Also, equations are developed to include the effects of component removal on variance reduction. Finally, a theoretical investigation into velocity biasing leads to a method for detecting the presence of biasing from the histogram of the number of points per lagged time slot. The theoretical predictions are then tested using data obtained from physical and numerical experiments.

II. ANALYSIS

Estimate of the Autocorrelation Function

To perform spectral analysis, the LV provides a data set consisting of a sequence of discrete velocity measurements $x(t_j)$ taken at times t_j . The analysis in this paper assumes the measured process to be stationary and that the exact mean has been subtracted from the measured values, so that the autocorrelation and autocovariance functions are equivalent. The estimate of the autocorrelation function given in Refs. 5-9 is

$$R_{xx}(k) = \frac{1}{N(k)} \sum_{i=1}^{N_i} x(t_i) \sum_j x(t_i + k \Delta\tau + t'_j) \quad (1)$$

where $N(k)$ is the number of lagged products in the k th time slot, k is the time lag at the center of the slot of width $\Delta\tau$, and t'_j is a random variable such that $-\Delta\tau/2 < t'_j < \Delta\tau/2$. The variable t'_j accounts for the random distribution of points over

the lagged time slot.

Assuming the autocorrelation function does not vary significantly over the lagged time slot, Scott (6) shows that the estimate given by Eq. (1) is asymptotically unbiased and consistent. Increasing the number of points per slot $N(k)$ increases the confidence of the estimate of the autocorrelation function. Thus, it is important to determine the parameters affecting $N(k)$.

To develop an expression for $N(k)$, assume that the time between measurements follows an exponential distribution. Then the probability of a measurement occurring within a time interval dt is

$$P(t < t' < t+dt \mid t' > t) = r dt$$

where r is the mean sampling rate and P is the probability. The total number of points per lagged time slot is the sum of the probabilities of a measurement occurring in time $t+dt$ and another occurring in time $t+\tau+dt$ over the total sampling interval. Thus

$$N(k) = \sum_{l=1}^{N_c} \int_0^{T_1 - \tau_k} r dt \int_{-\frac{\Delta\tau}{2}}^{\frac{\Delta\tau}{2}} r dt \quad (2)$$

$$= r^2 \Delta\tau \sum_{l=1}^{N_c} (T_1 - \tau_k)$$

where $\tau_k = k\Delta\tau$.

T_1 is the time over which the estimate of the autocorrelation function is formed. Interruptions to the data acquisition process can occur during a run (such as waiting for data output to a storage device, intervals of sparse seeding, etc.) which require that the estimation process be restarted N_c times. The average restart time is

$$\bar{T} = \frac{1}{N_c} \sum_{l=1}^{N_c} T_1$$

and the total effective sampling time is $T = N_c \bar{T}$. Thus the expression for $N(k)$ becomes

$$N(k) = N_T r \Delta\tau \left(1 - \frac{k\Delta\tau}{\bar{T}}\right) = r^2 T \Delta\tau \left(1 - \frac{k\Delta\tau}{\bar{T}}\right) \quad (3)$$

where $N_T = rT$ is the total number of points acquired.

Equation (3) indicates that the total number of points per lagged time slot is a function of the total number of samples N_T , the average sampling rate r , the average restart time \bar{T} , and the lagged time slot width $\Delta\tau$. Increasing any of these parameters increases the total number of points per slot. Equation (3) also shows $N(k)$ to be a linear function of $\Delta\tau$. If the maximum lag time is much less than the average restart time of the correlation estimate, then $N(k)$ is approximately constant for $\tau \neq 0$. Finally, Eq. (3) provides an estimate of the mean sampling rate from the histogram of the number of points per lagged time slot versus time lag. The rate can be estimated

from the relation

$$r = \frac{N(1)}{\Delta\tau N_T} \quad (4)$$

where $N(1)$ is the number of points in the first slot not including the zero time lag products. Equation (4) provides a relatively simple means of determining the effective sampling rate for an exponential distribution of the time between samples.

Biassing and Aliasing Analysis

In Ref. 6, Section IV, Scott shows that the estimate of the autocorrelation function given by Eq. (1) is biased for finite values of $\Delta\tau$. Using the techniques developed in Ref. 4, the expected value of $\hat{R}_{xx}(k\Delta\tau)$ in Eq. (1) is

$$E[\hat{R}_{xx}(k\Delta\tau)] = \frac{r^2}{N(k)} \int_{-\frac{\Delta\tau}{2}}^{\frac{\Delta\tau}{2}} \int_0^{T(1 - \frac{k\Delta\tau}{\bar{T}})} E[x(t)x(t+k\Delta\tau-t')] dt dt'$$

where a stationary process is assumed and $E[\]$ denotes the expected value. Now,

$$E[x(t)x(t+k\Delta\tau-t')] = R_{xx}(k\Delta\tau-t')$$

Thus, substituting for $N(k)$ from Eq. (3) gives

$$E[\hat{R}_{xx}(k\Delta\tau)] = \frac{1}{\Delta\tau} \int_{-\frac{\Delta\tau}{2}}^{\frac{\Delta\tau}{2}} R_{xx}(k\Delta\tau-t') dt' \quad (5)$$

According to Eq. (5), Eq. (1) is an unbiased estimate of the autocorrelation function if $R_{xx}(k\Delta\tau)$ is constant over the interval $\Delta\tau$. For infinitesimally small lagged time slots, unbiased estimates result. However, for finite slot widths, it can be shown that (6,7)

$$E[\hat{R}_{xx}(k\Delta\tau)] = \sum_{n=-\infty}^{\infty} \int_{-\frac{\pi}{\Delta\tau}}^{\frac{\pi}{\Delta\tau}} \left[\frac{\sin\left(\frac{\omega\Delta\tau}{2}\right)}{\frac{\omega\Delta\tau}{2}} \right] \exp(-i\omega'k\Delta\tau) S_{xx}(\omega) d\omega \quad (6)$$

where $\omega' = \omega - \frac{2\pi n}{\Delta\tau}$, ω is the angular frequency and $S_{xx}(\omega)$ is the power spectral density function.

Equation (6) shows that biasing occurs with the estimate given by Eq. (1) for finite lagged time slot widths. The $(\sin u)/u$ term represents the attenuation of the spectral components that make up the autocorrelation function. This attenuation arises from the smearing of the lagged products over the lagged time intervals and leads to the biased results. The magnitude of the bias error depends upon the size of $\Delta\tau$ relative to the maximum signal frequency. As $\Delta\tau$ approaches zero, the $(\sin u)/u$ function approaches unity and the estimate becomes essentially unbiased. However, according

to Eq. (3) decreasing $\Delta\tau$ also decreases the number of points per slot and thus the confidence of the autocorrelation estimate. In practice, the selection of $\Delta\tau$ requires a tradeoff between the minimization of the biasing error and the maximization of the number of points per slot.

With the LV the response of the seeding particles to flow oscillations limits the maximum frequency f_{max} that can be detected. In essence, the particle response acts as an aliasing filter. If the value of the lagged time slot width is less than $1/(2f_{max})$, then the maximum attenuation is 0.637 in the amplitude of the correlation function, which arises from the $(\sin u)/u$ function (6,7). Aliasing occurs only when $\Delta\tau$ is greater than $1/(2f_{max})$.

Feller and Meyers show in Ref. 12 that the temporal response of the seeding particles in a given fluid depends on the diameter and density of the particles. Since many seeders generate particles over a range of sizes, it is difficult to precisely determine the maximum frequency response and thus the value of $\Delta\tau$ which avoids aliasing. This lack of precision makes an algorithm for determining the presence of aliasing desirable. A relatively simple procedure consists of computing the spectral estimate from the autocorrelation function at a given value of $\Delta\tau$, then decreasing the size of $\Delta\tau$. If aliasing is present, a significant change in the power spectral density will result indicating that $\Delta\tau$ should be decreased further. This process of decreasing $\Delta\tau$ continues until minimal changes to the power spectral density are evident.

A final observation regarding aliasing with the slotted correlation technique is that aliasing is caused by the numerical approach - the randomly sampled data are not aliased. Thus, no reacquisition of the data set is required. With periodic sampling, however, aliasing arises from the sampling of the data set itself and, if present, requires a reacquisition of the data.

Variance of the Estimate of the Autocorrelation Function

Using the approach given in Ref. 13, the variance of the autocorrelation function estimate is shown in the Appendix to be

$$\text{Var}[\hat{R}_{xx}(\tau)] = \frac{R_{xx}^2(0) + R_{xx}^2(\tau)}{N(\tau)} + \frac{2\tau_c}{T^2} \int_0^{\tau_c} \left(2 - \frac{|\eta|}{\tau_c}\right) [R_{xx}^2(\eta) + R_{xx}(\eta - \tau) R_{xx}(\eta + \tau)] d\eta \quad (7)$$

where τ_c is the flow correlation time, and $T' = T(1 - \tau/T)$.

An expression similar to Eq. (7) is derived by Scott (6) using a different approach. Equation (7) shows that two terms contribute to the variance of the spectral estimate. The first term on the right hand side of Eq. (7) is simply the square of the standard deviation of the products within each lagged time slot. The second term represents the contribution to the variance from product pairs

that are not statistically independent.

Based on Eq. (7) there are several ways to decrease the variance. The first term decreases with increasing $N(\tau)$. According to Eq. (3), the number of points per lagged time slot can be increased by increasing the sampling rate, the total sampling time, or the lagged time slot width $\Delta\tau$. However, other factors come into play. Increasing $\Delta\tau$ also increases the bias of the estimate of the autocorrelation function and may introduce aliasing. Thus, increasing $\Delta\tau$ must be done judiciously. Since the first term on the right hand side of Eq. (7) varies inversely as the square of the sampling rate r according to Eq. (3), increasing r is the most effective way of decreasing this term. However, for a given number of samples, increasing the sampling rate decreases the total sampling time, which increases the contribution to the variance from the second term on the right hand side of Eq. (7). Therefore, increasing the sampling rate without regard for total sampling time does not necessarily reduce the variance, as pointed out in Ref. 10. In general, in order to achieve maximum reduction in the variance of the estimate of the autocorrelation function both the sampling rate and total sampling time should be increased.

If the second term on the right hand side of Eq. (7) can be neglected, then the variance of the estimate of the autocorrelation function reduces to the relatively simple expression

$$\text{var}[\hat{R}_{xx}(\tau)] = \frac{R_{xx}^2(0) + R_{xx}^2(\tau)}{N(\tau)} \quad (8)$$

A sufficient condition for Eq. (8) to hold will now be developed. For the second term on the right hand side of Eq. (7), the following inequality holds:

$$\begin{aligned} & \frac{4R_{xx}^2(0)}{T'^2} \int_0^{\tau_c} (2\tau_c - |\eta|) d\eta > \\ & \frac{2}{T'^2} \int_0^{\tau_c} (2\tau_c - |\eta|) [R_{xx}^2(\eta) + R_{xx}(\eta - \tau) R_{xx}(\eta + \tau)] d\eta \\ & = 6 R_{xx}^2(0) \frac{\tau_c^2}{T'^2} \end{aligned}$$

Similarly,

$$\frac{R_{xx}^2(0)}{N(\tau)} < \frac{R_{xx}^2(0) + R_{xx}^2(\tau)}{N(\tau)}$$

Thus, Eq. (8) is a good approximation to the variance if

$$\frac{R_{xx}^2(0)}{N(\tau)} \gg \frac{6R_{xx}^2(0)}{N_c T} \frac{\tau_c^2}{T^2} \quad (9)$$

$$N(\tau) \ll \frac{N_c T^2}{6}$$

where $N_c T = T/\tau_c$ is the number of flow correlation times contained within the total effective sampling interval. For Eq. (8) to be a good approximation of the variance, Eq. (9) requires that the total number of points within a lagged time slot be much less than the square of the number of flow correlation times within the sampling interval.

According to Eq. (7) or (8), the variance of the autocorrelation estimate can be reduced by controlling the sampling process. Reference 13 presents another method for further reductions in the variance. If the power of the signal $x(t)$ is concentrated at discrete frequencies, then an estimate of these discrete frequency components can be obtained and subtracted from the original data set. The resulting data set may then possess a smaller value of R_{xx} , which, according to Eqs. (7) and (8) produces a smaller variance. Estimates of the signals at the discrete frequencies can be obtained using either Fourier transform methods or performing a least squares fit of a sinusoid at the discrete frequency with $x(t)$. From Ref. 4, the estimate of $x(t)$ can be computed from

$$y(t_j) = \frac{1}{N_s} \sum_k \sum_m x(t_m) e^{-i\omega_k(t_m - t_j)}$$

where N_s is the number of samples over which the estimate is taken, and $y(t)$ is the estimate of $x(t)$. The new data set becomes

$$z(t_j) = x(t_j) - y(t_j)$$

The estimate of the autocorrelation function for $z(t)$ can be obtained from Eq. (1) and shown to be

$$\hat{R}_{zz}(\tau) = \frac{1}{N(\tau)} [\hat{R}_{xx}(\tau) - 2\hat{R}_{xy}(\tau) + \hat{R}_{yy}(\tau)] \quad (10)$$

The variance of \hat{R}_{zz} is given by Eq. (8) with R_{zz} replacing R_{xx} . From Eq. (10), the degree of variance reduction afforded by component removal depends upon how well $y(t)$ approximates $x(t)$. In the limiting case where there is no correlation between $x(t)$ and $y(t)$, then R_{xy} is zero and this method can increase the variance, as pointed out in Ref. 5. On the other hand, if $y(t)$ exactly duplicates $x(t)$, then $R_{xx} = R_{xy} = R_{yy}$ and the variance of R_{zz} is zero. For broadband signals this method of variance reduction yields at best marginal decreases (Ref. 5) since the signal power is distributed over a large number of frequency components.

This method works best when the signal power is confined to narrow frequency bands or discrete tones. In cases where this condition applies (such

as studies of tone excited jets and boundary layers and rotating blades), removal of these discrete frequency components allows for more accurate determination of the remaining power spectral density function. Without component removal, the variance introduced by the discrete tones can obscure the presence of other components of the spectra as shown in Ref. 5.

Velocity Biasing

Velocity biasing occurs with LV measurements when the sampling rate depends on the velocity magnitude (2,3). According to Ref. 3, this dependence can occur when the LV system reset time is much less than the arrival times between seeding particles and the flow correlation time scale. The sampling rate then becomes

$$r(t) = DAv(t) \quad (11)$$

where D is the particle density, A the measurement cross sectional area, and $v(t)$ is the velocity magnitude. Dividing the velocity into a mean and unsteady term such that $v(t) = \bar{v} + v'(t)$, Eq. (11) becomes

$$r(t) = \bar{r}[1 + v'(t)] \quad (12)$$

where \bar{r} is the mean sampling rate equal to $DA\bar{v}$ and \bar{v} is the mean velocity magnitude.

To determine the effect of biasing on the number of points per lagged time slot, substitute $r(t)$ into Eq. (2) and take the expected value to obtain, assuming that v' varies insignificantly over Δt .

$$E\{N_B(k)\} = N(k) \left[1 + \frac{R_{v'v'}(k\Delta t)}{\bar{v}^2} \right] \quad (13)$$

where N_B is the number of points at the k th lagged time slot when biasing is present. If velocity biasing exists in the LV measurements, Eq. (13) indicates that the histogram of the number of points per slot versus lagged time exhibits a dependency on the autocorrelation function. This fact can be used as a cue to the presence of velocity biasing. This point is explored further in the next section.

III. COMPARISON OF THEORY WITH EXPERIMENT

Biasing and Aliasing

According to Eq. (6), the amplitude of a signal at a given frequency will be attenuated by the $(\sin u)/u$ term, where $u = \omega\Delta t/2$. In addition, at frequencies above the value $1/(2\Delta t)$ aliasing results and the signal appears in the autocorrelation function at an aliased frequency, which can be determined by standard time series analysis (e.g. Ref. 14). The amplitude of the aliased signal is attenuated according to the $(\sin u)/u$ function.

To test these predictions, a sine wave at frequencies of 10 and 20 kHz was generated numerically and randomly sampled using an exponential distribution for the time between samples. The mean sampling rate was fixed at 5000 samples per second. The lagged time slot width

was then varied to produce both biasing and aliasing of the resulting estimates of the autocorrelation function.

Figure 1 presents the results of this numerical experiment. Here the normalized amplitude of the estimate of the autocorrelation function is plotted against the ratio of the signal frequency to the Nyquist value, ω/ω_{max} . The amplitude of the estimate of the autocorrelation function resulted from a least squares fit of the estimate with a sinusoid at the signal frequency. The amplitude attenuation resulting from the averaging of the autocorrelation estimate over $\Delta\tau$ agrees well with the predictions from Eq. (6).

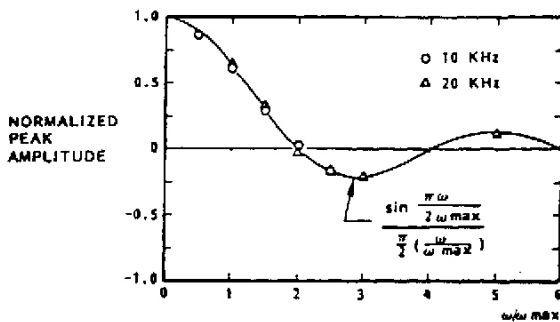


Figure 1. Comparison of the predicted and computed attenuation of the autocorrelation function caused by smearing. Discrete tone signal, $r = 5000$ samples/second.

For frequencies above the Nyquist value, the signal appears in the estimate of the autocorrelation function as a lower frequency signal. The measured and predicted folding frequencies are compared in Fig. 2. At frequencies above the Nyquist value, the signal frequency ω appears in the estimate of the correlation function as a lower frequency signal at frequency ω' . Excellent agreement exists between the predicted and measured folding frequencies as shown in Fig. 2.

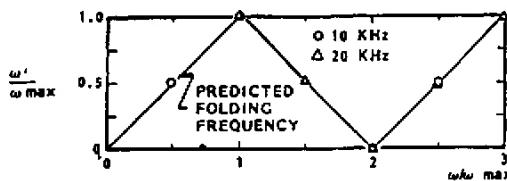


Figure 2. Comparison of the predicted and computed folding frequencies for a discrete tone signal, $r = 5000$ samples/second.

The effect of varying $\Delta\tau$ is shown in Fig. 3 in the plots of the normalized estimates of the autocorrelation function. These estimates are obtained from a sine wave at 10 kHz sampled at a mean rate of 5000 samples per second. For this frequency, aliasing occurs at values of $\Delta\tau$ above 50 microseconds. The values of $\Delta\tau$ in 3a and 3b were selected so that the signal frequency is below the Nyquist value. The attenuation in the peak

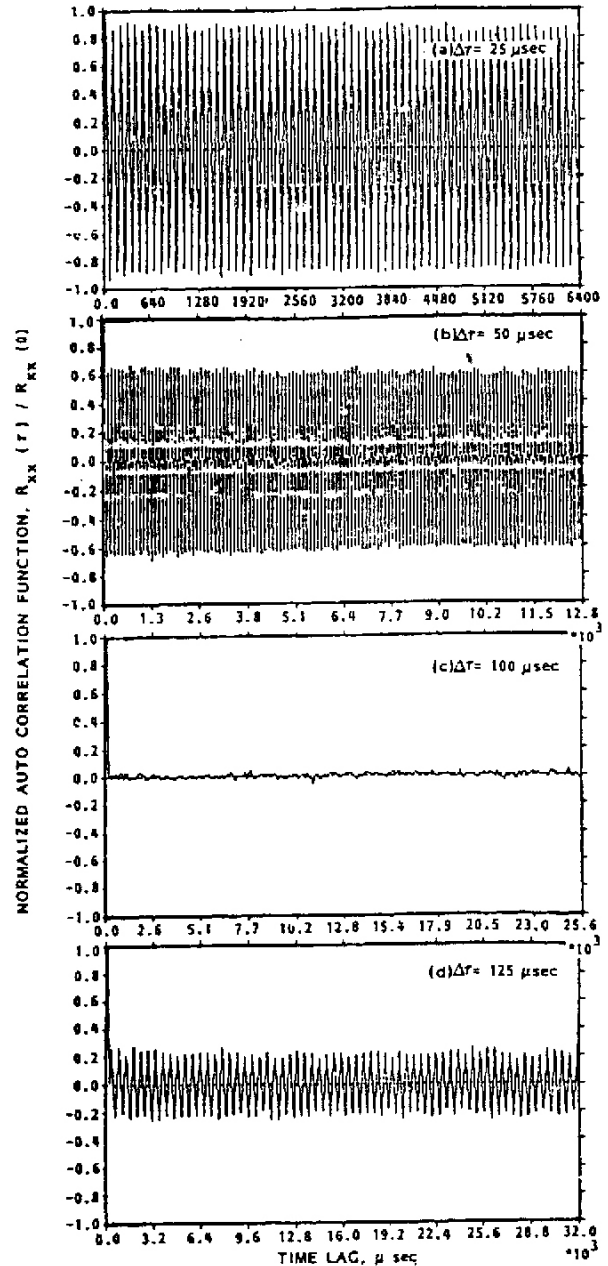


Figure 3. Effect of variations in the lagged time slot width on the estimate of the autocorrelation function for a discrete tone of 10 kHz, $r = 5000$ samples/second.

amplitude of the autocorrelation function is evident. As shown in Fig. 3c, the value of 100 microseconds is such that one cycle of the signal is contained within $\Delta\tau$. The average of the lagged products within $\Delta\tau$ is zero for this case and the only evidence of a signal present is the peak at $\tau=0$ and random fluctuations at the other values. An autocorrelation function of this type is characteristic of a signal comprised of white noise. For this case the high frequency signal contributes only noise to the power spectral density estimate. Finally, for a lagged time slot width of 125 microseconds, the signal appears at the folding frequency of 2000 kHz. The amplitude attenuation according to the $(\sin u)/u$ term in Eq. (6) is also evident.

Variance

Assuming that the data is sampled over a sufficient number of flow correlation times, then Eq. (8) provides a good approximation to the variance of the estimate of the correlation function. Since the variance depends only on the number of points $N(\tau)$ per lagged time slot for a given signal, results from the investigation of $N(\tau)$ are presented first.

Figure 4 shows the variation of $N(\tau)$ versus τ . These data were obtained from wake measurements behind a cylinder using the LV system at Lockheed-Georgia described in Ref. 15. The results are normalized with respect to $N(0)$, which contains $N\tau + N(\Delta\tau/2)$ samples. The distribution of $N(\tau)$ follows the trends predicted by Eq. (3). The linear decrease in N with τ is clearly evident. According to Eq. (3) the slope is the inverse of \bar{T} , the average restart time of the correlation estimate. The data acquisition software used with this LV system employs a double buffering scheme and the correlation estimates must be restarted every 512 to 1024 samples. Using Eq. (4) the sampling rate is approximately 4800 samples per second, which means that the average restart time falls between .11 and .21 seconds. From the slope of a line through the

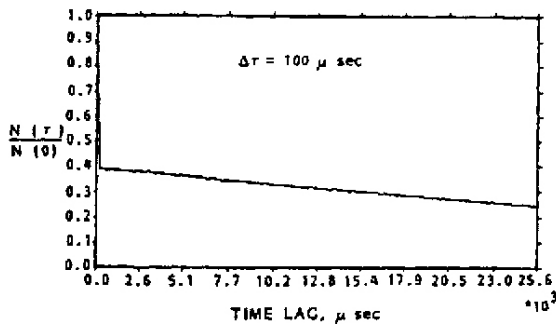


Figure 4. Measured variation in the number of points per lagged time slot. LV data obtained in the wake of a right circular cylinder.

data in Fig. 4, a value of \bar{T} of .15 results, which falls within the expected range.

The variance predicted by Eq. (8) is compared with results using simulated data in Figs. 5 and 6 for narrow band and broadband signals. The data were generated utilizing the algorithms presented in Ref. 16. As shown in Fig. 5a, the autocorrelation function follows an exponentially damped sine wave distribution for the narrow band signal described by the equation

$$\frac{R_{xx}(\tau)}{R_{xx}(0)} = e^{-488\tau} \sin(2000\pi\tau), \tau \text{ in microseconds}$$

The autocorrelation function for the broadband signal shown in Fig. 6a follows the equation

$$\frac{R_{xx}(\tau)}{R_{xx}(0)} = e^{-1000\tau}, \tau \text{ in microseconds}$$

Comparison of the computed and predicted variances are shown in Figs. 5b and 6b. These figures plot the parameter

$$\text{var}[R_{xx}(\tau)]N(\tau)/[2R_{xx}^2(0)] \text{ versus lagged time.}$$

According to Eq. (8), this parameter takes on values within the range 0.5 to 1.0. Good agreement exists between the predicted and computed values of this parameter indicating that Eq. (8) yields reliable predictions of the variance for these cases.

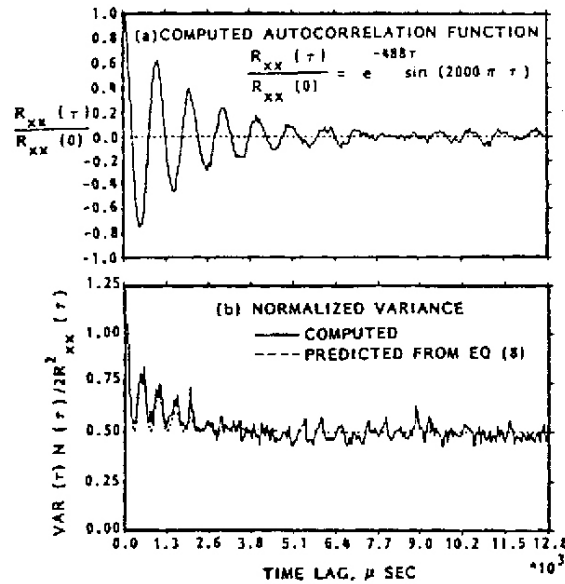


Figure 5. Estimate of the autocorrelation function and normalized variance for a narrowband signal. Lagged time slot width = 50 microseconds, $\tau = 5000$ samples/second.

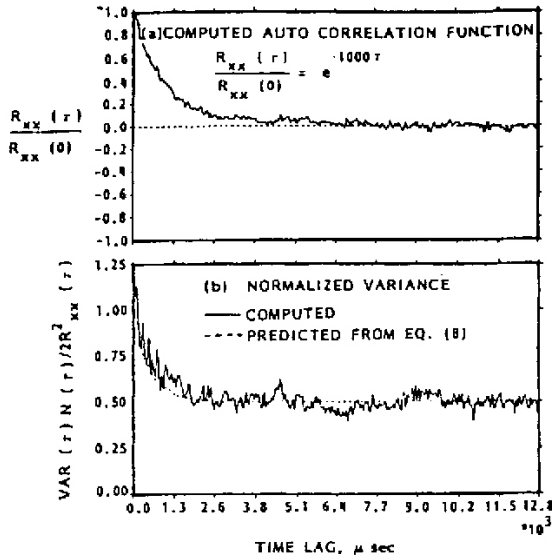


Figure 6. Estimate of the autocorrelation function and normalized variance for a broadband signal. Lagged time slot width = 50 microseconds, $r = 5000$ samples/second.

To test the variance reduction procedure based on component removal, a sinusoidal signal of 1000 Hz was added to the broadband signal of Fig. 6. The amplitude of the sinusoidal signal was 10 times that of the broadband signal. Figure 7 is a plot of the ratio of the variance after component removal to the variance before removal of the sinusoid. This figure indicates that the component removal scheme significantly reduces the variance of the estimate of the autocorrelation function for this case. Similar variance reductions are indicated in Ref. 5 where component removal is used to reduce the spectral variance. According to Fig. 7, this technique is also useful in reducing the variance of the estimate of the autocorrelation function as well when a dominant discrete tone is present in the signal.

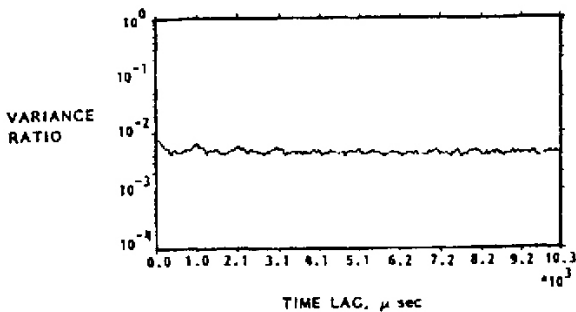


Figure 7. Effect of component removal on the variance of a discrete tone of 1000 Hz added to the broadband signal of Fig. 6. The amplitude of the discrete tone is 10 times that of the broadband signal. Lagged time slot width = 50 microseconds, $r = 5000$ samples/second.

Velocity Biasing

According to Eq. (13), velocity biasing introduces a coupling between the number of points per lagged time slot $N(\tau)$ and the autocorrelation function of the velocity magnitude. Estimates of the autocorrelation functions of the axial and vertical velocity components and the corresponding plots of $N(\tau)$ are shown in Figs. 8 through 10. The data were obtained experimentally using the LV system described in Ref. 15. The data in Fig. 8 for flow within a boundary layer shows a dependence of $N(\tau)$ in the correlation function. This dependence is also evident in Fig. 9 where the LV measurements were taken within a boundary layer excited by a discrete tone. On the other hand, Fig. 10 shows no coupling between the correlation function and $N(\tau)$, indicating no presence of biasing. The data in Fig. 10 were obtained from LV measurements in the wake of a cylinder.

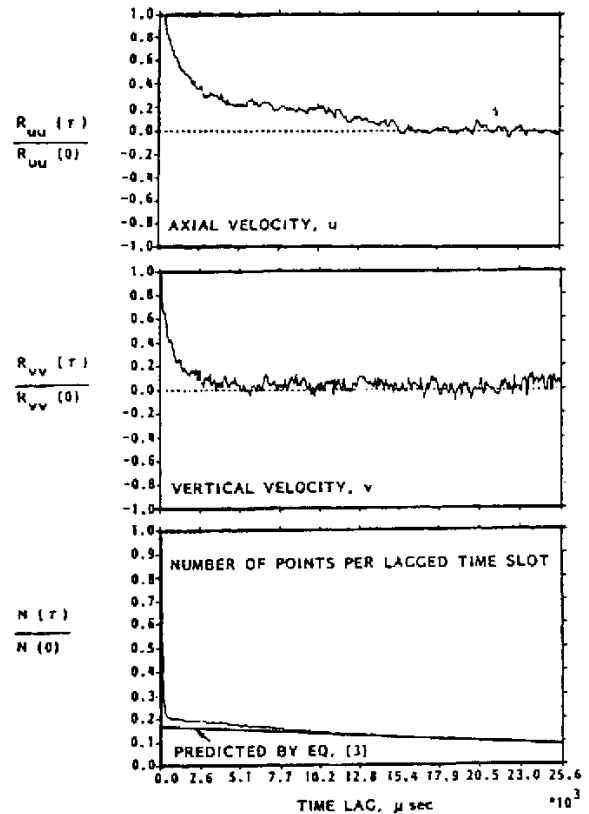


Figure 8. Estimates of the autocorrelation functions and normalized histogram of the number of points per lagged time slot. Data taken from LV measurements within an unexcited boundary layer. Lagged time slot width = 100 microseconds.

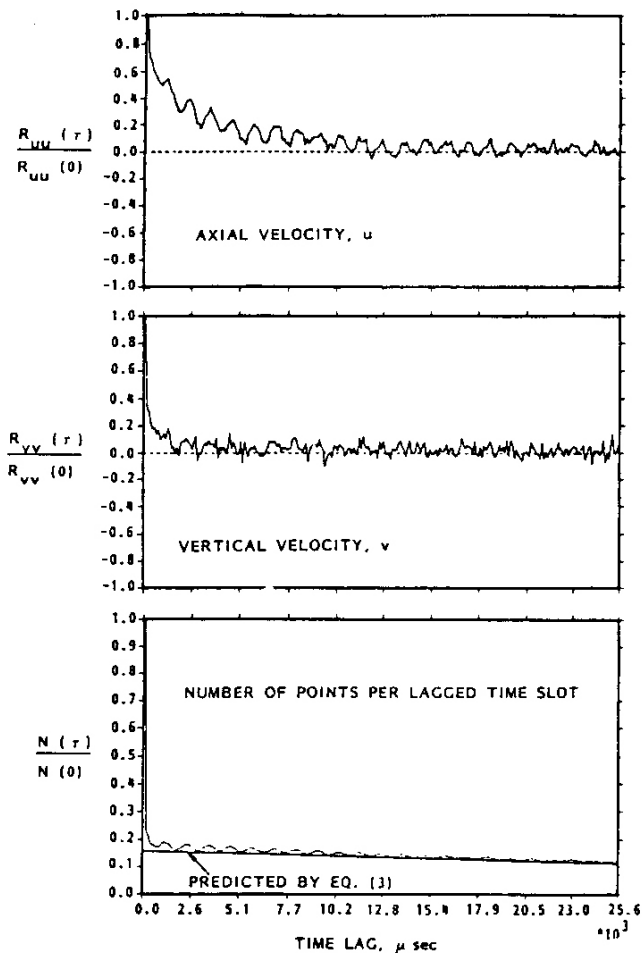


Figure 9. Estimates of the autocorrelation functions and normalized histogram of the number of points per lagged time slot within a boundary layer excited by a discrete tone of 900 Hz. Lagged time slot width = 100 microseconds.

Using the same data set employed in Figs. 8-10, the method of Edwards and Meyers in Ref. 3 was used to determine the dependence of the sampling rate on velocity magnitude. For the given data sets, the dependence is approximately linear and follows the relation

$$\frac{r(t)}{\bar{r}} = [1 + b v'(t)]$$

Table 1 presents the values of b . For the boundary layer data used in Figs. 8 and 9, the values of b in Table 1 show respectively a 1.8 and .8 per cent change in sampling rate for a one foot per second change in velocity magnitude, indicating the presence of biasing. The data from the histogram of the number of points versus τ also reflect the presence of biasing. For the cylinder wake data, biasing is not evident as reflected in the fact that $b = 0$ for this case and that the

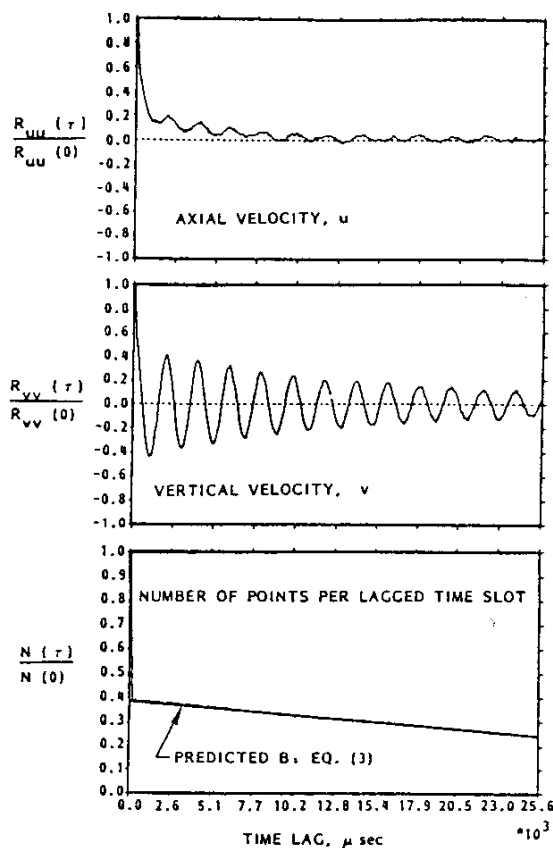


Figure 10. Estimates of the autocorrelation functions and the normalized histogram of the number of points per lagged time slot. Data set taken from 2-D LV measurements in the wake of a right circular cylinder. Lagged time slot width = 100 microseconds.

histogram of the number of points per $\Delta\tau$ shows no variation with the autocorrelation functions. Based on these results, the histogram plots provide an indication of the presence of biasing.

The negative values of b from the boundary layer measurements indicate a decrease in sampling rate r with increasing velocity, which is contrary to the assumption made in Refs. 2 and 9. However, the studies reported in Ref. 11 also show a decrease in sampling rate with velocity. One reason for these negative values lies in the fact that, with the boundary layer data, the mean velocity is low, approximately 10 feet per second from Table 1. Thus, there is a significant variation in the particle residence time with velocity. The low speed particles provide a signal of much longer duration which allows more time for signal validation by the LV electronics. As pointed out in

Table 1. Biasing coefficients and corrected means using the method of Edwards and Meyers.

DATA SET	1	2	3
b	-0.018	-0.008	0

BIASING COEFFICIENTS, sec/ft

DATA SET	1	2	3
UNCORRECTED	11.5	8.5	30.0
MEYERS/EDWARDS	11.8	9.2	30.0
McLAUGHLIN/TIEDERMAN	7.1	2.6	21.6

MEAN VELOCITY MAGNITUDE (ft/sec)

DATA SET 1 - UNEXCITED BOUNDARY LAYER (Fig. 8)

DATA SET 2 - EXCITED BOUNDARY LAYER (Fig. 9)

DATA SET 3 - CYLINDER WAKE (Fig. 10)

Ref. 10, at sufficiently low velocities multiple measurements from the same particle can also result, although these measurements were eliminated in the data sets used in Figs. 8 and 9.

An area requiring further investigation is the apparent lack of biasing in the data obtained in the cylinder wake. Here the turbulence intensities reach up to 30 per cent of free stream values. According to Ref. 2 significant biasing should result. A possible cause of this lack of biasing could arise from the sampling statistics inherent in the LV system used. The validation criterion for this system requires that the signal from a seeding particle be simultaneously validated on each of four channels within 10 microseconds. This validation criterion depends upon random processes such as photomultiplier tube noise, signal amplitudes, and threshold settings. These variables tend to decouple the particle arrival statistics from the sampling statistics, which would lead to unbiased results, as shown in Ref. 17.

Mean values of the velocity are also shown in Table 1 using three methods of computation. The first method assumes no biasing, the second uses a weighted average obtained using the value of b from the method of Meyers and Edwards, and the third method employs the McLaughlin-Tiederman correction. The data indicate that the method of McLaughlin and Tiederman overcompensates for the effects of biasing for these data sets. Similar results have been reported by other investigators (Refs. 10,11).

IV. SUMMARY AND CONCLUSIONS

This paper presents an analytical and experimental investigation into the estimation of the correlation function used to obtain the spectra from LV measurements. The estimate of the autocorrelation function based on the slotted correlation technique is biased for finite values of the lagged time slot width $\Delta\tau$. If $1/(2\Delta\tau)$ is less than the maximum signal frequency, aliasing results. Existing theories adequately describe the effects of biasing and aliasing. Aliasing can be detected and avoided without resampling the data set by decreasing $\Delta\tau$.

The variance of the estimate of the correlation function can be reduced by increasing the number of points per lagged time slot, increasing the total sampling time, or component removal. Increasing the total number of samples can be done by increasing the sampling rate, total sampling time, $\Delta\tau$, or the time between restarting the correlation estimate. The technique of removing a component of the input signal to reduce the variance works well when a dominant signal at a discrete tone is present in the data.

Velocity biasing in LV data causes the number of points per lagged time slot to depend on the correlation function. This fact serves as an indication of the presence of biasing.

REFERENCES

1. Shapiro, H. S. and Silverman, R. A., "Alias-Free Sampling of Random Noise", Journal of the Society of Industrial and Applied Mathematics, Vol. 8, No. 2, June 1960, pp. 225-248.
2. McLaughlin, D. K. and Tiederman, W. G., "Biasing Correction for Individual Realization of Laser Anemometer Measurements in Turbulent Flows", Physics of Fluids, Vol. 16, No. 12, 1973, pp. 2082-2088.
3. Edwards, R. V. and Meyers, J. F., "An Overview of Particle Sampling Bias", Proceedings of the Second International Symposium on Applications of Laser Velocimetry to Fluid Mechanics, Lisbon, Portugal, July 1984, pp. 2.1.1-2.1.5.
4. Gaster, M. and Roberts, J. B., "Spectral Analysis of Randomly Sampled Signals", J. Inst. Maths. Applics., Vol. 15, 1975, pp. 195-216.
5. Roberts, J. B. and Gaster, M. "On the Estimation of Spectra from Randomly Sampled Signals: A Method of Reducing Variability", Proc. of the Royal Society of London, Vol. A371, 1980, pp. 235-258.
6. Scott, P. F., "Theory and Implementation of Laser Velocimeter Turbulence Spectrum Measurements", Proceedings of the Second International Workshop on Laser Velocimetry, Purdue University, W. Lafayette, Indiana, March 1974, pp. 47-65.

7. Mayo, W. T., "Error Prediction of LV Turbulence Power Spectra", SDL No. 78-6378, Spectron Development Laboratories, Costa Mesa, CA, February 1979.

8. Smith, D. M. and Meadows, D. M., "Power Spectra from Random-Time Samples for Turbulence Measurements with a Laser Velocimeter", Proceedings of the Second International Workshop on Laser Velocimetry, Purdue University, W. Lafayette, Indiana, March 1974, pp. 1-18.

9. Buchhave, P. "The Measurement of Turbulence with the Burst-Type Laser Doppler Anemometer - Errors and Correction Methods", Ph. D. Dissertation, Technical Report No. TRL-106. Turbulence Research Laboratory, State University of New York at Buffalo, September 1979.

10. Edwards, R. V. and Jensen, A. S., "Particle Sampling Statistics in Laser Anemometers: Sample-and-Hold and Saturable Systems", Journal of Fluid Mechanics, Vol. 133, 1983, pp. 397-411.

11. Meyers, J. F. and Hepner, T. E., "Velocity Vector Analysis of a Flow Using a Three Component Laser Velocimeter", Proceedings of the Second International Symposium on Applications of Laser Velocimetry to Fluid Mechanics, Lisbon, Portugal, July 1984, pp. 3.1.1-3.1.5.

12. Feller, W. V. and Meyers, J. F., "Development of a Controllable Particle Generator for LV Seeding in Hypersonic Wind Tunnels", Proceedings of the Minnesota Symposium on Laser Anemometry, University of Minnesota, Bloomington, MN, October 1975, pp. 345-357.

13. Gaster, M. and Roberts, J. B., "The Spectral Analysis of Randomly Sampled Records by a Direct Transform", Proceedings of the Royal Society London, Vol. A 354, 1977, pp. 27-58.

14. Otnes, R. K. and Enochson, L., Applied Time Series Analysis, Vol. 1, John Wiley and Sons, Inc., 1978, pp. 24-27.

15. Braden, J. A., Whipkey, R. R., Lilley, D. E., Jones, G. S., and Morgan, H. L., "Application of Laser-Velocimetry to the Study of the Flow around a Two-Dimensional Airfoil", AIAA Paper 86-0505, January 1986, pp. 3-4.

16. Masry, E., Klammer, D. and Mirabile, C., "Spectral Estimation of Continuous-Time Processes; Performance Comparison Between Periodic and Poisson Sampling Schemes", IEEE Transactions on Automatic Control, Vol. AC-23, No. 4, August 1978, pp. 679-685.

17. Durao, D. F. G., Laker, J. and Whitelaw, J. H., "Bias Effects in Laser Doppler Anemometry", Journal of Physics E: Scientific Instruments, Vol. 13, 1980, pp. 442-445.

APPENDIX

To derive the variance of the estimate of the correlation function, begin with the definition of the variance

$$\text{var}[\hat{R}_{xx}(\tau)] = E[\hat{R}_{xx}^2(\tau)] - E^2[\hat{R}_{xx}(\tau)] \quad (A1)$$

Assuming no aliasing so that $x(t)x(t+\tau) = x(t)x(t-\tau)$ for $-\Delta\tau/2 < \tau < \Delta\tau/2$, then

$$\hat{R}_{xx}^2(\tau) = \frac{\tau^2 \Delta\tau}{N^2(\tau)} \left[\sum_i x(t_i) x(t_i + \tau) \right]^2 \quad (A2)$$

Following Ref. 13, it is convenient to introduce a function $Z(t)$ which jumps in value by $x(t_i)$ at every sampling time t_i and retains that value between samples. Then Eq. (A2) can be expressed as

$$\hat{R}_{xx}^2(\tau) = \frac{\tau^2 \Delta\tau}{N^2(\tau)} \int_0^{T'} d[Z(t)Z(t+\tau)] \int_0^{T'} d[Z(s)Z(s+\tau)] \quad (A3)$$

where $T' = T(1-\tau/T)$.

Taking the expected value of both sides of Eq. (A3) gives, when t and s overlap,

$$E[\hat{R}_{xx}^2(\tau)] = \frac{\tau^2 \Delta\tau}{N^2(\tau)} \int_0^{T'} E[x^2(t)x^2(t+\tau)] dt \quad (A4)$$

where $E[d\{Z^2(t)Z^2(t+\tau)\}] = \tau^2 E[x(t)x(t+\tau)] dt$ from Ref. 13. Assuming that the process has a normal distribution,

$$E[x^2(t)x^2(t+\tau)] = R_{xx}^2(0) + 2R_{xx}^2(\tau)$$

and Eq. (A4) gives

$$E[\hat{R}_{xx}^2(\tau)] = \frac{R_{xx}^2(0) + 2R_{xx}^2(\tau)}{N(\tau)} \quad (A5)$$

Similarly,

$$E^2[\hat{R}_{xx}(\tau)] = \frac{R_{xx}^2(\tau)}{N(\tau)} \quad (A6)$$

So for overlapping t and s

$$\text{var}[\hat{R}_{xx}(\tau)] = \frac{R_{xx}^2(0) + R_{xx}^2(\tau)}{N(\tau)} \quad (A7)$$

When t and s do not overlap

$$E[\hat{R}_{xx}^2(\tau)] = \frac{\tau^2 \Delta \tau}{N(\tau)} \int_0^{\tau'} \int_0^{\tau'} E[x(t)x(t+\tau)x(s)x(s+\tau)] \tau^2 dt ds \quad (A8)$$

For a normally distributed process

$$E[x(t)x(t+\tau)x(s)x(s+\tau)] = R_{xx}^2(t-s) + R_{xx}^2(\tau) + R_{xx}(t-s+\tau) R_{xx}(t-s-\tau)$$

Also, for nonoverlapping t and s ,

$$E^2[\hat{R}_{xx}(\tau)] = R_{xx}^2(\tau)$$

Thus, when t and s do not overlap

$$\text{var}[\hat{R}_{xx}(\tau)] = \frac{1}{\tau^2} \int_0^{\tau'} \int_0^{\tau'} [R_{xx}^2(t-s) + R_{xx}(t-s+\tau)R_{xx}(t-s-\tau)] dt ds \quad (A9)$$

The total variance is the sum of Eqs. (A7) and (A9). Making a change of variables, the double integral in Eq. (9) can be written as

$$\frac{2}{\tau^2} \int_0^{\tau_c} (2\tau_c - |\eta|) [R_{xx}^2(\eta) + R_{xx}(\eta-\tau)R_{xx}(\eta+\tau)] d\eta$$

The expression for the total variance then becomes

$$\text{var}[\hat{R}_{xx}(\tau)] = \frac{R_{xx}^2(0) + R_{xx}^2(\tau)}{N(\tau)} + \frac{2\tau_c}{\tau^2} \int_0^{\tau_c} \left(2 - \frac{|\eta|}{\tau_c}\right) [R_{xx}^2(\eta) + R_{xx}(\eta-\tau)R_{xx}(\eta+\tau)] d\eta \quad (A10)$$

Index

5

50% overlap, 9-3

A

A/D converter, A-14
Abs offset, 12-5
acceleration, 13-5
acousto-optic cell, A-11
analog, 8-2
analog data
 outputting, 11-1
analog input range, 8-2
analyze method, 9-2
apply, 12-6
apply current settings to all runs, 15-3
atomization, A-20
attenuation level, 5-3
auto, 9-3, 12-4, 13-6
auto dialog
 screen, 13-6
auto fill-column
 screen, 13-9
auto setup, 13-7
auto slope, 5-6
 error message, 5-7
axis labels dialog, 6-6
axis setup, 13-5
 dialog screen, 13-5

B

backscatter, A-7
band pass filter, 2-14, 2-16
bandwidth, A-6
bar graph parameters
 screen, 6-7
beam diameter values, 2-7
beam expander, 2-7
beam separation, 2-7
 values, 2-7
beamsplitter, A-3, A-11
bragg cell, A-11
bragg cell freq, 2-8
burst detector, A-14
burst eff (%), 2-18
burst inhibit connector, 2-9
burst monitor, 14-1
 window, 14-2

burst threshold, 2-16, 2-17

C

calibration, 3-7, 3-15
calibration diode setup page, 3-16
 screen, 3-18
capture run button, 4-1
cascade graphs, 6-11
caution and warning labels, xix
channel enable, 2-8
class IIIB laser, vi
class IV laser, vi
coincidence button, 10-9
coincidence data rate, 2-18
coincidence mode, 10-7
coincidence window
 coincidence int., 10-9
 gate scale, 10-8
 selection, 10-8
 setup, 10-8
collimating light, A-7
communication setup, 13-4
 dialog screen, 13-4
condensation, A-21
converted high, 8-2
converted low, 8-2
copy graph to clipboard, 6-10
correlation dT, 9-3
counters, A-12
covariance processor, A-12
create project directory, 1-2
creating
 graphs, 6-1
 new data structure, 1-1, 1-2
 simple traverse position list, 13-9
 statistics window, 7-1
customizing graph, 6-5
customizing statistics window, 7-5

D

data rate, 2-14
 as function of PMT voltage, 3-12
data storage, 1-3
decrease font size, 6-10
degrees per cycle, 12-2
deleting graph, 6-3
designing graph, 6-2
designing statistics window, 7-9

- detector separation values, 3-7
- diameter difference
 - screen, 3-14
- diameter distribution
 - screen, 4-14
- diameter fitting, 4-11
- diameter histogram
 - screen, 6-9
- diameter limit max, 3-4
- diameter limit min, 3-4
- diameter max, 2-8
- diameter measurement, 3-8, 3-10, 5-1, 5-6
 - page, 5-3
 - screen, 3-8
- diameter min, 2-8
- diameter statistics, 4-6
- diameter statistics window, 7-2
- diameter/channel 1 velocity control menu
 - screen, 3-11
- digital, 8-3
- digital signal analyzer, A-14
- digital signal processor, A-12
 - components, A-13
- direction, 12-2
- direction of fringe motion, 2-3, 3-2
- disable inhibit windows, 12-3
- domains, 5-3
- Doppler frequency, A-9
- Doppler frequency measurement, A-3
- Doppler signal, A-5, A-6
- downmixing, 2-12
- droplets, A-20
- dual-beam arrangement, A-2, A-7

E

- edit graph
 - edit graph window, 6-8
 - edit plot, 6-9
- edit graph window, 6-8
- edit histogram data sets
 - screen, 6-4
- editing commands, 13-9
- enable auto export, 2-4
- enable auto intensity limit calculation, 4-3
- enable bragg cell, 2-9
- enable gatetime weighting, 2-10
- enable intensity validation on velocity, 2-9
- enable power spectrum/correlation analysis, 9-1
- enable probe volume correction, 4-7
- enable range limits, 9-3
- enable software slave mode, 2-4
- enable sync pulse input, 2-9
- encoder parameters, 12-2
- error message
 - inconsistent entries for auto slope, 5-7
- ESD protection, xx
- estimated smallest measurable dia., 4-7
- evaporation, A-21

- even-time analysis, 9-2
- even-time sampling, 10-11
 - feature, 10-12
- example subrange analysis, 10-3
- export data dialog
 - screen, 15-1
- export file, 15-2
- export format, 15-2
- export headings, 15-2
- export to 1 file, 15-2
- exporting data in ASCII format, 15-1
- external input
 - screen, 8-1
 - statistics window, 7-4
 - tab, 8-1
 - using, 8-1

F

- fiberlight
 - power output, ix
- fiberoptic probe
 - power output, ix
- file
 - experiment manager, 15-2
- filters
 - high-pass, A-6
 - low-pass, A-6, A-14
- flow
 - reversal, A-9
- focal length, 2-6
- forward-scatter, A-8
- Fourier transform, A-14
- frequency
 - versus velocity, A-8
- frequency shifting, A-9, A-10
- fringe descriptions, A-4
- fringe motion
 - direction, 2-3
- fringe spacing, 2-8, A-4
- fringes, A-10
- FSA connection, 2-18

G

- gate scale, 10-8
- Gaussian, A-7
- Gaussian diameter, 2-7
- Gaussian intensity distribution, A-4, A-5
- graph
 - creating, 6-1
 - customizing, 6-5
 - data, 6-10
 - deleting, 6-3
 - designing, 6-2
 - modifying, 6-3
 - showing, 6-1
- graph designer, 6-3
- graph designer button, 6-2

- graph designer screen, 6-3
- graph parameters screen, 6-8
- graphs, 4-1
 - cascade graphs, 6-11
 - frequency1 histogram, 2-14
 - graph designer, 6-3
 - hide all graphs, 6-11
 - system graphs
 - intensity validation, 3-12
 - particle diameter distribution, 4-10
 - phase AB, phase AC, 3-16
 - tile graphs horizontally, 6-11
 - tile graphs vertically, 6-11

H

- hardware
 - burst monitor, 14-1
- hardware coincidence, 2-10
- hardware status, 2-14, 2-18
 - screen, 2-10
- help, xxi
- hide all graphs, 6-11
- high-pass filter, 2-9
- hints, 10-10
- histogram data set
 - modifying, 6-4
- horizontal axis dialog, 6-6

I-J-K

- increase font size, 6-10
- increment, 9-3
- inputting subrange values, 10-2
- installing software, 1-1
- intensity validation, 3-12
- intensity validation/PVC page, 4-7
- intensity/validation PVC tab, 4-2
- introduction, xix

L

- laser beam diam, 2-7
- laser diode calibration, 3-15
- laser diode calibration page, 3-17
- laser Doppler velocimetry
 - noise, A-16
- laser safety, v
- LDV
 - Doppler signal, A-5
 - frequency shifting, A-9
 - fringe spacing, A-4
 - laser source, A-3
 - measurement volume, A-4
 - noise, A-15
 - overview, 2-1, A-1
 - particle requirements, A-17
 - signal characteristics, A-6
 - system components, A-2

- LDV (*continued*)
 - system optimization, A-3
 - technique, A-1
- LDV controls, 2-11
 - menu screen, 2-12
 - tab, 2-11, 10-7
- light scattering, A-19
- liquid water content, 4-9
- log normal, 4-12
- lower-to-upper intensity ratio, 4-3
- LWC, 4-9

M

- manage experiments, 1-3
- manage experiments and runs, 1-3
- manual, 13-2
- manual history, ii
- manual input checkbox, 2-8
- manual setup, 13-2
- matrix, 13-7
 - open, 13-6
- matrix dialog screen, 13-8
- matrix transformation, 16-1
- matrix transformation page, 16-1
- Matsumoto-Takahashi, 4-13
- max travel steps, 13-5
- max. angle, 12-6
- maximum particle measurement attempts, 2-3, 2-5
- maximum run time, 2-5
- mean diameter as function of PMT voltage, 3-12
- measurement volume, A-4, A-5, A-20
 - dimensions, A-5
 - geometry, 4-7
- Mie scattering calculations, A-7
- min. angle, 12-6
- miscellaneous
 - decrease font size, 6-10
 - increase font size, 6-10
 - reset plot, 6-10
- mode, 12-2
- modifying graph, 6-3
- modifying histogram data set, 6-4
- modifying RMR window, 12-4
- modulus, 8-2
- monodisperse, A-19, A-21

N

- noise
 - laser Doppler velocimetry, A-16
- normal, 4-12
- Nukiyama-Tanasawa, 4-13
- number concentration, A-19
- number of diameter bins, 4-3
- number of windows, 12-5

O

- obtaining detailed flow information, 4-1
- offset, 8-2
- offset angle, 12-5
- once per rev., 12-3
- open current project directory, 1-4
- optical properties of common particle materials, 5-2
- optical setup page
 - screen, 2-6, 3-5
- optimizing particle size measurement, 4-1
- outputting analog data, 11-1
- overview
 - LDV, 2-1
 - phase Doppler, 3-1

P

- parameter description, 13-8
- particle, A-7
- particle diameter distribution, 4-10
- particle generating techniques, A-20
- particle lag, A-18
- particle sizing, 5-1
- particles, solid, A-21
- pedestal, A-5, A-6, A-7
- phase Doppler
 - overview, 3-1
- photodetector, A-3, A-6
- photodiode, A-5, A-6, A-9
- photon correlators, A-12
- playback button, 4-4
- plot parameters
 - screen, 6-8
- PMT volt sat, 2-18
- PMT voltage*, 2-16
- points per FFT, 9-3
- polydisperse, A-20
- post processing, 12-6
- power output, ix
- power spectrum analysis, 9-1
- power spectrum/correlation
 - screen, 9-1
 - tab, 9-1
- probe volume correction, 4-6
- processor/matrix
 - screen, 2-11, 3-6, 9-2
 - tab, 3-6, 11-1
- pulses per revolution, 12-3
- PVC, 4-6

Q

- quick capture mode, 2-5

R

- RCF front lens, 3-5
- RCV back lens, 3-5

- reader's comments sheet (*Reader's Comment Sheet*)

- receiver calibration
 - screen, 3-7
- receiving optics, A-4
- relative home, 13-5
- relative refractive index, 5-3
- reset plot, 6-10
- reset time stamp at OPR, 12-4
- RMR, 12-1
 - auto screen, 12-5
 - screen, 12-1
 - tab, 12-1
 - window
 - automatic generation parameters, 12-4
 - display graphic, 12-4
 - modifying, 12-4
- RMR off, 12-3
- Rosin Rammler, 4-11
- run
 - calibration
 - laser diode calibration, 3-15
 - real time view, 2-14
 - run setup, 3-3
 - diameter measurement, 5-1
 - run settings, 3-3
 - run setup processor/matrix, 16-8
 - save run, 4-2
- run settings, 3-3
 - screen, 2-4, 3-4
- run setup, 5-1, 5-3
 - calibration, 3-7
 - diameter measurement, 3-8
 - optics, 2-6, 3-4
 - beam expander, 2-7
 - beam separator, 2-7
 - bragg cell freq, 2-8
 - diameter limit max, 3-4
 - diameter limit min, 3-4
 - diameter max, 2-8
 - diameter min, 2-8
 - focal length, 2-6
 - fringe spacing, 2-8
 - laser beam diam, 2-7
 - RCV back lens, 3-5
 - RCV front lens, 3-5
 - slit aperture, 3-5
 - wavelength, 2-6
- processor/matrix, 2-8
 - burst inhibit connector, 2-9
 - channel enable, 2-8
 - enable bragg cell, 2-9
 - enable gatetime weighting, 2-10
 - enable intensity validation on velocity, 2-9
 - enable sync pulse input, 2-9
 - hardware coincidence, 2-10
 - high-pass filter, 2-9
 - single measurement/burst, 2-9

- run setup (*continued*)
 - run settings
 - enable auto export, 2-4
 - enable software slave mode, 2-4
 - maximum particle measurement attempts, 2-3, 2-5
 - maximum run time, 2-5
 - screen update interval, 2-4, 2-5
 - time out, 2-4, 2-5
 - sweep capture, 3-9

S

- safety
 - labels, xix
 - laser, v
 - warning labels, vii
- save graph, 6-10
- save run, 4-2
- scan capture, 13-1
- scattered light, 2-2, A-7
 - intensity, A-7
- scattering domain, 5-3
- scattering mode chart, 5-4, 5-5
- screen
 - hardware status, 2-10
- screen update interval, 2-4, 2-5
- selected, 12-6
- selecting
 - existing project, 1-3
 - experiment folder, 1-3
 - optical layout, 5-1
- selecting optical layout, 5-2
- service policy, iii
- setting traverse parameters, 13-1
- setting up
 - software, 3-3
 - traverse, 13-1
- shaft encoder, 12-3
- shaft encoder x4, 12-3
- showing graph, 6-1
- showing statistics window, 7-1
- signal processor, A-11
 - requirements, A-12
 - types, A-12
- signal-to-noise, 2-17
- signal-to-noise ratio, A-3
- single measurement/burst, 2-9
- slit aperture, 3-5
- slope of upper intensity curve, 4-3
- slot analysis, 9-2
 - options, 9-3
- SNR, 2-16, 2-17
- software
 - installation, 1-1
 - license, iv
 - setup, 3-3
- software coincidence, 10-9
- software coincidence capture, 10-10

- software coincidence mode
 - of operation, 10-9
- spectrum analyzer, A-12
- statistics
 - statistics designer, 7-9
- statistics designer
 - screen, 7-10
- statistics designer button, 7-9
- statistics output options, 7-5
- statistics selection menu, 7-1
- statistics summary report, 7-6
- statistics window
 - creating, 7-1
 - designing, 7-9
 - example, 7-10
 - showing, 7-1
- subrange
 - suggestions, 10-6
- subrange input menu, 10-3
- subranges (over/under)
 - tab, 10-2
- sweep capture, 3-9
 - screen, 3-9
- system graph
 - intensity validation
 - screen, 3-13
- system graphs, 3-12, 4-10
 - menu, 4-1

T

- taking size and velocity data, 3-1
- text parameters dialog, 6-5
- tile graphs horizontally, 6-11
- tile graphs vertically, 6-11
- time out, 2-4, 2-5, 13-5
- tolerance, 12-3
- total particle conc., 4-10
- trackers, A-12
- transformation matrix
 - setup, 16-8
- transformed velocity statistics window, 7-4
- traverse
 - scan capture, 13-1
 - setting parameters, 13-1
 - setting up, 13-1
 - start, 13-1
- traverse manager
 - screen, 13-2
- turbulent flow, A-9

U

- upper/lower intensity curve intercept, 4-4
- use transformed velocities, 9-2
- using external input, 8-1
- using subrange, coincidence modes and even-time sampling, 10-1

V

- various size distributions, 4-11
- vector to analyze, 9-2
- velocity, 13-5
- velocity and size subrange statistics window, 7-3
- velocity bias, 10-11, A-15
- velocity statistics, 4-4
 - screen, 4-5
 - window, 7-2
- velocity subrange, 10-4
- volume 1, 4-10
- volume 10, 4-10
- volume 50, 4-10
- volume 90, 4-10
- volume 99, 4-10
- volume distribution
 - screen, 4-14, 4-16
- volume distribution statistics, 4-8
 - window, 7-3
- volume flux x, y and z, 4-9

W-X-Y-Z

- wait time in pos (s), 13-5
- warning and caution labels, xix
- warning labels, vii
- warning message
 - auto-intensity option, 4-3
- warranty, iii
- wavelength, 2-6
- windowing method, 9-3
- windows, 12-4, 12-5

Reader's Comments

Please help us improve our manuals by completing and returning this questionnaire to the address listed in the "About This Manual" section. Feel free to attach a separate sheet of comments.

Manual Title Phase Doppler Particle Analyzer/Laser Doppler Velocimeter Operation Manual
P/N 1990048 **Rev.** E

1. Was the manual easy to understand and use?

Yes No

Please identify any problem area(s) _____

2. Was there any incorrect or missing information? (please explain) _____

3. Please rate the manual according to the following features:

Good Adequate Poor

- Readability
- Accuracy
- Completeness (is everything there?)
- Organization (finding what you need)
- Quality and number of illustrations
- Quality and number of examples

Comments: _____

4. Which part(s) of this manual did you find most helpful? _____

5. Rate your level of experience with the product:

Beginning Intermediate Expert

6. Please provide us with the following information:

Name _____ Address _____
Title _____
Company _____



TSI Incorporated
500 Cardigan Road, Shoreview, MN 55126 U.S.A.
Web: www.tsi.com

